Faculty of Pharmaceutical Sciences

STRUCTURE-AIDED DESIGN OF INHIBITORS OF *MYCOBACTERIUM TUBERCULOSIS* THYMIDYLATE KINASE

Veerle Vanheusden

Thesis submitted to the faculty of Pharmaceutical Sciences in order to obtain the degree of Doctor in the Pharmaceutical Sciences

Promoters
Prof. dr. S. Van Calenbergh
Prof. dr. P. Herdewijn

Academic year 2003-2004

TABLE OF CONTENTS

v............. *Acknowledgements, Dankwoord*

vii........... *Summary, Samenvatting*

xi............ *List of abbreviations*

1............. *Chapter 1*

State-of-the-art and research objectives

59........... *Chapter 2*

Synthesis and Biological Evaluation of Thymidine-5’-*O*-monophosphate Analogues as Inhibitors of *M. tuberculosis* Thymidylate Kinase (2'- and 3'-modifications)

71........... *Chapter 3*

Enzymatic and Structural Analysis of Inhibitors Designed against *Mycobacterium tuberculosis* Thymidylate Kinase: new insights into the phosphoryl transfer mechanism (5-modifications)

95........... *Chapter 4*

3’-*C*-Branched-Chain-Substituted Nucleosides And Nucleotides as Potent Inhibitors of *Mycobacterium tuberculosis* Thymidine Monophosphate Kinase

117.......... *Chapter 5*

Thymidine and Thymidine-5'-*O*-monophosphate Analogues as Inhibitors of *Mycobacterium tuberculosis* Thymidylate Kinase (2', 3', 5'- and 5- modifications)

125.......... *Chapter 6*

Discovery of Bicyclic Thymidine Analogues as Selective and High Affinity Inhibitors of *Mycobacterium tuberculosis* Thymidine Monophosphate Kinase

141.......... *Chapter 7*

Synthesis of 1-[2,4-dideoxy-4-*C*-hydroxymethyl-α-L-lyxopyranosyl]thymine: a Potential Inhibitor of *Mycobacterium tuberculosis* Thymidine Monophosphate Kinase

159.......... *Chapter 8*

General discussion, conclusions and perspectives

165.......... *Overview of evaluated compounds*

167.......... *List of publications*

DANKWOORD

The past four and a half years were fascinating, illuminating, frustrating, exhausting. This page is for all those who joined me in work and discussion, who lifted my moods when things went wrong and celebrated with me the good times. For all those who made this work possible. Thanks.

- *Prof. Serge Van Calenbergh*, mijn promotor, bedankt om mij in te wijden in de organische synthese en mij te betrekken in dit boeiende project. Bedankt voor de vele suggesties en tips. Ik heb je inzicht en kritische geest enorm geapprecieerd.

- *Prof. Piet Herdewijn* bedankt voor de waardevolle raadgevingen in de nucleosidenchemie en het corrigeren van mijn arikels en dit werk.

- Een bijzonder woord van dank, *Prof. Roger Busson*, voor je hulp bij het bepalen van de configuraties van een aantal verbindingen, *Prof. Jef Rozenski* voor het opnemen van de talrijke massapectra, *Dr. Arne Heyerick* voor de hulp bij de HPLC zuiveringen en *Mathy Froeyen*, voor de moddeling experimenten. *Dr. Hélène Munier* and *Dr. Marc Delarue*, thanks for testing my nucleosides and nucleotides for their biological activity. Zonder jullie hulp was dit werk niet mogelijk geweest !

- Voor de financiering van dit onderzoek ben ik dank verschuldigd aan het *FWO Vlaanderen*.

- *Philippe*, *Inge*, *Charlotte*, *Steven*, *Timothy*, *Liesbeth*, *Ineke*, *Helga*, *Ulrik* en *Izet* die samen met mij de voorbije jaren in het labo hebben gewerkt : jullie hulp en de toffe babbels heb ik enorm geapprecieerd. Ineke, ik ben blij dat je dit onderzoek zal verder zetten en ik wens je het allerbeste voor de toekomst .

- Mijn ouders, goede vrienden en familie: bedankt om het wel en wee van mijn nucleosiden te aanhoren, bedankt voor jullie interesse en vriendschap.

- *Peter*, toen we elkaar acht jaar geleden leerden kennen, was ik een meisje dat apotheker wou worden. Sindsdien hebben mijn studies en doctoraatsonderzoek vaak op de voorgrond gestaan. Op momenten dat het slecht ging heb je me, samen met Fientje, getroost en als het goed ging, hebben we samen gevierd. Bedankt ook om dit boekje in een mooie vorm te gieten.

- Ik heb geprobeerd om in dit dankwoord niemand te vergeten. Als ik toch nog iemand zou vergeten zijn, kom dan maar aan mijn oren trekken, je hebt nog iets te goed…

Iedereen heel erg bedankt,

Veerle

SUMMARY

The aim of this work was the search for selective inhibitors of *M. tuberculosis* thymidine monophosphate kinase (TMPKmt) as leads for the development of new anti-tuberculosis agents. Based on the X-ray structure of TMPKmt, it was decided to establish a preliminary structure-activity relationship by synthesising a series of nucleosides and nucleotides modified at the 2’-, 3’- and 5-positions of the dTMP-scaffold. These analogues were tested for their affinities for TMPKmt. From this, a 2'-chlorine and a 2'-fluorine substituent emerged as the most promising modifications of the dTMP scaffold. Furthermore, the affinities of a series nucleosides and their corresponding nucleotides were compared. The deletion of the phosphate moiety typically resulted in a modest, in many cases negligible affinity loss. In view of the drug delivery problems of phosphorylated compounds, nucleosides seemed more useful leads for further drug design.

The goal of the synthesis of a series 3'-*C*-branched-chain nucleosides and nucleotides (3'-CH_2N_3, 3'-CH_2NH_2, 3'-CH_2F, 3'-CH_2OH) was to occupy a cavity in the enzyme near the 3'-position. Biological results and modeling confirmed this hypothesis. 3'-Azidomethyl-3'-deoxy-thymidine (**4.9**), combining a low K_i-value (40 μM) with a high selectivity index for the tuberculosis enzyme (K_i TMPKh/ K_i TMPKmt = 26) emerged as the most promising lead for further optimisation. Attempts were made to combine these favourable 3'-substitution patterns with 2'-halogen substituents (**6.9**-**6.14**). However, introduction of the 2'-halogen led to a drastic decrease in affinity compared to the corresponding 2'-deoxy-nucleosides. Probably, the 2'-halogens compete with the 3'-substituents for the same binding pocket.

Furthermore, it was tried to supersede the good affinities of the 3'-*C*-branched-chain nucleosides, by further exploration of the enzyme cavity near the 3'-position with alternative nitrogen-containing substituents. However, attempted simultaneous reduction of the 6'-azido function and the 2'-hydroxyl of compound **19** (chapter 6) failed. Instead three peculiar nucleoside analogues (**6.10**, **6.11** and **6.12**) were isolated that were tested for their affinities for TMPKmt and TMPKh. Dinucleoside **6.12** unexpectedly showed a high affinity (K_i = 37 μM) and selectivity for the tuberculosis enzyme, indicating an exceptional flexibility of TMPKmt towards the orientation of the sugar ring. Also the bicyclic nucleosides **6.10** and **6.11** showed excellent affinities. With its K_i-value of 3.5 μM (exceeding the affinity of the natural substrate) and its selectivity index of 200, **6.10** represents the highest affinity and most selective inhibitor of TMPKmt found so far. The favourable affinities and selectivities of these three inhibitors will form the basis for further drug design, considerably increasing the variety of nucleoside analogues that may be envisaged for future synthesis.

Based on the encouraging affinity of anhydro-hexitol nucleotide **7.1**, the effects of six-membered sugar rings for the affinity for TMPKmt were further explored through the synthesis of 1-[2,4-dideoxy-4-*C*-hydroxymethyl-α-L-lyxopyranosyl]thymine (**7.4**). This nucleoside indeed showed the predicted equatorial orientation of the thymine ring ($^4C_1$). Affinity results were however disappointing.

In conclusion, this work yielded some high affinity and selective inhibitors for TMPKmt that open interesting perspectives in the search for new anti-tuberculosis agents. Based on their high selectivity indices, especially dinucleoside **6.12** and bicyclic nucleosides **6.10** and **6.11** will be used as the starting point for the search of inhibitors with an optimal fitting in the active pocket of TMPKmt.

SAMENVATTING

Het doel van dit werk was de zoektocht naar selectieve inhibitoren voor *M. tuberculosis* thymidine monofosfaat kinase (TMPKmt) als *leads* voor de ontwikkeling van nieuwe anti-tuberculose geneesmiddelen. Op basis van de X-straal structuur van TMPKmt, werd besloten een eerste structuur-activiteitsrelatie tot stand te brengen via de synthese van een reeks nucleosiden en nucleotiden, gemodificeerd op de 2'-, 3'- en 5-posities van het dTMP skelet. Deze verbindingen werden getest op hun affiniteit voor TMPKmt. Hieruit kwamen een 2'-chloor en een 2'-fluor substituent naar voor als de meest interessante modificaties. Verder werden de affiniteiten van een reeks nucleosiden en hun overeenkomstige nucleotiden vergeleken. Over het algemeen, veroorzaakte de verwijdering van de fosfaatgroep een bescheiden, meestal zelfs verwaarloosbaar, affiniteitsverlies. Aangezien gefosforyleerde verbindingen moeilijk door cellen opgenomen worden, zijn nucleosiden nuttigere *leads* voor verdere geneesmiddelontwikkeling.

Met de synthese van een reeks 3'-*C*-vertakte-keten nucleosiden en nucleotiden (3'-CH_2N_3, 3'-CH_2NH_2, 3'-CH_2F, 3'-CH_2OH) werd gepoogd een holte dicht bij de 3'-positie in het enzym op te vullen. Biologische resultaten en modeling bevestigden deze hypothese. 3'-Azido-methyl-3'-deoxy-thymidine (**4.9**), dat een lage K_i-waarde (40 μM) combineert met een hoge selectiviteitsindex voor het tuberculose enzym (K_i TMPKh/ K_i TMPKmt = 26) kwam naar voor als de meest interessante *lead* voor verdere geneesmiddelontwikkeling. Pogingen werden ondernomen om deze gunstige 3'-substitutiepatronen te combineren met 2'-halogeen substituenten (**6.9**-**6.14**). Invoering van deze 2'-halogenen leidde echter tot een sterke affiniteitsdaling in vergelijking met de overeenkomstige 2'-deoxy-nucleosiden. Waarschijnlijk treden de 2'-halogenen in competitie met de 3'-substituenten voor de zelfde bindingsplaats.

Verder werd gepoogd de goede affiniteiten van de 3'-*C*-vertakte keten nucleosiden te verbeteren via verdere verkenning van de holte in de buurt van de 3'-positie met andere stikstof-bevattende substituenten. Een poging tot simultane reductie van de 6'-azidofunctie en de 2'-hydroxylgroep van verbinding **19** (hoofdstuk 6) faalde. Niettemin werden hierdoor drie bijzondere nucleoside analogen (**6.10**, **6.11** and **6.12**) gevormd die getest werden op hun affiniteiten voor TMPKmt en TMPKh.

Dinucleoside **6.12** vertoonde een onverwacht hoge affiniteit (K_i = 37 μM) en selectiviteit voor het tuberculose enzym, wat wijst op een uitzonderlijke flexibiliteit van TMPKmt voor de oriëntatie van de suikerring. Ook de bicyclische nucleosiden **6.10** en **6.11** vertoonden uitmuntende affiniteiten: met zijn K_i-waarde van 3.5 μM (die de affiniteit van het natuurlijk substraat overtreft) en een selectiviteitsindex van 200 is **6.10** de beste en meest selectieve inhibitor voor TMPKmt die tot nu toe ontdekt is. De gunstige affiniteiten en selectiviteiten van deze drie inhibitoren zullen de basis vormen voor verdere geneesmiddelontwikkeling. Zij verhogen gevoelig de diversiteit van nucleoside analogen die voor verdere synthese in aanmerking komt.

Op basis van de bemoedigende affiniteit van anhydro-hexitol nucleotide **7.1**, werden de effecten van zesring suikers op de affiniteit voor TMPKmt verder verkend via de synthese van 1-[2,4-dideoxy-4-*C*-hydroxymethyl-α-L-lyxopyranosyl]thymine (**7.4**). Dit nucleoside vertoonde inderdaad de voorspelde equatoriale orientatie van de thymine ring ($^4C_1$). Affiniteitsresultaten van deze verbinding voor TMPKmt waren echter teleurstellend.

We mogen besluiten dat het beschreven onderzoek leidde tot de ontdekking van een aantal hoge affiniteitsinhibitoren voor TMPKmt, wat interessante perspectieven opent voor de zoektocht naar nieuwe anti-tuberculose geneesmiddelen. Op basis van hun hoge selectiviteitindices zullen vooral het dinucleoside **6.12** en de bicyclische nucleosiden **6.10** en **6.11** gebruikt worden als uitgangspunt in de zoektocht naar inhibitoren die nog beter passen in het actief centrum van TMPKmt.

LIST OF ABBREVIATIONS

ACP	Acyl Carrier Protein
AIDS	Acquired Immuno-Deficiency Syndrome
APC	Antigen Presenting Cell
ATP	Adenosine Triphosphate
BCG	Bovine Calmette Guérin
DNA	Deoxy ribo Nucleic Acid
DOTS	Directly Observed Treatment Short-course
FAD	Flavin Adenine Dinucleotide
FDA	Food and Drug Administration
HEPA	High Efficiency Particulate Air
HIV	Human Immuno-deficiency Virus
IFN	Interferon
Il	Interleukine
LDH	Lactate Dehydrogenase
MDR	Multi Drug Resistant
MHC	Major Histocompatibility Complex
MIC	Minimum Inhibitory Concentration
mRNA	messenger RNA
M. tuberculosis	*Mycobacterium tuberculosis*
NAD^+	Nicotinamide Adenine Dinucleotide (oxidised form)
NDP	Nucleoside Diphosphate
NDPK	Nucleoside Diphosphate Kinase
NMP	Nucleoside Monophosphate
NMPK	Nucleoside Monophosphate Kinase
NK cell	Natural Killer cell
PEP	Phosphoenol Pyruvate
PK	Pyruvate Kinase
RNA	Ribo Nucleic Acid
TB	Tuberculosis
TMPK	Thymidine Monophosphate Kinase
TMPKec	Thymidine Monophosphate Kinase of *E. coli*
TMPKh	Human Thymidine Monophosphate Kinase
TMPKmt	Thymidine Monophosphate Kinase of *M. tuberculosis*
TMPKy	Yeast Thymidine Monophosphate Kinase
TNF	Tumor Necrosis Factor
WHO	World Health Organisation

Chapter 1

STATE-OF-THE-ART AND RESEARCH OBJECTIVES

1 *Introduction* *5*

2 *Tuberculosis* *7*
2.1 Pathology 7
2.2 Immunology 9
2.3 Diagnosis 12
2.4 Resistance 13
2.5 Control and treatment 14

3 *Current research in preventing and curing TB* *21*
3.1 Vaccination 21
3.2 Drugs 23

4 *Thymidine monophosphate kinase* *29*
4.1 *Mycobacterium Tuberculosis* TMPK: an attractive target 29
4.2 Structure of TMPKmt 30
4.3 Human TMPK 37
4.4 Herpes TK (TKhsv) 41

5 *Initial Structure Activity Relationship* *43*
5.1 Base-modifications 43
5.2 Sugar modifications 44
5.3 Six-membered sugar rings 44

6 *Modeling and rational drug design* *45*

7 *Objectives* *47*
7.1 5-Modifiactions 47
7.2 2'-Modifications 47
7.3 3'-Modifications 48
7.4 5'-Modifications 48
7.5 Six-membered ring nucleosides 49
7.6 Biological evaluation 49
7.7 Further optimisation of the 3'-*C*-branched-chain nucleosides 50
7.8 General objective 50

8 *References* *51*

1 Introduction

Tuberculosis (TB), an infectious disease that usually attacks the lungs, is frighteningly on the rise. Once nearly vanquished by antibiotics, at least in the developed world, TB resurged in the late 1980's and now kills more than 2 million people a year – second only to AIDS among infectious diseases. Thirty million people are at risk of dying from TB in the next 10 years, most of them living in Africa (Figure 1).[1]

Mycobacterium tuberculosis, the causative agent of this disease is a slow-growing bacillus, primarily transmitted via the respiratory route, mostly causing pulmonary TB. Estimates are that one third of the world's population is infected with this organism, but infection usually does not lead to the active disease. Reactivation of this latent infection can be caused by immuno-deficiency, HIV-infection, use of corticosteroids, aging, alcohol and drug abuse.

In HIV infected patients, TB has become the main cause of death. At the moment one out of three HIV infected patients is co-infected with TB and 40% of them develops the active disease, rendering the HIV-problem countries (most of them lying in Africa) also the regions with the highest TB incidence in the world. Although it is a leading cause of HIV-related morbidity and mortality, only little attention is paid to TB in HIV/AIDS programs so far.[2]

Next to HIV-infection, demographic factors, socio-economic trends and the neglected TB control in many countries caused this vast epidemic. Efforts to stop the frightening trend are hampered by the lack of financial means in developing countries, the appearance of multi-drug resistant strains of *M. tuberculosis* and bad therapy compliance.

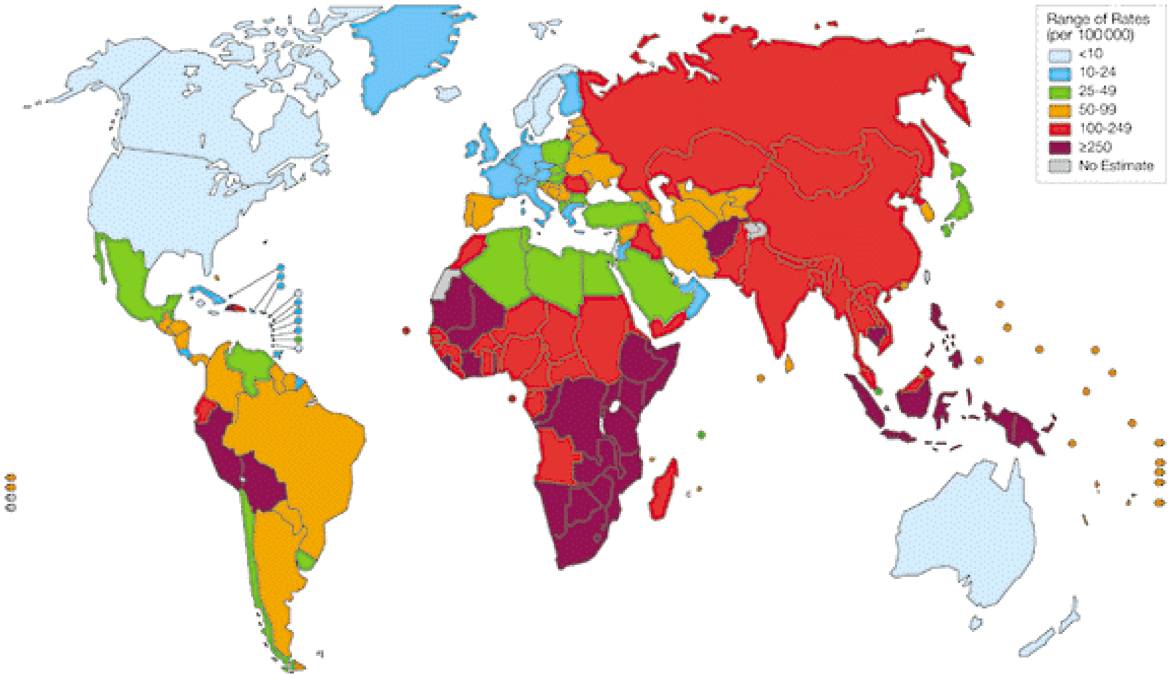

Figure 1: TB incidence per 100.000 inhabitants

The current strategy in the battle against TB is DOTS (Directly Observed Treatment Short-course). In DOTS, TB patients are subjected to standardised treatment regimens (generally consisting of combinations of the most powerful anti-TB drugs) that, with direct observation of drug intake, last 6-8 months. Such standardised treatment regimens reduce the duration of illness, the risk of death and the appearance of resistant strains. In this way, one can indeed prevent the development of resistance. However, for the unfortunate that are or will be infected with the multi-drug-resistant bacteria or develop resistance after a previous drug treatment (50-80% of previously treated cases), there's a large need for more effective drugs acting on novel targets. This has made the search for new targets and the development of new antibiotic drugs a global emergency.[3] However, in spite of its abundance and the considerable economic loss it causes, TB is one of the so-called neglected diseases. As the disease is generally spread in developing countries, the profitability of new anti-TB drug research is questionable, explaining the reluctant attitude of the pharmaceutical industry in this area.

The complete genome sequence of the best characterised strain of *M. tuberculosis*, H37Rv, has been recently determined and analysed.[4] The determination of its genome sequence was a great aid to the cloning and overexpression of mycobacterial proteins, necessary for their structure elucidation via crystallisation and X-ray analysis. In 2001 the structure of *M. tuberculosis* thymidine monophosphate kinase (TMPK) was elucidated by Li de la Sierra et al.[5] The high resolution structure of TMPKmt and the difference in structure with the human TMPK are a good starting point to devising novel inhibitory compounds using a structure-based drug design approach. It may be worth mentioning here that one of the most successful antiviral drugs against *herpes simplex* virus (aciclovir) targets thymidine kinase, a related enzyme, which is responsible for the synthesis of both dTMP and dTDP in cells infected by the virus.[6,7]

In this work the structure-based drug design of inhibitors for *M. tuberculosis* TMPK as potential leads for new anti-mycobacterial drugs will be described.

2 Tuberculosis

The genus of *M. tuberculosis* consists of aerobic rod-shaped organisms. Humans are the host organisms for *M. tuberculosis*, cows for *M. bovis*. On their surface, mycobacteria have unique lipid components called mycolic acids (see Figure 2). It is a group of complex branched-chain hydroxy lipids that are bound to the peptidoglycan layer on their cell wall via phosphodiester bonds. The mycobacteria use this layer for adhesion. Its hydrophobic character renders the cells highly impermeable, making these resistant against dryness and disinfectants. Its impermeability for nutrients causes the slow growth of these organisms (the generation time of *M. tuberculosis* in synthetic medium or infected animals is 24 hours). This contributes to the chronic nature of the disease, imposes lengthy treatment regimens and represents a formidable obstacle for researchers.

2.1 PATHOLOGY

The interaction of the human host and *M. tuberculosis* is extremely complex. Partly, it is determined by the virulence of the strain but probably more importantly by the specific and non-specific resistance of the host. Cell-mediated immunity plays an important role in the development of disease symptoms. It is convenient to distinguish between two kinds of human tuberculosis infections: *primary* and *postprimary* (or reinfection).

The primary infection is the first infection that an individual acquires and usually results from droplets containing viable bacteria from an individual with an active pulmonary infection.

The bacteria that reach the lungs are ingested by macrophages but often survive because the fusion between the phagosome and the lysosome is hindered. The bacteria multiplying in macrophages cause a chemotactic response that brings additional macrophages into the area, forming aggregates of macrophages, called tubercles in which *M. tuberculosis* continues to multiply intracellularly. After a few weeks many of the macrophages die, releasing TB bacteria and forming a liquid centre in the tubercle, which is surrounded by a mass of macrophages and lymphocytes. The disease may become dormant after this stage.

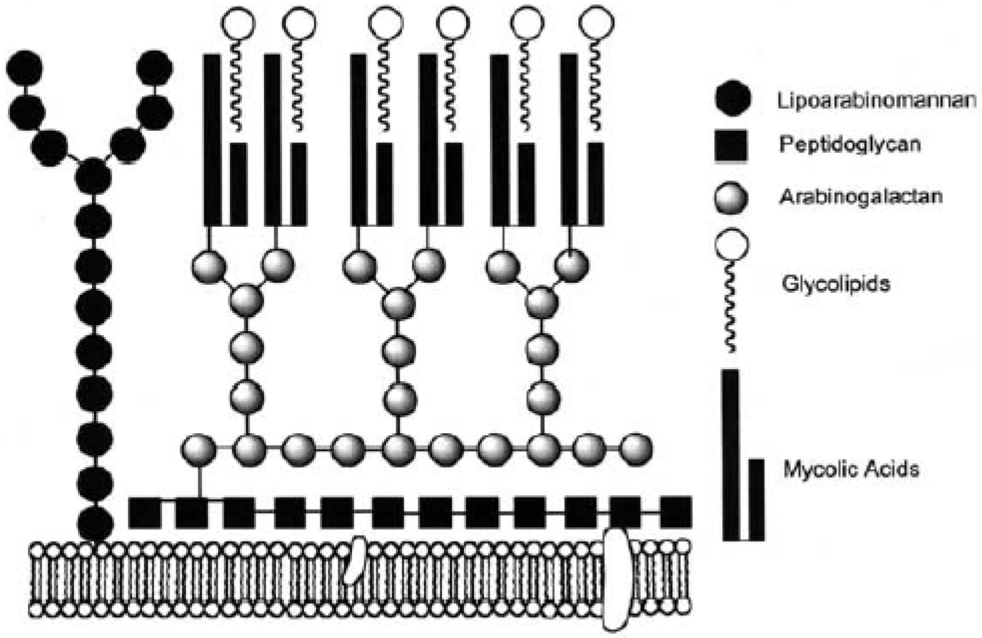

Figure 2. Schematic drawing of the mycobacterial cell wall. [8]

In a few individuals with low resistance, the bacteria are not effectively controlled. The centre of the tubercle enlarges in the process of liquefaction, forming an air-filled tuberculous cavity in which the bacilli multiply extracellularly. Liquefaction continues until the tubercle ruptures, allowing bacilli to spill into a bronchiole and thus be disseminated throughout the respiratory system to other systems. This causes an acute pulmonary infection which can lead to an extensive destruction of lung tissue, the spread of bacteria to other parts of the body and death.

However, in most cases of tuberculosis, acute infection does not occur and the infection remains localised and is usually inapparent.

The postprimary infection occurs when immunity wanes (e.g. HIV-infection, use of corticosteroids, alcoholism, lung emphysema, diabetes, malnutrition, stress, …). The mycobacteria can multiply again in macrophages, the tubercle wall breaks down and the infection spreads to different tissues. This causes symptoms like weight loss, night sweats, feverishness and a cough that produces greenish sputum flecked with blood.

2.2 IMMUNOLOGY

The immunological response to *M. tuberculosis* is complex and multi-faceted (Figure 3). *M. tuberculosis* succeeds in evading several toxic effects of this immune response, so that the immune system is generally successful in sequestering, although not eliminating the pathogen. *M. tuberculosis* then persists within a tubercle, composed of macrophages, T-cells and B cells. In most cases of *M. tuberculosis* infection, the individual is asymptomatic and non-infectious. This clinical latency often extends for the lifetime of the individual. Breakdown of the immune response, can result in reactivation and replication of the bacilli, with necrosis and damage to the lung tissue.

2.2.1 Macrophages

Interferon-gamma (IFN-γ) was found to be the key endogenous activating agent that triggers the anti-mycobacterial effects of murine macrophages. Tumor necrosis factor-alpha (TNF-α) although ineffective alone, synergises with INF-γ to induce the anti-mycobacterial effects of the macrophages.

The macrophages contain complex vacuolar organelles, lysosomes, that contain potent hydrolytic enzymes capable of degrading a whole range of macromolecules including those of micro-organisms. These enzymes function optimally at acidic pH, a condition found in the intralysosomal environment. They also produce reactive oxygen intermediates such as hydrogen peroxide and reactive nitrogen intermediates like nitric oxide, produced by inducible nitric oxide synthase. The phagosomes can fuse with lysosomes and the phagocytosed micro-organisms are subjected to degradation by intralysosomal acidic hydrolases and the reactive oxygen- and nitrogen- intermediates. Prevention of this phagolysosomal fusion is a mechanism by which *M. tuberculosis* survives within macrophages. Several theories to explain this escape mechanism have been proposed. Probably several of those mechanisms contribute to the prevention of the phagolysosmal fusion.[9]

- It has been reported that mycobacterial sulfatides, derivatives of multi acetylated trehalose 2-sulfate, a polyanionic glycolipid, would have the ability of inhibiting phagolysosomal fusion.

- Also, the large amounts of ammonia (regulated by mycobacterial urease and glutamine synthetase) that *M. tuberculosis* generates could be responsible for this, but the precise mechanism by which ammonia prevents phagolysosome fusion remains to be determined.

- Exclusion of ATPase proton pumps from phagosomes containing living *M. tuberculosis* provides another mechanism for the lack of acidification of mycobacterial phagosomes.

- A TACO (tryptophan aspartate containing coat) protein is present in lymphoid and myeloid cells and is associated with the cortical microtubule network in non infected macrophages. Two hours after infection it gets relocalised to the mycobacterium containing phagosomal membrane and it remains associated for a prolonged period of time, which inhibits the phagolysosomal fusion.

On top of the evasion of the phagolysosomal fusion, mycobacteria are also capable of partly evading the toxic effects of the reactive oxygen intermediates with oxygen radical scavengers like phenoglycolipid I and lipoarabinomannan.[9]

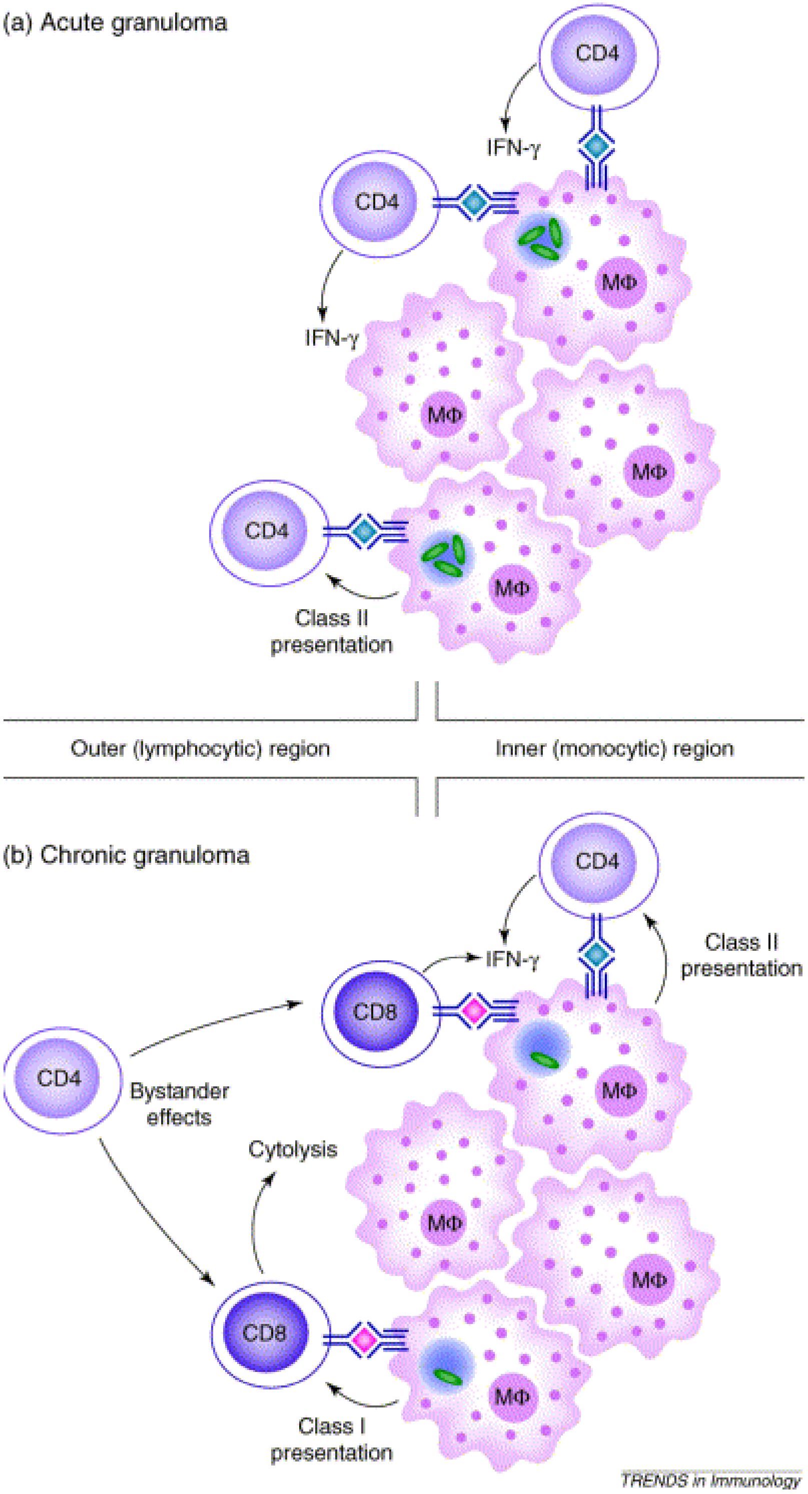
(a) Acute granuloma
CD4
IFN-γ
CD4
MΦ
IFN-γ
MΦ
MΦ
CD4
MΦ
Class II presentation
Outer (lymphocytic) region
Inner (monocytic) region
(b) Chronic granuloma
CD4
IFN-γ
Class II presentation
CD8
CD4
Bystander effects
MΦ
Cytolysis
MΦ
MΦ
CD8
MΦ
Class I presentation
TRENDS in Immunology

Figure 3: Cellular interactions in acute and latent TB infection. (a) The acute stage of infection is characterised by multiplying bacteria inside the phagosomes, which secrete or release proteins to the surroundings. These proteins are processed by the endosomal pathway and presented mainly by MHC class II molecules to CD4$^+$ T-cells. The CD4$^+$ T-cells secrete cytokines (e.g. IFN-g), which activate the macrophage and lead to killing of the intracellular mycobacteria through the production of reactive oxygen metabolites and phagosomal acidification. (b) During the chronic or latent stages of infection, low numbers of dormant or slowly replicating bacteria release antigens that enter both the MHC class I and the MHC class II pathway. CD8$^+$ cells play an important role in the control of infection mediated by their cytokine production and cytolytic activity. In this phase of infection the CD4$^+$ cells might serve more as bystanders promoting CD8 activity.[10]

2.2.2 Cytokines

The immune response to all pathogens is at least in part dependent on cytokines, which regulate all the cells of the immune system. *M. tuberculosis* is no exception and strongly induces cytokines during infection. This response is crucial for the control of the infection but may also contribute to the chronic infection and associated pathology.

- Immunologic control of *M. tuberculosis* infection is based on a type I T-cell response. Phagocytosis *of M. tuberculosis* bacilli by macrophages induces interleukine 12 (Il-12) production, which in its turn activates the production of IFN-γ by NK cells, CD4 and CD8 T-cells. IFN-γ is a key cytokine in the control of *M. tuberculosis* infection. Although its production alone is insufficient to control the infection, it is required for the protective response against the pathogen. *M. tuberculosis*, however, is able to prevent macrophages from responding adequately to IFN-γ.

- TNF-α plays multiple roles in immune and pathologic responses in tuberculosis. *M. tuberculosis* induces TNF-α secretion by macrophages and T-cells. This cytokine is required for control of acute *M. tuberculosis* infection. In synergy with IFN-γ, it induces nitric oxide synthase expression. It affects cell migration to tissues infected with *M. tuberculosis*. TNF-α also influences expression of adhesion molecules as well as chemokines and chemokine receptors and this is certain to affect formation of tubercles in infected tissues. It is major factor in host-mediated destruction of lung tissues.

- In contrast to TNF-α, Il-10 is generally considered to be primarily anti-inflammatory. This cytokine, produced by macrophages and T-cells, possesses macrophage deactivating properties, including down-regulation of Il-12 production, which, in its turn decreases IFN-γ production by T-cells. It directly inhibits $CD4^+$ T-cell responses as well as the antigen presenting cell (APC) function of cells infected with mycobacteria.

- Il-6 also plays multiple roles in the inflammation process, hematopoiesis and the differentiation of T-cells. It can be responsible for suppression of T-cell responses just as the transforming growth factor-β (TGF-β) does. The latter also participates in macrophage deactivation by inhibiting IFN-γ induced nitric oxide synthase production.[9]

2.2.3 T-cells

M. tuberculosis is a pathogen for which the protective response relies on cell mediated immunity. This is primarily because the organism lives within cells, usually macrophages. Thus T-cell effector mechanisms, rather than antibodies, are required to control or eliminate the bacteria. Activated T-cells migrate to the site of infection and are interacting with APC's. The tubercles contain both CD4 and CD8 T-cells that likely participate in the continuous battle to sequester the infection and prevent reactivation.

- *M. tuberculosis* primarily resides in a vacuole within the macrophage and as reported above MHC class II presentation triggers the action of the $CD4^+$ T-cells. $CD4^+$ T-cells from infected subjects produce IFN-γ in response to a wide variety of mycobacterial antigens to activate macrophages, which can then control or eliminate intracellular organisms. These macrophages can lyse infected cells. In humans, this happens via secretion of perforin and granulysin. Perforin is required to form a pore but granulysin, a cytotoxic granule protein is responsible for killing of the intracellular organism. These

CD4$^+$ T-cells also play a role in maturing APC's. *M. tuberculosis* infected macrophages are diminished in their ability to present antigens to the CD4$^+$ T-cells, which could contribute to the inability of the host to eliminate persistent infection. *M. tuberculosis* does this by down-regulation of cell surface expression of MHC class II molecules, which results in fewer antigen presentation.

- During the dormant stage of the infection, CD8$^+$ cells play an important role in sequestering the infection. They migrate to the lungs with kinetics similar to CD4$^+$ T-cells following *M. tuberculosis* infection. They lyse infected macrophages and produce IFN-γ that, in its turn activates macrophages.[9]

2.3 DIAGNOSIS

Because *M. tuberculosis* is a slow growing organism, diagnosis is difficult. A sputum smear microscopic analysis, typical symptoms, responsiveness to certain antibiotics and X-ray examinations can give an initial idea of *M. tuberculosis* infection. However, it takes weeks to grow it out of sputum, for unambiguous confirmation of *M. tuberculosis* infection.

2.3.1 Tuberculin skin test

This test measures the hypersensitivity of an individual against the bacteria or their products, caused by the primary infection. When tuberculin, a protein factor extracted from *M. tuberculosis*, is injected intradermally into a hypersensitive individual, it elicits a localised immune reaction (induration and swelling) within 1-3 days at the site of the injection. This test doesn't indicate the active disease but only that the individual has been exposed to the organism at some time. Vaccination with the BCG vaccine can also result in a positive tuberculin skin test.[11]

2.3.2 Sputum smear microscopy

M. tuberculosis gets visualised with a Zeehl-Neelsen stain. However, there is a 25% chance for a false negative result; 25% of the smear negative patients appear to be culture positive.

2.3.3 Culture

Viable bacteria are found in the sputum of individuals with extensive lung tissue destruction. The organism can be selectively isolated from sputum and other materials that are grossly contaminated. Because of the high lipid content of its cell walls, *M. tuberculosis* is able to resist alkali for a considerable amount of time. Therefore the sputum is first treated with 1N NaOH for 30 minutes. Subsequently, it is neutralised and streaked onto an isolation medium. Due to the slow growth of *M. tuberculosis,* visible colonies can only be observed after days to weeks of incubation.

2.3.4 Symptoms

Tuberculosis infection causes symptoms like cough, feverishness, weight loss and sputum production.

2.3.5 Responsiveness to antibiotics

Smear negative patients can be treated with amoxicillin and/or erythromycin. Patients who do not respond to either of these antibiotics have a 50-75% (depending on the chosen antibiotic(s)) chance of having TB anyway.

2.3.6 X-ray

Primary and reactivated tuberculosis have distinct radiographic patterns. When renewed pulmonary infection occurs, it is usually a chronic infection that involves destruction of lung tissue, followed by partial healing and slow spread of the lesions within the lungs. Those spots of damaged tissue may be revealed by X-ray examination. However, intercurrent pneumonia, pulmonary embolism or supervening carcinoma may be confounding factors.[3]

2.4 RESISTANCE

Unlike many drug resistant bacteria, TB does not acquire drug resistance through exchange of plasmids. Instead, normal error rates of DNA replication in *M. tuberculosis* ensure that spontaneous mutations arise that cause resistance in the absence of antibiotic exposure. Spontaneous mutation to isoniazid resistance, for example, occurs in about 1 in 10^6 bacteria; resistance rates for streptomycin and ethambutol are similar. About 1 in 10^8 bacteria is rifampicin-resistant. If the bacterial load is large enough, treating a patient with a single drug will lead to the suppression of susceptible bacteria and the selection for growth of a drug-resistant strain. Avoidance of selection for resistance is, in part, the reason for treating TB with multiple drugs. The probability of resistance arising when rifampicin and isoniazid are used in combination is only 1 in 10^{14}, sufficiently low to prevent resistance for either drug.[12]

2.4.1 Drug resistant tuberculosis

In drug resistant TB, the bacteria are resistant to one or more anti-tuberculosis drugs.

- In patients with some record of previous treatment, the bacterial resistance is called *acquired resistance*. Interruption of the therapy by the patient, prescription of inadequate chemotherapy, poor drug supply (especially in developing countries) may cause resurgence of the infection. The resurgent organisms are often resistant to the original treatment drug.

- In patients without prior treatment with anti-tuberculosis drugs, the bacterial resistance is called *primary resistance*. The occurrence of primary resistance is a consequence of the level of acquired resistance in the community. The rate of primary resistance is lower than the incidence of acquired one. It is also less severe than the acquired one. This resistance is more often to one drug (streptomycin or isoniazid) than to two drugs. Resistance to three drugs is exceptional. The level of resistance (measured by the minimum inhibitory concentration of antibiotics) is lower in primary than in acquired resistance.

2.4.2 Multi-drug resistant (MDR) tuberculosis

In MDR tuberculosis, bacteria are resistant to several anti-tuberculosis drugs and at least to isoniazid and rifampicin. It is a consequence of inappropriate use of essential anti-tuberculosis drugs. It is usually found in patients after failed treatment regimens and represents a significant proportion of tuberculosis patients with acquired resistance. Only exceptionally it is observed in new cases. Top priority is not the management, but the prevention of MDR tuberculosis.

2.4.3 Cross-resistance

Patients showing resistance to one drug often also show resistance against other drugs from that family or even drugs from other families. This should be taken into account when choosing a drug regimen for a patient with multi-drug resistant TB.

2.5 CONTROL AND TREATMENT

2.5.1 Prevention

Since tuberculosis is highly contagious, patients with infectious tuberculosis must be hospitalised in negative pressure rooms. People that have contact with the patients, have to wear face masks with HEPA filters (high energy particulate air).

The efficiency of the bacille Calmette Guérin (BCG) vaccine, containing an enfeebled live stem of *M. bovis*, is subject of controversy nowadays (see further).

2.5.2 Chemotherapy

The anti-tuberculosis drugs are divided into two categories: the *essential drugs*, used in patients without drug resistance or drug resistance against some drugs (as long as it isn't against isoniazid and rifampicin) and the *second line drugs* that are used in case of multi-drug resistant TB in combination with first-line drugs. These second line drugs are less effective, have more side effects and are more expensive than the present standard essential drugs.

- Essential drugs (Figure 4)

  → Streptomycin: was the first drug used against tuberculosis. It inhibits the translation of mRNA via interaction with the 30S ribosomal subunit. Mutations on the genes coding for the ribosomal protein S12, confer streptomycin resistance. Resistance to streptomycin has become less common since the wider use of ethambutol as fourth drug in the WHO standard regimen.[13]

  → Isoniazid: the discovery of isoniazid (isonicotinic acid hydrazide) caused a revolution in tuberculosis treatment. This agent is not only effective and free from toxicity, but also inexpensive and readily absorbed when orally given. Isoniazid affects the synthesis of mycolic acid by *M. tuberculosis*. It gets processed by mycobacterial catalase-peroxidase (katG), which transforms the drug into a nucleophilic radical. Reaction of this radical, with the cofactor NAD^+, yields a potent inhibitor of enoyl-

ACP (acyl carrying protein) reductase. This enzyme is necessary for the mycolic acid synthesis of the bacterial cell wall. The major class of mutations in isoniazid-resistant *M. tuberculosis* map to a gene which encodes the catalase-peroxidase.[14]

→ Rifampicin is an antibiotic drug that, by interacting with RNA-polymerase, blocks RNA-transcription. It binds a pocket of RNA polymerase within the DNA/RNA channel, but more than 12 Å away from the active site. It acts by directly blocking the path of the elongating RNA when the transcript becomes 2 to 3 nucleotides in length. Because it diffuses freely into tissues, living cells, and bacteria, it is extremely effective against intracellular pathogens like *M. tuberculosis*. However, bacteria develop resistance to rifampicin with high frequency. Mutations conferring rifampicin resistance map almost exclusively to the *rpoB* gene that encodes the RNA polymerase β subunit.[15]

→ Pyrazinamide: This drug has a special place in modern tuberculosis therapy, as it appears to kill semi dormant tubercle bacilli that are not affected by other anti-tuberculosis drugs. It has a bactericidal effect in an acid medium (bacilli inside macrophages). So, in order to obtain a maximal bactericidal effect, it is best combined with streptomycin or another aminoglycoside, effective against bacilli outside macrophages. Pyrazinamide blocks fatty acid synthesis through inhibition of the eukaryotic-like fatty acid synthetase I.[16] Intracellularly, it is converted to pyrazinoic acid by an amidase. Resistance to pyrazinamide is neither easily acquired nor proved by susceptibility testing. It is correlated with the amidase activity of the *M. tuberculosis* isolate in question: most pyrazinamide resistant isolates of *M. tuberculosis* have decreased or no amidase activity and are presumably unable to convert pyrazinamide into the active agent. However, this drug is toxic to retinal ganglion cells and ocular toxicity has also been reported.[17]

→ Ethambutol: The critical target for ethambutol lies in the pathway for the biosynthesis of cell wall arabinogalactane (see Figure 2); it inhibits arabinosyl transferase, responsible for the polymerisation of arabinose into the arabinan of arabinogalactane. Disruption of the biosynthesis of arabinogalactane would destroy the macromolecular assembly of the mycolyl-arabinogalactan-peptidoglycan complex of the cell wall, permitting drugs with intracellular targets (such as rifampicin) to enter the cell more easily. Ethambutol resistant *M. tuberculosis* strains carry mutations in one certain part of the gene encoding for arabinosyl transferase. In the case of MDR-TB, if there is still a reliable susceptibility, ethambutol might be valuable as a companion drug for preventing the emergence of resistance to other active drugs.[13,18]

→ Thioacetazone is a bacteriostatic agent, showing partial cross resistance with ethionamide.[19] Its mode of action has not been elucidated,[20] although it has been shown that thioacetazone forms copper complex salts that have been postulated to represent the effective compound.[21] The most frequently seen adverse effects include gastrointestinal burden and central nervous system disorders.[22]

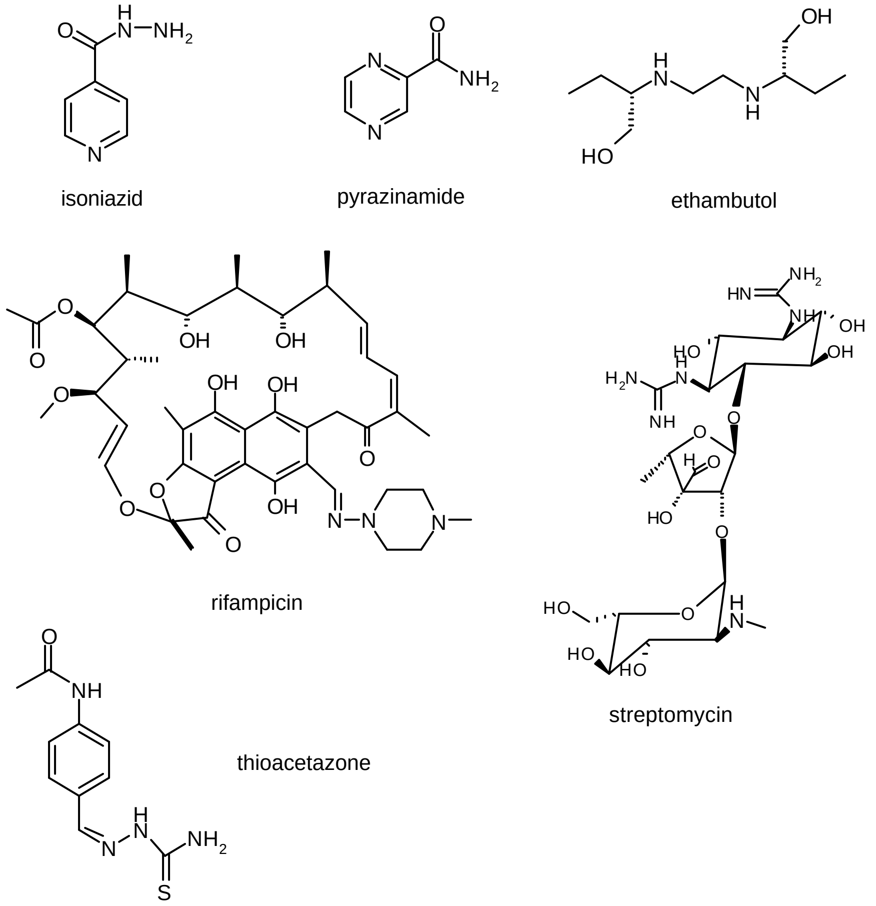

Figure 4: First-line anti-tuberculosis drugs

- *Second line drugs (Figure 5)*

  → Aminoglycosides (e.g., *kanamycin*, *amikacin* and *capreomycin)* can be used in case of resistance to streptomycin. These analogues also inhibit the translation of mRNA via interaction with the 30S ribosomal subunit. The main adverse effects are ototoxicity and reversible nephrotoxicity. Kanamycin-resistance is caused by mutations on the gene coding for the 16S ribosomal RNA.[13]

  → Thioamides (e.g., *ethionamide* and *prothionamide).* Thioamides show cross-resistance with thioacetazone. Their adverse effects include nausea, psychotic reactions, hypoglycaemia and hepatitis. Ethionamide gets activated by an FAD-containing enzyme which turns it in two steps into 2-ethyl-4-aminopyridine.[23] Like isoniazid it blocks the mycobacterial mycolic acid synthesis, but it binds enoyl-ACP reductase at a different part of the active site.[14]

  → Fluoroquinolones (e.g.,[2] *ofloxacin* and *ciprofloxacin)* have low bactericidal activity and are useful in association with other drugs. They inhibit DNA gyrase, responsible for supercoiling the bacterial DNA. Side effects are rare and consist of gastrointestinal disturbance, dizziness, headache and mood changes. Missense mutations in the DNA gyrase gene have been reported to be associated with increased levels of resistance to fluoroquinolones.[13]

→ Cycloserine blocks the mycobacterial peptidoglycan synthesis by inhibition of D-alanine racemase that catalyses the conversion of L-alanine into D-alanine. It has no cross-resistance with the other anti-tuberculosis drugs, so it might be valuable to prevent resistance to other active drugs but its high toxicity limits the use of cycloserine. Side effects are dizziness, convulsions, headache and depression.[24]

→ *Para*-aminosalicylic acid is a bacteriostatic agent, valuable for preventing resistance to other bactericidal drugs: it may prevent resistance to streptomycin and leads to a substantial enhancement of monotherapy with isoniazid. It has dose-related side effects such as vomiting, diarrhea, hepatotoxicity, fever, hypocalcaemia and rash.[25]

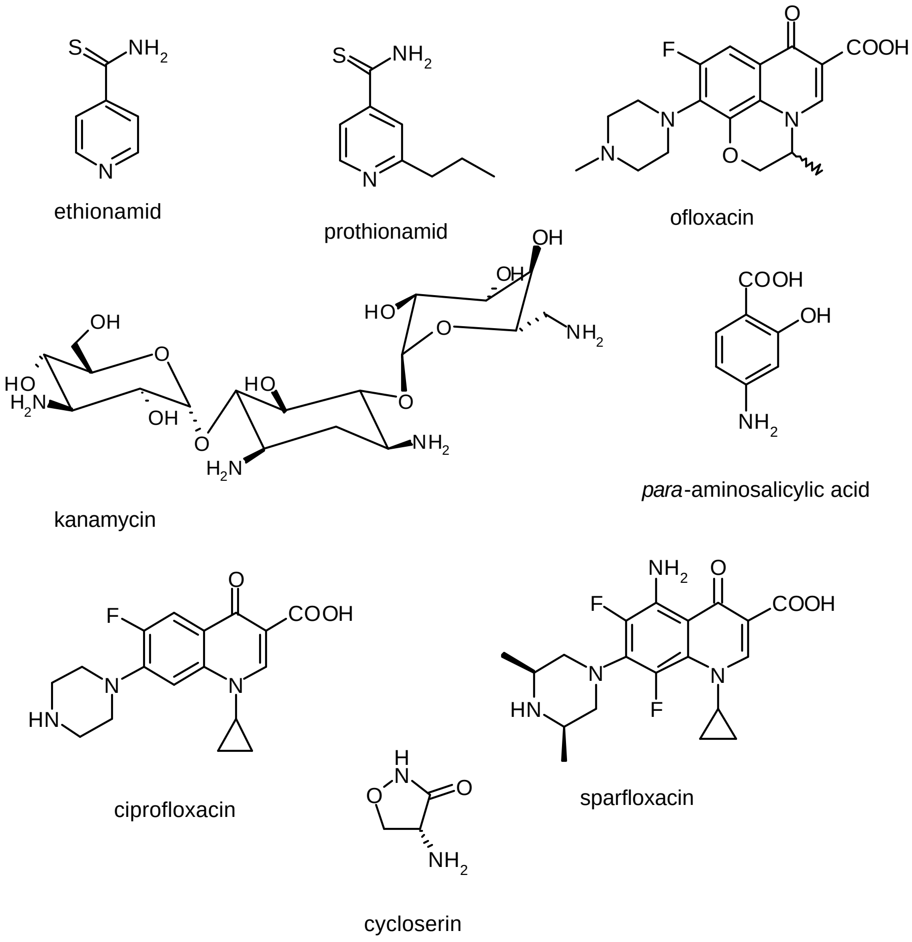

Figure 5: Second-line anti-tuberculosis drugs

Depending on whether it is the first drug treatment of the patient, whether a treatment regimen failed before and depending on the presence of drug-resistant TB, a different treatment regimen is chosen.

- *WHO standard first-line regimen*: This regimen, consisting of a combination of four drugs (isoniazid, rifampicin, pyrazinamide and ethambutol or streptomycin), is given during 6 to 8 months. This overcomes the risk of failure due to acquired resistance. Because primary resistance is less severe than acquired resistance, it hardly affects the outcome of this regimen.

- *WHO standard retreatment regimen*: This regimen is administered to patients, returning after premature interruption of the first-line treatment and/or after relapse. It combines four drugs during 8 months to reduce the risk of failure due to acquired resistance. It consists of three drugs throughout the whole period (isoniazid, rifampicin, ethambutol), supplemented by pyrazinamide during the first three months and streptomycin during the first two months. Any bacteria remaining after 5 months are usually resistant to one or two of the main bactericidal drugs (isoniazid and/or rifampicin). The vast majority of the patients will be cured with this retreatment regimen, failures are generally due to the use of an incorrect regimen and/or failure to ensure that the regimen is fully administered and directly observed.

- *Treatment regimen for chronic cases*: This regimen is administered to patients for whom the WHO retreatment regimen failed. They usually received at least two courses of chemotherapy, they are most of the time excreters of resistant bacilli and often of MDR bacilli. Treatment of patients with MDR tuberculosis involves ‘second line’ spare drugs. These are more expensive, less effective and have more side effects compared to the standard drugs. They should only be distributed by a specialised unit, equipped with a laboratory that is able to test for drug resistance in order to prevent incurable tuberculosis. The treatment consists of a mix of essential drugs and second-line drugs. The initial regimen should consist of 4 or 5 drugs to which the bacteria are likely to be fully sensitive, i.e. drugs not previously used for that patient. For this, it is crucial to take cross-resistance also into account. When the patient’s sputum has converted to negative, one or more drugs are withdrawn, preferably weaker drugs which are causing side effects. In order to prevent relapse, the treatment with this slimmed regimen is continued for at least 18 months after sputum conversion.

2.5.3 DOTS

The current strategy in the battle against TB is DOTS. DOTS combines five elements: political commitment, microscopy services, drug supplies, monitoring systems and direct observation of treatment. For the first, typically six, months of the disease (i.e. when the bacterial load is the highest), combinations of several drugs are administered to the patients, according to fixed patterns as presented by the WHO standard first-line regimen. This therapy, when closely monitored, considerably decreases the duration of illness, risk of death and the appearance of resistant strains. In all DOTS compliant countries the cure rates of smear-positive tuberculosis are already over 80%. When implemented over a long period, there will be a huge reduction in sources of infection and transmission.[3]

2.5.4 Surgery

For patients with bacilli resistant to all except 2 or 3 relatively weak drugs, surgery is considered. However, for many of these patients the infection has evolved too extensively and/or lung function has degraded too much for surgery to be possible. If the patient has a large localised lesion with little other disease, reasonable lung function and only 2 or 3 weak drugs available, surgery can be considered. To avoid serious and potentially fatal TB complications, the operation is performed when the bacterial load is the lowest, i.e. after 2 months of treatment. After surgery, the same drug regimen is continued for at least 18 months.

2.5.5 Vaccination

The current TB vaccine, *M. bovis* bacille Calmette-Guérin (BCG), was developed almost a century ago. Although several clinical studies showed this vaccine to be inefficient, it is still in widespread use. It was developed by attenuation of *M. bovis*, which is closely related to *M. tuberculosis* (>90% DNA homology). However, recent data indicate that a large number of mutations have taken place during the long *in vitro* propagation of this strain. It is known that these mutations have resulted in the deletion of many open reading frames, encoding several important T-cell antigens, thereby reducing the efficiency of the vaccine.

In experiments where animals were sensitised with environmental mycobacteria - which share many antigens with BCG- the multiplication of the attenuated BCG vaccine was inhibited. As such the protection provided by environmental mycobacteria partly masks the effect of BCG vaccination. These aspects could explain the failure of multiple BCG vaccinations and need to be taken into consideration when discussing the potential of substituting BCG with new attenuated mycobacterial vaccines, also sharing numerous antigens with environmental strains.[26]

3 Current research in preventing and curing TB

3.1 VACCINATION

Most current vaccines against bacterial and viral pathogens depend on long-lived humoral responses that can be induced by many different vaccine formulations. However, TB vaccines require the induction of a sustained cell-mediated immune response and for this purpose, the best choice of antigens and adjuvants is still an open question.

An ideal vaccine has following requirements: it has to be safe, stable and inexpensive; it has to provide worldwide protection against disease and infection, protect after single administration and induce long-lasting immunological memory; it needs to be compatible with childhood vaccines and should not compromise the tuberculin skin test.

So far none of the vaccine technologies tested, lives up to all of these ideal characteristics.[26]

3.1.1 Living mycobacterial vaccines

Living vaccines have the theoretical advantage that many antigens can act together to induce maximum protection. They would also be expected to survive in the tissues for prolonged periods of time, thereby ensuring that efficient immunological memory is induced and maintained. As development of molecular tools for manipulation of mycobacteria progresses, the number of reports on successful attenuation of mycobacterial strains increases rapidly. Selectable markers, such as antibiotic resistance genes, transposon mutagenesis and allelic exchange have resulted in the generation of several auxotrophic mutants that have reduced virulence owing to a lack of functional genes for the synthesis of nutritional growth factors.[27,28] Although several of these constructs are protective against subsequent infection with tuberculosis, there seems to be a correlation between virulence and protection, and none of the mutants tested so far has given higher levels of protection than BCG in the animal models.

It has been suggested that BCG could be augmented with some of the many genes lost during the *in vitro* attenuation of this strain. This idea is related to the argument that BCG might have been attenuated to impotence,[29] and one needs to reintroduce or overexpress some of the genes lost or expressed in insufficient quantities. Along this line, efficient protection was recently reported in the guinea pig model of pulmonary TB with a recombinant strain of BCG that overexpresses the AG85 protein (the major antigen of *M. tuberculosis* in cell wall biogenesis).[30] Similarly, attempts have been made to improve the immunogenicity of BCG, either by enhancing its CD8$^+$ T-cell stimulating capacity through the introduction of listeriolysin[31] or by the expression of Th1 cytokines.[32] However, these different approaches are always complicated by the potential risk of increasing the virulence of the vaccine strain.

3.1.2 Subunit and DNA vaccines

Both the subunit and DNA approach are based on the assumption that a few antigens are sufficient to induce and maintain a protective immune response. In addition, both approaches share the advantage of being stable and safe even in immunocompromised individuals. The development of DNA and subunit vaccines has benefited tremendously from the sequencing of the TB genome, and the accelerated identification of novel antigens has resulted in the identification of defined antigens that are protective in animal models. To include antigens that give rise to beneficial responses and exclude potential detrimental components is the ultimate advantage provided by subunit or DNA vaccines. In the development of subunit vaccines, the major focus has been on vaccines based on culture filtrates or secreted proteins from the latter, such as components of the 30-33 kDa AG85 complex, [30] the 38 kDa phosphate-binding protein[33] and the low molecular mass antigen ESAT-6.[34] The most promising vaccines have promoted protection against subsequent TB challenge at levels close to that provided by BCG, and one of the recent developments consists in combining these single protective antigens into subunit vaccines based on di- or tri-fusion molecules.

The demonstration in animal models that DNA vaccines could induce humoral as well as broad cellular responses with both CD4$^+$ and CD8$^+$ T-cells provided hope that they could become the vaccine of choice for infections that require cellular responses. This approach has been applied with success in several small animal models of infectious diseases and its potential is convincingly demonstrated for the development of TB vaccines based on HSP60 and AG85,[35] as well as other antigens recently evaluated. Most recently cocktails of different genes have resulted in levels of protection close to that of BCG[36]. The most promising of these vaccines still need further testing in animal models that mimic the human disease.

3.2 DRUGS

In the search for more potent anti-tuberculosis drugs there are two principal choices: synthesis of improved versions of existing drugs or discovery of new drugs with a novel mechanism of action.

3.2.1 *Improved versions of existing drugs*

Existing drugs are adapted to improve their activity or pharmacokinetic properties, or to circumvent the resistance mechanisms of *M. tuberculosis.*

- An example of the first option is rifapentine (Priftin), the first anti-tuberculosis drug to be approved in 25 years. Although the TB relapse rate for rifapentine is slightly higher (10%) than that of rifampicin (5%), the FDA approved the new medication because it only has to be taken once weekly during the last 4 months of treatment, as opposed to twice weekly for rifampicin. Another derivative of rifampicin, currently in phase II clinical trials, is rifalazil. *In vitro* studies have shown this analogue to be 10 to 100 times as potent as rifampicin, and, more importantly, it has a longer half-life. This longer half-life and increased potency could allow physicians to shorten the treatment period and lower the frequency of doses, reducing the overall cost of therapy. Indeed, the administration of the drugs and compliance surveillance are more expensive than the drugs themselves. [37]

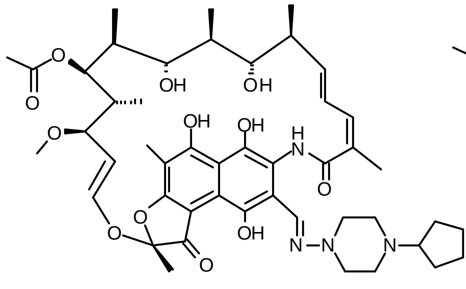
Rifapentine

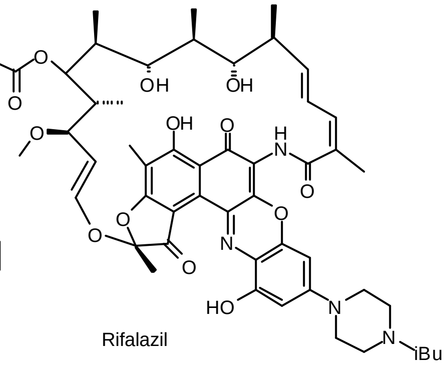
Rifalazil

- Reneau et al.[38-39] performed a study to optimise the quinolone anti-bacterials against *M. tuberculosis* by preparing a series of *N*-1 and *C*-7 substituted quinolones. A series of *N*-1 substituted anti-bacterials showed that increasing the lipophilic character of these compounds by itself does not correlate with increased potency against mycobacteria and none of the tested compounds was more effective against *M. tuberculosis* than the fluoroquinolone-drug sparfloxacin. However, in a series of *N*-1, *C*-7 disubstituted analogues, a cyclopropyl or a *tert*-butyl at the *N*-1 position in combination with a substituted piperazine yielded more potent inhibitors of *M. tuberculosis* than sparfloxacin (see Figure 4).

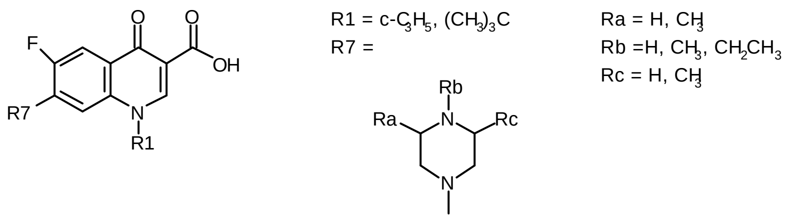

- Most cases of pyrazinamide resistance are due to low levels of pyrazinamidase activity, necessary to convert pyrazinamide into the active agent, pyrazinoic acid. Pyrazinoic acid esters that can be hydrolysed by an esterase, could equally well serve as prodrugs and could circumvent the requirement for activation by an amidase. Modification of both the pyrazine nucleus and the ester function proved to be successful. *n*-Propyl-, 2'-octyl- and *n*-octylesters of 5-chloro pyrazinoic acid showed *in vitro* activities against *M. tuberculosis* 100-1000-fold greater than pyrazinamide.[40] Recently several pyrazinoic acid ester derivatives were designed as potential prodrugs through a self-immolative process. These prodrugs generate an unstable intermediate that, following the activation process, will provide the active drug in a number of steps. The advantage of self-immolation is that it increases the diversity of prodrugs that can be activated by a certain enzyme. 4-Acetoxy-benzyl pyrazionic acid and 4'-acetoxybenzyl-2-quinoxalinecarboxylate showed excellent activities against TB (MIC values of 1-6.25 µg/mL). Enzymatic hydrolysis of the acetate yields a hydroxyl group. The increased electron density in the aromatic system then leads to the extrusion of pyrazinoic acid and a substituted quinone methide.[41]

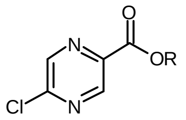

R= 2'-octyl, *n*-propyl, *n*-octyl

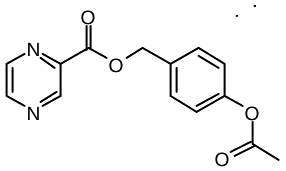

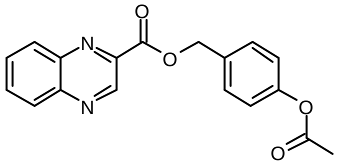

- Inspired by the anti-tubercular drugs isoniazid and pyrazinamide, it was assumed that precursors of isosteres of isonicotinic or pyrazinoic acid could possess anti-mycobacterial activity. Pyrazines and pyridines substituted with N1 and N2 alkylated tetrazoles, 1,2,4-oxadiazole-5-ones, 1,2,4-oxadiazole-5-thiones and 1,3,4-oxathiazoline-2-ones were synthesised. The 1,3,4-oxathiazoline-2-one derivatives were the most potent of the series, showing to be 8 to 16 times as effective as pyrazinamide. Although the compounds were not tested against pyrazinamide resistant strains of *M. tuberculosis*, it is expected that they are effective against the latter. Indeed, most pyrazinamide resistance generally results from lack of pyrazinamidase enzyme in the bacteria and the examined compounds do not contain an amide bond that has to be hydrolysed for activity.[42-43]

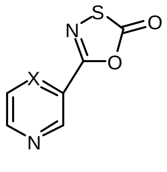

X= CH, N

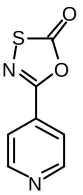

- A series of isonicotinoyl hydrazone derivatives showed interesting anti-mycobacterial activity against rifampicin-, pyrazinamide- and streptomycin resistant strains of *M. tuberculosis*, but lower activities against isoniazid resistant strains. Sub-inhibitory concentrations induced a significant increase in the anti-mycobacterial activities of rifampicin, ethambutol and *para*-aminosalicylic acid.[25,44]

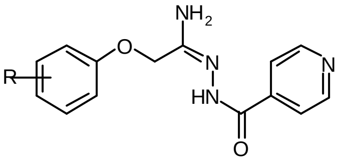

R= 2-CH_3, 3-CH_3, 4-CH_3, 3-Cl, 4-Cl, 4-NO_2

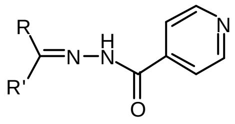

R= H, CH_3
R'= CH_3, 3FPh, 2FPh, CF_3

- Lee et al.[45] tried to find a better inhibitor of arabinosyltransferase than ethambutol. They studied a large group (63238 compounds) of ethylenediamine derivatives via the use of solide phase synthesis and found 26 compounds possessing MIC values lower than ethambutol. They are all characterised by large hydrophobic groups. The most active compound (MIC = 0.2 µg/mL), contained both an amantadyl and a geranyl group. It is suggested that this potent activity is a result of the geranyl group mimicking the polyprenol side chain of decaprenolphosphoarabinose in the active site of mycobacterial arabinosyl transferase.

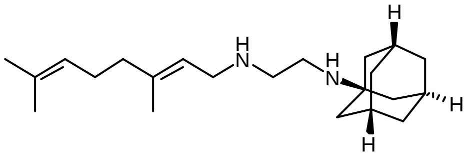

3.2.2 *Drugs with a novel mechanism of action*

Drugs with a novel mechanism of action are more likely to be active against strains of *M. tuberculosis* that are resistant to existing drugs. The ideal target for the design of novel anti-TB agents would be a *M. tuberculosis* enzyme that isn't found in humans or differs sufficiently from its human congener to allow selective blocking. The genome sequence of *M. tuberculosis* H37Rv, which was recently determined and analysed, shows that a very large portion of its coding capacity is devoted to the production of enzymes involved in lipogenesis, lipolysis and synthesis of cell wall sugars.[4] Lots of research is currently being directed against biological targets, taking part in the mycobacterial cell wall synthesis. Below, an overview is given of some of the most important recent achievements in that area of anti-tuberculosis drug design.

- 4,4'-Diisoamyloxy diphenyltiourea (ISO), a thiourea derivative successfully used in the 1960s to treat tuberculosis, recently showed to have considerable antimycobacterial activity against multi-drug-resistant TB strains (MIC 1-10 µM), without showing toxicity against macrophage cell cultures. This compound exerts its effect through inhibition of the mycobacterial oleic- and mycolic-acid synthesis.[46] Recently, membrane bound 9-stearoyl-desaturase was proven to be the biological target of this compound.[47] Several ISO analogues with various side chains of allyl, alkoxy and alkylthio units showed even superior activities against *M. tuberculois* (< 0.1µM for the propylthio- or butylthio- substituted diphenylthioureas).[47]

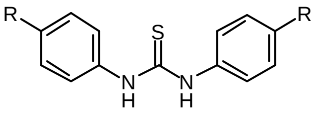

R = $OCH_2CH_2CH(CH_3)_2$
R = $SCH_2CH_2CH_2CH_3$
R = $SCH_2CH_2CH_3$

- While the synthesis of fatty acids occurs in all living organisms, mycobacteria possess accessory fatty acid synthase enzymes with specialised substrate and product specificities that are attractive targets for drug development. A new class of compounds designed to inhibit the β-ketoacyl synthase reaction of fatty acid synthesis has been developed. Out of more than thirty compounds, mimicking the transition state of the β-ketoacyl synthase reaction[48], the most active ones were 2-alkylsulphonylacetamides with an alkyl tail between eight and ten carbons in length (lower MIC than ethambutol, rifampicin, streptomycin and pyrazinamide, i.e. 1 µg/mL). The inhibitory activities were acutely sensitive to variations in alkyl tail length, charge and relative position of the sulfone to the amide. These compounds inhibit the growth of several species of mycobacteria, including both isoniazid-resistant and multi-drug resistant strains of *M. tuberculosis.*[49]

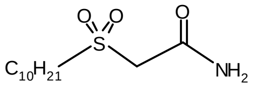

- From a series of 6-arylpurines, carrying a variety of substituents at the 9-position, the lowest minimum inhibitory concentration was found for 9-benzyl-2-chloro-6-(2-furyl)purine (0.78 µg/mL). Tests on its capacity to kill *M. tuberculosis* in monolayers of mouse bone marrow macrophages showed that it is able to penetrate inside macrophages. It exhibits low cytotoxicity and is active against several single drug-resistant strains of *M. tuberculosis*. The mechanism by which these purines exhibit their anti-mycobacterial activity is not known. However, the lack of cross-resistance with many known anti-mycobacterial drugs suggests that these compounds do not share the same mode of action.[50]

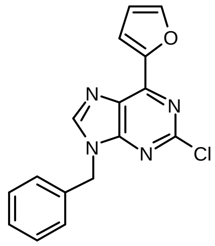

- 3-Aryl-2-oxazolidinones are a relatively new class of synthetic antibacterial agents, having a new mechanism of action which involves very early inhibition of protein synthesis. U-100593 and U-100766 demonstrate potent *in vitro* activity against *M. tuberculosis* (MIC < 0.125 µM).[51] A subclass with a thiomorpholine moiety showed markedly potent *in vitro* activity against *M. tuberculosis.* A representative of this class, U-100480, proved to be more active than isoniazid. Moreover it is also efficient against *M. tuberculosis* strains which are resistant to the conventional anti-tuberculosis drugs, without a sign of cross resistance.[52]

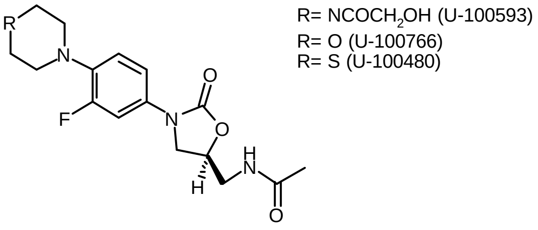

- Based on a series of *N*-hydroxyalkyl-1,2-benzisothiazol-3(2*H*)-ones (**1**), known to have anti-mycobacterial properties, a series isosteric 2-mercapto-pyridine-3-(*N*-alkyl-carbothioamides) (**2**) was evaluated for its activity against *M. tuberculosis*. All compounds showed anti-TB activity, especially the ethyl- and heptylamides proved to be more potent than ethambutol (MIC values of 0.5 μM). These compounds show low toxicity but very rapid elimination from the body after intravenous administration and poor absorption after oral administration.[53]

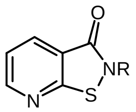

1

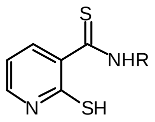

R = C_2H_5, C_7H_{15}

2

4 Thymidine monophosphate kinase

4.1 *MYCOBACTERIUM TUBERCULOSIS* TMPK: AN ATTRACTIVE TARGET

Thymidine monophsophate kinase (TMPK, ATP:dTMP phosphotransferase, thymidylate kinase) belongs to the large super family of nucleoside monophosphate kinases (NMPK's). It catalyses the reversible phosphorylation of thymidine monophosphate (dTMP) to thymidine diphosphate (dTDP) utilising ATP as its preferred phosphoryl donor.[54]

$$\mathrm{dTMP + ATP} \xrightleftharpoons{\text{TMPKmt}} \mathrm{dTDP + ADP}$$

The position of TMPK at the junction of the *de novo* and salvage pathways of the thymidine triphosphate (dTTP) metabolism, as the last specific enzyme for dTTP synthesis, makes it an interesting target for new drug design. With experiments using a *cdc*8 mutant of *Saccharomyces cerevisiae*, deficient in TMPK, Jong et al. proved that yeast TMPK (TMPKy) is essential for DNA replication and thus for cellular growth.[55,56] Furthermore, the thymidylate kinase activity of yeast shows to be a cell-cycle-regulated: enzyme activity is barely detectable in non-proliferating tissues, whereas in growing tissues, thymidylate kinase activity is increased considerably. A correlation between thymidylate kinase activity and the rate of DNA synthesis during rapid growth has been documented.[57]

Because studies using in vivo expression technology suggest that bacterial pathogenicity depends on genes essential for bacterial growth and intracellular survival,[58] blocking processes essential for the growth and replication of these organisms is believed to be an ideal way to beat them.

This has successfully been demonstrated by aciclovir, one of the most successful drugs against the *herpes simplex* virus. This drug is directed against thymidine kinase, which is responsible for the synthesis of both dTMP and dTDP in cells infected by the virus. Once selectively activated to its triphosphate form, it blocks the viral DNA synthesis through chain termination.

Although the global folding of TMPKmt is similar to that of TMPKh, sequence comparison showed only a 22% sequence identity between both enzymes, suggesting that selective blocking of the bacterial DNA synthesis should be feasible.[59] Moreover, AZTMP was already identified as a selective competitive inhibitor of TMPKmt.[59] TMPKmt represents the first reported TMPK that does not phosphorylate AZTMP, a feature that could be exploited in the search of selective inhibitors of TMPKmt.

4.2 Structure of TMPKmt

TMPKmt has recently been crystallised by Li de la Sierra et al.[60] The structural data used in this work are based on a 1.95 Å resolution X-ray image of TMPKmt bound to its natural substrate, dTMP, with a sulphate ion mimicking the β-phosphoryl of ATP.

4.2.1 Primary, secondary, tertiary and quaternary structure

TMPKmt has a molecular mass of 24 kDa and consists out of 214 amino acid residues. It is a homodimer in solution (Figure 6). In each monomer, nine α-helices surround a five-stranded β-sheet core. The interface of the dimer consists of three pairs of helices (α2, α3 and α6), kept together through hydrophobic interactions and an ion pair Glu50-Arg127.[60]

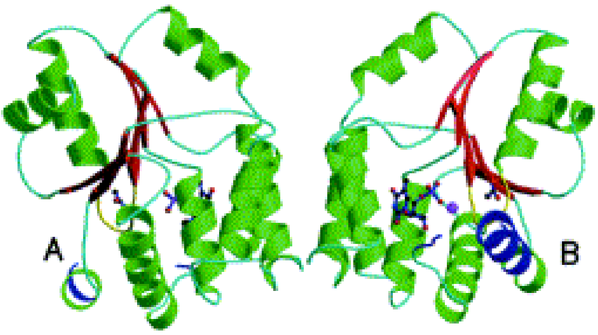

Figure 6: Stereo plot of the functional TMPKmt dimer crystallised in sodium malonate. The protein is shown in ribbon representation with helices shown in green and b-strands in red. The dTMP substrate as well as the acetate molecule found in the ATP-binding site are shown in a ball and stick representation. The magnesium ion found in the dTMP-binding site of one monomer (monomer B, on the right side) is shown in magenta. The P-loop is depicted in yellow and ordered parts of the LID are in dark blue.[61]

The global folding of TMPKmt is similar to that of other TMPKs, despite the low similarity of their amino acid sequences (26%, 25% and 22% sequence identity over about 200 aligned residues with TMPKec, TMPKy and TMPKh respectively) (Figure 7).

Like other NMPK's, TMPKmt undergoes large conformational changes upon substrate binding. One can distinguish between:

- the open conformation, observed without substrate
- the partially closed conformation with a single substrate
- the fully closed and active conformation, observed in the presence of both substrates (dTMP and ATP).

In the X-ray structure described by Li de la Sierra et al.,[60] the enzyme is in the fully closed conformation even though the presence of ATP is mimicked by SO_4^{2-}.

Three regions contain the essential residues for the function of this enzyme

- The P-loop motif (consensus sequence Gly $X_1X_2X_3X_4$ Gly Lys X_5)[62] controls the positioning of the phosphoryl groups of the phosphate donor. It binds and positions the α- and β-phosphoryl groups of ATP through interactions between amide backbone hydrogens and phosphate oxygen atoms. Unique to TMPKs is an interaction between the P-loop and the phosphoryl acceptor dTMP. This is achieved through a hydrogen bond between the 3'-hydroxyl group of dTMP and a carboxylic acid residue at position X_2 of the P-loop motif (Asp9 in TMPKmt). The exact function of this acidic amino acid is still unclear but it seems to be crucial for the catalytic mechanism of TMPK as any mutation of this residue in either the yeast, human or *E. coli* enzyme abolishes the phosphoryl transfer activity.[63]

- The DR(Y/H/F) motif is a loop containing a strictly conserved arginine residue, acting as a clip which favorably orients the phosphoryl donor and acceptor via an interaction with the phosphate group of dTMP and the γ-phosphate of ATP.

- The LID region is a flexible stretch that closes upon the phosphoryl donor when it binds the enzyme. This highly flexible stretch undergoes substantial conformational changes when the ATP molecule is fixed onto the enzyme. Simultaneously there is a transition from a coil to a helical conformation in the LID region when ATP gets bound.[64] Phosphoryl groups of both substrates interact with arginine side chains of the LID region, revealing their importance in catalysing phosphoryl transfer.[60]

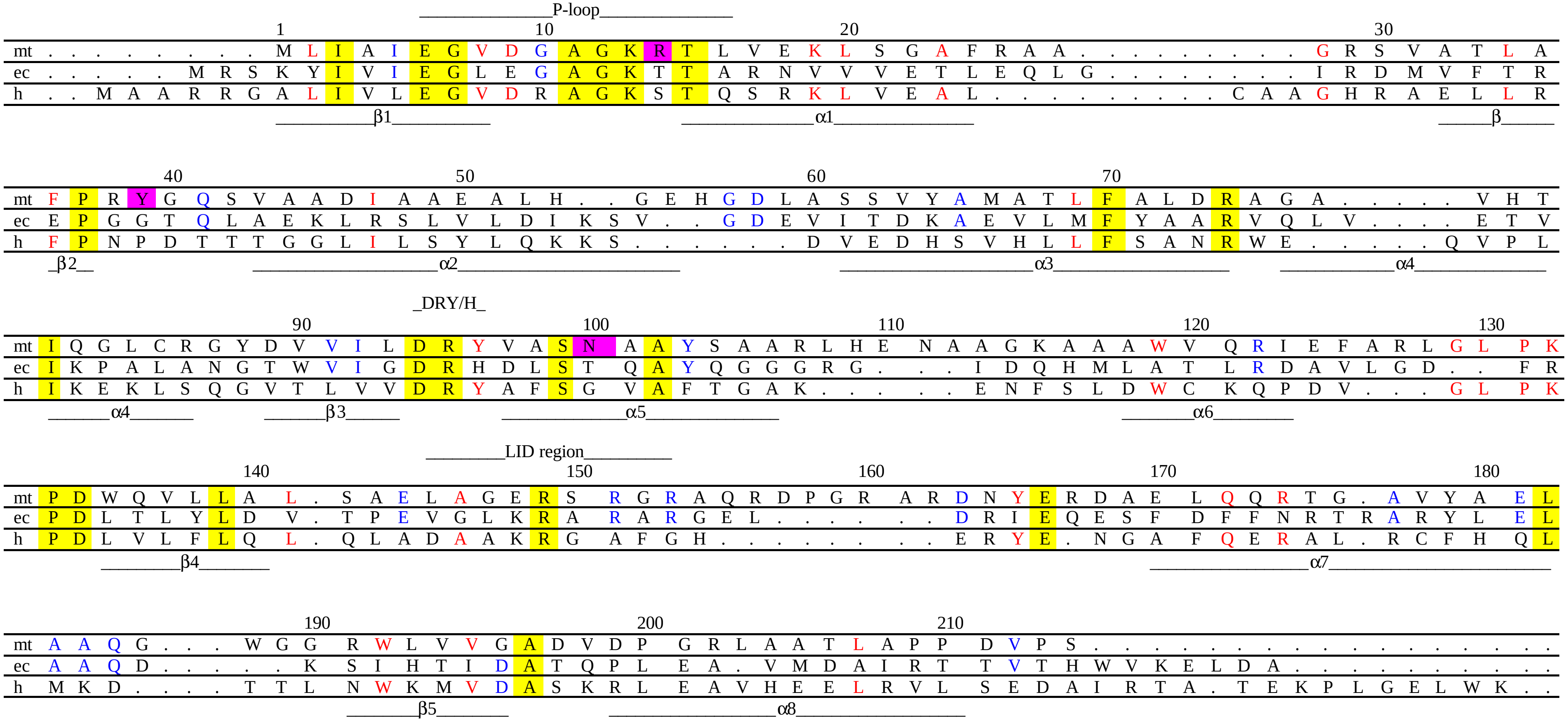
P-loop
1 10 20 30
mt . . . . M L I A I E G V D G A G K R T L V E K L S G A F R A A . . . . G R S V A T L A
ec . . . . . M R S K Y I V I E G L E G A G K T T A R N V V V E T L E Q L G . . . . I R D M V F T R
h . . M A A R R G A L I V L E G V D R A G K S T Q S R K L V E A L . . . . C A A G H R A E L L R
β1 α1 β
40 50 60 70
mt F P R Y G Q S V A A D I A A E A L H . . G E H G D L A S S V Y A M A T L F A L D R A G A . . . . . V H T
ec E P G G T Q L A E K L R S L V L D I K S V . . G D E V I T D K A E V L M F Y A A R V Q L V . . . . . E T V
h F P N P D T T T G G L I L S Y L Q K K S . . . . D V E D H S V H L L F S A N R W E . . . . . Q V P L
β2 α2 α3 α4
DRY/H
90 100 110 120 130
mt I Q G L C R G Y D V V I L D R Y V A S N A A Y S A A R L H E N A A G K A A A W V Q R I E F A R L G L P K
ec I K P A L A N G T W V I G D R H D L S T Q A Y Q G G G R G . . . I D Q H M L A T L R D A V L G D . . F R
h I K E K L S Q G V T L V V D R Y A F S G V A F T G A K . . . . . E N F S L D W C K Q P D V . . . G L P K
α4 β3 α5 α6
LID region
140 150 160 170 180
mt P D W Q V L L A L . S A E L A G E R S R G R A Q R D P G R A R D N Y E R D A E L Q Q R T G . A V Y A E L
ec P D L T L Y L D V . T P E V G L K R A R A R G E L . . . . . . D R I E Q E S F D F F N R T R A R Y L E L
h P D L V L F L Q L . Q L A D A A K R G A F G H . . . . E R Y E . N G A F Q E R A L . R C F H Q L
β4 α7
190 200 210
mt A A Q G . . . W G G R W L V V G A D V D P G R L A A T L A P P D V P S . . . .
ec A A Q D . . . . . K S I H T I D A T Q P L E A . V M D A I R T T V T H W V K E L D A . . . .
h M K D . . . . T T L N W K M V D A S K R L E A V H E E L R V L S E D A I R T A . T E K P L G E L W K . .
β5 α8

Figure 7: Alignment of the amino acid sequences of TMPKmt, TMPKec and TMPKh. Identical residues in all three sequences are shown in yellow. In red are amino acids common to TMPKmt and TMPKh and blue denotes commonalties between TMPKmt and TMPKec. Three positions occupied in TMPKmt by specific amino acids (Arg14, Tyr39 and Asn100) are shown in pink.

The phosphoryl transfer is catalysed by basic amino acids, mostly positively charged arginine residues that stabilise the negatively charged transition state. Based on the position of those arginines in the enzyme, TMPKs are categorised into two types:

- Type I TMPKs (e.g. yeast and human) have, in addition to the invariant lysine (residue 19 in the human enzyme), a basic residue (arginine) around position 16 in their P-loop sequence that can interact with the γ-phosphate group of ATP and lack such a positively charged residue in the LID region;

- Type II TMPKs (e.g. *E. coli*) have a glycine residue at that place in the P-loop and one additional basic residue in the LID region that interacts with ATP (Arg 153 in the *E. coli* enzyme).

This sequence variability in the catalytic region of eukaryotic versus prokaryotic TMPKs is associated with subtle but essential differences in phosphorylation mechanisms,[65] suggesting that inhibitors could be directed specifically against the enzyme of a pathogenic bacteria.

TMPKmt displays a configuration essentially representative of type II TMPKs, the LID region (residues 147-159) comprising a series of basic residues (Arg149, Arg151, Arg153 and Arg 156) and the P-loop (residues 7-14) having the usual glycine residue (Gly10) at position X_3. However, a peculiar additional basic residue, Arg14, is found at position X_5 in the P-loop, partly reminiscent of type I TMPKs, but unique among all TMPKs.

The observed magnesium ion is another unique feature of the TMPKmt structure: no magnesium atom was reported for the yeast or the *E. coli* enzyme.[64,65] For the human enzyme, one magnesium binding site has been reported but is located further away along the ATP-binding site, between the β- and γ-phosphate groups.[63] Three water molecules, an oxygen atom from the phosphoryl group and the carboxylate oxygen atoms of Asp9 and Glu166 coordinate the magnesium ion in an octahedral configuration. Fioravanti et al.[61] suggest this cation neutralises the electrostatic repulsion between the anionic substrates and optimises their proper alignment.

4.2.2 The dTMP-binding site

Examination of the X-ray structure of TMPKmt learns that the main bonding forces between dTMP and the enzyme are:

- a stacking interaction between the pyrimidine ring and Phe70;

- a hydrogen bond between *O*4 of thymine and the Arg74 side-chain, which results in a preference for thymine over cytosine;

- a hydrogen bond between Asn100 and *N*3 of the thymine ring;

- a hydrogen bond between the 3’-hydroxyl of dTMP and the terminal carboxyl of Asp9, that in its turn interacts with the magnesium ion, responsible for positioning the phosphate oxygen of dTMP;

- hydrogen bonds and an ionic interaction between the 5’-*O*-phosphoryl and Tyr39, Phe36, Arg95 and Mg^{2+} respectively;

- the presence of Tyr103 close to the 2'-position is believed to render the enzyme catalytically selective for 2'-deoxy-nucleotides versus *ribo*-nucleotides (Figure 8).

Several subtle differences are observed when comparing TMPKmt to other TMPK's. These include:

- the hydrogen bond between the *N*3 atom of the pyrimidine ring with the Asn100 side-chain (changed to a glycine residue in both yeast and human, and to a threonine residue in the *E. coli* enzyme);
- the Tyr39 residue makes two polar contacts with dTMP: one with the phosphate oxygen atom and the other with the oxygen atom at the 5'-position. Arginine and glycine residues replace this tyrosine in the human and yeast enzymes respectively;
- the 3'-hydroxyl group of the ribose moiety makes three polar contacts: one with a water molecule involved in the Mg^{2+}-coordination and two others with Asp9.[60]

These differences are potentially interesting starting points for finding selectivity for TMPKmt versus TMPKh.

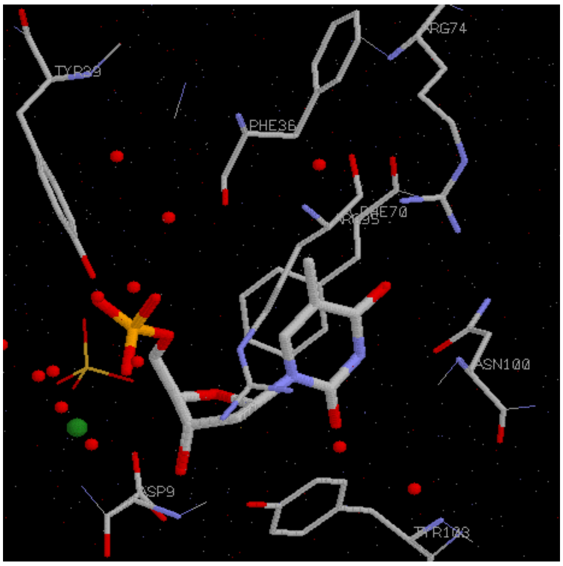

Figure 8: Image of the dTMP binding site of *M. tuberculosis*, complexed with dTMP, showing the most important amino acids interacting with dTMP. dTMP is pictured in bold, the water molecules as red spheres and the magnesium ion as a green sphere.

4.2.3 The ATP binding site

Despite the fact that TMPKmt was co-crystallised as a complex with dTMP and SO_4^{2-}, in the absence of ATP, the structural characteristics observed around the ATP binding site are similar to those observed in complexes from yeast and *E. coli* enzymes where ATP was fixed, indicating that the crystal structure represents the closed conformation. The LID region has made the transition from a coil to a helical conformation, normally seen upon ATP binding. Arg149 (part of the LID helix) and Thr15, which interacts via a stacking interaction with the adenine ring of ATP, are in the correct position to accommodate the adenine ring of ATP, just as observed in the closed conformation of the TMPKec.[60]

TMPKmt has a broader substrate specificity for nucleoside triphosphates than other NMPK's. The reaction rates with ATP or dATP as phosphate donors were similar. ITP, GTP, CTP and UTP could also serve as efficient phosphate donors (order of efficacy: ITP > GTP > CTP > UTP). Even dGTP, dCTP and dTTP act as phosphate donors, even though much less efficiently (1% for dTTP, 8% for dCTP and 35% for dGTP compared to ATP).[59]

4.2.4 Catalysis

4.2.4.1 Kinetic parameters for dTMP and ATP

TMPKmt has a high resistance to thermal denaturation, associated with a lower catalytic activity (the specific activity of TMPKmt is four- and six-fold lower compared to TMPKec and TMPKy, respectively). The K_m-values for dTMP and ATP lie in the same order of magnitude in TMPKmt, TMPKy, TMPKec and TMPKh.[59] (Table 1).

TMPK	K_m (ATP) (mM)	K_m (dTMP) (mM)	V_m (ATP, dTMP)[a]	k_{cat} (s^{-1})
M. tuberculosis	0.1	4.5	13	4.5
E. coli	0.04	15	50	10.5
Yeast	0.19	9	84	35
Human	5	5	2	0.7

Table 1: Kinetic parameters for dTMP and ATP in TMPKmt,[59] TMPKec[64] and TMPKy[59] and TMPKh.[59] .[a] V_m in mmole/min.mg of protein.

4.2.4.2 Structural changes of TMPKmt upon substrate binding

The structural changes of TMPKmt occurring upon binding of the substrates and subsequent catalysis were investigated by protein crystallography. Structures were determined at different pH values, in the presence and/or absence of sulphate ions, acetate ions and ATP, yielding different snapshots along the reaction pathway (Figure 9).[61]

- Structure 1 (apo-TMPKmt) shows a dTMP binding site completely ready to accommodate dTMP, the LID region is in a highly disordered conformation.

- Structure 2 (TMPKmt-dTMP) shows the native dTMP bound state of the enzyme, the partially closed conformation. The switch from the open to the closed conformation is triggered by the 3'-hydroxyl and the phosphoryl group of dTMP, attracting positively charged residues from the LID region (Arg149, Arg151, Arg153, Arg156, Arg160 and Arg162).

- Structure 3 (TMPKmt-dTMP-Mg^{2+}) shows that Mg^{2+} binds the enzyme transiently during catalysis. Structural changes of the LID region result in the correct positioning of Glu166 in order to trap the magnesium ion. The binding of magnesium orders Asp9 in the correct position to interact with Glu166, thereby establishing a link between the P-loop and the LID region.

- Structure 4 (TMPKmt-dTMP-Mg^{2+}-$SO4^{2-}$) represents the closed conformation, the sulphate ion mimicking the β-phosphate of ATP. Binding of ATP provides additional contacts between the LID region and the P-loop, through Arg153 and Lys13. Glu166 now coordinates the magnesium ion at in the correct position for catalysis.

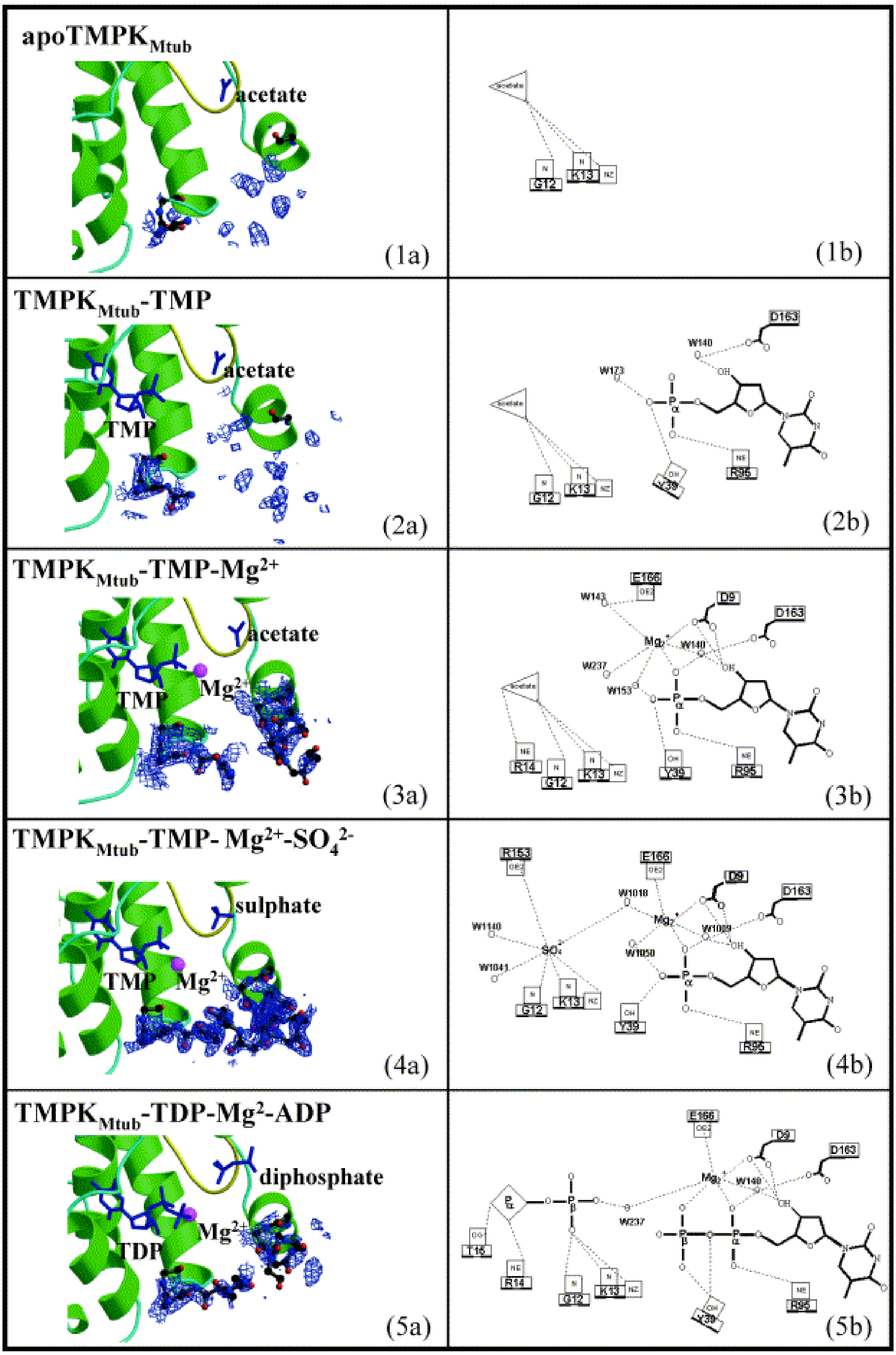
apoTMPKMtub
acetate
(1a)
acetate
N
G12
N
K13
NZ
(1b)
TMPKMtub-TMP
acetate
TMP
(2a)
D163
W140
OH
W173
acetate
P
α
N
G12
N
K13
NZ
OH
Y39
NE
R95
(2b)
TMPKMtub-TMP-Mg2+
acetate
TMP
Mg2+
(3a)
E166
OE2
W143
D9
D163
Mg2+
W140
W237
W153
OH
acetate
P
α
NE
R14
N
G12
N
K13
NZ
OH
Y39
NE
R95
(3b)
TMPKMtub-TMP- Mg2+-SO42-
sulphate
TMP
Mg2+
(4a)
R153
OE2
E166
OE2
D9
D163
W1018
W1140
Mg2+
W1089
SO42-
OH
W1050
W1041
P
α
N
G12
N
K13
NZ
OH
Y39
NE
R95
(4b)
TMPKMtub-TDP-Mg2-ADP
diphosphate
TDP
Mg2+
(5a)
E166
OE2
D9
D163
Mg2+
W140
OH
Pα
P
β
W237
P
β
P
α
OG
T15
NE
R14
N
G12
N
K13
NZ
OH
Y39
NE
R95
(5b)

Figure 9: Snapshots along the reaction coordinate of TMPKmt. The five described structures ((1) apo-TMPKmt; (2) TMPKmt-dTMP; (3) TMPKmt-dTMP-Mg^{2+}; (4) TMPKmt-dTMP-Mg^{2+}-SO$_4^{2-}$ and (5) TMPKmt-dTDP-Mg^{2+}-ADP) are shown from top to bottom. Nucleotides, sulphate and acetate ions are shown in blue. The part of the main chain in the LID region that could be modelled in the electron density is shown in ball-and-stick representation. The LID closes when going from (1) to (4) and re-opens in (5). (b) A drawing of the TMPKmt active site. [61]

- Structure 5 (TMPKmt-dTDP-Mg^{2+}-ADP) resembles the state of the enzyme immediately after phosphoryl transfer, with the LID region still fully closed. This structure is more relaxed with Gu166 at a greater distance from Mg^{2+}.

The scenario described above aligns with the induced-fit mechanism already suggested in several NMPK's[66,67,68,69] and with the idea of an ordered bi-bi-catalytic mechanism, in contrast to the random bi-bi-mechanism proposed for these enzymes.[70,71] The possibility of a mechanism, involving ATP binding first, cannot be excluded from this study completely. However, it has been shown that dTMP exhibits an affinity (K_m = 4.5 μM) for the enzyme more than 20 times stronger than ATP (K_m=100 μM),[59] suggesting that the pathway involving dTMP binding first is largely favoured when both substrates are present in the same concentration. Closure of the LID region upon ATP binding would sterically restrict the access of dTMP to its binding site. A mechanism starting with ATP binding first would probably require a secondary channel through which dTMP may enter the active site.

4.2.4.3 Possible catalytic residues

The magnesium ion provides a strong electrostatic potential, attracting the γ-phosphate of ATP sufficiently close to the α-phosphate of dTMP for phosphoryl transfer. It tightly coordinates these phosphoryl groups, thereby acting as a clamp between the phosphoryl donor and acceptor. The essential role of this ion in driving the catalysis suggests that structure-based design of inhibitors for the enzyme should focus on possibilities to destabilise this ion.[61]

In prokaryotic TMPKs, the arginine residues located in the LID region are responsible for stabilisation of the negatively charged transition state with their positive charges. In the eukaryotic enzymes, however, one of the key basic residues is located in the P-loop and not in the LID region. In TMPKmt, apart from the side-chains of Arg153, Arg156 and Arg160 of the LID region, the active site contains also an arginine residue (Arg14) in the P-loop, together creating a highly positive electrostatic potential at the location where the triphosphate moiety of the ATP molecule binds.

The phosphoryl group of dTMP makes direct polar contacts with three residues (Asp9, Tyr39 and Arg95) and solvent mediated contacts with six residues (Gly12, Lys13, Phe36, Arg153, Asp163 and Glu166) of the enzyme. These tyrosine and arginine residues are also good candidates in assisting the transfer of a phosphoryl group to dTMP.[5]

4.3 HUMAN TMPK

4.3.1 Structure and catalysis

Human TMPK (TMPKh) is a 24 kDa protein, consisting of 212 amino acid residues. It is a homodimer with a similar fold as described for the TMPKmt, TMPKy and TMPKec. Each monomer consists of a five-stranded parallel β-sheet core surrounded by nine α helices. The highly hydrophobic dimer interface is generated by the stacking of three nearly parallel helices from each monomer against the other. It is a type I TMPK with a basic residue in the P-loop that can interact with the substrate.

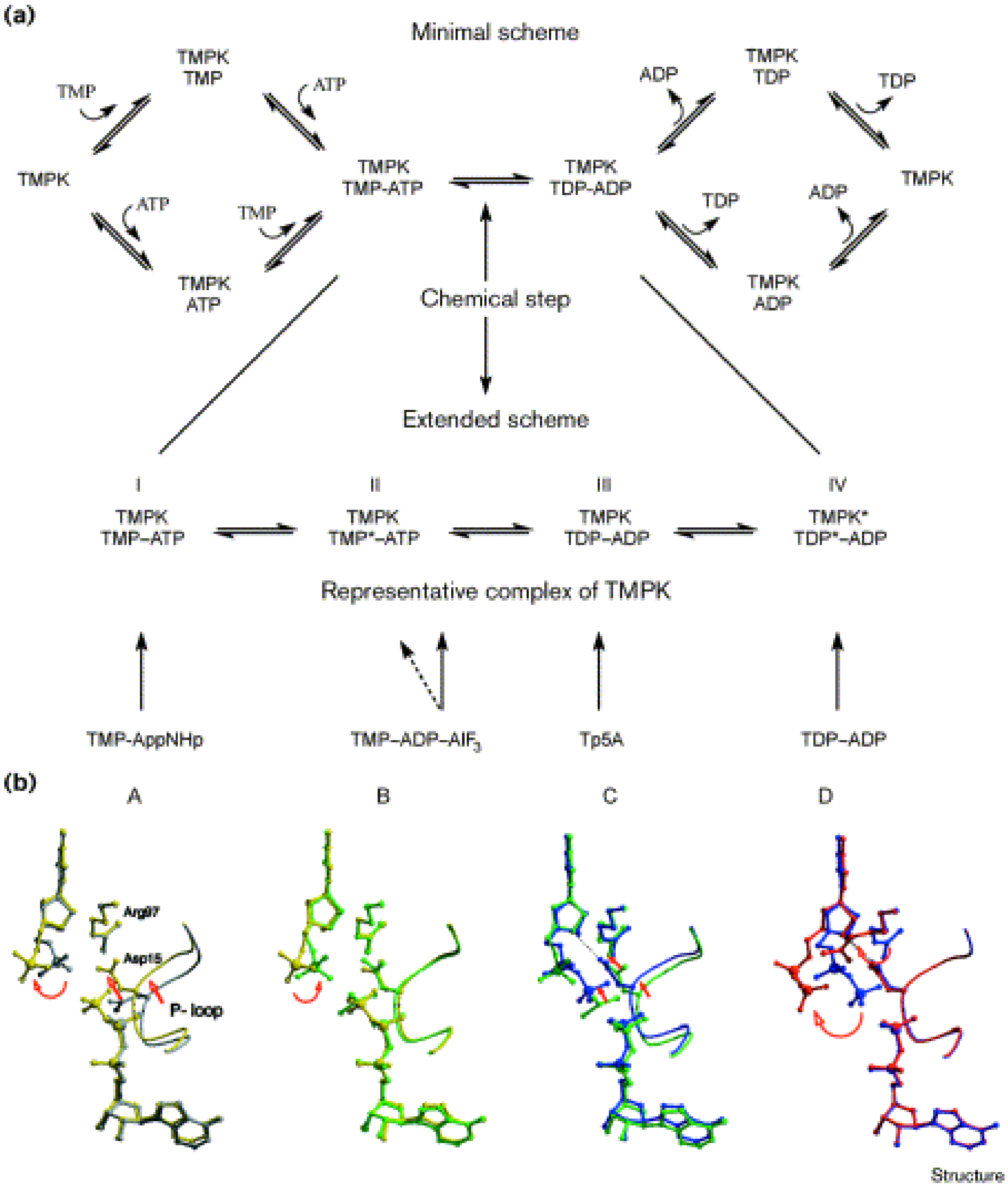
(a)
Minimal scheme
TMPK
TMP
TMP
ATP
TMPK
TMPK
TMP-ATP
TMPK
TDP-ADP
ADP
TMPK
TDP
TDP
TMPK
ATP
TMP
TMPK
ATP
TDP
ADP
TMPK
ADP
Chemical step
Extended scheme
I
TMPK
TMP–ATP
II
TMPK
TMP*–ATP
III
TMPK
TDP–ADP
IV
TMPK*
TDP*–ADP
Representative complex of TMPK
TMP-AppNHp
TMP–ADP–AlF3
Tp5A
TDP–ADP
(b)
A
B
C
D
Arg97
Asp15
P- loop
Structure

Figure 10: (a) The minimal scheme for a bi-bi-mechanism requires an expansion to account for the conformational changes that occur after both substrates are bound and prior to product release. States, I, II, III and IV are proposed on the basis of the different structural features observed in different complexes of human TMPK (b), labeled A, B, C and D: (A) overlay of the TMP–ADP (gray) and TMP–AppNHp (yellow) complexes; (B) TMP–AppNHp and TMP–ADP–AlF_3 (green); (C) TMP–ADP–AlF_3 and Tp_5A (blue; the b-phosphate group of Tp_5A is modeled; (D) Tp_5A and TDP–ADP (red). Superposition of the different states reveals the possible dynamics that occur during the phosphoryl transfer reaction. Note that the dTMP-ADP complex shown in A does not represent a state on the reaction coordinate, but rather reveals the conformational changes that occur upon the replacement of a diphosphate by a triphosphate at the phosphoryl donor site.

A special feature, only observed in the human TMPK structures are the additional conformational changes occurring within the globally closed conformation, which are dependent on the nature of the bound substrates. This feature entails the rigid-body movement of three loop regions: the P-loop, the LID region and the adenine-base binding loop. Several complexes of TMPKh (TMPKh with dTMP and ADP, with dTMP and AppNHp, with TP_5A, with ADP and dTDP and with dTMP, ADP and AlF_3) have been crystallised,[63] representing different states along the reaction coordinate and giving an image of the different conformations for these regions (Figure 10).

- P-loop open: is formed in the presence of dTMP and ADP

- P-loop partially closed: when ADP is replaced by AppNHp or when the phosphoryl group mimic AlF_3 is soaked into a dTMP-ADP crystal

- P-loop closed: is seen when the bisubstrate inhibitor TP_5A is present or when dTDP and ADP are present.

Although with each P-loop movement a concomitant shift in the position of the LID region and the adenine-base binding loop is also observed, the terminology used above focuses on the P-loop for reasons of clarity. However, at the moment we cannot be sure whether this novel feature is unique to the human enzyme, or if it is common for all TMPK’s.

The P-loop moves as a rigid body, with the hinges being formed by two highly conserved residues: Glu12, anchoring the P-loop via a bidentate interaction with Ser101 and Lys19, interacting with the phosphate(s).

There is no information available about the free and singly bound enzyme. The dTMP and AppNHp complex structure, represents the first step along the reaction coordinate of phosphoryl transfer: the P-loop and LID region have already undergone a conformational change from the open form to the P-loop partially closed state. However, in this state, the dTMP phosphoryl group is not ideally positioned for nucleophilic attack on the γ-phosphate of ATP. Therefore, it is assumed that, before the chemical step can take place, the dTMP phosphoryl group swings away from Arg45 towards Arg97 and the phosphate group of ATP, thus shortening the distance to the donor nucleotide. Arg97 now acts as a clamp bringing the donor and acceptor nucleotides together.

The structure of the AlF_3 bound complex is a model for the transition state of the phosphoryl transfer. The P-loop moves slightly further towards the monophosphate and in this state, the oxygen of the dTMP phosphoryl group is optimally positioned for attack on the γ-phosphate of ATP. It makes only one interaction with Arg97, leaving the attacking oxygen atom free for nucleophilic attack on the γ-phosphate of ATP.

The TP_5A complex structure is interpreted to represent the enzyme conformation just after the reaction has taken place. Probably this state is only observed because of the restraints imposed by using the covalently linked phosphate chain TP_5A. Without this constraint, the phosphate groups of dTDP and the sidechain of Arg97 rotate to the stable product conformation represented by the complex with dTDP and ADP. As in the TP_5A complex, also in this case the enzyme adopts the fully closed conformation. The diphosphate moiety of dTDP rotates with respect to the phosphate position when dTMP is bound. As a result, the β-phosphoryl group of dTDP does not interact with the catalytic magnesium ion, but rather forms two hydrogen bonds to Arg97, thereby forcing it in a new position so that it cannot act as a clamp anymore.

The magnesium ion, present in human TMPK, coordinates the β and γ-phosphates of ATP. By withdrawing negative charge from the reactive phosphate, the magnesium ion promotes nucleophilic attack on the phosphorus atom.[72] Instead of a magnesium ion at this position, in TMPKmt a coordination by the guanidinium-group of Arg14 is seen. Superposition of the human and the tuberculosis TMPK suggests that the two enzymes have evolved slightly differently by swapping the roles played by the two key positive charges in the active site (the metal ion and one arginine residue). Whereas an NTP-bound Mg^{2+} is required in TMPKh, Arg14 takes this role in TMPKmt. Conversely, a dTMP-bound Mg^{2+} is required for catalysis in TMPKmt whereas in TMPKh Arg45 interacts with the dTMP phosphate group. The roles of Arg97 (TMPKh) and Arg95 (TMPKmt), which superimpose very well in the two structures, are likely to be similar in the two enzymes, acting as a clamp during catalysis.[61]

4.3.2 The low catalytic efficiency of human TMPK

The P-loops of all eukaryotic TMPK’s contain an arginine residue that follows the strictly conserved carboxylic acid residue Asp15. A catalytic role was assigned to this residue because mutating this arginine to glycine in yeast, reduced the activity 200-fold. In all of the human TMPK complex structures, however, this arginine is observed in an extended conformation that precludes interaction with the phosphates. This result is consistent with mutagenesis experiments that show no appreciable decrease in catalytic rate upon mutating this residue to glycine. Interestingly the rate observed for the human enzyme ($0.7\ s^{-1}$) is similar to that of the yeast enzyme lacking this residue ($35\ s^{-1}$ for wild type, $0.2\ s^{-1}$ for the Asp15→Gly mutant).[63]

Of the two arginines (Arg15 and Arg97) that could potentially interact with the transferred phosphoryl group to stabilise the transition state only the latter is also seen to show this interaction with the γ-phosphate of ATP. Possibly in vivo an additional factor interacts with TMPKh and can induce the P-loop arginine to make the interaction mentioned above. It seems likely that this and also the extra conformational changes within the globally closed conformation limit the overall catalysis rate of human TMPK, which, in its isolated state, is several orders of magnitude less efficient than AMPK, UMPK or even the highly homologous yeast TMPK. Therefore, the question arises as to whether a mechanism or factor is present in the cell for acceleration of this surprisingly slow reaction. Such a factor or mechanism would add another level of control to the activity of the protein, in addition to that of cell-cycle-dependent transcriptional control.[63]

4.3.3 The role of human TMPK in activating AZT

The HIV-prodrug 3’-azido-3’-deoxy-thymidine (AZT) is converted by cellular enzymes to its active form 3'-azido-3'-deoxy-thymidine triphosphate (AZTTP). The most important antiviral effect of AZT is a consequence of efficient AZTTP incorporation into a growing DNA chain by HIV reverse transcriptase, but to a much lesser extent by human DNA polymerases, resulting in viral DNA chain termination in HIV infected cells. A prerequisite for AZT to be a potent drug is that all phosphorylation steps to the triphosphate are catalysed efficiently by the cellular enzymes. AZTMP, however, the substrate of TMPKh, accumulates in millimolar concentrations in cells treated with AZT, implicating TMPK to be the rate limiting kinase in AZT activation. Lavie et al.[73] crystallised AZTMP with TMPKh. The location of dTMP and

AZTMP in the enzyme is almost identical, which is in agreement with the kinetic data which show a very similar K_m value for dTMP and AZTMP. The enzyme-AZTMP interactions are identical to those made with dTMP, including those with the 3’ substituent: the azido group and the side chain of Asp14 lie in close proximity. These identical interactions are made possible by a rigid body movement of the entire P-loop by about 0.5 Å away from the azido group. Arg15 of the P-loop, involved in fixing the α- and β-phosphates of ATP, appears to play an important catalytic role but is mispositioned because of steric hindrance between the azido group of AZTMP and the carboxylic acid side chain of Asp14. So, as it is the P-loop which binds the phosphoryl donor, its position determines the relative orientation of the donor (ATP) and acceptor (dTMP or AZTMP) and the relative position of Arg15. Consequently, the 0.5 Å shift of the P-loop does not affect binding, as reflected in the unchanged K_m values, but rather increases the activation energy for the phosphoryl transfer step, thus lowering the rate (200 fold in comparison to dTMP). This low phosphorylation rate of AZT by TMPK does not only result in insufficient concentrations of the active AZTTP, but also in the accumulation of toxic AZTMP.

TMPKec has no arginine in its P-loop motif, but rather several arginine residues in its LID region. One or more of these arginines are predicted to assume the catalytic role assigned to the P-loop arginine of the yeast and human enzyme. Therefore, TMPKec is less affected by the presence of the azido group of AZTMP. Insertion of the LID domain of the bacterial TMPK into the human enzyme (and mutation of Arg15 to Gly15 to avoid a steric clash between this arginine and the LID region arginine) resulted in a pronounced acceptance of AZTMP such that it gets phosphorylated even faster than TMP.[74]

Because AZTMP behaves as a competitive inhibitor (K_i-value of 10μM) of TMPKmt, in contrast to the human enzyme, this feature could be exploited in the search of selective inhibitors of TMPKmt.

4.4 HERPES TK (TKHSV)

TKhsv1 (thymidine kinase of *herpes simplex* virus 1) is an example of a kinase of a pathogen whose differences with the human isozyme lead to the discovery of a series of antiviral drugs such as aciclovir and ganciclovir.

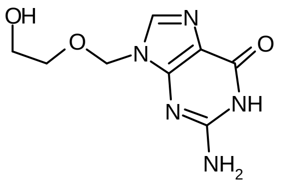

acyclovir

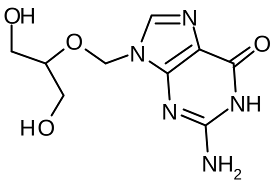

gancyclovir

In contrast to the human isozyme, TKhsv not only catalyses the transfer of the γ-phosphate from ATP to the 5’-hydroxyl of deoxythymidine (dT) to form dTMP, but also phosphorylates dTMP to dTDP. The catalysed phosphorylations of dT and dTMP have slow rates, with k_{cat} numbers around 5 s^{-1}. Both reactions occur successively and the phosphoryl acceptor remains in the binding site during the two phosphorylation steps. A superposition of the dT and dTMP complex structures shows only small differences. The largest one occurs around position 222, where the phosphate of dTMP pushes the backbone 1.5 Å outwards.[75]

Because it has a much broader substrate specificity than the human enzyme, TKhsv selectively helps activating antiviral drugs like aciclovir and ganciclovir to their triphosphates, which cause chain termination of the growing DNA chains in herpes viruses.[76]

This broad substrate specificity of TKhsv can be rationalised the fact that thymine, even though it is bound tightly, doesn’t fill up its binding pocket completely. In complex TK:ADP:dTMP, thymine leaves a non-polar 35 Å void close to its C5 position. In TK:ADP:5-iodo-dUMP, the large iodine replaces the smaller methyl group without steric hindrance and still leaves a void of 17 Å.[77,64]

Selectivity is ensured through the inability of the host-cell TK to phophorylate these drugs to an appreciable extent. These compounds can also be used in gene therapy for cancer, to achieve selective toxicity after introduction of the viral TK gene in tumor cells. TKhsv itself is not a direct target for antiviral therapy because the enzyme is not required for virus replication in proliferating cells. However, viral TK activity may be required for reactivation of the virus from latency in nerve cells so that TK inhibitors have potential use in treatment of recurrent herpes infections.[75]

TMPKmt, in contrast to TKhsv, is essential for the DNA replication and survival of *M. tuberculosis.* Therefore, selective inhibitors of TMPKmt hold great promise as anti-tuberculosis drugs. In spite of the similarities between the tuberculosis and the herpes enzyme, aciclovir and ganciclovir could never be accommodated by TMPKmt, since the 35 Å void close to the C5 position is not present in the tuberculosis enzyme. The inhibition of TMPKmt (in contrast to TMPKh) by AZTMP, however, indicates that the 3'-position holds great promise for differentiating between the human and the tuberculosis enzyme.

5 Initial Structure Activity Relationship

At the moment we became involved in this project, kinetic data for various base- and sugar-modified dTMP analogues were already available.

5.1 BASE-MODIFICATIONS

The 5-methyl was replaced by several halogen atoms.[59] All these compounds are substrates for TMPKmt, the best one being 5-Br-dUMP with a slight increase in K_m and V_m compared to dTMP (K_m = 30 μM). Substitution by a iodine (5-I-dUMP) or a fluorine (5-F-dUMP) drastically decreases the affinity for the enzyme. X-ray crystallography showed that 5I-dUMP binds to the phosphate acceptor binding site in a very similar fashion as dTMP.

Removal of the methyl group (dUMP) affects the affinity even more (50-fold increase in K_m-value and 44% decrease in reaction rate).

Furthermore, different substitution patterns at position 2 of the pyrimidine ring were probed and from this 5-methyl-iso-dCMP emerged as a competitive inhibitor with a K_i of 130 μM.

5.2 SUGAR MODIFICATIONS

Substitution of the 3'-hydroxyl by an azido group (AZTMP), yielded an inhibitor with a K_i-value of 10µM. Surprisingly, TMPKmt is the first reported TMPK (in contrast to TMPK's from eukaryotes and other prokaryotes) to be a competitively inhibited by AZTMP. AZTMP is a substrate for TMPKec and TMPKy, with only a 2-fold reduction of k_{cat} for the bacterial enzyme and 200-fold for the yeast enzyme. In TMPKmt, the presence of an azido group abolishes catalysis without changing the affinity. A plausible explanation for the inhibitory effect of AZTMP could be a direct interaction between the magnesium ion and the azido group of AZTMP. Modeling showed a distance of only 2 Å between the last nitrogen atom of the azido group and the ion. This would displace one of the ligands of the magnesium ion and significantly perturb the geometry of the active site. Since this ion is involved in the positioning of several key chemical groups for the reaction, i. e. one of the phosphate oxygen atoms and Asp9, this displacement of the magnesium ion is believed to cause the observed inhibition of the phosphoryl transfer.[59, 5]

5.3 SIX-MEMBERED SUGAR RINGS

1',5'-Anhydro-2',3'-dideoxy-5'-*O*-phosphoryl-2'-(thymin-1-yl)-D-arabino-hexitol was tested for its affinity for the enzyme to probe the effect of a six-membered sugar ring. It turned out to be an inhibitor of TMPKmt with a K_i-value of 31 µM, which indicates that six-membered sugar rings can be accepted by the substrate binding cavity.

NMP	**K_m (µM)**	**V_m ^{a}**	**K_i (mM)**
dTMP	4.5	10.60	
dUMP	2100	3.50	
5-Br-dUMP	33	9.82	
5-I-dUMP	140	7.46	
5-F-dUMP	420	4.66	
AZTMP			10
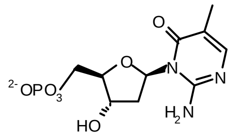			130
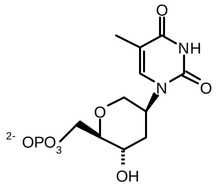			31

Table 2: Kinetic parameters of base and sugar modified nucleotides for TMPKmt; ^{a} V_m in (mmole/min.mg of protein)

6 Modeling and rational drug design

Accidental discoveries always played an important role in science, especially in the search for new drugs. Up to the eighties, drugs were discovered, rather than developed. Meanwhile, new scientific developments, especially in the areas of biological sciences, molecular modelling and spectroscopy, have brought irreversible changes in the organic chemistry and drug discovery culture. Since the fast evolving elucidation of protein structures, a new way of drug design was introduced: structure-based ('rational') drug design. Using computer modeling and target structures obtained through X-ray or NMR, new ligands with a higher chance of being active can be synthesised. The structural information is used for explaining the basis of effective inhibition and improving the potency and specificity of new lead compounds. The complementary methods of computer-aided molecular design and combinatorial chemistry are now routinely employed in both the lead identification and the development phases of drug design. Examples of therapeutically used drugs developed in this way are captopril, an anti-hypertensive Angiotensin-converting enzyme inhibitor (the first drug derived from a structural model of a protein), dorzolamide, a carbo-anhydrase inhibitor for the treatment of glaucoma and the HIV protease inhibitors Saquinavir, Indinavir, Ritonavir, and Nelfinavir. In the absence of a protein 3 dimensional (3D) structure, the 3D structures of certain ligands can also be used for rational design. This approach, called pharmacophore-based drug design, has been successfully applied the design of specifically acting integrin-receptor antagonists.[78]

Although it considerably increases the chance of finding effective drugs, there are some problems that rational drug design cannot overcome today;

- Our incomplete understanding of intermolecular interactions which may e.g. result in unexpected binding modes of newly synthesised compounds to the target protein. In order to increase the predictability of these models, the force fields currently used need further optimisation and gas-phase calculations should be replaced by calculations in an aqueous environment. Furthermore, not only the enthalpy component of the free energy should be considered but also the entropy component, which still remains a challenge today.
- The potential drug may not reach the target *in vivo*;
- Metabolic processes may transform the potential drug into an ineffective compound;
- New compounds may be toxic, teratogenic, mutagenic or carcinogenic.

In this work, most of the changes of the dTMP-scaffold were chosen, inspired by the X-ray structure of TMPK with dTMP and aimed to establish novel interactions with certain amino acids. Modeling was mainly used to explain the affinities of the best binding ligands. For those compounds, docking in GOLD was performed, using the AMBER force field. Although the enzyme stays rigid in these experiments, they are a fast and easy way to get an idea of the most likely binding modes of the nucleoside analogues. Finally, based on this most favourable binding way, an energy minimisation was performed, allowing the ligand and the amino acids in the active pocket to move towards the minimum energy conformation. The interactions observed in the resulting model were then used as the basis for further inhibitor design.

7 Objectives

TMPKmt emerged as an interesting target for the design of selective inhibitors as potential leads for the development of a new class of anti-tuberculosis agents. Based on the X-ray structure of TMPKmt and the known affinities of a few compounds for the enzyme,[59] it was decided to establish a preliminary SAR by synthesising a series of nucleotides modified at the 2'-, 3'- and 5-positions of the dTMP-scaffold and testing them on their affinity for TMPKmt (Figure 11).

7.1 5-MODIFIACTIONS

Because a 5-bromine (5Br-dUMP) is well accepted by the enzyme, we envisaged some larger substituents at the 5-position. The introduction of a furanyl or a thienyl substituent was aimed to form a stacking interaction with Phe36. A 5-CH_2OH, on the other hand, could interact with the side chain of Arg74 (Chapter 3).

7.2 2'-MODIFICATIONS

Near the 2'-position lies Tyr103, believed to be responsible for discrimination between *ribo*- and deoxy-nucleotides. By introducing a 2'-hydroxyl function on the α- or β-face of the sugar ring, the interactions with Tyr103 were investigated. An α-directed 2'-amine could indicate if this positively charged substituent is capable of interacting with Tyr103 via a cation-π interaction.[79] To sort out the influence of the size and electronegativity of 2'-substituents on the affinity for TMPKmt, the 2'-hydroxyl function of thymidine was replaced by a fluorine. ^{1}H-NMR studies have demonstrated a relation between the electronegativity and the size of the 2'-substituents and the sugar puckering in a series of 2'-substituted-2'-deoxy-adenosines.[80] In these studies, introduction of a fluorine increases the percentage of sugar that exhibits the 2'-*exo*-3'-*endo*-conformation, while a 2'-chloro-substitution favours the 2'-*endo*-3'-*exo*-conformation. The latter puckering is the one adopted by the furanose of dTMP when bound to TMPKmt. It could be expected that nucleotide-analogues that exhibit a similar *S*-type conformation will have a higher affinity for TMPK, than those that have to be forced into that configuration by the enzyme (Chapter 2).

7.3 3'-MODIFICATIONS

Due to the unique behaviour of AZTMP towards TMPKmt in comparison to other TMPKs, particularly the 3'-position was considered to have potential for finding good and selective inhibitors. Because AZTMP interacts through its azido group with Asp9, we intended to establish an ionic interaction with Asp9 by introducing a 3'-amino group. A 3'-fluorine, on the other hand, could show the effect of an electronegative substituent at that position (Chapter 3).

In the X-ray structure, a cavity near the 3'-position was observed with the potential of accommodating larger substituents. Li de la Sierra et al.[5] suggested that the azido group of AZTMP moves the magnesium ion away from the active site, thereby abolishing catalysis. We explored the feasibility to have a similar effect produced by a series of 3'-*C*-branched-chain nucleotides (the 3'-*C*-azidomethyl, 3'-*C*-aminomethyl, 3'-*C*-fluoromethyl and 3'-*C*-hydroxymethyl derivatives of dTMP) (Chapter 4).

7.4 5'-MODIFICATIONS

Initially, we focused on the synthesis of phosphorylated analogues of dTMP. Indeed, one can expect that the loss of the ionic interaction between the phosphate moiety and the enzyme will cause an unacceptable affinity drop. Furthermore, the phosphoryl group is believed to be important to correctly position dTMP in its binding site. By conserving the phosphate moiety in (closely) related analogues, their binding mode is believed to mimick that of dTMP, which renders prediction of the interactions with the enzyme easier. However, due to their inability to enter cells, monophosphate derivatives cannot be delivered as such. Generally, nucleosides cross the cell membrane barrier in a non-phosphorylated form and are then converted to the corresponding nucleotides by intracellular kinases. In this particular case, where TMPK is the drug target, a thymidine analogue could be activated by thymidine kinase (TK), which converts the analogue into the corresponding mono-phosphorylated compound. However, a search of the *M. tuberculosis* genome[4] did not identify any gene coding for TK. This result aligns with other biochemical studies indicating a lack of TK activity in mycobacteria.[81] These problems make it a challenge to find a 5'-substituent, undergoing high affinity interactions with the enzyme and not hampering the cellular uptake. As a starting point towards this, we will not only test nucleotides but also their corresponding nucleosides to probe the effect of the loss of the phosphoryl group on the affinity (Chapter 5).

7.5 SIX-MEMBERED RING NUCLEOSIDES

1',5'-Anhydro-2',3'-dideoxy-5'-*O*-phosphoryl-2'-(thymin-1-yl)-D-arabino-hexitol proved to be an inhibitor of TMPKmt with a K_i-value of 31 μM, indicating that six-membered sugar rings can be accepted by the substrate binding cavity. In this nucleotide the base is oriented axially ($^1C_4$ conformation), in contrast to dTMP, were thymine is in a more equatorial-like position. When co-crystallised with a similar enzyme, HSV-1 TK, the sugar ring of 1',5'-anhydro-2',3'-dideoxy-5'-*O*-phosphoryl-2'-(thymin-1-yl)-D-arabino-hexitol is forced in the $^4C_1$ (base equatorially) conformation.[82] Because this conformational change demands energy, 1-[2,4-di-deoxy-4-*C*-hydroxymethyl-α-L-lyxopyranosyl]thymine, carrying thymine in an equatorial position, seemed a very promising dTMP mimic (Chapter 7).

7.6 BIOLOGICAL EVALUATION

Via a reported spectrometric assay,[83] all compounds mentioned above were tested for their inhibitory activity for TMPKmt and those showing the most promising activity were also evaluated for their affinity for TMPKh.

In this spectrometric assay, the formation of nucleoside diphosphates (NDPs) is coupled to reactions catalyzed by pyruvate kinase (PK) and lactate dehydrogenase (LDH) in the presence of phosphoenolpyruvate (PEP) and NADH, using NADH as indicator. Each mole of transferred phosphoryl group generates two moles NDP (sum of ADP and NDP) and consequently two moles of NADH are oxidised to NAD^+.

$$\mathrm{ATP + NMP} \xrightarrow{\mathrm{NMPK}} \mathrm{ADP + NDP}$$

$$\mathrm{ADP + NDP + 2\ PEP} \xrightarrow{\mathrm{PK}} \mathrm{ATP + NTP + 2\ pyruvate}$$

$$\mathrm{2\ pyruvate + 2(NADH + H^+)} \xrightarrow{\mathrm{LDH}} \mathrm{2\ lactate + 2\ NAD^+}$$

Because the reactivity of various NDPs towards PK can vary a lot, the coupling system may become rate limiting, which leads to underestimation of the phosphorylation rate. Adding NDP-kinase (NDPK), that has a broad specificity for the phosphoryl donors and acceptors, can circumvent this problem.

$$\mathrm{ATP + NMP} \xrightarrow{\mathrm{TMPK}} \mathrm{ADP + NDP}$$

$$\mathrm{NDP + ATP} \xrightarrow{\mathrm{NDPK}} \mathrm{NTP + ADP}$$

$$\mathrm{2\ ADP + PEP} \xrightarrow{\mathrm{PK}} \mathrm{2\ ATP\ \ + 2\ pyruvate}$$

$$\mathrm{2\ pyruvate + 2(NADH + H^+)} \xrightarrow{\mathrm{LDH}} \mathrm{2\ lactate + 2\ NAD^+}$$

From the spectrometrically measured decrease in NADH, the phosphorylation rate can be calculated. In case the synthesised compounds were no substrates, their inhibitory capacity was determined. At a fixed concentration of dTMP, the decrease in phosphorylation rate was measured, allowing to calculate the K_i-value.

Modeling of the best binding inhibitors was then used to explain their interactions with the enzyme and to plan the synthesis of novel ligands with potentially higher affinity.

7.7 FURTHER OPTIMISATION OF THE 3'-*C*-BRANCHED-CHAIN NUCLEOSIDES

Based on the above mentioned biological results and modelling, the intended purpose was to synthesise a series of 3'-*C*-branched-chain nucleosides, containing larger nitrogen-containing substituents at the 6'-position. The synthesis of a series of 2'-halogeno-3'-*C*-branched-chain nucleosides was another object in view (Chapter 6-).

7.8 GENERAL OBJECTIVE

In summary, the objective of this Ph.D. study comprehends the design and synthesis of a series thymidine and thymidine-5'-*O*-monophosphate analogues as selective inhibitors of TMPKmt.

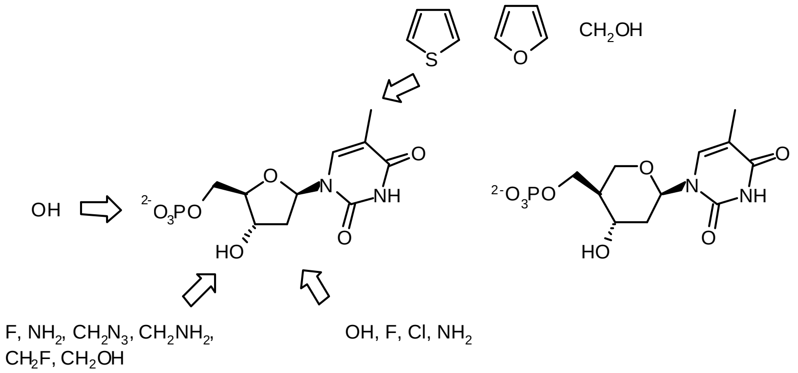

Figure 11: Aimed changes of the dTMP scaffold

8

References

---

[1] Stokstad, E. Drug-Resistant TB on The Rise. *Science* **2000**, *287*, 2391.

[2] Godfrey-Fausset, P.; Maher, D.; Mukadi, Y. D.; Nunn, P.; Perriëns, J.; Raviglione, M. How human immunodeficiency virus voluntary testing can contribute to tuberculosis control. *Bulletin of the World Health Organization* **2002**, *80*, 939-945.

[3] Web site://www.who.org.

[4] Cole, S. T.; Brosch, R. ; Parkhill, J. ; Garnier, T. ; Churcher, C. ; Harris, D.; Gordon, S. V.; Eiglmeier, K.; Gas, S.; Barry, C. E.; Tekaia, F.; Badcock, K.; Basham, D.; Brown, D.; Chillingworth, T.; Connor, R.; Davies, R. et al. Deciphering the biology of *Mycobacterium tuberculosis* from the complete genome sequence. *Nature*, **1998**, *393*, 537-544.

[5] Li de la Sierra, I.; Munier-Lehmann, H.; Gilles, A. M.; Bârzu, O.; Delarue, M. X-ray Structure of TMP Kinase from *Mycobacterium tuberculosis* Complexed with TMP at 1.95 Å Resolution. *J. Mol. Biol.* **2001**, *311*, 87–100.

[6] Wild, K.; Bohner, T.; Folkers, G.; Schulz, G. E. The structures of thymidine kinase from *Herpes simplex* virus type I in complex with substrates and a substrate analogue. *Protein Sci.* **1997**, *6*, 2097–2106.

[7] Champnesss, J. N.; Bennett, M. S.; Wien, F.; Visse, R.; Visser, R.; Summers, W. C.; Herdewijn; P. Exploring the active site of herpes simplex virus type-1 thymidine kinase by X-ray crystallography of complexes with aciclovir and other ligands. *Proteins: Struct. Funct. Genet.* **1998**, *32*, 350–361.

---

[8] Lowary, T. L. Recent Progress Towards the Identification of Inhibitors of Mycobacterial Cell Wall Polysaccharide Biosynthesis. *Mini reviews in Medicinal Chemistry* **2003**, *3*, 689-702.

[9] Flynn, J. L.; Chan, J. Immunology of tuberculososis. *Annu. Rev. Immunol.* **2001**, *19*, 93–129.

[10] Andersen, P. TB vaccines: progress and problems. *Trends in Tmmunology* **2001,** *22*, 160.

[11] Fjällbrant, H.; Ridell, M.; Larsson, L. O. The tuberculin skin test in relation to immunological *in vitro* reactions in BCG-vaccinated healthcare workers. *Eur. Respir. J.* **2001**, *18*, 376–380.

[12] *Anti-tuberculosis Drug Resistance in the World*. World Health Organisation: Geneva, Switserland, **1998**.

[13] Suzuki, Y.; Suzuki, A.; Tamaru, A.; Katsukawa, C.; Oda, H. Rapid detection of Pyrazinamide-resistant *Mycobacterium tuberculosis* by a PCR-based *in vitro* system. *J. Clin. Microbiol.* **2002**, 501–507.

[14] Heath, R. J.; White, S. W.; Rock, C. O. Lipid biosynthesis as a target for antibacterial agents. *Progress in lipid research* **2001** *40*, 467–497.

[15] Campbell, E. A.; Korzheva, N.; Mustaev, A.; Murakamin, K.; Nair, S.; Goldfarb, A.; Darst, S. Structural mechanism for rifampicin inhibition of bacterial RNA polymerase. *Cell* **2001**, *104*, 901–912.

[16] Zimhony, O.; Cox, J. S.; Welch, J.; Vilchese, C.; Jacobs, W. R. Pyrazinamide inhibits the Eukaryotic-like Fatty Acid Synthase I (FASI) of *Mycobactrium tuberculosis. Nat. Med.* **2000**, *6*, 1043–1047.

[17] Speirs, R. J.; Welch, J. T.; Cynnamon, M. H. Activity of *n*-propyl pyrazinoate against pyrazinamide-resistant *Mycobacterium tuberculosis*: investigations into the mechanism of action of and mechanism of resistance to pyrazinamide. *Antimicrob. Agents Chemother.* **1995**, *39*, 1269–1271.

[18] Belanger, A. E.; Besra, G. S.; Ford, M. E.; Mikusova, K.; Belisle, J. T.; Brennan, P. J.; Inamine, J. M. The *embAB* genes of *Mycobacterium avium* encode an arabinosyl transferase involved in cell wall arabinan biosynthesis that is the target for the antimycobacterial drug ethambutol. *Proc. Natl. Acad. Sci. USA* **1996**, *93*, 11919–11924.

[19] Grosset, J.; Benhassine, M. La thiacétazone (TB1): données expérimentales et cliniques récentes. *Adv. Tuberc. Res.* **1970**, *17*, 107–153.

[20] Protivinsky, R. Chemotherapeutics with tuberculostatic action. Antibiotics *Chemother*. **1971**, *17*, 101–121.

[21] Liebermeister, K. Zur Wirkung der tuberkulostatischen Chemotherapeutika. *Deutsch Med. Wschr.* **1950**, *75*, 621–622.

[22] Malluche, H. Die Thiosemicarbazone-Therapie der Tuberkulose. *Fortschr. Tuberk. Forsch*. **1952**, *5*, 152–154.

[23] Vannelli, T. A.; Dykman, A.; Ortiz de Montellano, P. R. The antituberculosis drug ethionamide is activated by a flavoprotein monooxygenase. *J. Biol. Chem.* **2002**, *277*, 12824–12829.

[24] Chacon, O.; Feng, Z.; Harris, N. B.; Caceres, N. E.; Adams, L. G.; Barletta, R. G. *Mycobacterium smegmatis* D-Alanine Racemase Mutants Are Not Dependent on D-Alanine for Growth. *Antimicrob. Agents Chemother.* **2002**, *46*, 47–54.

[25] De Logu, A.; Onnis, V.; Saddi, B.; Congiu, C.; Schivo, M. L.; Cocco, M. T. Activity of a new class of isonicotinoylhydrazones used alone in combination with isoniazid, rifampicin, ethambutol, para-aminosalicylic acid and clofazimine against *Mycobacterium tuberculosis*. *J. Antimicrob. Chemotherap.* **2002**, *49*, 275–282.

[26] Anderson, P. TB vaccines: progress and problems. *Trends in immunology* **2001**, *22*, 160–168.

---

[27] Jackson, M.; Phalen, S. W.; Lagranderie, M.; Ensergueix, D.; Chavarot, P.; Marchal, G.; McMurray, D. N.; Gicquel, B.; Guilhot, C. Persistence and protective efficacy of a *Mycobacterium tuberculosis* auxotroph vaccine. *Infection and immunity* **1999**, *67* , 2867–2873.

[28] McAdam, R. A.; Weisbrod, T. R.; Martin, J.; Scuderijd; Brown, A. M.; Cirillo, J. D.; Bloom, B. R.; Jacobs, W. R. In-vivo growth characteristics of leucine and methionine auxotrophic mutants of Mycobacterium-bovis BCG generated by transpososn mutagenesis. *Infection and immunity* **1995**, *63*, 1004–1012.

[29] Behr, M. A.; Small, P. M. Has BCG attenuated to impotence? *Nature* **1997**, *389*, 133–134.

[30] Horwitz, M. A.; Harth, G.; Dillon, B. J.; Maslesa-Galic, S. Recombinant bacillus Calmette-Guerin (BCG) vaccines expressing the Mycobacterium tuberculosis 30-kDa major secretory protein induce greater protective immunity against tuberculosis than conventional BCG vaccines in a highly susceptible animal model. *Proc. Natl. Acad. Sci.* **2000**, *97*, 13853–13858.

[31] Hess, J.; Miko, D.; Catic, A.; Lehmensiek, V.; Russell, D. G.; Kaufmann, S. H. E. *Mycobacterium bovis* bacille Calmette-Guerin strains secreting listeriolysin of Listeria monocytogenes. *Proc. Natl. Acad. Sci.* **1998**, *95*, 5299–5304.

[32] Murray, P. J.; Aldovini, A.; Young, R. A. Manipulation and potentiation of antimycobacterial immunity using recombinant bacille Calmette-Guerin strains that secrete cytokines. *Proc. Natl. Acad. Sci.* **1996**, *93*, 934-939.

[33] Falero-Diaz, G.; Challacombe, S.; Banerjee, D.; Douce, G.; Boyd, A.; Ivanyi, J. Intranasal vaccination of mice against infection with *Mycobacterium tuberculosis*. *Vaccine* **2000**, *18*, 3223–3229.

[34] Brandt, L.; Elhay, M.; Rosenkrands, I.; Lindblad, E. B.; Andersen, P. ESAT-6 subunit vaccination against *Mycobacterium tuberculosis*. *Infection and immunity* **2000**, 68, 791–795.

[35] Huygen, K.; Content, J.; Denis, O.; Montgomery, D. L.; Yawman, A. M.; Deck, R. R.; DeWitt, C. M.; Orme, I. M.; Baldwin, S. D.; Souza, C.; Drowart, A.; Lozes, E.; Vandenbussche, P.; VanVooren, J. P.; Liu, M. A.; Ulmer, J. B. Immunogenicity and protective efficacy of a tuberculosis DNA vaccine. *Nature medicine* **1996**, *2*, 893–898.

[36] Morris, S.; Kelley, C.; Howard, A.; Li, Z. M.; Collins, F. The immunogenicity of single and combination DNA vaccines against tuberculosis. *Vaccine* **2000**, *18*, 2155–2163.

[37] Kling, J. Genomics: enlisting a genome to fight MDR tuberculosis. *Modern Drug Discovery* **1999**, 33–45.

[38] Renau, T. E.; Sanchez, J. P.; Gage, J. W.; Dever, J. A.; Shapiro, M. A.; Gracheck, S. J.; Domagala, J. M. Structure-activity relationships of quinolone antibacterials against mycobacteria: effect of structural changes at N-1 and C-7. *J. Med. Chem.* **1996**, *39*, 729–735.

[39] Renau, E. R.; Sanchez, J. P.; Shapiro, M. A.; Dever, J. A.; Gracheck, S. J.; Domagala, J. M. Effect of lipophilicity at N-1 on activity of fluoroquinolones against mycobacteria. *J. Med. Chem.* **1995**, *38*, 2974–2977.

[40] Cynamon, M. H.; Gimi, R.; Gyenes, F.; Sharpe, C. A.; Bergmann, K. E.; Han, H. Y.; Gregor, L. B.; Rapolu, R.; Luciano, G.; Welch, J. T. Pyrazinoic acid esters with broad spectrum *in vitro* antimycobacterial activity. *J. Med. Chem.* **1995**, *38*, 3902–3907.

[41] Seitz, L. E.; Suling, W. J.; Reynolds, R. C. Synthesis and Antimycobacterial Activity of Pyrazine and Quinoaline Derivatives. *J. Med. Chem.* **2002**, *45*, 5604–5606.

[42] Wächter, G. A.; Davis, M. C.; Martin, A. R.; Franzblau, S. G. Antimycobacterial activity of substituted isosteres of pyridine- and pyrazinecarboxylic acids. *J. Med. Chem.* **1998**, *41*, 2436–2438.

---

[43] Gezginci, M. H.; Martin, A. R.; Franzblau, S. G. Antimycobacterial activity of substituted isosteres of pyridine- and pyrazinecarboxylic acids. *J. Med. Chem.* **2001**, *44*, 1560–1563.

[44] Bottari, B.; Maccari, R.; Monforte, F.; Ottana, R.; Rotondo, E.; Vigorita, M. G. Isoniazid-related copper (II) and nickel (II) complexes with antimycobacterial *in vitro* activity. *Bioorg. Med. Chem. Lett.* **2000**, *10*, 657–660.

[45] Lee, R. E. Protopopova, M. ; Crooks, E. Slay, R. A.; Terrot, M.; Barry, C. E. Combinatorial lead optimisation of [1,2]-diamines based on ethambutol as potential antituberculosis preclinical candidates III *J. Com. Chem.* **2003**, *5*, 172-187.

[46] Phetsuksiri, B.; Baulard, A. R.; Cooper, A. M.; Minnikin, D. E.; Douglas, J. D.; Besra, G. S.; Brennan, P. J.; Antimycobacterial activities of isoxyl and new derivatives through the inhibition of mycolic acid synthesis.*Antimicrobial Agents and Chemotherapy.* **1999**, *43*, 1042–1051.

[47] Phetsuksiri, B.; Jackson, M.; Scherman, H.; McNeil, M. R.; Besra, G. S.; Baulard, A. R.; Slayden, R. A.; DeBarber, A. E.; Barry, C. E.; Baird, M. S.; Crick, D. C.; Brennan, P. J. Unique mechanism of action of the Thiourea drug, isoxyl, on Mycobacterium tuberculosis; *J. Biol. Chem.* **2003,** accepted on october 14.

[48] Jones, P. B.; Parrish, N. M.; Houston, T. A.; Stapon, A.; Bansal, N. P.; Dick, J. D.; Townsend, C. A. A new class of antituberculosis agents. *J. Med. Chem.* **2000**, *43*, 3304–3314.

[49] Parrish, N. M.; Houston, T.; Jones, P. B.; Townsend, C.; Dick, J. D. *In vitro* activity of a novel antimycobacterial compound, *N*-octanesulfonylacetamide and its effects on lipid and mycolic acid synthesis. *Antimicrob. Agents Chemother.* **2001**, *45*, 1143–1150.

[50] Gundersen, L. L.; Nissen-Meyer, J.; Spilsberg, B. Synthesis and antimycobacterial activity of 6-arylpurines: the requirements for the *N*-9 substituent in active antimycobacterial purines. *J. Med. Chem.* **2002**, *45*, 1383–1386.

[51] Brickner, S. J.; Hutchinson, D. K.; Barbachyn, M. R.; Manninen, P. R.; Ulanowicz, D. A.; Garmon, S. A.; Grega, K. C.; Hendges, S. K.; Toops, D. S.; Ford, C. W.; Zurenko, G. E. Synthesis and antibacterial activity of U-100592 and U-100766, two oxazolidinone antibacterial agents for the potential treatment of multidrug-resistant gram-positive bacterial infections. *J. Med. Chem.* **1996**, *39*, 673–679.

[52] Barbachyn, M. R.; Hutchinson, D. K.; Brickner, S. J.; Cynamon, M. H.; Kilburn, J. O.; Klemens, S. P.; Glickman, S. E.; Grega, K. C.; Hendges, S. K.; Toops, D. S.; Ford, C. W.; Zurenko, G. E. Identification of novel oxazolidinone (U-100480) with potent antimycobacterial activity. *J. Med. Chem.* **1996**, *39*, 680–685.

[53] Pagani, G.; Pregnolato, M.; Ubiali, D.; Terreni, M.; Piersimoni, C.; Scaglione, F.; Fraschini, F.; Gascon, A. R.; Muñoz, J. L. P. Synthesis and *in vitro* anti-mycobacterium activity of *N*-alkyl-1,2-dihydro-2-thioxo-3-pyridinecarbothioamides. Preliminary toxicity and pharmakokinetic evaluation. *J. Med. Chem.* **2000**, *43*, 199–204.

[54] Anderson, E. **1973** Nucleoside and nucleotide kinases. In *The enzymes* (Boyer, P. D., ed.), 3rd edit., vol. 8, pp. 49–96, Academic Press, New York.

[55] Jong, A. Y. S.; Kuo, C. L.; Campbell, J. L. The *cdc8* gene of yeast encodes thymidylate kinase. *J. Biol. Chem.* **1984**, *259*, 11052–11059.

[56] Sclafani, R. A.; Fangman, W. L. Yeast gene *cdc8* encodes thymidilate kinase and is complemented by herpes thymidine kinase gene TK. *Poc. Natl. Acad. Sci.* **1984**, *81*, 5821–5825.

[57] Jong, A. Y. S.; Campbell, J. L. Characterisation of *Saccharomyces cerevisiae* Thymidylate Kinase, the *CDC8* Gene Product. *J. Biol. Chem.* **1984**, *259*, 14394–14398.

[58] Valvidia, R. H. M.; Falkow, S. Fluoresence-based isolation of bacterial genes expressed within host-cells. *Science* **1997**, *277*, 2007–2011.

---

[59] Munier-Lehman H.; Chaffotte A.; Pochet S.; Labesse G. Thymidylate kinase of *Mycobaterium tuberculosis*: A chimera sharing properties common to eukaryotic and bacterial enzymes. *Protein Science* **2001**, *10*, 1195–1205.

[60] Li de la Sierra, I.; Munier-Lehmann, H.; Gilles, A. M.; Bârzu, O.; Delarue, M. X-ray Structure of TMP Kinase from *Mycobacterium tuberculosis* Complexed with TMP at 1.95 Å Resolution. *J. Mol. Biol.* **2001**, *311*, 87–100.

[61] Fioravanti, E.; Haouz, A.; Ursby, T.; Munier-Lehmann, H.; Delarue, M.; Bourgeois, D. *Mycobacterium tuberculosis* Thymidylate Kinase: Structural Studies of Intermediates along the Reaction pathway. *J. Mol. Biol.* **2003**, *327*, 1077–1092.

[62] Saraste, M.; Sibbald, P. R.; Wittinghofer, A. The P-loop - a common motif in ATP- and GTP-binding proteins. *Trends Biochem. Sci.* **1990**, 430–434.

[63] Ostermann, N.; Schlichting, I.; Brundiers, R.; Konrad, M.; Reinstein, J.; Veit, T.; Goody, R. S.; Lavie, A. Insights into the phosphoryltransfer mechanism of human thymidilate kinase gained from crystal structures of enzyme complexes along the reaction coordinate. *Structure* **2000**, *8*, 629–642.

[64] Lavie, A.; Konrad, M.; Brundiers, R.; Goody, R. S.; Schlichting, I.; Reinstein, J. Crystal structure of yeast thymidilate kinase complexed with the bisubstrate inhibitor P5-(5'-adenosyl) P5-(5'-thymidyl) pentaphosphate (TP_5A) at 2.0 Å resolution: implications for catalysis and AZT activation. *Biochemistry* **1998**, *37*, 3677–3686.

[65] Lavie, A.; Osterman, N.; Brundiers, R.; Goody, R.; Reinstein, J.; Konrad, M.; Schlichting, I. Structural basis for efficient phosphorylation of 3'-azidothymidine monophosphate by *Escherichia Coli* thymidilate kinase. *Proc. Natl. Acad. Sci. USA* **1998**, *95*, 14045–14050.

[66] Vonrhein, C.; Schlauderer, G. J.; Schulz, G. E. Movie of the structural changes during a catalytic cycle of nucleoside monophosphate kinases. *Struct. Fold. Des.* **1995**, *3*, 483–490.

[67] Matte, A.; Tari, L. W. Delbaere, L. T. How do kinases transfer phosphoryl groups? *Struct. Fold. Des.* **1998**, *6*, 413–419.

[68] Blaszczyk, J.; Li, Y.; Yan, H.; Ji, X. Crystal structure of unligated guanylate kinase from yeast reveals Gmp-induced conformational changes. *J. Mol. Biol.* **2001**, *307*, 247–257.

[69] Schulz, G. E.; Müller, C. W.; Diederichs, K. Induced-fit movements in adenylate kinases. *J. Mol. Biol.* **1990**, *213*, 627–630.

[70] Cheng, Y. C.; Prusoff, W. H. Mouse ascites sarcoma 180 thymidylate kinase. General properties, kinetic analyses and inhibition studies. *Biochemistry* **1973**, *12*, 2612–2619.

[71] Li, Y.; Zhang, Y.; Yan, H. Kinetic and thermodynamic characterisations of yeast guanylate kinase. *J. Biol. Chem.* **1999**, *271*, 28038–28044.

[72] Pappu, K. M.; Gregory, J. D.; Serpersu, E. H. Substrate activity of Rh(III)ATP with phosphoglycerate kinase and the role of the metal ion in catalysis. *Arch. Biochem. Biophys.* **1994**, *311***,** 503–508.

[73] Lavie, A.; Vetter, I. R.; Konrad, M.; Goody, R. S.; Reinstein, J.; Sclichting, I. Structure of thymidilate kinase reveals the cause behind the limiting step in AZT activation. *Nat. Struct. Biol.* **1997**, *4*, 601–604.

[74] Brundiers, A.; Lavie, A.; Veit, T.; Reinstein, J.; Schlichting, I.; Ostermann, N.; Goody, R. S.; Konrad, M. Modifying human thymidylate kinase to potentiate azidothymidine activation. *J. Biol. Chem.* **1999**, *274*, 35289–35292.

[75] Bennet, M. S.; Wien, F.; Champness, J. N.; Batuwangala, T.; Rutherford, T.; Summers, W. C.; Sun, H.; Wright, G.; Sanderson, M. R. Structure to 1.9 Å resolution of a complex with herpes simplex virus type-1 thymidine kinase of a novel, non-substrate inhibitor: X-ray crystallographic comparison with binding of aciclovir. *FEBS Letters* **1999**, *443*, 121–125.

---

[76] De Winter, H.; Herdewijn, P. Understanding the binding of 5-Substituted 2'-Deoxyuridine Substrates to Thymidine Kinase of Herpes Siplex Virus Type-1. *J. Med. Chem.* **1996**, *39*, 4727–4737.

[77] Wild, K.; Bohner, T.; Folkers, G.; Schulz, G. E. The structure of thymidine kinase from *Herpes simplex* virus type 1 in complex with substrates and a substrate analogue. *Prot. Sci.* **1997**, *6*, 2097–2106.

[78] Kubinyi, H. Chance favors the prepared mind - From serendipity to rational drug design. *Journal of receptor and signal transduction research* **1999**, *19*, 15–39.

[79] Mo, Y.; Subramanian, G.; Gai, J.; Fergusion, D. M. Cation-π Interactions: an energy decomposition analysis and its implication in δ-opioid receptor-ligand binding. *J. Am. Chem. Soc.* **2001**, *124*, 4832–4837.

[80] Uesugi, S.; Miki, H.; Ikehara, M.; Iwahashi, H.; Kyogoku, Y. Linear relationship between electronegativity of 2'-substituents and conformation of adenine nucleosides. *Tetrahedron. Lett.* **1979**, *42*, 4073–4076**.**

[81] Saito, H.; Tomioka, H. Thymidine kinase of bacteria - activity of the enzyme in actinomycetes and related organisms. *J. Gen. Microbiol.* **1984** *130*, 1863.

[82] Ostrowski, T.; Wroblowski, B.; Busson, R.; Rozenski, J.; De Clercq, E.; Bennet, M. S.; Champness, J. N.; Summers, W. C.; Sanderson, M. R.; Herdewijn, P. 5-Substitted pyrimidines with a 1,5-anhydro-2,3-dideoxy-D-arabino-hexitol moiety at N-1: Synthesis, antiviral activity, conformational analysis, and interaction with viral thymidine kinase. *J. Med. Chem.* **1998**, *41*, 4343–4353.

[83] Blondin, C.; Serina, L.; Wiesmüller, L.; Gilles, A. M.; Bârzu, O. Improved Spectrophotometric Assay of Nucleoside Monophosphate Kinase Activity Using Pyruvate Kinase/Lactate Dehydrogenase Coupling System. *Anal. Biochem.* **1994**, *220*, 219–222.

Chapter 2

SYNTHESIS AND BIOLOGICAL EVALUATION OF THYMIDINE-5′-*O*-MONOPHOSPHATE ANALOGUES AS INHIBITORS OF *M. TUBERCULOSIS* THYMIDYLATE KINASE

Veerle Vanheusden, Hélène Munier-Lehmann, Sylvie Pochet, Piet Herdewijn, Serge Van Calenbergh

Bioorg. Med. Chem. Lett. **2002**, *12*, 2695-2698

SYNTHESIS AND BIOLOGICAL EVALUATION OF THYMIDINE-5′-*O*-MONOPHOSPHATE ANALOGUES AS INHIBITORS OF *M. TUBERCULOSIS* THYMIDYLATE KINASE

Veerle Vanheusden, Hélène Munier-Lehmann, Sylvie Pochet, Piet Herdewijn, Serge Van Calenbergh

Bioorg. Med. Chem. Lett. **2002**, *12*, 2695-2698

A number of 2’- and 3’-modified thymidine 5’-O-monophosphate analogues were synthesised as potential leads for new anti-mycobacterial drugs. Evaluation of their affinity for Mycobacterium tuberculosis thymidine monophosphate kinase showed that a 2’-halogeno-substituent and a 3’-azido function are the most favourable leads for further development of potent inhibitors of this enzyme.

Tuberculosis (TB) is frighteningly on the rise. Once nearly vanquished by antibiotics, at least in the developed world, tuberculosis resurged in the late 1980’s and now kills more than two million people a year – second only to AIDS among infectious diseases.[1]

Mycobacterium tuberculosis, the causative agent of this disease, is primarily transmitted via the respiratory route and mostly causes pulmonary tuberculosis. Estimates are that one third of the world’s population is infected with this organism, but infection does not usually lead to the active disease. Reactivation of this latent infection can be caused by immunodeficiency, HIV-infection, use of corticosteroids, aging, alcohol and drug abuse.

TB has re-emerged as a serious public health threat worldwide because of a significant increase in multiple-drug-resistant TB and synergism between HIV and *M. tuberculosis* infection. Resolution of the current TB epidemic will require prevention of new TB infections as well as improved methods for treating existing ones. All this has made the search for new targets and the development of new antibiotic drugs a global emergency.

M. tuberculosis thymidine monophosphate kinase (TMPKmt), which phosphorylates dTMP to dTDP, is believed to be an attractive potential target for chemotherapeutic intervention because: (i) the enzyme lies at the junction of the *de novo* and salvage pathways for thymidine triphosphate (dTTP) and is the last specific enzyme for its synthesis,[2] (ii) *in vivo* studies with the *cdc*8 mutant in *Saccharomyces cerevisiae* have demonstrated that it is essential for DNA synthesis,[3,4] and (iii) sequence comparison of TMPKmt with the human enzyme reveals only a 22% sequence identity which should make the design of selective inhibitors possible.[5]

This enzyme has recently been crystallised by Li de la Sierra et al.[5] Examination of its X-ray structure (Figure 1) reveals that the main bonding forces between dTMP and the enzyme are: (i) a stacking interaction between the pyrimidine ring and Phe70, (ii) a hydrogen bond between *O*4 of thymine and the Arg74 side-chain which results in a preference for thymine over cytosine, (iii) a hydrogen bond between Asn100 and *N*3 of the thymine ring, (iv) a hydrogen bond between the 3’-hydroxyl of dTMP and the terminal carboxyl of Asp9, that in its turn interacts with the magnesium ion that is responsible for positioning the phosphate oxygen of TMP, and (v) hydrogen bonds and an ionic interaction between the 5’-*O*-phosphoryl group and Tyr39, Phe36, Arg95 and Mg^{2+} respectively.[5]

The presence of Tyr103 close to the 2'-position is believed to render the enzyme catalytically selective for 2'-deoxynucleotides versus *ribo* nucleotides.

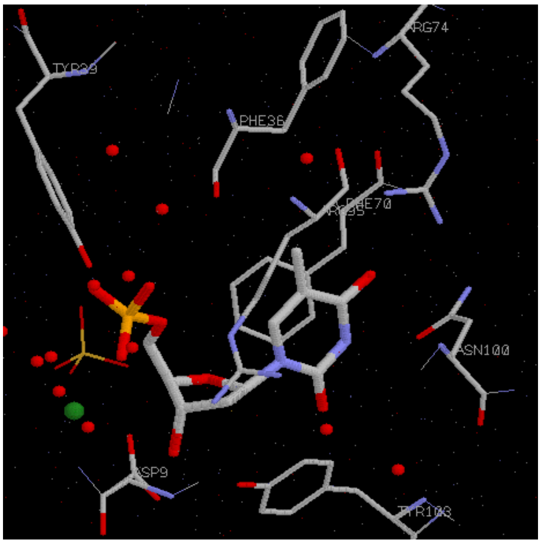

Figure 1: Simplified image of the dTMP binding site of M. tuberculosis*, complexed with dTMP and* SO_4^{2-}*, showing the most important amino acids interacting with dTMP. dTMP is pictured in bold, the water molecules as red spheres and the magnesium ion as a green sphere. A sulphate ion is located at the place normally occupied by the b -phosphate of ATP.*

Considering these interactions and the available K_i and K_m values of some nucleotides for TMPKmt,[6] we decided to make a series of nucleotides with modifications at the 2'- and 3'-positions of the dTMP scaffold in order to establish a preliminar structure activity relationship (SAR), that should be directive for the further design of inhibitors of TMPKmt.

3'-Azido-3'-deoxythymidine 5'-*O*-monophosphate (AZTMP) was the best known inhibitor so far with a K_i value of 10 μM.[6] Remarkably, the presence of the 3'-azido group totally abolishes its conversion by TMPKmt without significantly altering the affinity in comparison to dTMP. We assume that the azide moiety interacts directly with Asp9 and displaces the magnesium ion, which seriously disturbs the geometry of the active site.[5] To probe the effect of an amino group at the 3'-position, AZTMP was reduced to 3'-amino-3'-deoxythymidine 5'-*O*-monophosphate (**1**). The corresponding *ribo*-analogue **8**, was synthesised to examine the capability of Tyr103 to discriminate between *ribo*- and deoxy nucleotides. Introduction of an amino group at the 2'-position in **9**, on the other hand, could indicate if the positively charged nitrogen is able to interact with Tyr103 by a cation-π interaction.

To sort out the influence of the size and the electronegativity of 2'- and 3'-groups on the affinity for TMPKmt, a fluorine (**13**) and a chlorine (**12**) were introduced at C-2', and the 3'-hydroxyl was replaced by a fluorine (**20**). ^{1}H-NMR studies have demonstrated a relation between the electronegativity and the size of the substituents and the sugar puckering in a series of 2'-substituted-2'-deoxyadenosines.[7] Introduction of a fluorine increased the percentage of sugar that exhibits the 2'-*exo*-3'-*endo* conformation, while a 2'-chloro substitution favoured the 2'-*endo*-3'-*exo* conformation. The latter puckering is the one adopted by the sugar part of dTMP when bound to TMPKmt. It could be expected that nucleotide analogues that exhibit a similar S-type conformation would have a higher affinity for TMPKmt, than those that have to be forced into that configuration by the enzyme.

The synthetic methods used to prepare the desired dTMP analogues are outlined into Schemes 1 and 2. All phosphorylation steps were performed using the procedure of Yoshikawa et al.,[8] i.e. treatment with $POCl_3$ (3 eq.) in $(MeO)_3PO$. The obtained compounds were purified by column chromatography (iPrOH/ NH_4OH/H_2O : 77.5/15/2.5→60/30/5), followed by HPLC (C-18, CH_3CN/MeOH/0.05% HCOOH in H_2O : 45/45/10, 3 mL/min).

1-(3'-Azido-3'-deoxy-β-D-ribofuranosyl)thymine (**4**) was prepared by Vorbrüggen coupling[9] of sugar synthon **2**[10] with 5-methyl-2,4-bis[(trimethylsilyl)oxy]pyrimidine followed by alkaline deprotection, while its 2'-azido isomer **5** was obtained via opening of 2,2'-anhydro-thymidine (**3**) with NaN_3 in DMF according to the method of Verheyden.[11] Azidonucleosides **4** and **5** were converted to the corresponding amino nucleoside monophosphates **8** and **9** by sequential 5'-*O*-phosphorylation and reduction of the azido group with Ph_3P and NH_4OH.[12]

Compound **3** also served as synthon for the preparation of 2'-chlorothymidine[13] (**10**) and 2'-fluorothymidine (**11**). For the synthesis of the latter, **3** was treated with 3,4-dihydropyran in DMF, followed by saponification to yield its 3',5'-bisprotected arabinosyl derivative. Fluorination with DAST, followed by deprotection with *p*-toluenesulfonic acid in MeOH, afforded **11**.[14] Nucleosides **10** and **11** were converted to their monophosphates **12** and **13** in 53% and 55 % yield, respectively (Scheme 1).

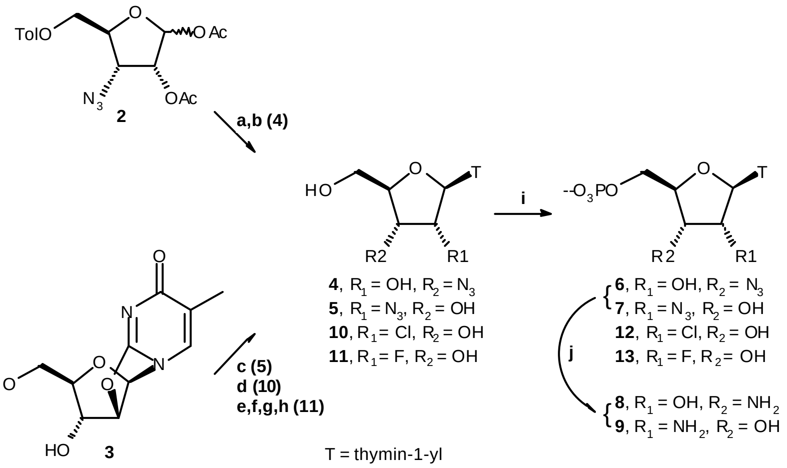

Scheme 1: Synthetic pathways of nucleotides 8, 9, 12 and 13. Reagents and conditions: (a) 5-methyl-2,4-bis[(trimethylsilyl)oxy]pyrimidine, $(CH_3)_3SiOSO_2CF_3$, $Cl_2(CH_2)_2$; (b) NH_3, MeOH; (c) NaN_3, DMF; (d) HCl, dioxane; (e) 3,4-dihydropyran, p*-toluenesulfonic acid, DMF; (f) 1N NaOH, MeOH; (g) DAST, CH_2Cl_2, pyridine; (h)* p*-toluenesulfonic acid, MeOH; (i) $POCl_3$, $(MeO)_3PO$; (j) Ph_3P, NH_4OH, pyridine.*

3'-Deoxy-3'-fluorothymidine (**19**) was synthesised from 5'-*O*-tritylthymidine (**14**), using the method of von Janta-Lipinski.[15] In our hands, treatment of the intermediate 3'-mesyl ester of **14** with NaOH in ethanol resulted in the formation of four reaction products: the desired SN2 product **18** (17% yield), as well as the 5'-*O*-tritylethers of 3'-*O*-ethylthymidine (**16**, 26 %), 3'-deoxy-2',3'-didehydrothymidine (**15**, 12 %) and 2,3'-anhydrothymidine (**17**, 33 %). **18** was then converted into **19** via treatment with DAST[16] and subsequent detritylation, and phosphorylation of **19** to give **20** (Scheme 2).

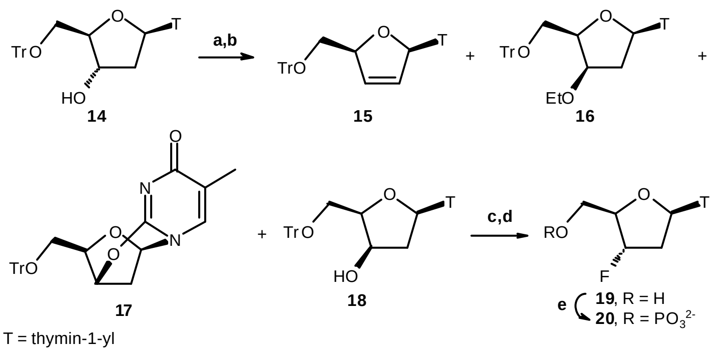

*Scheme 2: Synthetic pathway of nucleotide **20**. Reagents and conditions: (a) MsCl, pyridine; (b) NaOH, EtOH; (c) DAST, CH_2Cl_2, pyridine; (d) CH_3COOH, H_2O, 90°C; (e) $POCl_3$, $(MeO)_3PO$.*

All compounds were tested with the reported spectrophotometric assay.[17] The results are given in Table 1.

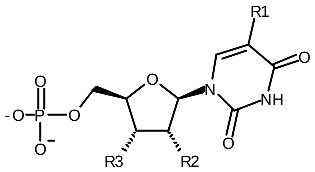

Compounds	R1	R2	R3	K_m (µM)	V_m[a]	K_i (µM)
dTMP	CH_3	H	OH	4.5	10.6	
dUMP[6]	H	H	OH	2100	3.5	
5F-dUMP[6]	F	H	OH	420	4.7	
5Br-dUMP[6]	Br	H	OH	33	9.8	
5I-dUMP[6]	I	H	OH	140	7.5	
AZTMP[6]	CH_3	H	N_3			10
1	CH_3	H	NH_2			235
8	CH_3	OH	NH_2			45
9	CH_3	NH_2	OH			120
12	CH_3	Cl	OH			19
13	CH_3	F	OH			43
D_4T-MP	CH_3	dehydro	dehydro	140	0.16	
20	CH_3	H	F	30	0.11	

Table 1: Kinetic parameters of TMPKmt with various nucleoside monophosphates.
[a] V_m in mmole/min.mg of protein

The K_i value of **1** increases 20-fold compared to AZTMP. This strongly suggests that the 3'-amino group doesn't succeed in interacting with Asp9 in contrast to AZTMP. To our surprise the *ribo*-analogue **8** shows good affinity (45 µM) for TMPKmt. A modeling experiment was suggestive for an interaction between the 3'-amino group and the carboxyl function of Asp9. According to the model, Tyr103, believed to discriminate between deoxy- and *ribo* nucleotides, remained further away from the C-2' compared to the X-ray structure of TMPKmt with dTMP. Analogue **8** represents a first example of a *ribo*-nucleotide with good affinity for TMPKmt. The higher K_i value of 2'-amino dTMP (**9**) suggests that the positively charged nitrogen is not capable of interacting favourably with Tyr103 or Asp9. The monophosphate of d_4T (D_4TMP) behaves as substrate for TMPKmt, although its K_m-value is 30 times larger than that of the natural substrate.

The introduction of halogens at the 2'-position appears to be better tolerated than a hydroxyl group at that position. **12** exhibits appreciable affinity with a K_i value of 19 µM. Changing the chlorine of **12** for a fluorine (**13**) leads to a 2-fold affinity drop. A modeling experiment of **12** (results not shown) showed that introduction of the chlorine affects the relative position of the sugar ring. As a result, the 2'-chlorine occupies the pocket where normally the 3'-hydroxyl group resides. Indeed, the 3'-analogues indicate that this particular domain can accommodate larger substituents. The somewhat lower affinity of the 2'-fluoro nucleotide could be due to the fact that the smaller and more electronegative fluorine is not able to fill up that cavity, perhaps as a result of a different preferential sugar pucker.

Replacement of the 3'-OH of dTMP by a 3'-F in **20** affords an analogue that behaves as a substrate with a K_m of 30 µM.

In conclusion, only a few dTMP analogues, i.e. the 5-halogeno derivatives, d_4T-MP, dUMP and 3'-deoxy-3'-fluorothymidine 5'-*O*-monophosphate (**20**), remain substrates for TMPKmt, while other modifications lead up to competitive inhibitors. The introduction of a bromine, the best known 5-modification so far, doesn't drastically lower the affinity in comparison to dTMP.

Among the tested analogues in the ribo configuration (**8**, **9**, **12**, **13**), the best inhibition is obtained by the introduction of a 2'-chlorine and the replacement of the 3'-OH by an azido group. From these results it seems interesting to combine a 2'-chlorine and 3'-azido group and to explore other substitution patterns at the 3'-position. Because modeling experiments show that there's a lot of space at the 3'-position, introduction of larger nitrogen containing compounds that could interact with Asp9 will be the basis for further development of more potent ligands.

Experimental section

NMR spectra were obtained with Varian Mercury 300 and 500 spectrometers. Chemical shifts are given in ppm (δ) relative to residual solvent peak of DMSO-d_6 (2.5 ppm). All signals assigned to amino and hydroxyl groups were exchangeable with D_2O. Mass spectra and exact mass measurements were performed on a quadrupole/orthogonal-acceleration time-of-flight (Q/oaTOF) tandem mass spectrometer (qTof 2, Micromass, Manchester, UK) equipped with a standard electrospray ionisation (ESI) interface. Samples were infused in a 2-propanol:water (1:1) mixture at 3 µL/min. Precoated Merck silica gel F_{254} plates were used for TLC and spots were examined under UV light at 254 nm and revealed by sulfuric acid-anisaldehyde spray. Column chromatography was performed on Uetikon silica (0.2-0.06 mm). Anhydrous solvents were purchased from Acros Organics.

General procedure for the selective phosphorylation of the 5'-hydroxylgroup

A solution of the nucleoside (0.42 mmol) in trimethyl phosphate (4 mL) was cooled to 0° C, $POCl_3$ (0.25 mL, 2.70 mmol) was added dropwise and the mixture was stirred for 5 h at 0° C and for 30 min at room temperature. The mixture was poured into ice-water (10 mL), neutralised with concentrated NH_4OH and evaporated to dryness. The resulting residue was purified by column chromatography (iPrOH-NH_4OH-H_2O 77.5:15:2.5→60:30:5). Further purification of the white powder by HPLC (C-18, CH_3CN-MeOH-0.05% HCOOH in H_2O 45:45:10, 3 mL/min) and lyophilisation of the fractions containing the formed nucleotide, provided it as a white powder.

1-(3-Amino-3-deoxy-5-*O*-phosphoryl-b -D-ribofuranosyl)thymine (8)

1-(3-Azido-3-deoxy-β-D-ribofuranosyl)thymine[18] was phosphorylated according to the general procedure described above in a 48 % yield. The obtained nucleotide **6** (145 mg, 0.40 mmol) and triphenylphosphine (230 mg, 1.22 mmol) were then dissolved in pyridine (6 mL) and stirred at room temperature. After 1h, concentrated NH_4OH (4 mL) was added and the solution was allowed to stir for an additional 6.5 h. Pyridine was removed under reduced pressure, water (20 mL) was added and the unreacted triphenylphosphine and triphenylphosphine oxide were removed by filtration. The filtrate was extracted with toluene and the water layer was evaporated under reduced pressure to give a syrup. The syrup was purified via column chromatography (iPrOH-NH_4OH-H_2O 77.5:15:2.5→60:30:5). Further purification of the white powder by HPLC (C-18, CH_3CN-MeOH-0.05% HCOOH in H_2O 45:45:10, 3 mL/min) and lyophilisation of the fractions containing the formed nucleotide, yielded **8** (101 mg, 71 %) as a white powder. ^1H-NMR: (300 MHz, D_2O) *d* 1.75 (3 H, d, 5-CH_3), 3.82 (1H, t, H-3'), 3.93 (2H, dd, H-5'), 4.27 (1H, dt, H-4'), 4.49 (1H, dd, *J* = 3.6 and 6.3 Hz, H-2'), 5.77 (1H, dd, *J* = 3.6 Hz, H-1'), 7.58 (1H, d, *J* = 1.2 Hz, H-6); ^{13}C-NMR: (125 MHz, D_2O) *d* 14.21 (5-CH_3), 54.20 (C-3'), 65.72 (C-5', $^2J_{C, P}$ = 3.9 Hz), 75.10 (C-2'), 82.84 (C-4', $^3J_{C, P}$ = 6.8 Hz), 95.35 (C-1'), 114.29 (C-5), 140.19 (C-6), 154.30 (C-2), 169.19 (C-4); ^{31}P-NMR: (500 MHz, D_2O) *d* 3.40; HRMS (ESI-MS) for $C_{10}H_{17}N_3O_8P$ $[M+H]^+$: found 338.0745; calcd, 338.0753.

1-(2-Amino-2-deoxy-5-*O*-phosphoryl-b -D-ribofuranosyl)thymine (9)

2'-Azido-2'-deoxythymidine[11] (**5**) was phosphorylated according to the general procedure described above in a 56 % yield. The obtained nucleotide **7** (201 mg, 0.51 mmol) and triphenylphosphine (410 mg, 1.56 mmol) were dissolved in pyridine (8 mL) and stirred at room temperature. After 1h, concentrated NH_4OH (5 mL) was added and the solution was allowed to stir for an additional 4 h. Pyridine was removed at reduced pressure, water (20 mL) was added and the unreacted triphenylphosphine and triphenylphosphine oxide were removed by filtration. The filtrate was extracted with toluene and the water layer was evaporated under reduced pressure to give a syrup. The resulting syrup was purified by column chromatography (iPrOH-NH_4OH-H_2O 77.5:15:2.5→60:30:5). Further purification of the white powder by HPLC (C-18, CH_3CN-MeOH-0.05% HCOOH in H_2O 45:45:10, 3 mL/min) and lyophilisation of the fractions containing the formed nucleotide yielded **9** (101 mg, 71 %) as a white powder. ^1H-NMR: (300 MHz, D_2O) *d* 1.77 (3 H, s, 5-CH_3), 3.84 (3H, m, H-2' and H-5'), 4.20 and 4.39 (2H, br s and app. d, H3' and H-4'), 6.06 (1H, d, *J* = 8.4 Hz, H-1'), 7.68 (1H, s, H-6); ^{13}C-NMR: (125 MHz, D_2O) *d* 14.28 (5-CH_3), 58.88 (C-2'), 66.81 (C-5', $^2J_{C, P}$ = 3.9 Hz), 73.32 (C-3'), 88.43 (C-4', $^3J_{C, P}$ = 7.8 Hz), 88.88 (C-1'), 114.93 (C-5), 139.54 (C-6), 154.81 (C-2), 169.08 (C-4); ^{31}P-NMR: (500 MHz, D_2O) *d* 2.83; HRMS (ESI-MS) for $C_{10}H_{17}N_3O_8P$ $[M+H]^+$: found 338.0750; calcd, 338.0753.

1-(2'-Chloro-2'-deoxy-b -D-ribofuranosyl)thymine (10)[13]

An ice-cooled suspension of 2,2'-anhydrothymidine[13] (340 mg, 1.41 mmol) in dry dioxane (20 mL) was saturated with anhydrous hydrogen chloride. The mixture was heated in a glass cylinder at 75-80° C for 24 h. After cooling, the yellow solution was concentrated and the obtained residue purified by column chromatography (CH_2Cl_2-MeOH 99:1→97:3), yielding **10** (195 mg, 50%) as a white foam. ^1H-NMR: (300 MHz, DMSO-d6) *d* 1.78 (3 H, s, 5-CH_3), 3.57-3.70 (2H, m, H-5'), 3.93 (1H, app. q, H-4'), 4.21 (1H, dd, H-3'), 4.55 (1H, t, H-2'), 5.23 (1H, t, *J* = 5.1 Hz, 5'-OH), 5.84 (1H, d, *J* = 5.5 Hz, 3'-OH), 6.03 (1H, d, *J* = 6.3 Hz, H-1'), 7.78 (1H, d, *J* = 1.1 Hz, 6-H); HRMS (ESI-MS) for $C_{10}H_{13}ClN_2O_5Na$ $[M+Na]^+$: found 299.0443; calcd, 299.0410.

1-(2’-Chloro-2’-deoxy-5’-*O*-phosphoryl-β-D-ribofuranosyl)thymine (12)

10 (116 mg, 0.42 mmol) was phosphorylated according to the general procedure described above yielding **12** (78.94 mg, 53 %) as a white powder. ^{1}H-NMR: (300 MHz, D_2O) δ 1.93 (3 H, s, 5-CH_3), 4.00-4.22 (2H, m, H-5’), 4.39 (1H, m, H-4’), 4.54 (1H, t, H-3’), 4.66 (1H, t, H-2’), 6.20 (1H, d, *J* = 6.0 Hz, H-1’), 7.82 (1H, d, *J* = 1.0 Hz, H-6); ^{31}P-NMR: (500 MHz, D_2O) δ 0.88 ppm; HRMS (ESI-MS) for $C_{10}H_{14}ClN_2O_8PNa$ $[M+Na]^+$: found 379.0112; calcd, 379.0112.

1-(2’-Deoxy-2’-fluoro-β-D-ribofuranosyl)thymine (11)[14]

To a suspension of 2,2'-anhydrothymidine[13] (880 mg, 3.46 mmol) in DMF (15 mL) and 3,4-dihydro-2*H*-pyran (8.8 mL, 96.45 mmol) was added *p*-toluenesulfonic acid (683 mg, 3.59 mmol) at 0° C for 4 h, at which time a clear solution was obtained. This was neutralised with Et_3N (1.5 mL) and concentrated. The residue was dissolved in EtOAc, washed with saturated $NaHCO_3$ and dried over $MgSO_4$. Removal of the solvent gave a residue which was triturated with hexane. The solid cake was collected and washed with hexane to give 1-[2,2'-anhydro-3-*O*-5-*O*-di(tetrahydro-2*H*-pyran-2-yl)-β-D-arabinofuranosyl]thymine as a white solid. This was dissolved in MeOH (11 mL) and 1 N NaOH (11 mL) and was stirred at room temperature for 2 h. The solution was then neutralised with diluted acetic acid. The mixture was evaporated to dryness and the residue was purified by column chromatography (EtOAc) to give 1-[3-*O*-5-*O*-di(tetrahydro-2*H*-pyran-2-yl)-β-D-arabinofuranosyl]thymine (750 mg, 51 %) as a white solid. To a stirred mixture of the aforementioned nucleoside (750 mg, 1.76 mmol) in CH_2Cl_2 (10 mL) and pyridine (2 mL), cooled at -60°C under a nitrogen atmosphere, was added DAST (0.72 mL, 5.46 mmol). The resulting mixture was slowly warmed to room temperature and then refluxed for 4 h. The reaction was quenched with aqueous saturated $NaHCO_3$ and ice-water, extracted with CH_2Cl_2 (3 x 10 mL) and dried ($MgSO_4$). Removal of the solvent yielded crude 1-(2-deoxy-3,5-*O*-di(tetrahydro-2*H*-pyran-2-yl)-2-fluoro-β-D-ribofuranosyl)thymine as a dark-brown syrup. This was dissolved in MeOH (10 mL) and treated with *p*-toluenesulfonic acid (420 mg, 2.21 mmol) at room temperature for 3 h. The mixture was then neutralised with Et_3N (7 mL) and evaporated under reduced pressure. The obtained residue was purified by column chromatography (CH_2Cl_2-MeOH, 97:3 → 95:5) to yield **11**(270 mg, 59 %) as a white foam.^{1}H-NMR: (300 MHz, DMSO-d_6) δ 1.76 (3 H, s, 5-CH_3), 3.57-3.79 (2H, m, H-5’), 3.86 (1H, m, H-4’), 4.17 (1H, m, $J_{3’\text{-H, F}}$ = 20.2 Hz, 3’-H), 5.03 (1H, ddd, $J_{\text{H-2’, F}}$ = 53.2 Hz, 2’-H), 5.24 (1H, t, *J* = 4.8 Hz, 5’-OH), 5.61 (1H, d, *J* = 6.3 Hz, 3’-OH), 5.91 (1H, dd, $J_{\text{H-1’, H-2’}}$ = 2.3 Hz, $J_{\text{H-1’, F}}$ = 17.6 Hz, H-1’), 7.62 (1H, d, *J* = 1.2 Hz, 6-H); ^{19}F-NMR: (300 MHz, D_2O) δ -203.08; HRMS (ESI-MS) for $C_{10}H_{13}FN_2O_5Na$ $[M+Na]^+$: found 283.0733; calcd, 283.0706.

1-(2’-Deoxy-2’-fluoro-5’-*O*-phosphoryl-β-D-ribofuranosyl)thymine (13)

11 was phosphorylated according to the general procedure affording **13** (65.16 mg, 48 %) as a white powder. ^{1}H-NMR: (300 MHz, D_2O) δ 1.92 (3 H, s, 5-CH_3), 4.07 (1H, m, H-5'A), 4.23 (1H, m, H-5'B), 4.27 (1H, app. d, H-4’), 4.49 (1H, ddd, $J_{\text{H-3,’ F}}$ = 19.9 Hz, H-3’), 5.14-5.25 (1H, ddd, $J_{\text{H-2’, F}}$ = 52,5 Hz, H-2’), 6.06 (1H, dd, $J_{\text{H-1’, H-2’}}$ = 7.9 Hz, $J_{\text{H-1’, F}}$ = 18.1 Hz, H-1’), 7.76 (1H, d, $J_{\text{H-6, 5-CH3}}$ = 1.2 Hz, H-6) ppm; ^{13}C-NMR: (125 MHz, D_2O) δ 14.19 (5-CH_3), 65.60 (C-5’, $^2J_{\text{C, P}}$ = 3.9 Hz), 70.52 (C-3’, $^2J_{\text{C, F}}$ = 15.6 Hz), 84.30 (C-4’, $^3J_{\text{C, P}}$ = 9.8 Hz), 90.76 (C-1’, $^2J_{\text{C, F}}$ = 35.1Hz), 95.91 (C-2’, $^1J_{\text{C, F}}$ = 185.6 Hz), 114.17 (C-5), 140.08 (C-6); ^{19}F-NMR: (300 MHz, D_2O) δ -203.63 ppm; ^{31}P-NMR: (500 MHz, D_2O) δ 1.22; HRMS (ESI-MS) for $C_{10}H_{14}FN_2O_8P$ $[M+H]^+$: found 341.0576; calcd, 341.0549.

1-(2’-Deoxy-5’-*O*-trityl-b-D-*threo*-pentofuranosyl)thymine (18)

To an ice-cooled solution of **14**[15] (1.45 g, 3.39 mmol) in pyridine (15 mL), was added methanesulfonyl chloride (0.70 mL, 8.75 mmol). The reaction mixture was kept overnight at room temperature. Water (0.5 mL) was added and the solution was poured into vigorously stirring ice-water (540 mL). The resulting amorphous precipitate was collected by filtration, washed with water and coevaporated with EtOH to yield pure 1-(2’-deoxy-3’-*O*-methanesulfonyl-5’-*O*-trityl-β-D-*erythro*-pentofuranosyl)thymine, which was immediately used in the next step without further purification. It was dissolved in EtOH (25 mL) and heated at reflux. Sodium hydroxide (156 mg, 3.9 mmol) was added, and refluxing was continued for 1.5 h. After cooling to room temperature, the reaction mixture was concentrated to 10 mL and poured into water (250 mL). The turbid solution was extracted with $CHCl_3$ (2 x 150 mL). The combined organic layers were dried over $MgSO_4$, filtered and evaporated. The resulting residue was purified by column chromatography ($CHCl_3$-MeOH-Et_3N, 99:1:0.1) yielding **18** (279 mg, 17 %) as a foam. Apart from the expected **18**, three other products were formed. These were isolated and characterised as 1-(2’-deoxy-3'-*O*-ethtyl-5’-*O*-trityl-β-D-*threo*-pentofuranosyl)thymine (**16**) (452 mg, 26 %), 3'-deoxy-2',3'-didehydro-5'-*O*-tritylthymidine (**15**) (189 mg, 12 %) and 2,3'-anhydro-5'-*O*-tritylthymidine (**17**) (522 mg, 33 %). **18** ^{1}H-NMR: (300 MHz, DMSO-d_6) *d* 1.66 (3 H, s, 5-CH_3), 1.86 (1H, app d, H-2’), 2.54 (1H, m, H-2’), 3.19-3.34 (2H, m, H-5’), 4.11 (1H, m, H-4’), 4.22 (1H, m, H-3’), 5.22 (1H, br. s, 3’-OH), 6.14 (1H, app. d, *J* = 8.0 Hz, H-1’), 7.25-7.45 (15 H, m, CPh_3), 7.61 (1H, br. s, 6-H); MS (ES, iPrOH/H_2O): m/z (%) 507.1 ($[M+Na]^+$, 100); **17** ^{1}H-NMR: (300 MHz, DMSO-d_6) *d* 1.79 (3H, s, 5-CH_3), 2.43-2.61 (2H, m, H-2’), 3.09-3.16 (2H, m, H-5’), 4.47 (1H, m, H-4’), 5.33 (1H, br. s, H-3’), 5.90 (1H, d, *J* = 3.3 Hz, H-1’), 7.20-7.40 (15H, m, CPh_3), 7.64 (1H, s, H-6) ppm; MS(ES, iPrOH/H_2O): m/z (%) 467.2 ($[M+H]^+$, 100); **15** ^{1}H-NMR: (300 MHz, DMSO-d_6) *d* 1.24 (3H, s, 5-CH_3), 3.19 (2H, m, H-5’), 4.97 (1H, br. s, H-4’), 6.03 and 6.54 (2H, 2d, H-2’ and H-3’), 6.85 (1H, t, *J* = 1.6 Hz, H-1’), 7.24-7.38 (15H, m, Ph_3C); MS(ES, iPrOH/H_2O): m/z (%) 489.1 ($[M+Na]^+$, 100); **16** ^{1}H-NMR: (300 MHz, DMSO-d_6) *d* 1.33 (3H, t, *J* = 7.06 Hz, OCH_2CH_3), 1.67 (3H, s, 5-CH_3), 1.95 (1H, d), 2.57 (1H, m, H-2’A and H-2’B), 3.20-3.44 (4H, m, H-3’, H-4’ and H-5’), 4.36 (2H, q, CH_2CH_3), 6.10 (1H, dd, *J* = 1.6 and 7.9 Hz, H-1’), 7.25-7.36 (15H, m, Ph_3C), 7.44 (1H, s, 6-H); MS(ES, iPrOH/H_2O): m/z (%) 513.2 ($[M+H]^+$, 100). Treatment of **17** (460 mg, 0.95 mmol) with a mixture of NaOH 1 N (7 mL), MeOH (12 mL) and dioxane (15 mL) at room temperature during 2 h, followed by neutralisation with diluted acetic acid, evaporation en column chromatography (EtOAc, 100 %) yielded **18** (377 mg, 82 %).

3'-Deoxy-3'-fluorothymidine (19)

A solution of **18** (480 mg, 0.99 mmol) in dichloromethane (10 mL) was treated with DAST (0.23 mL, 1.73 mmol) and the reaction mixture was stirred at room temperature for 3h. The mixture was diluted with chloroform (30 mL) and extracted with saturated aqueous $NaHCO_3$ (40 mL). The organic layer was dried over $MgSO_4$, evaporated and the obtained residue was purified by column chromatography ($CHCl_3$-MeOH-Et_3N 99:1:0.1) yielding 3'-deoxy-3'-fluoro-5'-*O*-tritylthymidine (130 mg, 27 %) as a white foam. This foam (120 mg, 0.25 mmol) was treated with aqueous acetic acid (80%, 10 mL) and was heated at 90° C for 15 min. After cooling, the solvent was removed under reduced pressure, and the residue purified by column chromatography (CH_2Cl_2-MeOH, 98:2) yielding **19** (24.11 mg, 40 %) as a white foam. ^{1}H-NMR: (300 MHz, DMSO-d_6) *d* 1.78 (3 H, s, 5-CH_3), 2.21-2.45 (2H, m, H-2’), 2.55-2.67 (1H, m, H-5’), 4.13 and 4.17 (1H, dt, $J_{H\text{-}4', F}$ = 27.8 Hz, H-4’), 5.23 (1H, under signal 3’-H, 5’-OH), 5.24 and 5.36 (1H, app. dd, $J_{H\text{-}3', F}$ = 53.9 Hz, H-3’), 6.22 (1H, dd, $J_{H\text{-}1', H\text{-}2'}$ = 5.5 Hz and 9.3 Hz, H-1’), 7.72 (1H, br. s, 6-H); HRMS (ESI-MS) for $C_{10}H_{13}FN_2O_4Na$ $[M+Na]^+$: found 267.0770; calcd, 267.0757.

References

---

[1] Stokstad, E. Infectious Disease - Drug-Resistant TB on The Rise. *Science* **2000**, *287*, 2391.

[2] Anderson, E. P. In *The enzymes*; Boyer P. D., Ed.; Academic Press: New York, 1973; Academic Press, New York Vol. 8, pp 49-96.

[3] Jong, A. Y. S.; Campbell, J. L. Characterisation of *Saccharomyces cerevisiae* thymidylate kinase, the CDC8 gene product. General properties, kinetic analysis, and subcellular localisation. *J. Biol. Chem.* **1984**, *259*, 14394–14398.

[4] Sclafani, R. A.; Fangman, W. L. Yeast gene *cdc8* encodes thymidilate kinase and is complemented by herpes thymidine kinase gene TK. *Proc. Natl. Acad. Sci.* **1984**, *81*, 5821–5825.

[5] Li de la Sierra, I.; Munier-Lehmann, H.; Gilles, A. M.; Bârzu, O.; Delarue, M. X-ray Structure of TMP Kinase from *Mycobacterium tuberculosis* Complexed with TMP at 1.95 Å Resolution. *J. Mol. Biol.* **2001**, *311*, 87–100.

[6] Munier-Lehmann, H.; Chaffotte, A.; Pochet, S.; Labesse, G. Thymidylate kinase of *Mycobaterium tuberculosis*: A chimera sharing properties common to eukaryotic and bacterial enzymes. *Protein Sci.* **2001**, *10*, 1195–1205.

[7] Uesugi, S.; Miki, H.; Ikehara, M.; Iwahashi, H.; Kyogoku, Y. Linear Relationship Between Electronegativity of 2'-Substituents and Conformation of Adenine Nucleosides. *Tetrahedron Lett.* **1979**, *42*, 4073–4076.

[8] Yoshikawa, M.; Kato, T.; Takenishi, T. *B.* Studies of Phosphorylation. III. Selective Phosphorylation of Unprotected Nucleosides. *Chem. Soc. Jpn.* **1969**, *42*, 3505–3508.

[9] Vorbrüggen, H.; Krolikiewicz, K.; Bennua, B. Synthesis with Trimethylsilyl Triflate and Perchlorate as Catalists. *Chem. Ber.* **1981**, *114*, 1234–1255.

[10] Ozols, A. M.; Azhayev, A. V.; Dyatkina, N. B.; Krayevsky, A. A. Aminonucleosides and their derivatives. 6. A new synthesis of 1,2,5-tri-*O*-acyl-3-azido-3-deoxy-beta-D-ribofuranose. *Synthesis.* **1980**, *7*, 557–559.

[11] Verheyden, J. P. H.; Wagner, D.; Moffat, J. G. Synthesis of Some Pyrimidine 2'-Amino-2'-deoxynucleosides. *J. Org. Chem.* **1971**, *36*, 250–254.

[12] Azhayev, A. V.; Ozols, A.; Bushnev, A. S.; Dyatkina, N. B.; Kochetkova, S. V.; Viktorova, L. S.; Kukhanova, M. K.; Kraevskii, A. A.; Gottikh, B. P. Aminonucleosides and their derivatives. 4. Synthesis of the 3'-amino-3'-deoxynucleoside 5'-phosphates *Nucleic Acids Res.* **1979**, *6*, 625–643.

[13] Codington, J. F.; Doerr, I. L.; Fox, J. J. Synthesis of 2’-Fluorothymidine, 2’-Fluorodeoxyuridine and Other 2’-Halogeno-2’-Deoxy Nucleosides. *J. Am. Chem. Soc.* **1964**, *29*, 558–564.

[14] Choi, Y.; Li L.; Grill, S.; Gullen E.; Lee, C. S.; Gumina, G.; Tsujii E.; Cheng, Y. C. Chu, C. K. Structure-Activity Relationships of (*E*)-5-(2-Bromovinyl)uracil and Related Pyrimidine Nucleosides as Antiviral Agents for Herpes Viruses. *J. Med. Chem.* **2000**, *43*, 2538–2546.

[15] Von Janta-Lipinski, M.; ,Costisella, B.; Ochs, H.; Hübscher, U.; Hafkemeyer, P.; Matthes, E. Newly Synthesised L-Enantiomers of 3'-Fluoro-Modified β-2'-Deoxyribonucleoside 5'-Triphosphates Inhibit Hepatitis B DNA Polymerase But Not the Five Cellular DNA Polymerases α, β, γ, δ, ε Nor HIV-1 Reverse Transcriptase. *J. Med. Chem.* **1998**, *41*, 2040–2046.

[16] Herdewijn, P.; Van Aerschot, A.; Kerremans, L. Synthesis of nucleosides fluorinated in the sugar moiety- the application of diethylaminosulfur trifluoride to the synthesis of fluorinated nucleosides. *Nucleosides and Nucleotides* **1989**, *8*, 65–96.

[17] Blondin, C.; Serina, L.; Wiesmüller, L.; Gilles, A. M.; Bârzu, O. Improved Spectrophotometric Assay of Nucleoside Monophosphate Kinase Activity Using Pyruvate Kinase/Lactate Dehydrogenase Coupling System. *Anal. Biochem.* **1994**, *220*, 219–222.

[18] Gryaznov, S.; Winter, H. RNA mimetics: oligoribonucleotide N3'→P5' phospohoramidates. *Nucleic Acids Research.* **1998**, *26*, 4160–4167.

Chapter 3

ENZYMATIC AND STRUCTURAL ANALYSIS OF INHIBITORS DESIGNED AGAINST *M. TUBERCULOSIS* THYMIDYLATE KINASE: NEW INSIGHTS INTO THE PHOSPHORYL TRANSFER MECHANISM

Ahmed Haouz, Veerle Vanheusden, Hélène Munier-Lehmann, Matheus Froeyen, Piet Herdewijn, Serge Van Calenbergh and Marc Delarue

J. Biol. Chem. **2003**, *278*, 4963-4971

ENZYMATIC AND STRUCTURAL ANALYSIS OF INHIBITORS DESIGNED AGAINST *M. TUBERCULOSIS* THYMIDYLATE KINASE: NEW INSIGHTS INTO THE PHOSPHORYL TRANSFER MECHANISM

Ahmed Haouz, Veerle Vanheusden, Hélène Munier-Lehmann, Matheus Froeyen, Piet Herdewijn, Serge Van Calenbergh and Marc Delarue

J. Biol. Chem. **2003**, *278*, 4963-4971

Abstract

The chemical synthesis of new compounds designed as inhibitors of M. tuberculosis *thymidine monophosphate kinase (TMPK) is reported. The synthesis concerns dTMP analogues modified at the 5-position of the thymine ring, as well as a novel compound with a six-membered sugar ring. The binding properties of the analogues are compared with the known inhibitor AZTMP, which is postulated here to work by excluding the dTMP-bound magnesium-ion. The crystallographic structure of the complex of one of the compounds, 5-*CH_2OH*-dUMP, with TMPK has been determined at 2.0 Å. It reveals a major conformation for the hydroxyl group in contact with a water molecule and a minor conformation pointing towards Ser99. Looking for a role for Ser99, we have identified an unusual catalytic triad, or a proton wire, made of strictly conserved residues (including Glu6, Ser99, Arg95 and Asp9), that probably serves to protonate the transferred* PO_3^{2-} *group. The crystallographic structure of the commercially available bisubstrate analog* Ap_5T *bound to TMPK is also reported at 2.45 Å and reveals an alternative binding pocket for the adenine moiety of the molecule, compared with what is observed either in the* E. coli *or the yeast enzyme structures. This alternative binding pocket opens a way for the design of a new family of specific inhibitors.*

Introduction

The incidence of tuberculosis (TB) has been increasing during the last twenty years; it is now the first cause of mortality among infectious diseases in the world.[1] The combination of four active drugs (rifampicin, isoniazid, pyrazinamide and ethambutol or streptomycin) is currently used in *Mycobacterium tuberculosis* treatment but this has led to the appearance of resistant bacterial strains.[2] These resistant strains are alarming for two reasons. First, as there are only few effective drugs available, infection with drug-resistant strains could give rise to a potentially untreatable form of the disease. Second, although only 5% of immunocompetent people infected with *M. tuberculosis* succumb to the disease, it is nevertheless highly contagious.[3] Therefore, a large effort is necessary to identify potential new targets and inhibitors.

An attractive potential target is thymidylate kinase (EC. 2.7.4.9; ATP: dTMP phosphotransferase; TMPK)[1], an essential enzyme that catalyses an obligatory step in the synthesis of thymidine triphosphate (dTTP) either from thymidine via thymidine kinase (salvage pathway) or from dUMP via thymidylate synthase in all living cells.[4] This enzyme phosphorylates thymidine monophosphate (dTMP) into thymidine diphosphate (dTDP), using ATP as the preferred phosphoryl donor.

In the case of the herpes simplex virus (HSV), the most successful antiviral drug (acyclovir) available on the market is directed against thymidine kinase (TK). Acyclovir is phosphorylated by several viral or host kinases into acyclovir triphosphate, which terminates DNA synthesis when incorporated into the viral DNA.[5,6] The comparative X-ray structures of different enzyme/ligands complexes of HSV-1 thymidine kinase[7,8,9,10] revealed a number of interesting structural features and paved the way for rational structure-based drug design of antiviral compounds.[11,12] A similar approach might lead to potent anti-tuberculosis agents.

TMPK from *M. tuberculosis* is a homodimer with 214 amino acids per monomer.[13] The X-ray three-dimensional structure has been recently solved at 1.95 Å resolution[14,15] as a complex with dTMP, thereby making it possible to initiate structure-based drug design studies. The global folding of the protein is similar to that of the other TMPKs and NMPKs despite the low similarity of their amino-acid sequences. The TMPK backbone is characterised by nine solvent-exposed α-helices surrounding a central β-sheet made of five β-strands, typical of the so-called Rossmann-fold.[16,17,18,19,20] However, the dimerisation mode of the *M. tuberculosis* enzyme differs from that reported in the yeast, human and *E. coli* enzymes.[15]

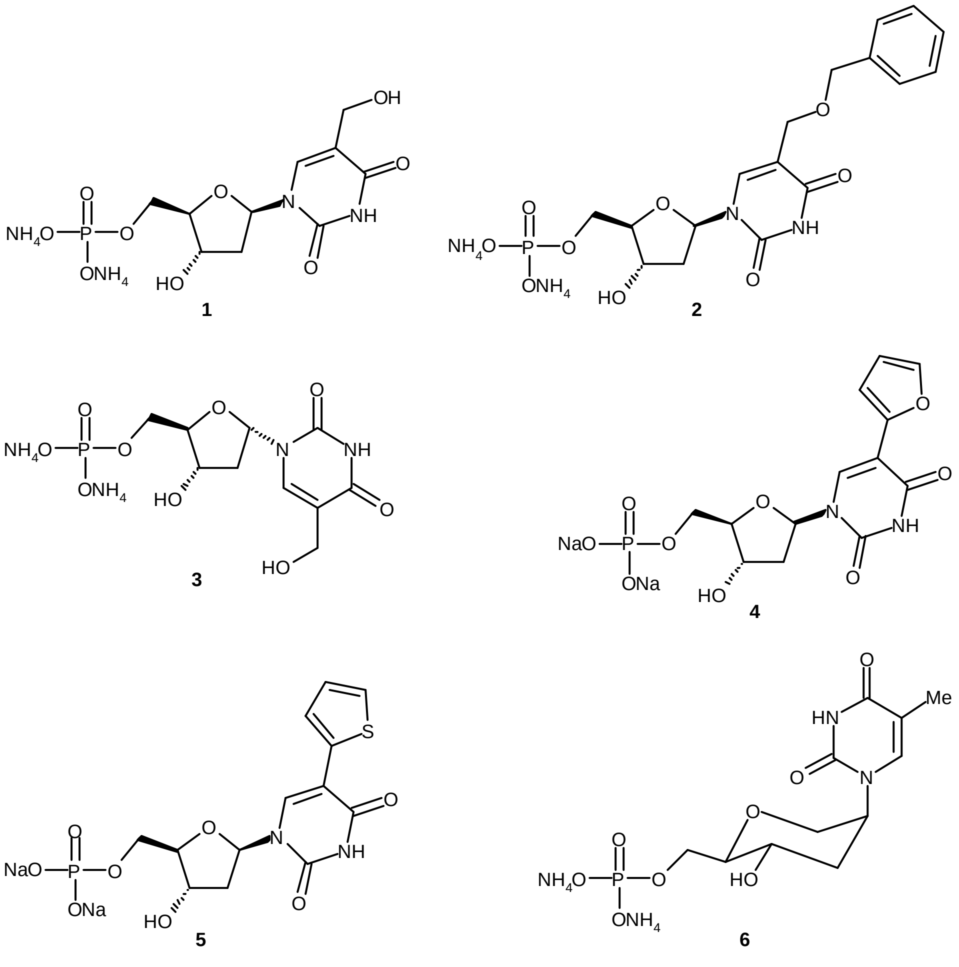

Figure 1: Chemical structure of synthesised dTMP analogues.

The active site of *M. tuberculosis* TMPK complexed with dTMP differs from the other known TMPKs in the following ways.[15] It is in a fully closed conformation, with the ATP binding site being already preformed and the LID region well ordered into an α-helical conformation, even though the second substrate ATP (or non-hydrolysable ATP) is absent from the structure. In the dTMP binding site, the protein-dTMP interaction shows three specific features when compared to yeast, human or *E. coli* enzyme structures. The first feature involves both a magnesium ion and Tyr39; they interact with two opposite non-bridging oxygens of the phosphate moiety of dTMP. The second feature involves Asn100 in contact with atom N3 of the base moiety.[15] The third feature, perhaps more amenable to the design of new inhibitors, is the interaction of the 3'-OH atom of dTMP with both the side chain of Asp9 and a water molecule, W9, which is a ligand of the Mg^{++} ion. In addition, there is a high concentration of positively charged side chains both from the LID region and from the P-loop, with arginine residues 14, 95, 149, and 160 as well as Lys13.[15] Examination of the structure therefore suggested the following targets for species-specific inhibitors.

Target 1. The 3'-OH and 2'-OH groups of the ribose ring could be systematically replaced with different chemical groups; this has been recently reported.[21]

Target 2. The 5-position of the thymine ring is another possibility, which has also been considered in the past for HSV thymidine kinase inhibitors.[11,12] Preliminary results of compounds modified at this position have already been reported.[13] Here we report results on other compounds, with the aim of adding an extra hydrogen bond with water molecule W12 detected in the three-dimensional structure. W12 is located close to Pro37 (which is in a cis conformation) and forms hydrogen bonds with residues building up the thymidine binding cavity, such as Phe70, Asp73 and Arg74.

Target 3. The 2-position of the thymine ring could also be explored and preliminary but encouraging results have been reported for one compound modified at this position.[13] The aim here is to replace the inserted (space filling) water molecules W2 and W3 which, if removed, give rise to a well defined cavity that can be readily materialised with computer programs such as VOIDOO.[22]

In this study we have synthesised five dTMP analogues (**1**-**5**, Figure 1), modified at the thymine moiety and focused on target 2. In addition, one member of a new class of nucleotide analogues has been tested,[23,24] namely a 1-5 anhydrohexitol analog **6** of dTMP, where the 3'-OH and/or of the 5'-*O*-phosphate positions are expected to depend on the sugar conformation. The inhibitiory effect of these dTMP analogues has been measured in vitro by a novel direct specific enzymatic activity test using HPLC and compared to the reference compound AZTMP, which is a good inhibitor.[13]

All compounds have been subjected to co-crystallisation experiments as well as soaking experiments for exchange with dTMP in dTMP-TMPK crystals (*M. tuberculosis* TMPK does not crystallise in the absence of dTMP). We solved the structure of one promising enzyme-inhibitor complex by X-ray diffraction and have determined the rearrangement of side chains in the active site and the concomitant modification of the water molecules network around the thymine moiety of the dTMP substrate. In addition, we have co-crystallised and solved the structure of the complex between TMPK and the bisubstrate analogue Ap_5T.

Altogether, considerable new insight into the possible mechanism of phosphoryl transfer has been gained, as described at the end of the discussion.

Experimental procedures

Protein and reagents

The *M. tuberculosis* TMPK was overexpressed in *E. coli* and purified as described previously.[13] The protein was stored at -20 °C in aliquots of 100 µL at 4 mg/ml in a buffer containing

20 mM Tris-HCl pH 7.5, 0.5 mM dithiothreitol and 1 mM EDTA, conditions at which it is stable over several months. Ap_5T was purchased from Jena Bioscience (Germany). All other reagents used were purchased from Sigma® (St. Louis), including the reference inhibitor AZTMP. All solutions were made with pyrolyzed water.

Inhibitors synthesis

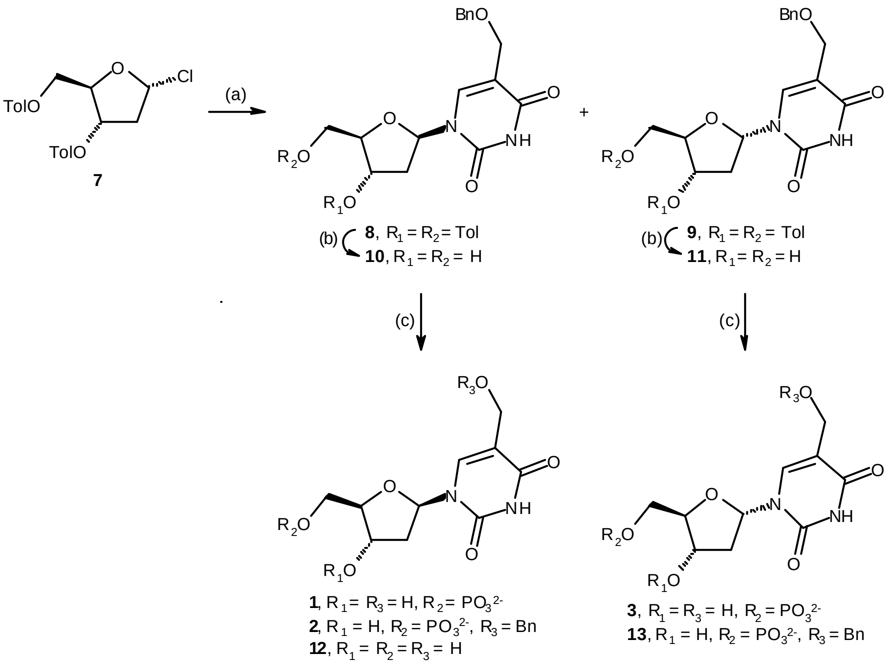

Scheme 1: Reagents and conditions: (a) 5-benzyloxymethyl-2,4-bis[(trimethylsilyl)oxy]pyrimidine, CH_3CN; (b) NH_3, MeOH; (c) $POCl_3$, $(MeO)_3PO$.

Several methods have already been reported for the synthesis of 5-hydroxymethyl-2’-deoxy-uridine. We found that hydroxymethylation of 2’-deoxyuridine with formaldehyde under acidic[25] or basic[26] catalysis gave only low yields. Therefore, we decided to couple 5-benzyl-oxymethyluracil with an appropriate sugar. In Ref. 27, the base is coupled with 1,2,3,5-tetra-acetylribose.[27] Since this method requires subsequent 2’-deoxygenation, we chose to glycosylate the silylated base with 2-deoxy-3,5-*O*-di-toluoyl-α-D-*eryhtro*-pentafuranosylchloride.[28] Unfortunately racemisation of the sugar prior to coupling led to a hardly separable mixture of the α- and β-anomers of the protected nucleoside. After alkaline removal of the acyl groups, however, the anomeric mixture could be separated via column chromatography to give the α- en β-anomers **10** and **11** as white foams. Both isomers were then phosphorylated. We noticed that the 5-*O*-benzyl group got partly removed during this step. Thus phosphorylation of the β-nucleoside gave three compounds: 2’-deoxy-5-hydroxymethyl-5’-*O*-phosphoryluridine (**1**), its benzyl-protected analogue (**2**) and 2’-deoxy-5-hydroxy-methyluridine (**12**). Phosphorylation of the α-nucleoside gave the corresponding benzylated and non-benzylated nucleotides **13** and **3** (Scheme 1).

2’-Deoxy-5-(furan-2-yl)uridine (**15**) and 2’-deoxy-5-(thien-2-yl)uridine (**16**) were synthesised according to a published procedure from unprotected 2’-deoxy-5-iodouridine (**14**).[29] Phosphorylation of these two nucleosides yielded the two desired 5-hetero-aryl substituted nucleotides **4** and **5** (Scheme 2).

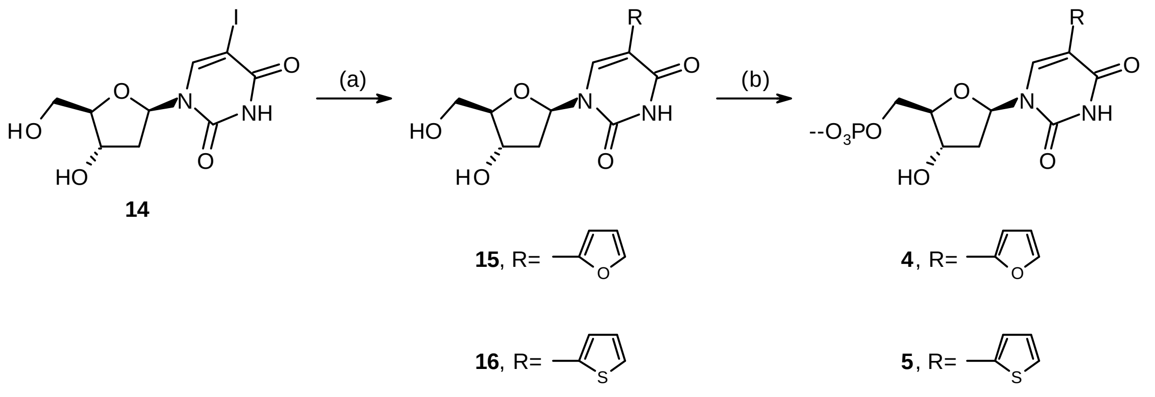

Scheme 2: Reagents and conditions: (a) 2-(tributylstannyl)furan, $(Ph_3P)_2Pd(II)Cl_2$, dioxane or 2-(tri-butylstannyl)thiophene, $Pd(OAc)_2$, Ph_3P, Et_3N, dioxane, (b) $POCl_3$, $(MeO)_3PO$

Synthesis

General

NMR spectra were obtained with a Varian Mercury 300 or 500 spectrometer using the solvent signal of DMSO-d_6 as a secondary reference. All signals assigned to amino and hydroxyl groups were exchangeable with D_2O. Mass spectra and exact mass measurements were performed on a quadrupole/orthogonal-acceleration time-of-flight tandem mass spectrometer (qTof 2, Micromass, Manchester, UK) equipped with a standard electrospray ionisation interface (ESI). Samples were infused in a 2-propanol:water (1:1) mixture at 3 µL/min. If necessary, nucleoside 5-*O*-monophosphates were ultimately purified using a Gilson HPLC system with a Gilson 322 pump, a UV/VIS-156 detector on a C18 column (10 µM; Altech; Altima; 250 × 22 mm). Precoated Merck silica gel F_{254} plates were used for TLC and spots were examined with UV light at 254 nm and sulfuric acid-anisaldehyde spray or phosphomolybdic acid (0.5% in EtOH) solution. Column chromatography was performed on Uetikon 560 silica (0.2-0.06 mm) and Amersham Biosciences DEAE Sephadex^{TM} A-25.

5-Benzyloxymethyl-1-[2-deoxy-3,5-*O*-di-(toluoyl)-b -D-*erythro*-pentafuranosyl]thymine (8) and 5-benzyloxymethyl-1-[2-deoxy-3-5-*O*-di-(toluoyl)-a -D-*erythro*-pentafuranosyl]thymine (9)

5-Benzyloxymethyluracil (680 mg, 2.93 mmol) was suspended in a mixture of hexamethyldisilazane (62 mL), trimethylsilyl chloride (0.5 mL, 3.94 mmol) and pyridine (5 mL). The mixture was refluxed overnight. The resulting solution was evaporated and coevaporated with toluene. The obtained residue was suspended in anhydrous CH_3CN (3.5 mL) and 2-deoxy-3,5-*O*-di-(toluoyl)-α-D-*erythro*-pentofuranosyl chloride (1 g, 2.58 mmol) was added. The reaction mixture was stirred 3 h at room temperature. CH_2Cl_2 (25 mL) was added and the organic layer was washed with a 7 % solution of $NaHCO_3$ (25 mL). The water layer was washed twice with CH_2Cl_2 (25 mL). The combined organic layers were dried over $MgSO_4$ and evaporated. The residue was purified by column chromatography (silica, CH_2Cl_2-MeOH, 98:2) to give a mixture of α- and β- anomers (0.932 g, 62 %). The anomers were partly separated by a combination of precipitation (ether-MeOH, 13:8) and column chromatography (silica, CH_2Cl_2-MeOH, 100:0→99:1→98:2). The two mixtures, enriched in either anomer, were used without further purification in the next step. **8**: ^{1}H-NMR: (300 MHz, DMSO-d_6) *d* 2.35 (3H, s, CH_3 toluoyl), 2.42 (3H, s, CH_3 toluoyl), 2.60 (2H, m, H-2’), 4.02 and 4.08 (2H, 2 d, $^2J = -11.7$ Hz, 5-CH_2), 4.52 (2H, s, *CH_2*Ph), 4.51-4.64 (3H, m, H-5’ and H-4’), 5.62 (1H, m, H-3’), 6.32 (1H, t, $J = 7.1$ Hz, H-1’), 7.25-7.39 (9H, m, 4H toluoyl and 5H benzyl), 7.73 (1H, s, 6-H), 7.88 (2H, d, toluoyl), 7.94 (2H, d, *J* = 7.5 Hz, toluoyl); HRMS (ESI-MS) for $C_{33}H_{32}N_2O_8Na$ [M+Na]$^+$: found, 607.2081; calcd, 607.2056.

1-(2-Deoxy-b-D-*erythro*-pentofuranosyl)-5-(benzyloxymethyl)thymine (10) and 1-(2-deoxy-a-D-*erythro*-pentofuranosyl)-5-(benzyloxymethyl)thymine (11)

A mixture of **8** and **9** (932 mg, 1.70 mmol) was dissolved in EtOH (60 mL) and NaOH 2N (37 mL) was added. The mixture was stirred at room temperature for 15 min and evaporated. The obtained residue was dissolved in 5 mL H_2O and neutralised with HCl. The precipitate was filtered and the filtrate was evaporated and coevaporated with EtOH. The obtained residue was purified by column chromatography (silica, CH_2Cl_2-MeOH, 93:7), to give **10** (261 mg, 44%) and **11** (284 mg, 48%) as white foams. **10**: ^{1}H-NMR: (500 MHz, DMSO-d_6) *d* 2.08 (1H, ddd, H-2'A), 2.12 (1H, ddd, *J* = -13.4 Hz, H-2'B), 3.54 (1H, m, dd after addition of D_2O, *J* = 3.9 and -12.0 Hz, H-5'A), 3.58 (1H, m, H-5'B), 3.79 (1H, q, H-4'), 4.15 (1H, d, *J* = -14.8 Hz, H-5A), 4.19 (1H, d, H-5B), 4.24 (1H, m, dt after addition of D_2O, H-3'), 4.48 (2H, s, $\mathit{CH_2}$Ph), 5.04 (1H, t, *J* = 4.9 Hz, 5'-OH), 5.26 (1H, d, *J* = 4.0 Hz, 3'-OH), 6.16 (1H, t, *J* = 6.8 Hz, H-1'), 7.25-7.34 (5H, m, CH_2*Ph*), 7.93 (1H, s, 6-H); ^{13}C-NMR: (125 MHz, DMSO-d_6) *d* 39.83 (C-2'), 61.38 (C-5'), 64.56 (5-CH_2), 70.48 (C-3'), 71.61 ($\mathit{CH_2}$Ph), 84.45 (C-1'), 87.52 (C-4'), 110.76 (C-5), 127.58 (C_p arom), 127.63 (C_o arom), 128.43 (C_m arom), 138.61 (C_i arom), 139.31 (C-6), 150.42 (C-2), 162 (C-4); HRMS (ESI-MS) for $C_{17}H_{20}N_2O_6$ [M+H]$^+$: found, 371.1187; calcd, 371.1219.

1-(2-Deoxy-5-*O*-phosphoryl-b-D-*erythro*-pentofuranosyl)-5-(hydroxymethyl)thymine (1), 1-(2-deoxy-5-*O*-phosphoryl-b-D-*erythro*-pentofuranosyl)-5-(benzyloxymethyl)thymine (2) and 1-(2-deoxy-b-D-*erythro*-pentofuranosyl)-5-(hydroxymethyl)thymine (12)

A solution of **10** (261 mg, 0.75 mmol) in trimethyl phosphate (3.5 mL) was cooled to 0° C, $POCl_3$ (0.22 mL, 2.4 mmol) was added dropwise and the mixture was stirred for 4 h at 0° C. The mixture was poured into crushed ice-water (20 mL), neutralised with concentrated NH_4OH and evaporated to dryness. The residue was subjected to column chromatography (silica, iPrOH-NH_4OH-H_2O, 77.5:15:2.5→60:30:5), yielding **12** (38.7 mg, 20 %) as a white foam, as well as an oily mixture of **1** and **2**. This mixture was further purified by HPLC (C-18, CH_3CN-MeOH-0.05% HCOOH in H_2O, 45:45:10 3 mL/min) and the fractions containing the nucleotides were lyophilised yielding **2** (47 mg, 14 %) and **1** (109 mg, 41 %) as white powders. **12**: ^{1}H-NMR: (300 MHz, DMSO-d_6) *d* 2.09 (2H, m, H-2'), 3.55 (2H, m, H-5'), 3.78 (1H, dd, H-4'), 4.13 (2H, d, 5-CH_2), 4.24 (1H, m, H-3'), 4.92 (1H, t, *J* = 5.09 Hz, 5-CH_2*OH*), 4.99 (1H, t, *J* = 4.8 Hz, 5'-CH_2OH), 5.27 (1H, d, *J* = 4.0 Hz, 3'-OH), 6.19 (1H, t, *J* = 7.2 Hz, H-1'), 7.74 (1H, s, 6-H); MS(ESI): m/z (%) 259.1 ([M+H]$^+$, 100); **2**: ^{1}H-NMR: (300 MHz, D_2O) *d* 2.35 (2H, m, H-2'), 4.03 (2H, m, H-5'), 4.19 (1H, m, H-4'), 4.43 (2H, s, 5-CH_2), 4.55 (1H, dt, H-3'), 4.63 (2H, s, $\mathit{CH_2}$PH), 6.28 (1H, t, *J* = 6.7 Hz, H-1'), 7.35-7.48 (5H, m, arom. H), 8.09 (1H, s, 6-H); ^{31}P-NMR: (500 MHz, D_2O) *d* 1.58; HRMS (ESI-MS) for $C_{17}H_{21}N_2O_9PNa$ [M+Na]$^+$: found, 451.0860; calcd, 451.0882; **1**: ^{1}H-NMR: (300 MHz, D_2O) *d* 2.39 (2H, m, H-2'), 4.05 (1H, ddd, H-5'A), 4.11 (ddd, *J* = -11.58 Hz, H-5'B), 4.19 (1H, m, H-4'), 4.39 (2H, s, 5-CH_2), 4.59 (1H, dt, H-3'), 6.34 (1H, t, *J* = 6.8 Hz, H-1'), 8.04 (1H, s, H-6); ^{13}C-NMR: (125 MHz, D_2O) *d* 41.73 (C-2'), 59.06 (C-5), 67.02 (C-5', $^2J_{C,P}$ = 4.9 Hz), 73.60 (C-3'), 88.20 (C-1'), 88.57 (C-4', $^3J_{C,P}$ = 8.8 Hz), 116.49 (C-5), 142.44 (C-6), 154.27 (C-2), 167.74 (C-4); ^{31}P-NMR: (500 MHz, D_2O) *d* 1.58; HRMS (ESI-MS) for $C_{10}H_{15}N_2O_9PNa$ [M+Na]$^+$: found, 361.0419; calcd, 361.0413.

1-(2-Deoxy-5-*O*-phosphoryl-a-D-*erythro*-pentofuranosyl)-5-(hydroxymethyl)thymine (3) and 1-(2-deoxy-5-*O*-phosphoryl-a-D-*erythro*-pentofuranosyl)-5-(benzyloxymethyl)thymine (13)

A solution of **11** (248 mg, 0.71 mmol) in trimethyl phosphate (3.5 mL) was cooled to 0° C, $POCl_3$ (0.21 mL, 2.3 mmol) was added dropwise and the mixture was stirred for 4 h at 0° C. The mixture was poured into crushed ice-water (20 mL), neutralised with NH_4OH and evaporated to dryness. **3** and **13** were separated by column chromatography (silica, iPrOH-NH_4OH-H_2O, 77.5:15:2.5→60:30:5). Further purification was accomplished by HPLC (C-18, CH_3CN-MeOH-0.05% HCOOH in H_2O, 45:45:10, 3 mL/ min). The fractions containing the title nucleotides were lyophilised yielding **3** (106 mg, 42 %) and **13** (47 mg, 15 %) as white powders. **3**: ^1H-NMR: (300 MHz, D_2O) ***d*** 2.15 (1H, dt, H-2'A), 2.79 (1H, ddd, H-2'B), 3.82 (2H, t, *J* = 5.2 Hz, 5'-CH_2), 4.37 (2H, s, 5-CH_2), 4.53 (2H, m, H-3' and H-4'), 6.22 (1H, dd, *J* = 2.5 Hz and 7.3 Hz, H-1'), 7.95 (1H, s, H-6); ^{13}C-NMR: (125 MHz, D_2O) ***d*** 42.06 (C-2'), 59.40, 66.73 (5-CH_2 and C-5'), 73.83 (C-3'), 90.25 (C-1'), 90.84 and 90.90 (C-4', $J_{C,P}$ = 7.5 Hz), 115.53 (C-5), 143.15 (C-6), 154.28 (C-2), 168 .03 (C-4); ^{31}P-NMR: (500 MHz, D_2O) ***d*** 2.64; MS (ESI): m/z (%) 361.0 ($[M+Na]^+$,100); **13**: ^1H-NMR: (300 MHz, D_2O) ***d*** 2.13 (1H, dt, H-2'A), 2.78 (1H, ddd, H-2'B), 3.88 (2H, dd, *J* = 5.8 and 4.4 Hz), 4.34 (1H, d, 5-CH_2A), 4.37 (1H, d, *J* = -12.2 Hz, 5-CH_2B), 4.52 (2H, m, H-3' and H-4'), 4.58 (2H, s, $\mathit{CH_2}$Ph), 6.20 (1H, dd, *J* = 2.5 Hz and 8.0 Hz, H-1'), 7.40 (5H, m, arom H), 7.96 (1H, s, H-6); ^{13}C-NMR: (125 MHz, D_2O) ***d*** 42.20 (C-2'), 67.25, 67.34 (5-CH_2 and C-5'), 73.81 (C-3'), 74.55 and 74.57 ($\mathit{CH_2}$Ph), 90.40 (C-1'), 90.76 and 90.83 (C-4', $J_{C,P}$ = 7.8 Hz), 112.72 (C-5), 130.94 (C_p benzyl), 131.18 (C_m benzyl), 131.34 (C_o benzyl), 140.18 (C_i benzyl), 144.65 (C-6), 167.93 (C-4); ^{31}P-NMR: (500 MHz, D_2O) ***d*** 2.29; MS(ESI): m/z (%) 451.0 ($[M+Na]^+$, 100).

2'-Deoxy-5-(furan-2-yl)-5'-*O*-phosphoryluridine (4)

A solution of **15** (382 mg, 1.22 mmol) in trimethyl phosphate (5.8 mL) was cooled to 0° C. $POCl_3$ (0.4 mL, 4.29 mmol) was added dropwise and the mixture was stirred for 4 h at 0° C. It was poured into crushed ice-water (40 mL), was neutralised with NH_4OH and evaporated to dryness. The resulting residue was purified by column chromatography (silica, iPrOH-NH_4OH-H_2O, 77.5:15:2.5→60:30:5). The obtained white powder was further purified on DEAE Sephadex™ A-25 (triethylammoniumbicarbonate 0 → 0.5 M) yielding the triethylammonium salt of **4**. This was converted to its corresponding sodium salt (NaI, acetone) (248 mg, 51 %) as a white powder. ^1H-NMR: (300 MHz, D_2O) ***d*** 2.43 (2H, m, H-2'), 4.09 (2H, app. t, H-5'), 4.23 (1H, m, H-4'), 4.59 (1H, dt, H-3'), 6.38 (1H, t, *J* = 7.1 Hz, H-1'), 6.57 (1H, dd, H-4''), 6.89 (1H, d, H-3''), 7.57 (1H, d, H-5''), 8.21 (1H, s, H-6); ^{13}C-NMR: (125 MHz, D_2O) ***d*** 41.45 (C-2'), 67.41 (C-5'), 73.76 (C-3'), 88.49 (C-4' and C-1'), 111.52 and 114.16 (C-5', C-3'' and C-4''), 138.69 (C-6), 145.22 (C-5''), 151.15 (C-2''); ^{31}P-NMR: (500 MHz, D_2O) ***d*** 1.10; HRMS (ESI-MS) for $C_{13}H_{14}N_2O_9P$ $[M-H]^-$: found, 373.0448; calcd, 373.0436.

2'-deoxy-5-(thien-2-yl)-5'-*O*-phosphoryluridine (5)

A solution of **16** (320 mg, 1.03 mmol) in trimethyl phosphate (4.6 mL) was cooled to 0° C, $POCl_3$ (0.31 mL, 3.3 mmol) was added dropwise and the mixture was stirred for 4 h at 0° C. The mixture was poured into crushed ice-water (20 mL), neutralised with 28 % ammonia and was evaporated to dryness. The resulting residue was purified by column chromatography (silica, iPrOH-NH_4OH-H_2O, 77.5:15:2.5→60:30:5). The obtained white powder was further purified on DEAE Sephadex A-25 (triethylammonium bicarbonate 0 → 0.5 M) yielding the triethylammonium salt of **5**. This was converted to its corresponding sodium salt (NaI, acetone) (240 mg, 57 %) as a white powder. ^{1}H-NMR: (300 MHz, D_2O) *d* 2.45 (2H, m, H-2’), 4.03 (2H, m, H-5’), 4.22 (1H, m, H-4’), 4.59 (1H, dt, H-3’), 6.36 (1H, t, *J* = 7.3 Hz, H-1’), 7.17 (1H, dd, H-4’’), 7.49 (2H, m, H-3’’ and H-5’’), 8.14 (1H, s, H-6) ppm; ^{13}C-NMR: (125 MHz, D_2O) *d* 41.29 (C-2’), 66.83 (C-5’, $^2J_{C,P}$ = 4.9 Hz), 73.93 (C-3’), 88.54 (C-1’), 88.81 (C-4’, $^3J_{C,P}$ = 8.3 Hz), 112.85 (C-5), 128.14 (C-5’’), 129.34 (C-4’’), 129.99 (C-3’’), 135.26 (C-2’’), 139.77 (C-6), 153.50 (C-2); ^{31}P-NMR: (500 MHz, D_2O) *d* 3.11 ppm; HRMS (ESI-MS) for $C_{13}H_{14}N_2O_8SP$ [M+H]: found, 389.0181; calcd, 389.0208.

Enzymatic assay

The TMPK activity was measured by HPLC separation of nucleotide substrates and products, as described below. The major reason for using this test instead of the more rapid coupled spectrophotometric assay[30] is that some inhibitors absorb light at 340 nm (**4** and **5**), thereby rendering difficult the evaluation of NADH concentration in the coupled reaction. Also, coupled enzymatic tests might be error-prone in the determination of the true value of K_i and K_m of inhibitors and substrate respectively, through the recycling of some substrate or product during the reaction coupling.[31] The reaction is carried out in a 1 ml final volume of a solution 50 mM Tris-HCl, pH 7.5, 20 mM magnesium acetate, 100 mM KCl, 1 mM EDTA, 0.5 mM DTT, using different initial concentrations of ATP and dTMP, in the presence or absence of various inhibitors. To follow the enzymatic kinetics an aliquot of 100 µl is taken at different times after enzyme addition and the reaction is quenched by adding 900 µl of 100 mM sodium phosphate pH 7. The concentration of each nucleotide at different times during the reaction is measured at 260 nm by HPLC (isocratic mode) using a Sephasil^{TM} C18, 5 µm SC 2.1/10 (Amersham Biosciences) column. The buffer used for elution is 50 mM sodium phosphate, pH 6.5, 2.5% (V/V) ethanol, 40 mM of tetrabutyl ammonium bromide with a flow rate of 250 µl per minute. All the reaction velocities are calculated by monitoring the production of dTDP expressed in terms of optical absorbance per minute at 260 nm. It was checked that all four sources of information (appearance of dTDP or ADP, disappearance of ATP or dTMP) can be used and lead to the same results (see also Ref. 11).

Crystallisation and diffraction data collection

Co-crystals of *M. tuberculosis* TMPK in complex with compound **1** (see Figure 1) were obtained as described for crystals with the dTMP substrate.[14] Briefly, a 6 µl drop of 1:1 mixture of the protein solution 3.5 mg/ml incubated overnight with 5 mM of analog **1** and the reservoir solution was equilibrated with 34 % (w/v) ammonium sulphate solution, 100 mM HEPES pH 6.0, containing 2 % (w/v) PEG2000, 20 mM magnesium acetate, and 0.5 mM β-mercaptoethanol. Crystals grew in 1-3 weeks to bipyramids of 400x200x200 µm^3. X-ray data were collected from cryo-cooled crystals using 25 % (w/v) glycerol as cryoprotectant.

Soaking experiments were performed by first transferring dTMP-TMPK co-crystals to a stabilising solution containing 70 % ammonium sulfate and 1 mM dTMP, and then to a fresh solution containing 70 % ammonium sulfate and 10 mM inhibitor (but no dTMP). This last solution was replaced three times, each soaking time being 24 hours.

Diffraction data were processed using DENZO/SCALEPACK[32] package. The CCP4 package[33] was used to calculate structure factors from the observed intensities (TRUNCATE). Reflections in the resolution ranges 2.28-2.22 and 2.70-2.64 Å had to be suppressed due to the presence of ice rings during data collection for the **1**-TMPK complex.

Model building and refinement

Refinement was performed up to 2.0 Å resolution with CNS.[34] Standards protocols, including maximum likelihood target, bulk solvent correction and isotropic B-factors were used.[34,35] The model was inspected manually with SIGMAA-weighted $2F_0$ - F_c and F_0 - F_c maps,[36] and progress in the model refinement was evaluated by the decrease in the free R-factor. Manual rebuilding in the electron density maps was done with O.[37] Stereochemistry of the final model was assessed using PROCHECK.[38] Coordinates of the **1**-TMPKmt binary complex have been deposited in the Research Collaboratroy for Structural Bio-informatics (RSCB) Protein Databank (access code: 1MRS). Similar structural details apply to the Ap_5T-TMPK complex, where all the dictionaries necessary for O and CNS come from the database of G. Kleywegt[2]. The coordinates have been deposited in the RSCB Protein Databank (access code: 1MRN).

Results

Enzymatic test: calibration with the natural substrates

In all experiments, the enzyme concentration was set to a value at least 200 times lower than the substrates concentrations, i.e. typically $5*10^{-8}$ M. The reaction catalytised by TMPK was found to follow the Michaelis model.[39] The initial velocity of the reaction at different fixed (saturating) concentrations of ATP and different concentrations of dTMP allows for the determination of the apparent K_m for dTMP and for ATP. With this protocol we find an apparent $K_m = 40$ µM dTMP. For ATP, we measured $K_m = 100$ µM. Both values compare well with the ones obtained with the coupled assay.[13] The K_m of 40 µM for dTMP has been measured at the fixed concentration of ATP of 0.5 mM and shows some dependence upon ATP concentration. The K_m value of dTMP extrapolated at zero ATP concentration is 4-5 µM, in agreement with results reported earlier.[13]

The role of ATP as the phosphoryl donor has been explored in Ref. 13, where other NTP were tried and found to be less efficient than ATP. Similar results were obtained using the direct assay method described here (data not shown).

Inhibition of TMPK activity with synthetic compounds

Measuring the initial velocity of the reaction at a fixed saturating concentration of ATP and different concentrations of dTMP, both in the absence and in presence of inhibitors, allows to test the nature of the inhibition.[39,40] In our case, the reciprocal plot confirms that all inhibitors are competitive with dTMP because the least-squares fitted best lines in absence and presence of the inhibitor cross exactly on the y-axis. In the classical competitive inhibition model (with the Lineweaver-Burk representation), we can use the equation[39]:

$$K_m = K_m(1+\frac{[I]}{K_i})$$

where K'_m and K_m are the apparent Michaelis constants determined in the presence and the absence of inhibitor, respectively. Knowing the concentration of inhibitor *[I]*, it is possible to calculate K_i, which is shown in Table 1.

For AZTMP, the dependence of the K_i value upon ATP concentration was found to be significant, in accordance with Ref. 13. However, for all the inhibitors reported here, we report only the apparent K_i value at the fixed concentration of ATP of 1.0 mM. AZTMP will serve as a reference compound here since our aim is to do better than this compound.

Exploring the 5-position of the thymine ring.

Systematic substitution of the methyl group in the 5-position of the base into halogen atoms was explored in ref 8.[8] Bromine, which has the same size as CH_3, was found previously to be very similar to dTMP in terms of both K_i and V_{max}.[13] The difference in the kinetic parameters of these compounds reflects essentially a size effect, with the halogen atoms serving as cavity filling atoms. In this work, other compounds substituted at the 5-position of the base moiety of dTMP have been synthesised and will be described here.

Nucleotide analog 1 was designed in an effort to induce an additional contact between the 5-CH_2OH group and the side chain of Arg74. The value of the K_i constant indicates a moderately active inhibitor, as compared to AZTMP (Table 1).

Analog number or name	**5-position of the pyrimidine ring**	**1' (sugar)**	**5' (sugar)**	**3' (sugar)**	**K_i ^{app} (mM)**
1[a]	CH_2OH	β	Phosphate	OH	110
2[a]	CH_2-O-CH_2-phenyl	β	Phosphate	OH	280
3[a]	CH_2OH	α	Phosphate	OH	450
4[a]	Furan-2-yl	β	Phosphate	OH	140
5[a]	Thien-2-yl	β	Phosphate	OH	270
BVDU[b]	CH=CHBr	β	OH	OH	900
Thymidine	CH_3	β	OH	OH	280
dUMP (8)	H	β	Phosphate	OH	substrate
5-F-dUMP (8)	F	β	Phosphate	OH	substrate
5-Br-dUMP (8)	Br	β	Phosphate	OH	substrate
5-I-dUMP (8)	I	β	Phosphate	OH	substrate
6[a]	CH_3	Hexose	Phosphate	OH	150
AZTMP	CH_3	β	Phosphate	N_3	50
Ap_5T	CH_3	β	p_5A[c]	OH	30

Table 1: Apparent Inhibition Constant (K_i ^{app}) of different synthesised inhibitors.

[a] *See Figure 1 for the structures of compounds 1-6.*

[b] *BVDU: (*E*)-5-(2-bromovinyl)-2'-deoxyuridine*

[c] *p_5A: adenosine 5'-pentaphosphate*

Other dTMP analogues were synthesised in which the volume of the substituent at this position was further increased while maintaining one polar atom, namely a thiophene and a furane derivative. The resulting compounds (**4** and **5**) were less active than the 5-CH_2OH dUMP, indicating that the volume of this cavity cannot be stretched too much. Another compound (**2**) aiming towards a stacking interaction with Phe36 residue resulted in a less active compound (Table 1).

The unnatural α-isomer of **1** was also synthesised (**3**, see Figure 1) and assayed but proved less active than **1** (see Table 1).

Another possibility would be to increase the length of the linker from the C5 position up to a polar atom to replace directly the W12 water molecule, which is located at 3.95 Å from the C5 atom of dTMP, behind the pyrolidine ring of Pro37. Pro37 has a cis-peptide bond conformation that is maintained through an hydrogen-bond between its carbonyl atom and a water molecule W26, which is also in contact with one of the oxygens of the phosphate group of dTMP. Therefore, the exact position of Pro37 is expected to be important for catalysis. This cis-peptide bond is also present in the three other known structures of dTMP kinases.[16,17,18,19,20] The deoxyribose analog of dU with a substituent of exactly the size to reach out for the water molecule W12 (-CH=CH-Br) has been tried and compared to dT. This compound, BVDU, has already proved efficient for inhibition of HSV-type 1 thymidine kinase.[12] It was predicted that the electronegative bromine atom would play the role of W12. However, this compound proved relatively inefficient for *M. tuberculosis* TMPK (Table 1).

Inhibition by Ap$_5$T

The bisubstrate analogue Ap$_5$T has been found to be more efficient than AZTMP with an inhibition constant $K_i = 30\mu M$, making it one of the most powerful inhibitors of *M. tuberculosis* TMPK known to date. This compares well with similar inhibitors designed against other NMP kinases.[18,41] The inhibition mechanism inferred from the reciprocal plot analysis is compatible with the one described for adenylate kinase, where it is a competitive inhibitor for the forward reaction and a mixed noncompetitive inhibitor for the backward reaction.[42] To understand the chemical nature of the interaction of this inhibitor with its target and to further increase the efficiency of this compound, the structure determination of its complex with its TMPK was undertaken (see below).

Inhibition by the 1-5 anhydrohexitol analogue of dTMP

Modification of the sugar moiety of dTMP into an 1,5-anhydrohexitol was performed (**6**). This analogue is actually a member of a novel series of inhibitors already tried for HSV-type 1 TK.[24] The 5'-*O*-monophosphate was tested against *M. tuberculosis* TMPK but proved to be a moderately potent competitive inhibitor, again using AZTMP as a reference (see Table 1).

Structure determination of bound drugs in the dTMP binding site of TMPK

In order to better understand the molecular origin of the differences in the K_i inhibition constants of all these compounds, we tried either to co-crystallise them with TMPK or to exchange them with dTMP by soaking TMPK-dTMP crystals with an excess of inhibitor.

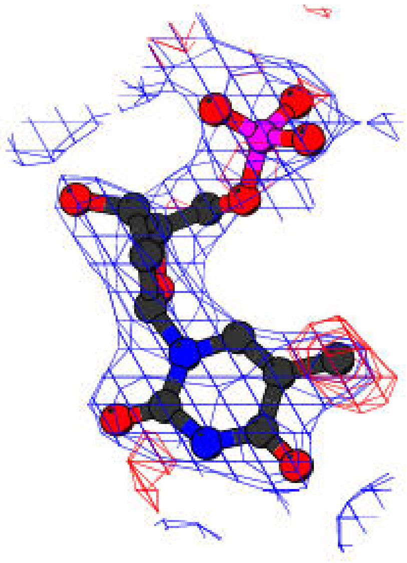

Figure 2: Electron density difference map around the analog 1 (drawn with Bobscript[43]). The F_0-F_c SIGMAA-weighted map is contoured at 3.0 s (red), while the 2F_0-F_c is contoured at 1.0 s (blue).

No exchange of dTMP by any of the analogues studied here was observed even after extensive soaking experiments on TMPK-dTMP crystals, in contrast with the control experiment with I-dUMP, which worked well as already reported in ref 15.[15] However, one should bear in mind that I-dUMP is a substrate whereas none of the compounds tried here are substrates.

No co-crystals were obtained either except with compound **1**, whose structure was determined at 2.0 Å resolution (see Tables 2 and 3 for data collection and refinement statistics, respectively). The Fourier difference map clearly shows density for the OH group of CH_2OH (Figure 2). The hydroxyl group makes an extra hydrogen bond with W12, which is also held in place by the side chain of Asp73 and the essential Arg74. After inspection of the residual SIGMAA-weighted $F_0 - F_c$ map, we found density at the 2.5 σ level for a possible alternative conformation of the hydroxyl group that reaches out for the side chain of the strictly conserved Ser99 (for which no definite role has been proposed yet).

	TMPK-1 cocrystals	**TMPK-Ap$_5$T cocrystals**
X-ray source	ESRF[a], ID14-3	Rotating anode (lab.)
Wavelength in (Å)	0.940	1.5418
Detector	MARCCD	MAR-IP
Space group	$P6_522$	$P6_522$
***a* = *b*, *c* (Å)**	76.34, 134.42	75.48, 133.35
Resolution (Å)	25.0-2.00 (2.07-2.00)	30.0-2.45 (2.54-2.45)
Total of unique refl.	14739 (1575)	8407 (768)
Multiplicity	6.0 (5.9)	3.3 (3.0)
Completeness (%)	89.5 (98.6)	95.1 (90.1)
R_{merge}[b]	0.082 (0.271)	0.066 (0.366)
I/s(I)	27.8 (18.8)	10.2 (9.2)

Table 2: Data-collection statistics of the TMPK-1 and TMPK-Ap$_5$T complexes.

[a] *ESRF: European Synchrotron Radiation Facility*

[b] $R_{merge} = S_h S_i ô I_{hi} - <I_h> ô/\Sigma_h \Sigma_i I_{hi}$, *where* I_{hi} *is the* i*th observation of the reflection* h, *while* $<I_h>$ *is the mean intensity of reflection* h

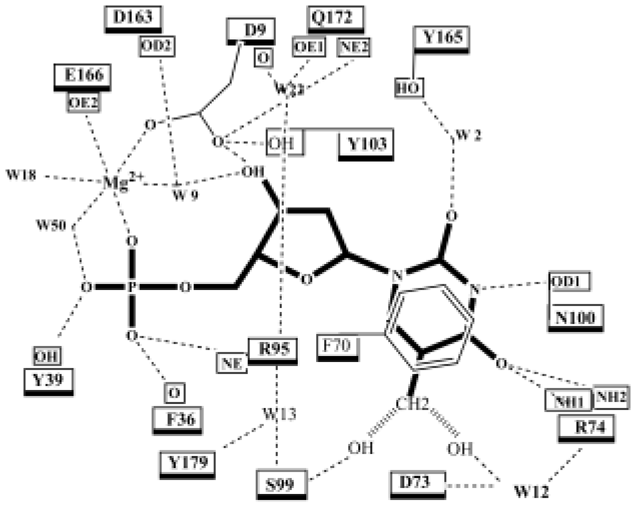

Figure 3: Network of interactions of the analog **1** *in the active site of TMPK (drawn with Chemdraw).*

No attempt has been made to refine this alternative conformation since the limited resolution of our data makes it difficult to estimate their relative occupancies. Ser99 is part of a hydrogen bond network involving both Glu6 (strictly conserved) and Tyr179 and helps to position Arg95 correctly (Figure 3), which is strictly conserved among all known TMPKs, except for the one from African swine fever virus, where it is a histidine.[15] Arg95 is the only residue of the whole protein whose main chain dihedral angles lie outside the "allowed" regions in a Ramachandran plot (Table 3), an observation that holds true in the other structures of TMPKs known, so it must have an important functional role. The guanidinium group of Arg95 is located 3.2 Å away from the carboxylate group of Asp9. Although the conformation of the side chain Arg95 is well conserved in the different TMPK structures, it has been shown that it can exist in another conformation in the complex with the products dTDP and ADP, pointing towards the carbonyl of residue 36, just before the cis-peptide bond of Pro37.[17]

	1-TMPK	Ap$_5$T-TMPK
Resolution range (Å)	25.0-2.00	30.0-2.45
Cutoff I/σ (I)	1.0	0.1
Number of reflections used for refinement	12400	7769
Number of reflections used for R$_{free}$ calculation	641	379
Number of non hydrogen atoms		
Protein	1543	1543
Inhibitor	22	53
SO$_4^{--}$ (two molecules)	10	10
Mg^{++}	1	1
Water	77	58
Refinement statistics		
R$_{factor}^{a}$ (%)	22.8	23.6
R$_{free}^{b}$ (%)	26.5	28.4
Root mean square deviations from ideality		
Bond lengths (Å)	0.0068	0.0079
Bond angles (°)	1.19	1.21
Dihedral angles (°)	20.67	20.1
Average temperature factors		
Main chain	35.35	38.2
Side chain atoms	38.2	39.2
Inhibitor	31.2	40.4
SO$_4^{-}$ molecule 1 (molecule 2)	30.1 (34.4)	30.1 (36.2)
Mg^{++}	46.96	34.5
Water	43.7	42.6
Scaling parameters (k in e/Å^3, overall B-factor in Å^2)	0.333 (50.5)	0.359 (42.56)
Ramanchandran plot		
Residues in most favoured regions (%)	96.1	91.1
Residues in additional allowed regions (%)	3.4	8.4
Residue in disallowed regions (%)	0.5 (Arg95)	0.5 (Arg95)
Overall G-factor^{c}	0.36	0.31

Table 3: Refinement statistics of the TMPK-1 and the TMPK-Ap$_5$T complexes.

[a] $R_{factor} = S\, ||F_o| - |F_c|| / |F_o|$

[b] R$_{free}$ *is calculated with 5% of randomly selected reflections*

[c] *G-factor is an overall measure of the structure quality calculated with PROCHECK.*[38]

Structure determination of bound Ap$_5$T

The crystal structure of the complex of *M. tuberculosis* TMPK with Ap$_5$T has been determined at 2.45 Å resolution (see Tables 2 and 3 for data collection and refinement statistics, respectively). The structure reveals an unexpected binding mode for the adenine moiety of this compound. While the thymidine moiety of the bisubstrate analogue indeed occupies the binding pocket of the dTMP substrate, the rest of the molecule departs from its expected position after the 5'-*O*-phosphate of the dTMP moiety (Figure 4). This is inferred from the superimposed crystal structures of both the *E. coli* and *H. sapiens* enzymes complexed with the same bisubstrate analog.[18,19] The phosphate backbone of the bound Ap_5T is making an angle of almost 90° with the superposed same molecule from *E. coli* at the alpha phosphate. The surprise comes from the fact that the ADP moiety of the Ap_5T molecule snugly fits into a cavity on the surface of TMPK that appears to be specific to the *M. tuberculosis* enzyme (Figure 5). This cavity involves packing interactions against helix $\alpha 2$ (residues 42-53) on one side and the region 152-162 on the other side. His53 is nicely stacked on the adenine ring.

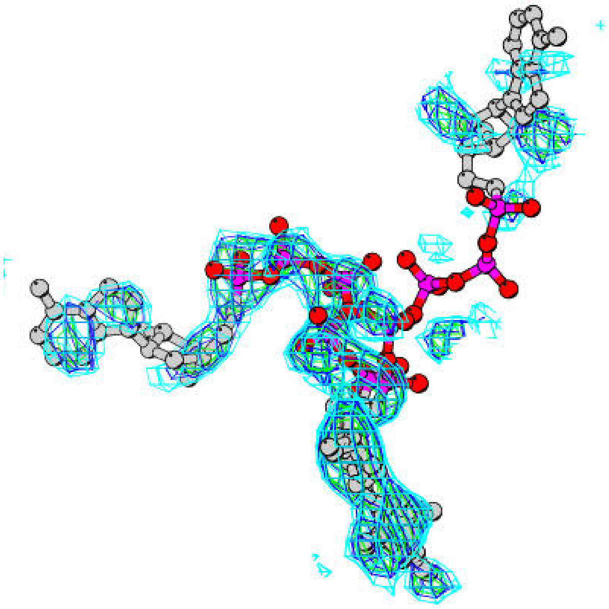

Figure 4: Electron density difference map around the Ap_5T compound (drawn with Bobscript[43]). The Fo-Fc SIGMAA-weighted map with phases calculated with a model deprived of the inhibitor is contoured at 2.5 s (blue). Both the refined model and the expected binding mode of the same molecule in the E. coli *TMPK complex structure are shown, for comparison (ball and stick representation).*

Discussion

One of the most striking findings of this study is that none of the 5-substituted dUMP analogues investigated here behaves as a substrate for *M. tuberculosis* TMPK, contrary to what had been observed for halogen-substituted compounds at the same position.[13,15] Our current interpretation is that any modification that significantly perturbs the volume of the substituent at this position will change the orientation of the sugar moiety of the dTMP molecule as well as that of the alpha phosphate. Indeed, recent results obtained on a series of compounds modified at the 3’ and 2’ positions of the sugar[21] indicated an extreme sensitivity of the reaction to the exact positioning of at least the 3’-OH group of the sugar moiety, which is in a C2’-*endo* conformation in the active site. This is also illustrated in the present study with compound **6**, which behaves as an inhibitor probably because of its inability to place correctly both the 5’-*O*-phosphate and the 3’-OH groups in a favorable arrangement for catalysis.

Similarly, AZTMP is an inhibitor of the *M. tuberculosis* enzyme contrary to what is observed in TMPKs of other species,[13] where it is either a weak substrate (in *H. sapiens*) or a good substrate (*E. coli*). This may be related to a unique feature of this enzyme revealed by its three-dimensional structure, namely the presence of a Mg^{++} ion in the vicinity of Asp9 and the 3'-OH position. Inhibition by AZTMP in the *M. tuberculosis* TMPK is probably due to a steric and/or electrostatic effect of the azido group, which would prevent the binding of the Mg^{++} ion.

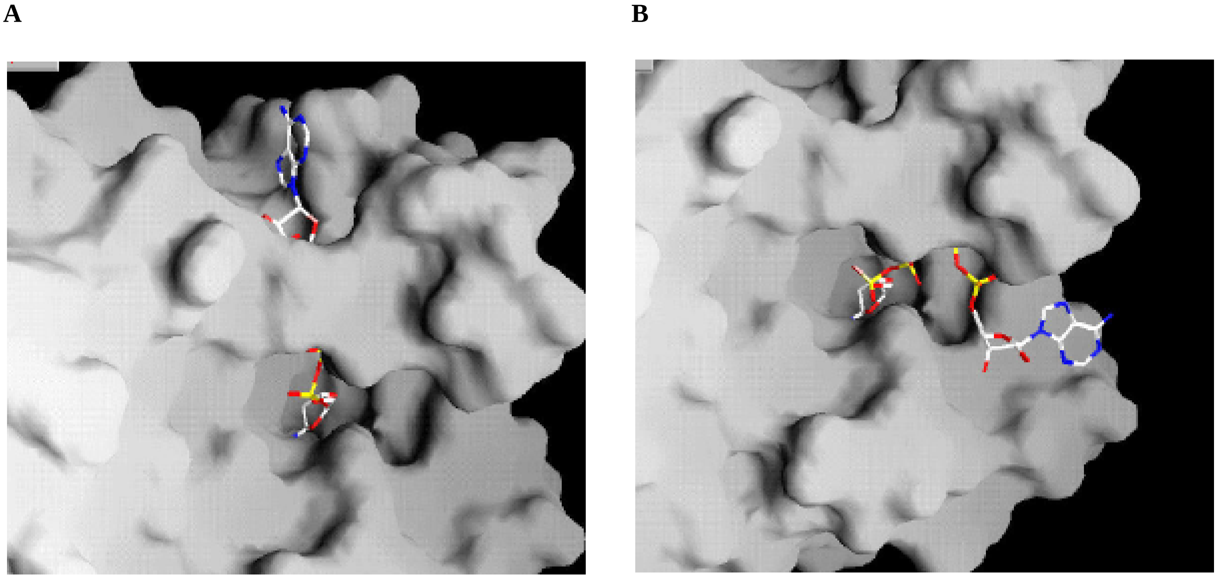

Figure 5: Comparison of the observed binding mode of Ap$_5$T both in the crystal state (A) and in the binding mode (B) expected from the structure of the same compound with the E. coli *enzyme.*[19] *Surface representation was drawn using Grasp.*[44] *The thymidine moiety of the molecule is hidden in its binding pocket.*

No Mg^{++} ion has been observed in this position in any of the three other structures of TMPK reported so far (*E. coli*, yeast and human enzymes) in various complexes.[16,17,18,19,20] This is especially intriguing since most of the side chain ligands for the divalent cation observed in the *M. tuberculosis* are conserved in the three other known TMPK structures. A possible explanation for this phenomenon may be the peculiar coordination of the 5'-*O*-phosphate of dTMP, which involves not only the Mg^{++} ion but also Tyr39, a specific feature of the *M. tuberculosis* sequence. Normally, at this Tyr39 position, an arginine or a lysine residue is expected, as seen in the human, yeast and *E. coli* enzyme structures and in the multialignment, to neutralise the dTMP phosphate negative charge. Since Tyr39 cannot play this role, it is tempting to postulate that it is fulfilled by the Mg^{++} cation in both *M. tuberculosis* and *M. leprae* enzymes, but then the positive charge is located on the opposite side of the phosphate, compared to the other known TMPKs, i.e. close to the essential Asp9. Mg^{++} may also contribute to deprotonate both the Asp9 residue and the phosphate of dTMP. We note that one of the water molecule ligands of the octahedral environment of the Mg^{++} ion is likely to be replaced by one of the non-bridging oxygens of the γ-phosphate of ATP, as seen in the structure of the complex with Ap$_5$T, thereby contributing to the exact positioning of all the reactants and stabilising the transition state. This is inferred from the superimposed structures of the complex of Ap$_5$T with the enzymes from *E. coli*[19] and/or *H. sapiens*[17] with the *M. tuberculosis* TMPK-dTMP structure.[15]

In the human enzyme, a magnesium ion is found on the ATP molecule. Since *M. tuberculosis* TMPK has been crystallised only in the presence of dTMP, one can only speculate about the presence of a second magnesium ion in the active site when ATP is bound. This (ATP-bound) second magnesium ion, weakening the bond between the beta and gamma phosphates and therefore assisting in the departure of the leaving group, is a general feature of various kinases and is therefore expected also in the *M. tuberculosis* enzyme.[45] Two magnesium ions in the active site of kinases would not be surprising, as this has been observed in several instances already. However, looking again at the multialignement of all known TMPK sequences,[15] one notices that Thr14 of the Walker A motif, which is essential in the coordination of this second magnesium ion, is not conserved in both *M. leprae* and *M. tuberculosis* sequences. Instead, it is replaced by an arginine residue whose guanidinium group can easily be brought, through a simple chi-1 rotation, at the expected binding site of the ATP-bound Mg^{++} ion.

The next surprising point is that most crystal soaking experiments did not work, indicating that the dTMP molecule could not be exchanged, at least in the conformation of the enzyme that has been captured in the crystal. In very much the same way, most co-crystallisations did not work (except for **1**), indicating the inability of the analogues tried here to induce the conformational change leading to the form of the enzyme that crystallises, namely the closed form. Our current interpretation is that the crystal structure has trapped an intermediate already well engaged along the reaction coordinate pathway: most of the inhibitors described here exert their binding abilities on a more open form of the enzyme but are unable to induce the transition from this open form to the closed form. In that sense, the transition to the closed form deserves the name of an induced fit mechanism.[46,47] *M. tuberculosis* TMPK is unique among the other known crystal structures of TMPKs in that the closed form is already formed upon dTMP binding, with the ATP binding site clearly preformed, whereas virtually all other NMP kinases need the binding of the two substrates to be in the fully closed form.[16,17,18,19,20] Two extrinsic factors contribute to this phenomenon: one is the Mg^{++} ion and the other is the sulphate ion, which drives the closing and the disorder-order transition of the LID region and which comes from the precipitating agent used to obtain crystals. The Mg^{++} role has been mentioned above while discussing the inhibition by AZTMP. The role of the sulphate is worth discussing in light of the Ap_5T complex structure.

Even though the ATP binding site is preformed in our crystal form, the “ADP” part of Ap_5T was found to bind to an unexpected site. This probably results from the inability of Ap_5T to displace the strongly bound sulphate ion that is located at the ATP beta phosphate binding site. Since this sulphate ion comes from the mother liquor of crystallisation, the alternative binding mode of the ADP moiety of Ap_5T might be seen as an artefact of crystallisation. However, since it binds already well into a cavity on the surface of the molecule for which it has not been especially designed, it is easy to imagine how one might improve its binding energy. For instance, it might be possible to take advantage of the close proximity of Glu55 to C2 of the adenine ring and of Glu50 and Asp46 to two different water molecules bound to the 2’ and 3’ position of ADP. It should then be possible to design new drugs against TMPK by synthesising branched molecules at the alpha phosphate of Ap_5T, with an extra chemical group reaching out to this cavity that is present only in the *M. tuberculosis* enzyme and designed specifically to bind there.

An important finding of the present study is the structural characterisation of the binding of TMPK to compound **1**. The structure partly verifies our expectation, by showing an anticipated hydrogen-bond between **1** and a known water molecule (W12 in PDB structure 1G3U), and partly brings a surprise, by displaying an alternative binding mode, with the hydroxyl group pointing towards the network of interactions between Glu6, Arg95, Tyr179 and Ser99. Both binding modes contribute to the rigidification of the dTMP binding pocket and explain why this compound is an inhibitor rather than a substrate, compared to 5-I-dUMP,[13,15] of comparable volume.

We now discuss in more detail the role of Ser99, a strictly conserved residue whose function has remained unclear up to now. First we observe that the network of interactions in which Ser99 is involved contains Glu6, the only other *non-glycine strictly conserved residue* among all known TMPK sequences,[15] as well as Arg95, which is almost universally conserved (except for one exception out of 32 sequences, where it is an histidine). It is tempting therefore to assume a central role in catalysis for this cluster of interacting residues.

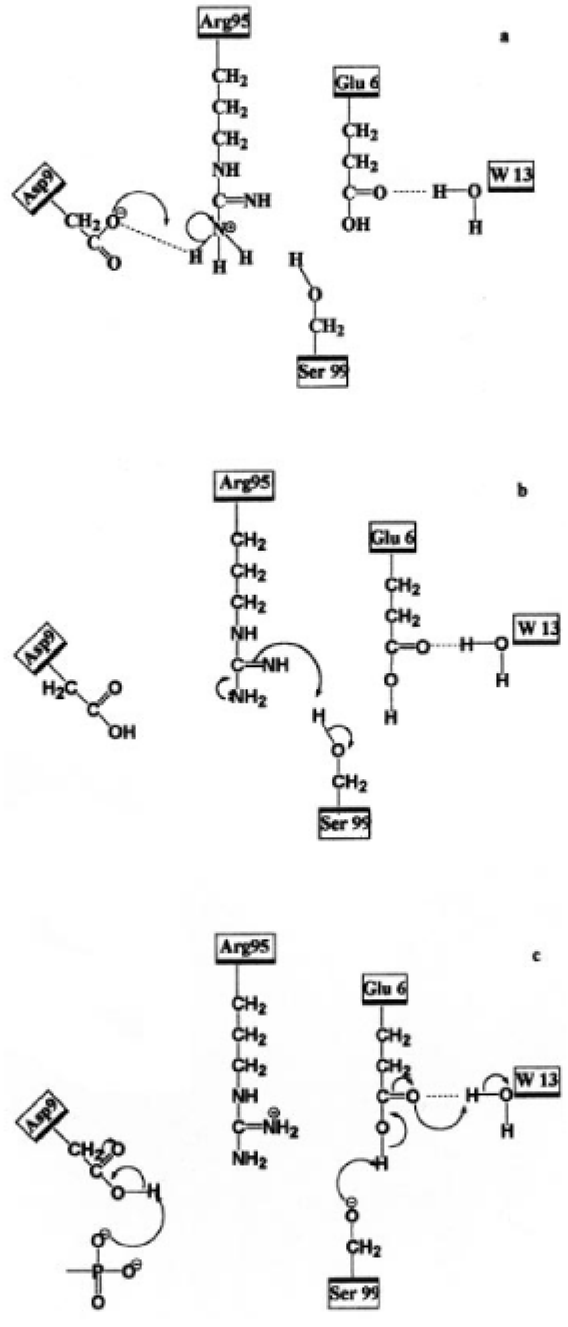

Figure 6: Proton wire involving Glu6, Ser99, Arg95 and Asp9. Glu6 and Ser99 are the only non-glycine residues strictly conserved among all known TMPK sequences, Arg95 has only one exception (where it is replaced by an histidine) and Asp9 is always either an aspartate or a glutamate residue.[15] *A) Asp9 gets its proton from Arg95. B) Arg95 gets its proton back from Ser99. C) Ser99 draws a proton from water through Glu6, while Asp9 gives its proton to the newly transferred phosphoryl group.*

In fact, we can describe this structural catalytic core as a “proton wire” in the active site of TMPKs, i.e. a continuous chain of several side chains in line and sharing a proton, including W13, Glu6, Ser99, Arg95 and Asp9 (Figure 6). W13 is in contact with the solvant, so this “proton wire” couples Asp9 to a reservoir of water molecules (and protons). Asp9, which is always either an aspartate or a glutamate in all known TMPK sequences, is within hydrogen bond distance of two non-bridging oxygens of phosphates, one from the α-phosphate of dTMP (acceptor) and the other from the γ-phosphate of ATP (donor). The distances between the residues in this “proton wire” are within 2.55-2.85 Å, with the exception of one definitely weak link between Arg95 and Asp9 (3.19 Å). We suggest that this distance becomes shorter upon ATP binding, making it possible to consider the Ser99-Arg95-Asp9 set as yet another variation of the well known catalytic triad of serine proteases (Ser-His-Asp/Glu). Asp9 could get a proton from Arg95 (Figure 6a), which immeditaely gets reprotonated from Ser99 and Glu6 (Figure 6b and 6c). The role of Asp9 would then be to provide the proton for the transferred phosphoryl group, playing the role of a general acid (Figure 6c). We believe that the proton from the hydroxyl group of the 5’-phosphate of dTMP has already been removed by the Mg^{++} ion. In that sense, we are one step further along the reaction pathway, compared to all other transition-state analog complex structures of other TMPKs. To sustain this hypothesis, we note that catalytic triads show considerable variation of sequence in the three different positions of the classical catalytic triad.[48] There is even one case where the histidine residue is replaced by a lysine, so arginine is not unconceivable between a serine and an aspartate.[48] Second, it has recently been observed that a previously hitherto unidentified catalytic triad is present in different families of cellulases, where the Asp/Glu residue plays the role of a proton donor.[49] Third, the recent work of Hutter and Helms[50] urges one to find a proton donor since their QMM calculations point to a concerted phosphoryl transfer mechanism involving the synchronous shift of a proton from the nucleotide monophosphate to the transferred PO_3 in the related enzyme UMP/CMP kinase. According to these authors[50], most of the activation energy of the phosphoryl transfer is spent on moving the proton towards its destination on the γ-phosphate group, so it is perhaps not surprising to find that TMPKs have evolved such a sophisticated network of four interacting highly conserved residues to accomplish this process.

References

---

[1] Stokstad, E. Infectious Disease - Drug-Resistant TB on The Rise. *Science* **2000**, *287*, 2391.

[2] Cole, S. T. *Mycobacterium tuberculosis*: drug-resistance mechanisms. *Trends in Microbiology* **1994**, *2*, 411–415.

[3] Tsuyuguchi, I. Dialogue between *Mycobacterium tuberculosis* and Homo sapiens. *Tuberculosis* **2001**, *81*, 221–227.

[4] Anderson, E. P. In The enzymes; Boyer P. D., Ed.; Academic Press: New York, 1973; Academic Press, New York Vol. 8, pp 49–96.

[5] Darby, G. K. In search of the perfect antiviral. *Antiviral Chem. Chemother.* **1995**, 6, 54-63.

[6] Griffiths, P. D. Progress in the clinical management of herpes virus infections. *Antiviral Chem. Chemother.* **1995**, *6*, 191–209.

[7] Champness, J. N.; Bennett, M. S.; Wien, F.; Visse, R.; Summers, W. C.; Herdewijn, P.; de Clercq, E.; Ostrowski, T.; Jarvest, R. L.; Sanderson, M. R. Exploring the active site of herpes simplex virus type-1 thymidine kinase by X-ray crystallography of complexes with aciclovir and other ligands. *Proteins: Struct., Funct. & Gen*. **1998**, *32*, 350–361.

[8] Bennett, M. S.; Wien, F.; Champness, J. N.; Batuwangala, T.; Rutherford, T.; Summers, W. C.; Sun, H.; Wright, G.; Sanderson, M. R. Structure to 1.9 angstrom resolution of a complex with herpes simplex virus type-1 thymidine kinase of a novel, non-substrate inhibitor: X-ray crystallographic comparison with binding of aciclovir. *FEBS Lett*. **1999**, *443*, 121–125.

[9] Wild, K.; Bohner, T.; Folkers, G; Schlulz, G. E. The structures of thymidine kinase from Herpes simplex virus type 1 in complex with substrates and a substrate analogue *Prot. Sci.* **1997**, *6*, 2097–2106.

[10] Vogt, J.; Perozzo, R.; Pautsch, A.; Prota, A.; Schelling, P.; Pilger, B.; Folkers, G.; Scapozza, L.; Schulz, G. E. Nucleoside binding site of Herpes simplex type 1 thymidine kinase analyzed by X-ray crystallography *Proteins* **2000**, *41*, 545–551.

[11] Manallack, D.; Pitt, W. R.; Herdewijn, P.; Balzarini, J.; De Clercq, E., Sanderson, M.R., Sohi, M., Wien, F., Munier-Lehmann, H., Haouz, Delarue, M. Database searching for thymidine and thymidylate kinase inhibitors using three-dimensional structure-based methods *Enz. Inh. & Medicinal Chem*. **2002**, *17*, 167–174.

[12] De Winter, H.; Herdewijn, P. Understanding the binding of base-substituted 2'-deoxyuridine substrates to thymidine kinase of herpes simplex virus type-1. *J. Med. Chem.* **1996**, *39*, 4727–4737.

[13] Munier-Lehmann, H.; Chafotte, A.; Pochet, S.; Labesse, G. Thymidylate kinase of *Mycobacterium tuberculosis*: a chimera sharing properties common to eukaryotic and bacterial enzymes. *Protein Sci.* **2001**, *10*, 1195–1205.

[14] Li de la Sierra, I.; Munier-Lehmann, H.; Gilles, A. M.; Bârzu, O.; Delarue, M. Crystallisation and preliminary X-ray analysis of the thymidylate kinase from *Mycobacterium tuberculosis*, *Acta Cryst.* **2000**, *D56*, 226–228.

[15] Li de la Sierra, I.; Munier-Lehmann, H.; Gilles, A. M.; Bârzu, O.; Delarue, M. X-ray Structure of TMP Kinase from *Mycobacterium tuberculosis* Complexed with TMP at 1.95 Å Resolution. *J. Mol. Biol.* **2001**, *311*, 87–100.

[16] Ostermann, N.; Lavie, A.; Padiyar, S.; Brundiers, R.; Veit, T.; Reinstein, J.; Goody, R. S.; Konrad, M; Schlichting, I. Potentiating AZT activation: Structures of wild-type and mutant human thymidylate kinase suggest reasons for the mutants' improved kinetics with the HIV prodrug metabolite AZTMP *J. Mol. Biol*. **2000**, *304*, 43–53.

[17] Ostermann, N.; Schlichting, I.; Brundiers, R.; Konrad, M.; Reinstein, J.; Veit, T.; Goody, R. S.; Lavie, A. Insights into the phosphoryltransfer mechanism of human thymidylate kinase gained from crystal structures of enzyme complexes along the reaction coordinate. *Structure* **2000**, *8*, 629–642.

[18] Lavie, A.; Konrad, M.; Brundiers, R.; Goody, R. S.; Schlichting, I.; Reinstein, J. Crystal structure of yeast thymidylate kinase complexed with the bisubstrate inhibitor P-1-(5 '-adenosyl) P-5-(5 '-thymidyl) pentaphosphate (TP(5)A) at 2.0 angstrom resolution: Implications for catalysis and AZT activation *Biochemistry* **1998a**, *37*, 3677–3686.

---

[19] Lavie, A.; Ostermann, N.; Brundiers, R.; Goody, R.; Reinstein, J.; Konrad, M.; Schlichting, I. Structural basis for efficient phosphorylation of 3 '-azidothymidine monophosphate by Escherichia coli thymidylate kinase *Proc. Natl. Acad. Sci. U.S.A.* **1998b**, *95*, 14045–14050.

[20] Lavie, A.; Vetter, I. R.; Konrad, M.; Goody, R. S.; Reinstein, J.; Schlichting, I. Structure of thymidylate kinase reveals the cause behind the limiting step in AZT activation. *Nature Struct. Biol.* **1997**, *4*, 601–604.

[21] Vanheusden, V.; Munier-Lehmann, H.; Pochet, S.; Herdewijn, P.; Van Calenbergh, S. Synthesis and evaluation of thymidine-5'-*O*-monophosphate analogues as inhibitors of *Mycobacterium tuberculosis* thymidylate kinase. *Bioorg. Med. Chem. Lett.* **2002**, *12*, 2695–2698.

[22] Kleywegt, G.; Jones, T. A. Detection, delineation, measurement and display of cavities in macromomlecular structures. *Acta Cryst*. **1994**, *D50*, 178–185.

[23] Ostrowski, T.; Wroblowski, B.; Busson, R.; Rozenski, J.; De Clercq, E.; Bennet, M. S.; Champness, J. N.; Summers, W. C.; Sanderson, M. R.; Herdewijn, P. 5-Substitted pyrimidines with a 1,5-anhydro-2,3-dideoxy-D-arabino-hexitol moiety at N-1: Synthesis, antiviral activity, conformational analysis, and interaction with viral thymidine kinase. *J. Med. Chem.* **1998**, *41*, 4343–4353.

[24] Vastmans, K.; Froeyen, M.; Kerremans, L.; Pochet, S.; Herdewijn, P. Reverse transcriptase incorporation of 1,5-anhydrohexitol nucleotides *Nucl.Acids.Res.* **2001**, *29*, 3154-3163.

[25] Cline, R. E.; Fink, R. M.; Fink, K. Synthesis of 5-Substituted Pyrimidines via Formaldehyde Addition. *J. Am. Chem. Soc.* **1958**, *80*, 2521–2525.

[26] Scheit, K. H. Die Synthese der 5'-Diphosphate von 5-Methyl-uridin, 5-Hydroxymethyl-uridin und 3.5-Dimethyl-uridin. *Chem. Ber*. **1966**, *99*, 3884–3891.

[27] Tona, R.; Bertolini, R.; Hunziker, J. Synthesis of aminoglycoside-modified oligonucleotides *Org. Lett.* **2000**, *2*, 1693–1696.

[28] Gupta, V. S.; Bubbar G. L. Synthesis and Properties of 5-Hydroxymethyl-2'-deoxyuridine and its α-Anomer. *Can. J. Chemistry*. **1971**, *49*, 719–722.

[29] Wigerinck, P.; Pannecouque, C.; Snoeck, R.; Claes, P.; De Clercq, E.; Herdewijn P. 5-(5-Bromothien-2-yl)-2'-deoxyuridine and 5-(5-chlorothien-2-yl)-2'-deoxyuridine are equipotent to (*E*)-5-(2-bromovinyl)-2'-deoxyuridine in the inhibition of herpes-simplex virus type-I replication. *J. Med. Chem*. **1991**, *34*, 2383–2389.

[30] Blondin, C.; Serina, L.; Wiesmüller, L.; Gilles, A. M.; Bârzu, O. Improved Spectrophotometric Assay of Nucleoside Monophosphate Kinase Activity Using Pyruvate Kinase/Lactate Dehydrogenase Coupling System. *Anal. Biochem.* **1994**, *220*, 219–222.

[31] Haouz, A.; Geleso-Meyer, A.; Burstein C. Assay of dehydrogenases with an O-2-consuming biosensor. *Enzyme Microbial Technology*, **1994**, *16*, 292–297.

[32] Otwinowski, Z.; Minor, W. Processing of X-ray diffraction data collected in oscillation mode. *Methods Enzymol.* **1997**, *276*, 307–326.

[33] CCP4 The CCP4 Suite: Programs for Protein Crystallography. *Acta Cryst*. 1994, *D50*, 760–763.

[34] Brunger, A. T.; Adams, P. D.; Clore, G. M.; DeLano, W. L.; Gros, P.; Grosse-Kunstleve, R. W.; Jiang, J. S.; Kuszewski, J.; Nilges, M.; Pannu, N. S.; Read, R. J.; Rice, L. M.; Simonson, T.; Warren, G. L. Crystallography & NMR system: A new software suite for macromolecular structure determination *Acta Cryst*. **1998**, *D54*, 905–921.

[35] Murshudov, G.; Vagin, A.; Dodson, E. Refinement of macromolecular structures by the maximum-likelihood method. *Acta Cryst*. **1997**, *D53*, 240–255.

[36] Read, R. J. Improved Fourier coefficients for maps using phases from partial structures with errors. *Acta Cryst.* **1986**, *A42*, 140–149.

[37] Jones, T. A.; Zou, J. Y.; Cowan, S. W.; Kjeldgaard, M. Improved methods for building protein models in electron-density maps and the location of errors in these models. *Acta Cryst.* **1991**, *A47*, 110–119.

[38] Laskowski, R. A.; McArthur, M. W.; Moss, D. S.; Thornton, J. M. Procheck- a program to check the stereochemical quality of protein structures. *J. Appl. Cryst*. **1993**, *21*, 283–291.

[39] Segel, I. H. **1993** *Enzyme Kinetics*. Wiley-Interscience Publication, John Wiley, New York.

---

[40] Jencks, W.P. **1987** *Catalysis in chemistry and enzymology*. Dover Publication New-York.

[41] Scheffzek, K.; Kliche, W.; Wiesmüller, L.; Reinstein, J. Crystal structure of the complex of UMP/CMP kinase from Dictyostelium discoideum and the bisubstrate inhibitor P-1-(5'-adenosyl) P-5-(5'-uridyl) pentaphosphate (UP(5)A) and Mg^{2+} at 2.2 Angstrom: Implications for water-mediated specificity. *Biochemistry*, **1996**, *35*, 9716–9727.

[42] Sheng, X. R.; Li, X.; Pan, X. M. An iso-random BiBi mechanism for adenylate kinase. *J. Biol. Chem.* **1999**, *274*, 22238–42.

[43] Esnouf, R. Further additions to MolScript version 1.4, including reading and contouring of electron-density maps. *Acta Cryst.* **1999**, *D55*, 938–940.

[44] Nicholls, A.; Sharp, K.; Honig, B. Protein folding and association - insights from the interfacial and thermodynamic properties of hydrocarbons. *Proteins* **1991**, *11*, 281–291.

[45] Cheek, S.; Zhang, H.; Grishin, N. V. Sequence and structure classification of kinases *J. Mol. Biol*. **2002**, *320*, 855–881.

[46] Schulz, G. E.; Muller, C. W.; Diederichs, K. Induced-fit movements in adenylate kinases. *J. Mol. Biol*.**1990**, *213*, 627–630.

[47] Muller, C. W.; Schlauderer, G. J.; Reinstein, J.; Schulz, G. E. Adenylate kinase motions during catalysis: An energetic counterweight balancing substrate binding *Structure* **1996**, *4*, 147–156.

[48] Dodson, G.; Wlodawer, A. Catalytic triads and their relatives *Trends Biochem. Sci.* **1998**, *23*, 347–352.

[49] Shaw, A .; Bott, R.; Vonrhein, C.; Bricogne, G.; Power, S.; Day, A. G. A novel combination of two classic catalytic schemes. *J. Mol. Biol*. **2002**, *320*, 303–309.

[50] Hutter, M. C.; Helms, V. Influence of key residues on the reaction mechanism of the cAMP-dependent protein kinase. *Prot. Sci*. **2000**, *9*, 2225–2231.

Chapter 4

3′-*C*-BRANCHED-CHAIN-SUBSTITUTED NUCLEOSIDES AND NUCLEOTIDES AS POTENT INHIBITORS OF *MYCOBACTERIUM TUBERCULOSIS* THYMIDINE MONOPHOSPHATE KINASE

Veerle Vanheusden, Hélène Munier-Lehmann, Matheus Froeyen, Laurence Dugué, Arne Heyerick, Denis De Keukeleire, Sylvie Pochet, Piet Herdewijn and Serge Van Calenbergh

J. Med. Chem. **2003**, *46*, 3811-3821

3′-*C*-BRANCHED-CHAIN-SUBSTITUTED NUCLEOSIDES AND NUCLEOTIDES AS POTENT INHIBITORS OF *MYCOBACTERIUM TUBERCULOSIS* THYMIDINE MONOPHOSPHATE KINASE

Veerle Vanheusden, Hélène Munier-Lehmann, Matheus Froeyen, Laurence Dugué, Arne Heyerick, Denis De Keukeleire, Sylvie Pochet, Piet Herdewijn and Serge Van Calenbergh

J. Med. Chem. **2003**, *46*, 3811-3821

Abstract

Thymidine monophosphate kinase of Mycobacterium tuberculosis *(TMPKmt) represents an attractive target for blocking the bacterial DNA synthesis. In an attempt to find high-affinity inhibitors of TMPKmt, a cavity in the enzyme at the 3'-position was explored* via *the introduction of various substituents at the 3'-position of the thymidine monophosphate (dTMP) scaffold. Various 3'-*C*-branched chain substituted nucleotides in the 2'-deoxyribo (**3**-**6**) and ribo series (**7**-**8**) were synthesised from one key intermediate (**23**). 2'-Deoxy analogues proved to be potent inhibitors of TMPKmt: 3'-CH_2NH_2 (**4**), 3'-CH_2N_3 (**3**) and 3'-CH_2F (**5**) nucleotides exhibit the highest affinities within this series with* K_i *values of 10.5, 12 and 15 mM, respectively. These results show that TMPKmt tolerates the introduction of sterically demanding substituents at the 3'-position. Ribo analogues experience a significant affinity decrease, which is probably due to steric hindrance of Tyr103 in close vicinity of the 2'-position. Although the 5'-*O*-phosphorylated compounds have somewhat higher affinities for the enzyme, the parent nucleosides generally exhibit affinities for TMPKmt in the same order of magnitude and display a superior selectivity profile versus human TMPK (TMPKh). This series of inhibitors holds promise for the development of a new class of anti-tuberculosis agents.*

Introduction

Mycobacterium tuberculosis is responsible for at least 2 million deaths per year worldwide and 30 million people are at risk of dying from tuberculosis (TB) in the next 10 years.[1] Due to demographic factors, socio-economic trends, neglected tuberculosis control in many countries and HIV-infection, this epidemic has been able to adopt such proportions. Efforts to stop this frightening trend are hampered by the lack of financial resources in developing countries, the appearance of multi-drug resistant strains of *M. tuberculosis* and bad therapy compliance. As a current strategy in the battle against TB, *Directly Observed Treatment Short-course* (DOTS) is preferred. In DOTS, TB patients are subjected to standardised treatment regimens (generally consisting of combinations of the most powerful anti-TB drugs), which last 6-8 months under direct observation of drug intake. As a consequence, the duration of illness, the risk of death and the appearance of resistant strains are reduced. For those that are or will be infected with the multi-drug-resistant bacteria or that develop resistance after a previous drug treatment (50-80% of previously treated cases), however, more effective drugs acting on novel targets are eagerly awaited.[2]

Thymidine monophosphate kinase (TMPK) catalyzes the conversion of dTMP to dTDP. This enzyme is ubiquitous in all living organisms. It lies at the junction of the *de novo* and salvage pathways for thymidine triphosphate (dTTP) synthesis. These enzymes are well characterised, both at biochemical[3] and structural[4] levels. Li de la Sierra et al. recently determined the structure of *M. tuberculosis* TMPK (TMPKmt) using X-ray diffraction.[5] Because of its crucial role in thymidine metabolism and in view of its low (22%) sequence identity with the human isozyme, it represents an attractive target for blocking mycobacterial DNA synthesis. The main interactions between dTMP and the enzyme are depicted in Figure 1. The most important catalytic regions are:

- the P-loop (amino acid residues 6–17), which binds and positions the α- and β-phosphoryl groups of the phosphate donor (ATP); it is unique among all known TMPK sequences in that it does not have an arginine at the position where it is found in the yeast and human enzymes; instead, it possesses a distant arginine residue four amino acids further;
- the DRY/H-motif (residues 94–96), which acts as a clip that favorably orients the phosphate donor and acceptor;
- the LID-region (residues 144–154) that leans over the phosphoryl donor, when dTMP binds the enzyme; it is very similar to *E. coli* TMPK having three arginines.

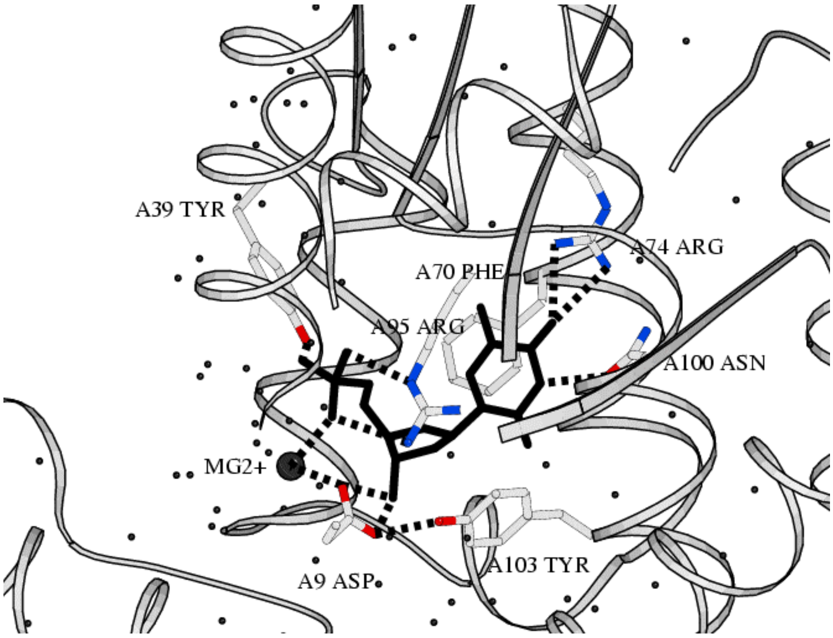

Figure 1: Schematic representation of the most important amino acid residues of TMPKmt interacting with dTMP (in black). The main bonding forces between dTMP and the enzyme are: (i) a stacking interaction between the pyrimidine ring and Phe70, (ii) a hydrogen bond between O4 of thymine and the Arg74 side-chain, which results in a preference for thymine over cytosine, (iii) a hydrogen bond between Asn100 and N3 of the thymine ring, (iv) a hydrogen bond between the 3'-hydroxyl of dTMP and the terminal carboxyl of Asp9, that in its turn interacts with the magnesium ion that is responsible for positioning the phosphate oxygen of dTMP, and (v) hydrogen bonds and an ionic interaction between the 5'-O-phosphoryl and Tyr39, Arg95 and Mg^{2+}*, respectively. The presence of Tyr103 close to the 2'-position is believed to render the enzyme catalytically selective for 2'-deoxy nucleotides versus ribo nucleotides.*

Moreover, 3'-azido-3'-deoxythymidine monophosphate (AZTMP) was identified as a competitive inhibitor of TMPKmt with a K_i of 10 μM.[5] TMPKmt represents the first reported TMPK that does not phosphorylate AZTMP, a feature that could be exploited in the search for other selective inhibitors of TMPKmt. Lavie et al.[4a] postulated that, in yeast TMPK, the azido group interacts via its terminal nitrogen with the side-chain carboxyl of Asp9, resulting in a

P-loop displacement. Thus, Arg15 binds ATP less efficiently, slowing down catalysis. A similar mechanism may account for the lack of phosphorylation of AZTMP by TMPKmt. Li de la Sierra et al. suggested that the azido group displaces the magnesium ion in the active site of TMPKmt (responsible for positioning one oxygen of the phosphate and Asp9), thereby abolishing catalysis.[5] Despite the uncertainty of the mechanism, it should be interesting to explore changes at position 3' of the dTMP-scaffold for finding more potent inhibitors of TMPKmt. The X-ray structure of TMPK complexed with dTMP reveals that relatively bulky substituents at the 3'-position could be accommodated.[5] Therefore, we decided to synthesise a series of 3'-*C*-branched-chain nucleotides, namely the 3'-*C*-azidomethyl, 3'-*C*-aminomethyl, 3'-*C*-fluoromethyl, and 3'-*C*-hydroxymethyl derivatives of dTMP (**3**-**6**). To delineate the most appropriate length of the spacer between the 3'-carbon and the introduced functionality, also 3'-deoxy-3'-hydroxyethylthymidine (**15**) was investigated for its affinity for TMPKmt.

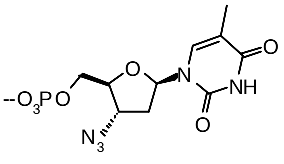

AZTMP

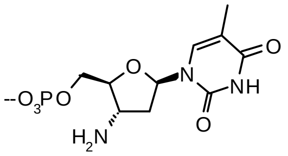

1

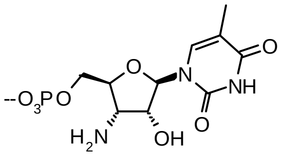

2

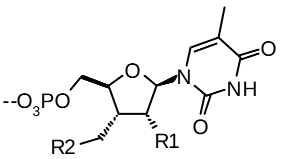

3 R1= H, R2= N_3
4 R1= H, R2= NH_2
5 R1= H, R2= F
6 R1= H, R2= OH
7 R1= OH, R2= N_3
8 R1= OH, R2= NH_2

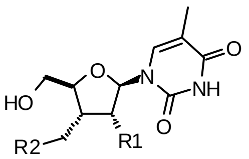

9 R1= H, R2= N_3
10 R1= H, R2= NH_2
11 R1= H, R2= F
12 R1= H, R2= OH
13 R1= OH, R2= N_3
14 R1= OH, R2= NH_2
15 R1= H, R2= CH_2OH

We have already reported that a ribo analogue exhibits a higher affinity for TMPKmt than its corresponding 2'-deoxy analogue, i.e. the ribo analogue of 3'-amino-3'-deoxy-5'-*O*-phosphorylthymidine (**2**) with a K_i of 27 μM versus 235 μM for **1**.[6] In order to gain detailed insight in the postulated steric hindrance caused by Tyr103 at the 2'-position, the ribo analogues of the azido and amino compounds were also synthesised (**7**-**8**). The non-phosphorylated analogues **9**-**14** of the above-mentioned compounds were included in this report as well.

Results and Discussion

Chemistry

Although an efficient synthetic route for the synthesis of 3'-*C*-branched-chain 2',3'-deoxy substituted thymidine has been established,[7] we developed a route that gives access to both 2'-deoxy and ribo analogues and allows easier conversion to the corresponding monophosphates. The synthesis of the parent 3'-*C*-branched-chain substituted nucleosides **9-14** was described by Lin et al.[8] In this procedure, all 3'-*C*-modifications are introduced on the sugar moiety before coupling with thymine. In our approach, the 3'-*C*-modifications are effected following sugar-base coupling, which allows synthesising all derivatives from a unique key intermediate. This approach requires a judicious choice of 5'- and 6'-*O*-protective groups, which must be stable under various reaction conditions and be chemoselectively removed to permit conversion of the key compound to the 3'-hydroxymethylnucleotide, on one hand and to the 3'-azidomethyl-, 3'-aminomethyl- and 3'-fluoromethyl-derivatives, on the other hand.

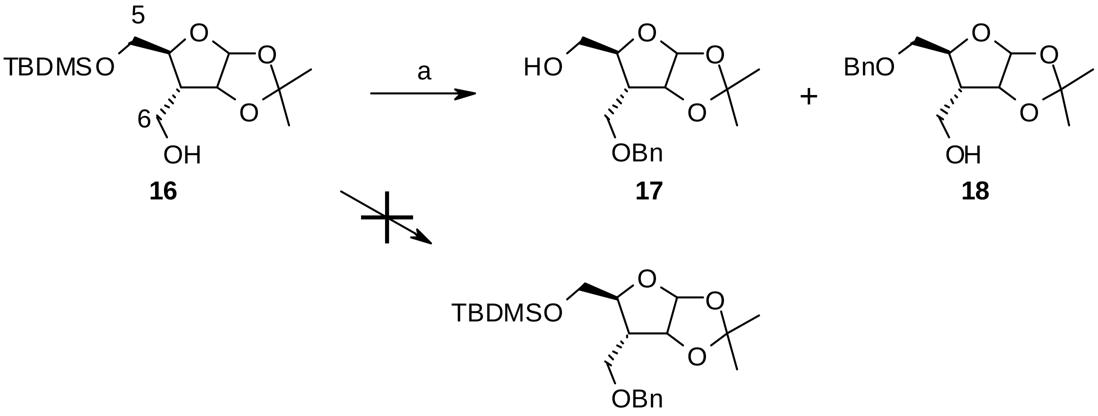

Scheme 1: Reagents: (a) BnCl, NaH, DMF.

First, we chose to combine 5-*O*-(*tert*-butyldimethyl)silyl and a 6-*O*-benzyl protecting groups (Scheme 1). However, introduction of the 6-*O*-protective group in **16** (prepared in 3 steps from 1,2-*O*-isopropylidene-α-D-xylofuranose[8]) using BnCl and NaH in DMF[9] was cumbersome. The 5-*O*-(*tert*-buthyldimethyl)silyl group was cleaved thereby furnishing a mixture of 3-deoxy-3-(benzyloxymethyl)-1,2-*O*-isopropylidene-α-D-ribofuranose (**17**) (17%) and 5-*O*-benzyl-3-deoxy-3-(hydroxymethyl)-1,2-*O*-isopropylidene-α-D-ribofuranose (68%) (**18**) resulting from silyl ether cleavage under basic conditions.[10] Therefore, we decided to take the 5-*O*-*p*-anisyl protecting group instead of the 5-*O*-(*tert*-butyldimethyl)silyl, as cleavage during introduction of the benzyl would be obviated under the given reaction conditions (Scheme 2). Unfortunately, attempts to selectively protect the primary hydroxyl of 1,2-*O*-isopropylidene-α-D-xylofuranose (**19**) with *p*-methoxyphenol under Mitsunobu conditions[11] did not afford the desired 5'-*O*-protected derivative. Instead, 3,5-anhydro-1,2-*O*-isopropylidene-α-D-xylofuranose[12] (**20**) was formed via intramolecular dehydration.

To circumvent this problem, we protected the 5-hydroxyl as a benzyl ether and the 6-hydroxyl with a *p*-anisyl group (Scheme 3). 5-*O*-Benzyl-3-deoxy-3-(hydroxymethyl)-1,2-*O*-isopropylidene-α-D-ribofuranose (**18**) was prepared using the method of Tino et al.[12] The 3-hydroxymethyl group was protected as a *p*-anisyl ether under Mitsunobu conditions,[11] affording the fully protected sugar **21**. Acidic cleavage of the 1,2-*O*-isopropylidene group, followed by acetylation, provided **22**. Vorbrüggen-type coupling[13] of this acetylated sugar with silylated thymine, followed by alkaline removal of the 2'-*O*-acetyl protecting group yielded **23** (78% in two steps), a convenient key intermediate for further derivatisation. Removal of the 2'-hydroxyl function was performed by reduction of its phenoxythiocarbonate ester with AIBN and *n*Bu$_3$SnH affording **24** (40% yield from **18**). Selective deprotection of the 5'-*O*-benzyl group of **24** by catalytic hydrogenolysis, followed by 5'-*O*-phosphorylation and removal of the

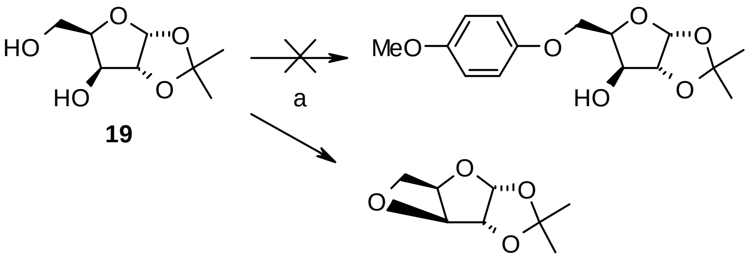

Scheme 2: Reagents: (a) p-*methoxyphenol, DEAD, Ph$_3$P, THF.*

p-anisyl group, gave the desired 2',3'-dideoxy-3'-*C*-hydroxymethylthymidine-5'-*O*-monophosphate (**6**) (Scheme 4). To obtain the corresponding free nucleoside **12**, **25** was treated with ceric ammonium nitrate. Besides the removal of the 6'-*O*-anisyl group, oxidation of the 5-methyl group occurred during work-up of the aqueous layer (possibly by residual ceric ammonium nitrate) thereby leading to the undesired 5-hydroxymethylthymine analogue **27**. The 5-hydroxymethyl was identified by COSY (an extra hydroxymethyl was present that did not show COSY contacts with any other proton) and gHMBC experiments (^3J contact between 5-*C*H$_2$OH and H-6 and between 5-C*H*$_2$OH and C-4 and C-6; ^2J contact between 5-C*H*$_2$OH and C-5). Consequently, we interchanged the deprotection steps c and a described in Scheme 4 and obtained **12** via **28** (68% yield from **24**).

Compound **28** also served as precursor for the synthesis of the 3'-CH$_2$N$_3$, 3'-CH$_2$NH$_2$ and 3'-CH$_2$F derivatives. Fluorination of **28** with (diethylamino)sulfur trifluoride (DAST), followed by reductive debenzylation, afforded the desired 2',3'-dideoxy-3'-fluoromethyl-nucleoside **11**. Phosphorylation of the 5'-hydroxyl group led to the corresponding nucleotide **5** (Scheme 4).

Mesylation of **28** followed by treatment with NaN$_3$ afforded azide **30** in 79% yield (2 steps) (Scheme 5). Debenzylation (BCl$_3$ in CH$_2$Cl$_2$), followed by 5'-phosphorylation, furnished 3'-*C*-azidomethyl nucleotide **3**. Reduction of the azido group in **3** with Ph$_3$P and NH$_4$OH in pyridine led to the 3'-CH$_2$NH$_2$ derivative **4**. Likewise **9** was converted to **10**.

The synthesis of the 3'-*C*-aminomethyl and 3'-*C*-azidomethyl ribo analogues from **23** was performed in a similar way as for the 2'-deoxy analogues. After selective removal of the *p*-anisyl group of **23**, the 6'-azido moiety was introduced via mesylation and treatment with NaN$_3$ to yield nucleoside **13** after deprotection. Phosphorylation of **13** led to analogue **7** and subsequent reduction of the 6'-azido group afforded analogue **8**. Similarly, reduction of the azido group of **13** afforded **14**.

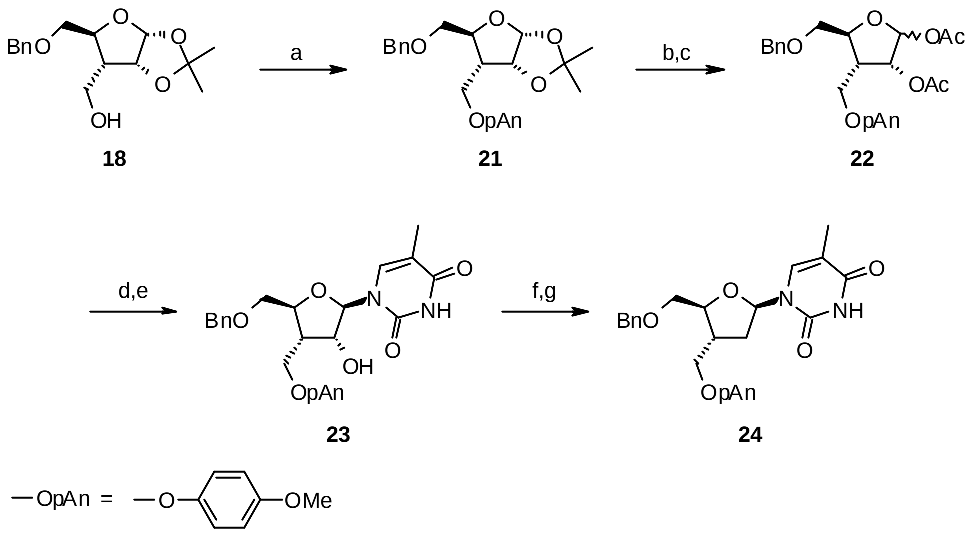
BnO
OH
18
a
OpAn
21
b,c
OAc
22
d,e
OH
23
f,g
24
—OpAn = —O—⟨⟩—OMe

Scheme 3: Reagents: (a) p-*methoxyphenol, DEAD,* Ph_3P*, THF, 80 °C; (b) HOAc 75%, 80 °C; (c)* Ac_2O*, pyridine; (d) 5-methyl-2,4-bis[(trimethylsilyl)oxy]pyrimidine,* $(CH_3)_3SiOSO_2CF_3$*,* $Cl_2(CH_2)_2$*; (e)* NH_3*, MeOH; (f) phenylchlorothionocarbonate, DMAP,* CH_3CN*; (g) AIBN,* nBu_3SnH*, toluene.*

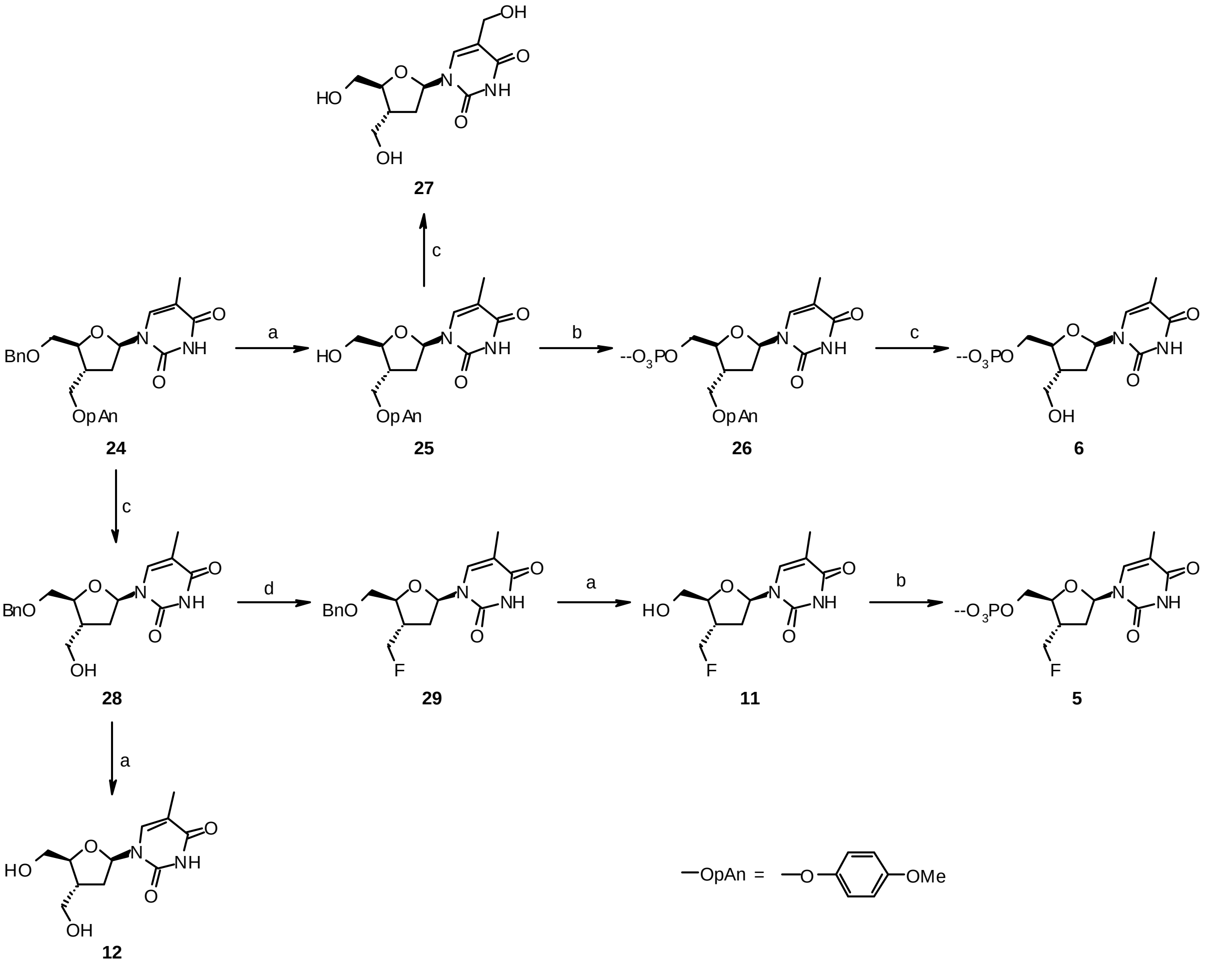
27
c
24
a
25
b
--O3PO
26
c
6
c
28
d
29
a
11
b
5
a
12
F
—OpAn = —O—⟨⟩—OMe

Scheme 4: Reagents: (a) H_2*, 10% Pd/C, MeOH; (b)* $POCl_3$*,* $(MeO)_3PO$*; (c) ceric ammonium nitrate,* CH_3CN*,* H_2O*; (d) DAST,* CH_2Cl_2*.*

Compound **15** was obtained according to reported procedures with slight modifications (Scheme 6). An allyl group was introduced at the 3'-position of 5'-silylated thymidine by a free-radical coupling described by C.K. Chu[14] to give nucleoside **33**. Aldehyde **34** was obtained from **33** by a two-step one-pot procedure involving *cis*-hydroxylation with osmium tetraoxide in the presence of 4-methylmorpholine *N*-oxide and sodium periodate cleavage of the diol.[15] Reduction of **34** with sodium borohydride in aqueous ethanol, followed by 5'-desilylation of the alcohol **35**, afforded the free nucleoside **15** in 24% yield from **33**.[16]

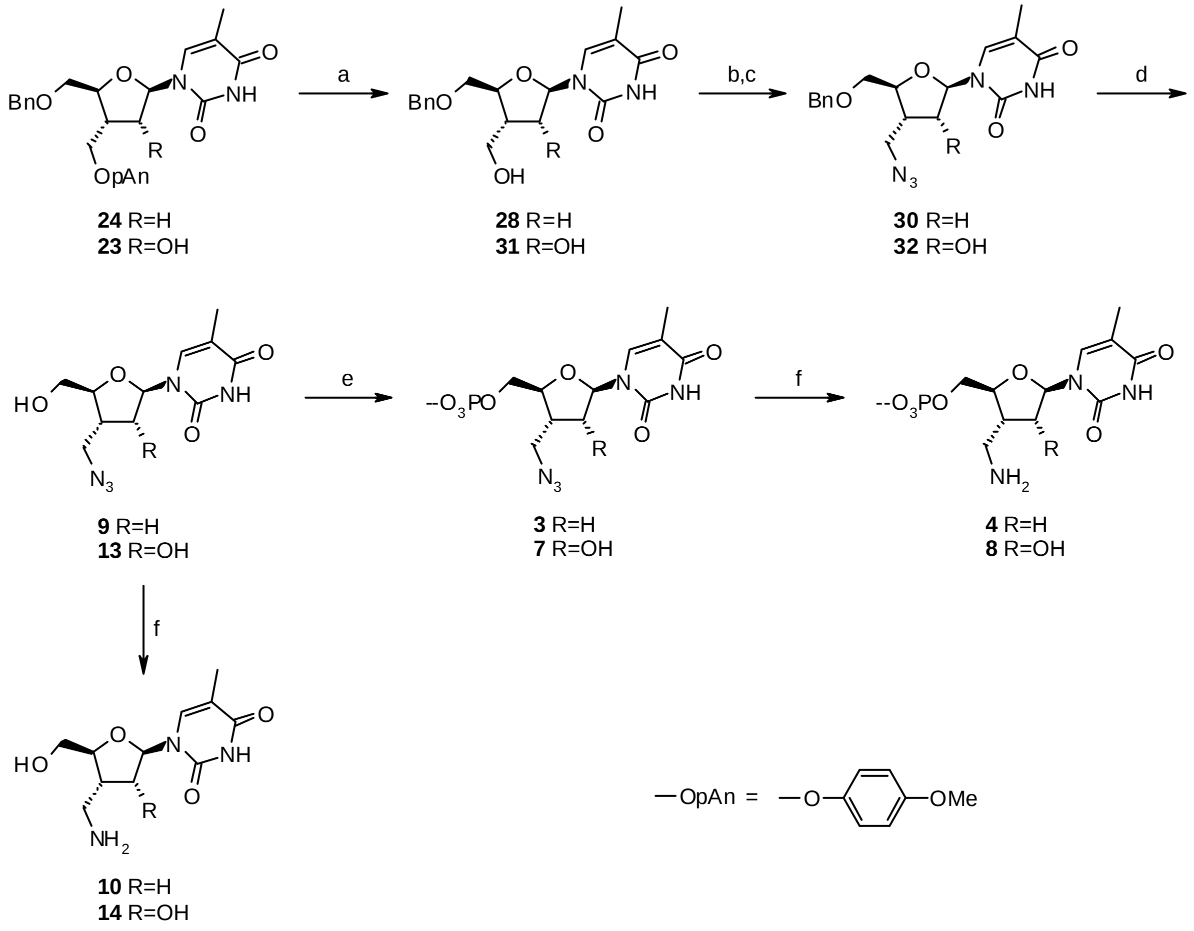
BnO
OpAn
R
a
b,c
d
OH
N3
e
f
HO
--O3PO
NH2
24 R=H
23 R=OH
28 R=H
31 R=OH
30 R=H
32 R=OH
9 R=H
13 R=OH
3 R=H
7 R=OH
4 R=H
8 R=OH
10 R=H
14 R=OH
—OpAn = —O—⟨⟩—OMe

Scheme 5: Reagents: (a) ceric ammonium nitrate, CH_3CN, H_2O; (b) methanesulfonyl chloride, pyridine; (c) NaN_3, DMF, 95 °C; (d) BCl_3, CH_2Cl_2, -78°C; (e) $POCl_3$, $(MeO)_3PO$; (f) Ph_3P, NH_4OH, pyridine.

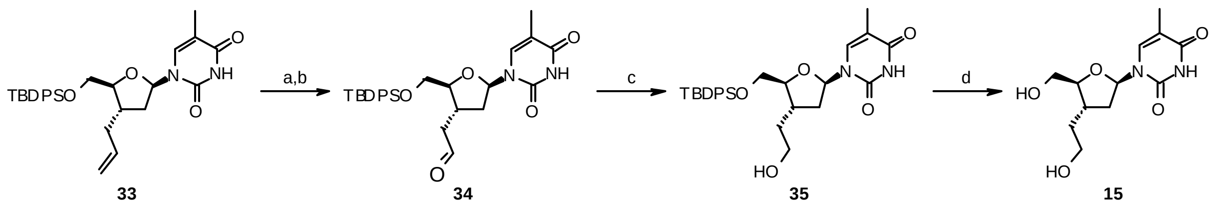
TBDPSO
a,b
c
d
HO
33
34
35
15

Scheme 6: Reagents: (a) OsO_4, 4-methylmorpholine N*-oxide, dioxane; (b) $NaIO_4$; (c) $NaBH_4$, EtOH, H_2O; (d) TBAF, THF.*

Binding Assay

All compounds were tested as described in the experimental section[17] and are presented in Table 1. Clearly, 2'-deoxy nucleotides **3**-**6** are potent inhibitors of the enzyme. The 3'-CH_2NH_2 nucleotide **4** , its 3'-CH_2N_3 precursor **3** and the 3'-CH_2F nucleotide **5** exhibit the highest affinities within this series with K_i values of 10.5 µM, 12 µM and 15 µM, respectively. A modeling experiment (in GOLD) showed that **4** adopts a 2'-*exo*-3'-*endo* conformation (dTMP, in contrast, is in the 2'-*endo*-3'-*exo* conformation). Consequently, the amino group occupies the same space as the 3'-hydroxylgroup of dTMP, hence it is in an appropriate position to interact with Asp9 (Figure 2).

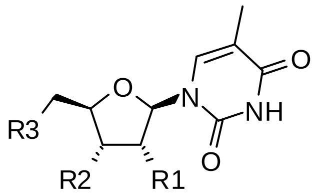

Compound code	R1	R2	R3	K_i (mM) TMPKmt	K_i (mM) TMPKh	SI(K_i TMPKh/ K_i TMPKmt)
dTMP	H	OH	OPO_3^{2-}	4.5[a]	5.0[a]	1.1[a]
Thymidine[33]	H	OH	OH	27	n.d.	n.d.
AZTMP[34]	H	N3	OPO_3^{2}-	10	n.d.	n.d.
AZT[33]	H	N3	OH	28	n.d.	n.d.
1[6]	H	NH2	OPO_3^{2}-	235	n.d.	n.d.
2[6]	OH	NH2	OPO_3^{2}-	27	n.d.	n.d.
3	H	CH2N3	OPO_3^{2}-	12	32	2.7
4	H	CH_2NH_2	OPO_3^{2-}	10.5	4.7	0.4
5	H	CH_2F	OPO_3^{2-}	15	40	2.7
6	H	CH_2OH	OPO_3^{2-}	29	43.5[a]	1.5
7	OH	CH_2N_3	OPO_3^{2-}	116	n.i.[b]	>9
8	OH	CH_2NH_2	OPO_3^{2-}	315	280	0.9
9	H	CH_2N_3	OH	40	1040	26
10	H	CH_2NH_2	OH	57	220	3.9
11	H	CH_2F	OH	45	970	21.6
12	H	CH_2OH	OH	41	420	103
13	OH	CH_2N_3	OH	770	n.i.[c]	>5
14	OH	CH_2NH_2	OH	393	110	0.3
15	H	$(CH_2)_2OH$	OH	156	n.d.	n.d.

*Table 1: Kinetic parameters of TMPKmt with the 3'-deoxy-3'-*C*-branched-chain-substituted nucleosides and nucleotides. Abbreviation n.d.: not determined*

[a] K_m*-value*

[b] *No inhibition (n. i.) at 1000 mM*

[c] *No inhibition (n. i.) at 4000 mM*

These results indicate that the enzyme can accommodate sterically more demanding substituents at the 3'-position. Since **5** binds the enzyme as efficiently as **3** and **4**, ionic interaction with Asp9 seems not a prerequisite for effective affinity. Interestingly, deletion of the phosphate moiety typically results in a modest (at most 6-fold) affinity loss, while this effect is negligible in the case of the 3'-CH_2OH substituent. The largest discrepancy between the K_i values of the free and phosphorylated forms is found for the 3'-CH_2NH_2 couple. The positively charged ammonium ion may well interact with the negatively charged phosphate moiety, thereby forcing the nucleotide in a favorable conformation for interaction with

TMPKmt. In the absence of the phosphoryl group, this conformation is no longer preferred and the conformational mobility of the 3’-CH_2NH_2 may account for the loss of affinity.

Because nucleotide **2** has a much higher affinity than the corresponding 2’-deoxyribo analogue **1**, compound **8** was expected to be active. However, introduction of a methylene spacer between the NH_2-group and C-3’ of **2**, leads to **8** with a 30-fold lower affinity than the deoxyribo analogue **4**. The affinities of the other ribo analogues were weak, the smallest decrease (6-fold) in affinity upon introduction of the 2’-hydroxyl being found for **14**. Apparently, the presence of Tyr103 close to the 2’-position impedes favorable binding characteristics of these ribo analogues. Thus, compound **2** is the only ribo analogue with a higher affinity than its deoxy counterpart.

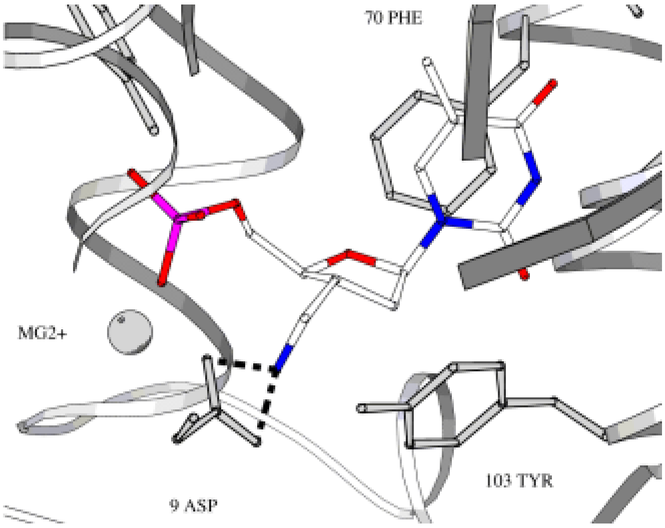

*Figure 2: Predicted binding mode of **4** with TMPKmt. The sugar ring is in the 2’-*exo*-3’-*endo *conformation and the 6'-amine lies at 2.64 Å of the carboxylic oxygen of Asp9.*

In order to probe the influence of the arm length at position 3’, **15** was synthesised. Its K_i value was 5.8 and 3.8 times higher than that of dT (n = 0) and **12** (n = 1), respectively.

The selectivity of all target compounds for TMPKmt versus TMPKh was evaluated . All are inhibitors of TMPKh except the 3'-hydroxymethylnucleotide **6,** which behaves as a weak substrate. Most nucleotides (**3**, **5**, **6** and **8**) show affinities for the human enzyme that lie in the same order of magnitude as those for the *Mycobacterium tuberculosis* enzyme. The non-phosphorylated 3'-*C*-branched-chain nucleosides **9**, **11** and **12**, on the other hand exhibit very low affinities for the human enzyme, which results in selectivity indices between 10 and 26. Somehow a 3'-CH_2N_3 functionality combined with a 2'-hydroxyl seems to introduce a TMPKmt versus TMPKh selectivity in these 3'-*C*-branched-chain analogues, whereas an opposite tendency is observed upon reduction of the 3'-CH_2N_3 group. To conclude, nucleosides **9**, **11** and **12** emerge as the inhibitors that combine a low K_i-value with a favourable SI ratio and are therefore put forward as promising leads for further research.

Conclusions

In the search for more potent drugs to treat tuberculosis, the discovery of new leads with a novel mechanism of action is of utmost importance. From this point of view, TMPKmt represents an attractive potential target for the rational design of inhibitors, mainly because of its crucial positioning in the metabolic activation of thymidine and because of the different structures between the enzymes of the bacterium and the host. This work describes the synthesis of a number of 3’-*C*-branched chain-substituted substrate analogues of dTMP in the ribo and 2’-deoxyribo series.

Several 3'-deoxy 3'-*C*-branched chain-substituted dTMP analogues (**3**-**5**) emerged as promising leads for the design of novel anti-tuberculosis agents. These molecules have a high diversity at the 3’-substitution site: the fluorine atom in **5** is sterically much smaller than an azido group in **3**, while the amino group of **4** is positively charged. The K_i values of these compounds are very similar. This suggests that they bind in a different way, involving (most probably) Asp9 and Tyr103 and the Mg^{2+} ion present near the 5’-*O*-phosphate group. As these nucleosides have a 3’-C substituent, they lack the *gauche* effect that might stabilise 2’-deoxy-nucleosides in the South type conformation. In a cooperative manner, a voluminous 3’-substituent should preferably occupy a pseudoequatorial position, which is achieved in the North type conformation. On the other hand, the steric interactions between the 3'-H and the thymine base should theoretically drive their pseudorotational equilibria to the South type sugar conformation. This conformational mobility, together with the flexibility of the amino acid side chain in the active site, renders prediction of binding affinities of nucleoside analogues difficult.

Importantly, it should be noted that introduction of a hydroxyl group at the 2’-position leads to an increase in affinity for the 3’-amino analogues **1** and **2**, which is a remarkable feature for an enzyme that metabolises only 2’-deoxynucleotides. However, protonation of the 3’-amino group may affect the conformation of the nucleotide, as well as its interaction with the enzyme. The most important observation refers to the small differences in binding affinities of the 5’-*O*-phosphorylated and non-phosphorylated analogues, as adequately shown in the very similar activities of **6** and **12**. This result facilitates further elaboration, as it is generally accepted that 5’-*O*-phosphorylated nucleosides are hardly taken up by cells. Originally, our objective was to synthesise modified nucleoside 5’-*O*-phosphates that are not prone to further phosphorylation in order to avoid cell toxicity. However, we confirmed that non-phosphorylated analogues are as active as their phosphorylated analogues. In addition affinity tests on TMPKh indicated that nucleosides have a significantly better selectivity profile vis à vis TMPKh. Therefore, we will pursue in this area. Further research will be directed to (i) exploration of other 3’-substituents of 2’,3’-dideoxythymidine with increased affinities and (ii) investigation of the most appropriate 5’-substituent devoid of phosphorylation capacity and, thus, associated to a low risk of toxicity.

Experimental Section

Spectrophotometric binding assay.

The *in vitro* tests were done on recombinant enzymes overexpressed in *E. coli*: TMPKmt[34] and TMPKh (will be described elsewhere by Pochet et al.). TMPKmt and TMPKh activity was determined using the coupled spectrophotometric assay described by Blondin et al.[17] at 334 nm in an Eppendorf ECOM 6122 photometer. The reaction medium (0.5 ml final volume) contained 50 mM Tris-HCl pH 7.4, 50 mM KCl, 2 mM $MgCl_2$, 0.2 mM NADH, 1 mM phosphoenol pyruvate and 2 units each of lactate dehydrogenase, pyruvate kinase and nucleoside diphosphate kinase. The concentrations of ATP and dTMP were kept constant at 0.5 mM and 0.05 mM respectively, whereas the concentrations of analogues varied between 0.01 and 2 mM.

Modeling

The X-ray structure published by de la Sierra et al.[5] (pdb entry 1G3U) was used in all docking experiments. Water molecules and sulphate counter ions were removed. The Mg^{2+} was considered as being part of the enzyme. Explicit hydrogen atoms were added to the enzyme and inhibitor structures using Reduce.[18] PDB files were then converted to mol2 files using Babel.[19] The position of atom C1' in the dTMP ligand in the pdb file 1G3U was used as the center of a 20 Å docking sphere. Default settings were used in Gold for all dockings.[20,21] The structures in the top 25 of the docking scores were retained for visual inspection and analysis. Figures 1 and 2 were generated using Molscript.[22]

Synthesis

General

NMR spectra were obtained with a Varian Mercury 300 or a Unity 500 spectrometer. Chemical shifts are given in ppm (δ) relative to residual solvent peak in the case of DMSO-d_6 (2.5 ppm). All signals assigned to amino and hydroxyl groups were exchangeable with D_2O. Mass spectra and exact mass measurements were performed on a quadrupole/orthogonal-acceleration time-of-flight (Q/oaTOF) tandem mass spectrometer (qTof 2, Micromass, Manchester, UK) equipped with a standard electrospray ionisation (ESI) interface. Samples were infused in a 2-propanol:water (1:1) mixture at 3 µL/min. The final nucleoside 5'-*O*-monophosphates were ultimately purified using a Gilson HPLC system with a Gilson 322 pump, a UV/VIS-156 detector on a C18 column (10 µM; Altech; Altima; 250 × 22 mm). The final nucleosides were purified by HPLC on a Perkin Elmer system with a diode-array ultraviolet absorption detector. A Kromasil reverse phase column (C18, 250 x 4.6 mm) was used with a linear gradient of acetonitrile (A) in 10 mM triethylammonium acetate buffer at pH 7.5 (B) over 20 min at a flow rate of 5.5 ml/min. The purity of all target compounds was assessed by HPLC using either a reverse phase column (Kromasil C18) with a linear gradient of A in B at a flow rate of 1 ml/min over 20 min (method A) or an anion-exchange column (Mono Q HR5/5) with a linear gradient of 1 M triethylammonium bicarbonate buffer at pH 7.8 in water (method B).

Precoated Merck silica gel F_{254} plates were used for TLC and spots were examined under UV light at 254 nm and revealed by sulfuric acid-anisaldehyde spray or phosphomolybdic acid (0.5% in EtOH) solution. Column chromatography was performed on Uetikon silica (0.2-0.06 mm).

Anhydrous solvents were obtained as follows: THF was distilled from sodium/benzophenone; pyridine was refluxed overnight over potassium hydroxide and distilled; dichloromethane, dichloroethane and toluene were stored over calcium hydride, refluxed, and distilled; DMF was stored over Linde 4 Å molecular sieves, followed by distillation under reduced pressure.

3-[(*p*-Anisyloxy)methyl]-5-*O*-benzyl-3-deoxy-1,2-*O*-(isopropylidene)-a-D-ribofuranose (21)

To a solution of **18**[12] (612 mg, 2.08 mmol), Ph_3P (708 mg, 2.7 mmol) and *p*-methoxyphenol (775 mg, 6.24 mmol) in THF (6 mL) was added dropwise diethyl azodicarboxylate (0.42 mL, 2.7 mmol). The reaction mixture was heated to 80 °C and stirred for 1.5 h. The mixture was diluted with ether (150 mL) and the organic layer was washed with water (150 mL), dried over $MgSO_4$ and evaporated. The resulting residue was purified by column chromatography (pentane−EtOAc, 9:1) yielding **21** (724 mg, 87%) as a foam. ^{1}H NMR (300 MHz, $CDCl_3$): *d* 1.28 and 1.43 (6 H, 2s, CMe_2), 2.38 (1H, m, H-3), 3.63 (1H, dd, H-5A), 3.78 (3H, s, OCH_3), 3.83 (1H, dd, $J_{5A,\,5B} = -10.8$ Hz, H-5B), 3.97 and 4.25 (2H, 2dd, 6-H) , 4.15 (1H, m, H-4), 4.54 and 4.66 (2H, 2d, C*H*$_2$Ph), 4.79 (1H, app t, H-2,) 5.89 (1H, d, *J* = 3.7 Hz, H-1), 6.80 (4H, m, 4-MeO*Ph*), 7.34 (5H, m, CH$_2$*Ph*); HRMS (ESI-MS) for $C_{23}H_{28}O_6Na$ [M + Na]$^+$: found, 423.1813; calcd, 423.1783.

1,2-Di-*O*-Acetyl-3-[(*p*-anisyloxy)methyl]-5-*O*-benzyl-3-deoxy-a -D-ribofuranose (22)

A solution of **21** (7.812 g, 19.51 mmol) in 75% HOAc (200 mL) was stirred at 80 °C for 8 h. The reaction mixture was evaporated to give crude 5-*O*-benzyl-3-deoxy-3-[(*p*-anisyloxy)methyl]-α-D-ribofuranose as a syrup. The obtained residue was dissolved in pyridine (150 mL) and acetic anhydride (23 mL, 246 mmol) was added. The solution was stirred at room temperature for 3 h. The solvent was removed under vacuum and the resulting residue was purified by column chromatography (pentane–EtOAc, 8:2) to yield **22** (8.039 g, 93%) as a foam. ^{1}H NMR (300 MHz, $CDCl_3$): *d* 1.96 and 2.05 (6H, 2s, 2 $COCH_3$), 2.96 (1H, m, H-3), 3.57-3.73 and 4.00-4.14 (4H, 2m, H-5 and H-6), 3.78 (3H, s, OCH_3), 4.33 (1H, m, H-4), 4.59 (2H, app d, C*H*$_2$Ph), 5.40 (1H, m, H-2), 6.12 and 6.46 (1H, s and d, H-1α and H-1β), 6.81 (4H, m, 4-MeO*Ph*), 7.34 (5H, m, CH$_2$*Ph*); HRMS (ESI-MS) for $C_{24}H_{28}O_8Na$ [M + Na]$^+$: found, 467.1707; calcd, 467.1682.

1-{3-[(*p*-Anisyloxy)methyl]-5-*O*-benzyl-3-deoxy-b -D-ribofuranosyl}thymine (23)

Thymine (225 mg, 1.78 mmol) was suspended in hexamethyldisilazane (20 mL, 95 mmol) containing trimethylsilylchloride (0.16 mL, 1.26 mmol) and pyridine (1.6 mL). The mixture was heated at reflux overnight. The reaction mixture was evaporated and coevaporated with toluene. The resulting residue and **22** (720 mg, 1.62 mmol) were dissolved in dry 1,2-dichloroethane (12 ml) and trimethylsilyl triflate (0.34 ml, 1.88 mmol) was added dropwise. The clear solution was stirred 5 h at room temperature. The reaction mixture was diluted with CH_2Cl_2 (200 mL) and washed with saturated aqueous $NaHCO_3$. The organic layer was dried over $MgSO_4$ and evaporated. The resulting crude 1-[2-*O*-acetyl-3-[(*p*-anisyloxy)methyl]-5-*O*-benzyl-3-deoxy-β-D-ribofuranosyl]thymine was treated with a 7N methanolic ammonia solution (19 mL) at room temperature for 15 h. Evaporation yielded a residue which was purified by column chromatography (CH_2Cl_2–MeOH, 98:2) to afford **23** (592 mg, 78%) as a white foam. ^{1}H NMR (300 MHz, DMSO-d_6): *d* 1.39 (3 H, s, 5-CH_3), 2.68 (1H, m, H-3’), 3.69 (3H, s, OCH_3), 3.73 (1H, app dd, H-2’), 3.95 (2H, m, H-5’), 4.17–4.31 (3H, m, H-4’ and H-6’), 4.59 (2H, 2 app d, C*H*$_2$Ph), 5.72 (1H, app s, H-1’), 5.88 (1H, d, 2’-OH), 6.85 (4H, s, 4-MeO*Ph*), 7.33 (5H, m, CH$_2$*Ph*), 7.74 (1H, d, $J_{6,\ 5\text{-}CH3}$ = 1.0, H-6); HRMS (ESI-MS) for $C_{25}H_{28}N_2O_7Na$ [M + Na]$^+$: found, 491.1820; calcd, 491.1794.

1-{3-[(*p*-Anisyloxy)methyl]-5-*O*-benzyl-2,3-dideoxy-b -D-*erythro*-pentofuranosyl}thymine (24)

To an ice-cold solution of **23** (6.55 g, 14.0 mmol) and DMAP (3.42 g, 28.0 mmol) in CH_3CN (290 mL) was gradually added phenyl chlorothionocarbonate (2.6 mL, 18.8 mmol). The mixture was stirred at 0 °C for 1.5 h. The solvent was removed *in vacuo*, and the residue was dissolved in EtOAc (500 mL). The solution was washed with water (2 x 500 mL), dried over anhydrous $MgSO_4$, filtered, and evaporated *in vacuo* to give 1-[3-[(*p*-anisyloxy)methyl]-5-*O*-benzyl-3-deoxy-2-*O*-(phenoxythiocarbonyl)-β-D-ribofuranosyl]thymine as a syrup. The syrup was dissolved in toluene (290 mL) to which 2,2’-azobis(2-methyl-propionitrile) (AIBN, 5.89 g, 35.87 mmol) and tri-*n*-butyltinhydride (8.00 g, 27.5 mmol) were added at 50-60 °C under N_2. The reaction mixture was stirred at 95-100 °C for 1 h. The solvent was removed in vacuo and the residue was purified by column chromatography (pentane–EtOAc, 2:1) to yield **24** (3.98 g, 63%) as a foam. ^{1}H NMR (300 MHz, DMSO-d_6): *d* 1.52 (3 H, s, 5-CH_3), 2.24-2.29 (2H, m, H-2’), 2.80 (1H, m, H-3’), 3.69 (3 H, s, OCH_3), 3.71 (1H, m, H-5’A), 3.87 (1H, dd,

$J_{5'A,\ 5'B}$ = −10.9 Hz, H-5'B), 3.94–4.06 (3H, m, H-4' and H-6'), 4.53 and 4.57 (2H, 2d, C*H*$_2$Ph), 6.1 (1H, dd, *J* = 7.0 Hz, H-1'), 6.87 (4H, s, 4-MeO*Ph*), 7.28–7.36 (5H, m, CH$_2$*Ph*), 7.67 (1H, br s, H-6); MS (ESI) *m/z* (%) 475.2 ($[M + Na]^+$, 100), 453.2 ($[M + H]^+$, 47).

1-{3-[(*p*-Anisyloxy)methyl]-2,3-dideoxy-b-D-*erythro*-pentofuranosyl}thymine (25)

A solution of **24** (730 mg, 1.61 mmol) in MeOH (40 ml) was hydrogenated at atmospheric pressure for 5h in the presence of 10% Pd/C (390 mg). The catalyst was removed by filtration through celite and the filtrate was concentrated *in vacuo*. The residue was purified by column chromatography (CH_2Cl_2–MeOH, 98:2) to give 496 mg (85%) of the debenzylated intermediate **25** as a white foam. ^{1}H NMR (300 MHz, DMSO-d_6): *d* 1.78 (3 H, s, 5-CH_3), 2.13–2.28 (2H, m, H-2'), 2.70 (1H, m, H-3'), 3.64 (1H, m, H-5'A), 3.69 (3H, s, OCH_3) 3.78 (1H, m, H-5'B), 3.88 (1H, m, H-4'), 3.96 (2H, d, H-6'), 5.13 (1H, t, *J* = 5.3 Hz, 5'-OH), 6.09 (1H, dd, H-1'), 6.87 (4H, m, 4-MeO*Ph*), 7.88 (1H, d, *J* = 1.2 Hz, H-6); HRMS (ESI-MS) for $C_{18}H_{22}N_2O_6Na$ $[M + Na]^+$: found, 385.1413; calcd, 385.1375.

1-(2,3-Dideoxy-3-hydroxymethyl-b-D-*erythro*-pentofuranosyl)-5-hydroxymethylthymine (27)

To a solution of **25** (124 mg, 0.34 mmol) in CH_3CN–H_2O (4:1) (5.5 mL) was added ceric ammonium nitrate (940 mg, 1.70 mmol). After 5 min the mixture was diluted with water (20 mL), washed with $CHCl_3$ (20 mL) and the aqueous layer was evaporated. The residue was purified by column chromatography (CH_2Cl_2–MeOH, 95:5→90:10) to give **27** (36 mg, 39%) as a foam. ^{1}H NMR (500 MHz, DMSO-d_6): *d* 2.17 (ddd, $J_{1',\ 2'}$ = 4.6 Hz, H-2'), 2.00 (1H, dt, $J_{2',\ 2''}$ = 13.7 Hz, $J_{1',\ 2''}$ = 7.2 Hz, H-2''), 2.31 (1H, m, H-3'), 3.44 (2H, m, H-6'), 3.67 and 3.55 (2H, 2m, H-5'), 3.78 (1H, dt, H-4'), 4.13 (2H, s, 5-CH_2), 4.76 (1H, t, 6'-OH), 4.86 (1H, t, 5-CH_2O*H*), 4.94 (1H, t, 5'-CH_2O*H*), 6.01 (1H, dd, $J_{1',\ 2'}$ = 4.4 and $J_{1',\ 2''}$ = 6.9 Hz, H-1'), 7.81 (1H, s, H-6), 11.24 (1H, s, H-3); ^{13}C NMR (125 MHz, DMSO-d_6): *d* 35.04 (C-2'), 40.82 (C-3'), 56.07 (5-CH_2), 61.59 (C-6'), 62.62 (C-5'), 83.47 (C-4'), 84.26 (C-1'), 113.7 (C-5), 137.01 (C-6), 150.33 (C-2), 162.98 (C-4); MS (ESI) *m/z* (%) 295.1 ($[M + Na]^+$, 70).

General procedure for the selective phosphorylation of the 5'-hydroxylgroup

To a cooled (0 °C) solution of the nucleoside (0.42 mmol) in trimethyl phosphate (10 mL/mmol), $POCl_3$ (6.5 eq) was added dropwise and the mixture was stirred for 5 h at 0° C and for 30 min at room temperature, after which it was poured into crushed ice-water (10 mL), neutralised with concentrated NH_4OH and evaporated to dryness. The resulting residue was purified by column chromatography (iPrOH–NH_4OH–H_2O, 77.5:15:2.5→60:30:5). Further purification of the white powder by HPLC (C-18, CH_3CN–MeOH–0.05% HCOOH in H_2O 45:45:10, 3 mL/min) and lyophilisation of the appropriate fractions, provided the nucleotide as a white powder.

1-{3-[(*p*-Anisyloxy)methyl]-2,3-dideoxy-5-*O*-phosphoryl-b-D-*erythro*-pentofuranosyl}thymine (26)

25 was phosphorylated as described in the general procedure and nucleotide **26** isolated in 52% yield. ^{1}H NMR (300 MHz, D_2O): *d* 1.94 (3 H, s, 5-CH_3), 2.28–2.44 (2H, m, H-2'), 2.86 (1H, m, H-3'), 3.81 (3H, s, OCH_3), 4.05–4.26 (5H, m, H-6', H-4' and H-5'), 6.22 (1H, dd, *J* = 5.2 and 6.6 Hz, H-1'), 6.98 (4H, m, 4-MeO*Ph*), 7.80 (1H, d, *J* = 0.9 Hz, H-6); ^{13}C NMR (125 MHz, D_2O): *d* 14.26 (5-CH_3), 37.21 (C-2'), 40.77 (C-3'), 58.51 (OCH_3), 68.36 (C-5', $^2J_{C,P}$ = 19.6 Hz), 72.19 (C-6'), 84.83 (C-4', $^3J_{C,\ P}$ = 8.8 Hz), 88.15 (C-1'), 113.86, 117.71 and 118.76 (C-5 and arom H), 140.13 (C-6), 154.18, 155.28, 156.10 (C-2 and arom H), 169 (C-4);

^{31}P NMR (500 MHz, D_2O): δ 1.03; HRMS (ESI-MS) for $C_{18}H_{24}N_2O_9P$ [M + H]$^+$: found, 443.1231; calcd, 443.1219.

1-[2,3-Dideoxy-3-(hydroxymethyl)-5-*O*-phosphoryl-β-D-*erythro*-pentofuranosyl]thymine (6)

To a solution of **26** (106 mg, 0.23 mmol) in H_2O (2 mL) was added ceric ammonium nitrate (162 mg, 0.29 mmol). After 15 min iPrOH–NH_4OH–H_2O (60:30:5) (20 mL) was added, the resulting suspension was filtered and the precipitate washed with water. The combined filtrates were evaporated under reduced pressure and the residue was purified by column chromatography (iPrOH–NH_4OH–H_2O, 77.5:15:2.5→60:30:5). The resulting white powder was further purified by HPLC (C-18, CH_3CN–MeOH–0.05% HCOOH in H_2O, 45:45:10, 3 mL/min) and the appropriate fractions were lyophilised yielding **6** (62 mg, 76%) as a white powder. ^{1}H NMR (300 MHz, D_2O): δ 1.93 (3 H, d, 5-CH_3), 2.30 (2H, m, H-2'), 2.62 (1H, m, H-3'), 3.70 (2H, d, $J_{6',3'}$ = 6.1 Hz, H-6'), 4.01 (1H, m, H-4'), 4.14 (2H, m, H-5'), 6.16 (1H, dd, J = 5.0 and 6.7 Hz, H-1'), 7.83 (1H, d, J = 1.2 Hz, H-6); ^{13}C NMR (125 MHz, D_2O): δ 14.28 (5-CH_3), 37.10 (C-2'), 43.04 (C-3'), 64.75 (C-6'), 67.88 (C-5'), 85.21 (C-4'), 88.01 (C-1'), 140.42 (C-6); ^{31}P NMR (500 MHz, D_2O): δ 1.03; HRMS (ESI-MS) for $C_{11}H_{18}N_2O_8P$ [M + H]$^+$: found, 337.0817; calcd, 337.0800.

1-[5-*O*-Benzyl-2,3-dideoxy-3-(hydroxymethyl)-β-D-*erythro*-pentofuranosyl]thymine (28)

To a solution of **24** (3.3 g, 7.29 mmol) in CH_3CN–H_2O (4:1) (120 mL) was added ceric ammonium nitrate (19.89 g, 36.68 mmol). After 5 min the mixture was diluted with $CHCl_3$ (300 mL), washed with brine (200 mL) and a saturated solution of $Na_2S_2O_5$ (200 mL), dried over $MgSO_4$, filtered and evaporated. The residue was purified by column chromatography (CH_2Cl_2–MeOH, 97:3) to give the expected product **28** (1.810 g, 72%) as a foam. ^{1}H NMR (300 MHz, DMSO-d_6): δ 1.52 (3 H, d, 5-CH_3), 2.01–2.19 (2H, m, H-2'), 2.44 (1H, m, H-3'), 3.46 (2H, app t, H-6'), 3.64 (1H, dd, H-5'A), 3.79 (1H, dd, $J_{5'A,5'B}$ = –10.8 Hz, H-5'B), 3.95 (1H, m, H-4'), 4.56 (2H, app s, C*H*$_2$Ph), 4.82 (1H, t, 6'-CH_2OH), 6.01 (1H, dd, J = 7.0 and 4.5 Hz, H-1'), 7.36 (5H, m, CH_2*Ph*), 7.64 (1H, d, J = 1.1 Hz, H-6); HRMS (ESI-MS) for $C_{18}H_{22}N_2O_5Na$ [M + Na]$^+$: found, 369.1455; calcd, 369.1426.

1-[2,3-Dideoxy-3-(hydroxymethyl)-β-D-*erythro*-pentofuranosyl]thymine (12)

Hydrogenation of **28** (62.0 mg, 0.179 mmol) was accomplished at atmospheric pressure of H_2 at room temperature for 45 min using 10% Pd/C (50 mg) in MeOH (5 mL). Column chromatography (CH_2Cl_2–MeOH, 95:5) yielded **12** (43.4 mg, 95%) as a white foam. ^{1}H NMR (300 MHz, DMSO-d_6): δ 1.78 (3 H, d, J = 1.0 Hz, 5-CH_3), 1.97–2.04 (2H, m, H-2'), 2.36 (1H, m, H-3'), 3.44 (2H, app d, $J_{6',3'}$ = 5.7 Hz, 6'-H), 3.56 (1H, dd, H-5'A) 3.69 (1H, dd, $J_{5'A,5'B}$ = –11.9 Hz, H-5'B), 3.78 (1H, m, H-4'), 4.76 and 5.03 (2H, 2t, 5'-OH and 3'-OH), 5.98 (1H, dd, J = 4.6 and 6.9 Hz, H-1'), 7.84 (1H, br s, H-6); HRMS (ESI-MS) for $C_{11}H_{16}N_2O_5Na$ [M + Na]$^+$: found, 279.0953; calcd, 279.0957. Anal. ($C_{11}H_{16}N_2O_5$) C, H, N.

1-[5-*O*-Benzyl-2,3-dideoxy-3-(fluoromethyl)-β-D-*erythro*-pentofuranosyl]thymine (29)

DAST (0.280 mL, 2.12 mmol) was dissolved in CH_2Cl_2 (5 mL) and pyridine (0.36 mL) at 0 °C under nitrogen. Nucleoside **28** (619 mg, 1.79 mmol) was added in several portions and the solution was allowed to warm to room temperature. After 7 h, the solvent was removed under vacuum to give a syrup which was purified by column chromatography (CH_2Cl_2–MeOH, 99:1) to yield **29** (185 mg, 30%) as a white foam. ^{1}H NMR (300 MHz, DMSO-d_6): *d* 1.54 (3 H, s, 5-CH_3), 2.10–2.23 (2H, m, H-2’), 2.69–2.80 (1H, m, H-3’), 3.65 (1H, dd, H-5’A), 3.80 (1H, dd, $J_{5'A,\,5'B}$ = –10.9 Hz, H-5’B), 4.02 (1H, m, H-4’), 4.45–4.61 (4H, m, H-6’ and C*H*$_2$Ph), 6.05 (1H, dd, *J* = 4.7 and 7.0 Hz, H-1’), 7.35 (5H, m, CH_2*Ph*), 7.62 (1H, d, *J* = 1.1 Hz, H-6); HRMS (ESI-MS) for $C_{18}H_{22}FN_2O_4$ [M + H]$^+$: found, 349.1586; calcd. 349.1563.

1-[2,3-Dideoxy-3-(fluoromethyl)-b-D-*erythro*-pentofuranosyl]thymine (11)

A solution of compound **29** (185 mg, 0.531 mmol) in MeOH (8 mL) was hydrogenated at atmospheric pressure in the presence of Pd/C 10% (107 mg) for 5 h. The catalyst was removed by filtration over a celite path, the solvent evaporated *in vacuo* and the residue purified by column chromatography (CH_2Cl_2–MeOH, 95:5) yielding **11** (134 mg, 98%) as a white foam. ^{1}H NMR (300 MHz, DMSO-d_6): *d* 1.78 (3 H, s, 5-CH_3), 2.06–2.21 (2H, m, H-2’), 2.60–2.71 (1H, m, H-3’), 3.56 (1H, dd, H-5’A), 3.71 (1H, dd, $J_{5'A,\,5'B}$ = –12.0 Hz, H-5’B), 3.84 (1H, m, H-4’), 4.44–4.57 (2H, dd, $J_{6',\,F}$ = 47.3 Hz, H-6’), 5.14 (1H, br s, 5’-OH), 6.02 (1H, dd, *J* = 4.9 and 6.7, H-1’), 7.82 (1H, s, H-6); ^{13}C NMR (75 MHz, DMSO-d_6): *d* 62.19 (C-5’), 83.04 (C-4’, $J_{4',\,F}$ = 4.5 Hz), 84.50 (C-1’), 85.64 (C-6’, $J_{6',\,F}$ = 179 Hz), 109.64 (C-5), 136.96 (C-6), 151.06 (C-2), 164.50 (C-4), under DMSO-signal (C-3’), 34.50 (C-2’, $J_{2',\,F}$ = 5.3 Hz), 12.95 (5-CH_3); ^{19}F NMR (300MHz, DMSO-d_6): *d* –222.73; HRMS (ESI-MS) for $C_{11}H_{16}FN_2O_4$ [M + H]$^+$: found, 259.1119; calcd, 259.1093. Anal. ($C_{11}H_{15}FN_2O_4$) C, H, N.

1-[2,3-Dideoxy-3-(fluoromethyl)-5-*O*-phosphoryl-b-D-*erythro*-pentofuranosyl]thymine (5)

Phosphorylation of **11** was performed as described in the general procedure and the title compound isolated in 49% yield. ^{1}H NMR (300 MHz, D_2O): *d* 1.94 (3 H, s, 5-CH_3), 2.29–2.44 (2H, m, H-2’), 2.77–2.89 (1H, m, H-3’), 4.00–4.22 (2H, m, H-5’), 4.25 (1H, m, H-4’), 4.53–4.70 (2H, m, H-6’), 6.16 (1H, dd, *J* = 5.0 and 7.0 Hz, H-1’), 7.84 (1H, d, *J* = 1.2 Hz, H-6); ^{13}C NMR (75 MHz, D_2O): *d* 11.69 (5-CH_3), 33.45 (C-2’, $J_{2',\,F}$ = 6.0 Hz), 65.30 (C-5’), 38.66 (C-3’, $J_{3',\,F}$ = 19.6 Hz), 81.50 (C-4’, $J_{4',\,F}$ = 6.7 Hz), 84.10 (C-6’, $J_{6',\,F}$ = 165.2 Hz), 85.43 (C-1’), 111.40 (C-5), 137.69 (C-6), 151.80 (C-2), 166.80 (C-4); ^{19}F NMR (300 MHz, D_2O): *d* –224.50; ^{31}P NMR (500 MHz, D_2O): *d* 1.12; HRMS (ESI-MS) for $C_{11}H_{17}FN_2O_7P$ [M + H]$^+$: found, 339.0806; calcd, 339.0757.

1-[3-(Azidomethyl)-5-*O*-benzyl-2,3-dideoxy-b-D-*erythro*-pentofuranosyl]thymine (30)

Methanesulfonyl chloride (0.180 mL, 2.33 mmol) was added to a solution of compound **28** (306 mg, 0.883 mmol) in pyridine (3 mL) at 0 °C. The reaction mixture was stirred at 0° C during 1 h. Then it was diluted with CH_2Cl_2 (50 mL), washed with saturated aqueous $NaHCO_3$ (50 mL) and dried over anhydrous $MgSO_4$. The solvent was removed under diminished pressure to give the crude mesylate. The obtained residue was dissolved in DMF (16 mL) and treated with NaN_3 (574 mg 8.83 mmol) at 95 °C for 1.5 h to complete the reaction. The reaction mixture was evaporated to dryness *in vacuo* and the residue was dissolved in CH_2Cl_2 (50 mL). The organic layer was washed with water (50 mL), dried over anhydrous $MgSO_4$ and evaporated to give a sirup which was purified by column chromatography (CH_2Cl_2–MeOH, 99:1) yielding **30** (260 mg, 79%) as a white foam. ^{1}H NMR (300 MHz, DMSO-d_6): *d* 1.52 (3 H, d, 5-CH_3), 2.50 (2H, m, H-2’), 2.60 (1H, m, H-3’), 3.46–3.59 (2H, 2dd, H-6’), 3.66 (1H, dd, H-5’A), 3.83 (1H, dd, $J_{5'A,\,5'B}$ = –10.4 Hz, H-5’B), 3.93 (1H, m, H-4’), 4.57 (2H, app s, C*H*$_2$Ph), 6.04 (1H, app t, *J* = 5.9 Hz, H-1’), 7.31 (5H, m, CH_2*Ph*), 7.62 (1H, br s, H-6); HRMS (ESI-MS) for $C_{18}H_{21}N_5O_4Na$ [M + Na]$^+$: found, 394.1489; calcd, 394.1491.

1-[3-(Azidomethyl)-2,3-dideoxy-b-D-*erythro*-pentofuranosyl]thymine (9)

To a solution of **30** (1.49 g, 4.01 mmol) in CH_2Cl_2 (160 mL) at -78 °C was slowly added a 1M solution of BCl_3 in CH_2Cl_2 (16.1 mL, 16.1 mmol). After 15 min MeOH (5 mL) was added and the reaction mixture was evaporated to dryness under reduced pressure. The resulting residue was purified by column chromatography (CH_2Cl_2–MeOH, 90:10) affording **9** (1.00 g, 89%) as a white foam. ^{1}H NMR (300 MHz, DMSO-d_6): *d* 1.78 (3 H, d, 5-CH_3), 2.13 (2H, m, H-2’), 2.51 (1H, m, H-3’), 3.51 (2H, app d, H-6’), 3.55–3.61 (1H, m, H-4'), 3.69–3.74 (2H, m, H-5’), 5.13 (1H, app t, 5’-OH), 6.02 (1H, dd, *J* = 5.0 and 6.3 Hz, H-1’), 7.82 (1H, d, *J* = 1.1 Hz, H-6); ^{13}C NMR (125 MHz, DMSO-d_6): *d* 12.96 (5-CH_3), 36.36 (C-2’), 38.07 (C-3’), 52.71 (C-6’), 61.90 (C-5’), 84.45 and 84.13 (C-1’ and C-4’), 109.56 (C-5), 136.97 (C-6), 151.05 (C-2), 164.51 (C-4); HRMS (ESI-MS) for $C_{11}H_{15}N_5O_4Na$ [M + Na]$^+$: found, 304.1033; calcd, 304.1021. Anal. ($C_{11}H_{15}N_5O_4$) C, H, N.

1-[3-(Aminomethyl)-2,3-dideoxy-b-D-*erythro*-pentofuranosyl]thymine (10)

Compound **9** (169 mg, 0.60 mmol) and triphenylphosphine (252 mg, 0.96 mmol) were dissolved in pyridine (7 mL) and stirred at room temperature. After 1h, concentrated NH_4OH (6 mL) was added and the solution was allowed to stir for an additional 2h. Pyridine was removed under reduced pressure, water (8 mL) was added and the unreacted triphenylphosphine and triphenylphosphine oxide were removed by filtration. The filtrate was extracted with toluene and the water layer was evaporated under reduced pressure to give a syrup. The syrup was purified by column chromatography (0.175 N NH_3 in CH_2Cl_2–MeOH, 80:20) to yield amine **10** (112 mg, 73%) as a white foam. ^{1}H NMR (300 MHz, DMSO-d_6): *d* 1.78 (3 H, s, 5-CH_3), 2.3–2.14 (2H, m, H-2’), 2.24 (1H, m, H-3’), 2.55–2.65 (2H, m, H-6’), 3.55-3.71 (3H, m, H-5’ and H-4’), 5.95 (1H, dd, *J* = 3.9 and 6.9 Hz, H-1’), 7.8 (1H, d, *J* = 1.1 Hz, H-6); ^{13}C NMR (75 MHz, DMSO-d_6): *d* 12.98 (5-CH_3), 43.38, 41.60 and 37.05 (C-6’, C-3’ and C-2’), 62.27 (C-5’), 85.49 (C-4’), 85.24 (C-1’), 109.37 (C-5), 136.95 (C-6), 151.04 (C-2), 164.51 (C-4); HRMS (ESI-MS) for $C_{11}H_{18}N_3O_4$ [M + H]$^+$: found, 256.1293; calcd, 256,1296. Anal. ($C_{11}H_{17}N_3O_4$) C, H, N.

1-[3-(Azidomethyl)-2,3-dideoxy-5-*O*-phosphoryl-b-D-*erythro*-pentofuranosyl]thymine (3)

9 was phosphorylated as described in the general procedure to yield 53% of the title compound. ^{1}H NMR (300 MHz, D_2O): *d* 1.91 (3 H, s, 5-CH_3), 2.33 (2H, app dd, H-2’), 2.68 (1H, m, H-3’), 3.54 (2H, app d, $J_{6’,3’}$ = 6.3 Hz, H-6’), 4.00–4.19 (3H, m, H-5’ and H-4’), 6.16 (1H, app t, *J* = 5.8 Hz, H-1’), 7.80 (1H, d, *J* = 1.1 Hz, 6-H); ^{13}C NMR (75 MHz, D_2O): *d* 11.75 (5-CH_3), 35.36 (C-2’), 37.71 (C-3’), 52.15 (C-6’), 65.13 (C-5’), 82.62 (C-4’), 85.36 (C-1’), 111.36 (C-5), 137.71 (C-6), 151.79 (C-2), 166.79 (C-4); ^{31}P NMR (500 MHz, D_2O): *d* 1.14; HRMS (ESI-MS) for $C_{11}H_{16}N_5O_7P$ [M + H]$^+$: found, 362.0889; calcd, 362.0865.

1-[3-(Aminomethyl)-2,3-dideoxy-5-*O*-phosphoryl-b-D-*erythro*-pentofuranosyl]thymine (4)

Compound **3** (476 mg, 1.26 mmol) and triphenylphosphine (528 mg, 2.01 mmol) were dissolved in pyridine (15 mL) and stirred at room temperature. After 1h, concentrated NH_4OH (12.6 mL) was added and the solution was allowed to stir for an additional 6.5 h. Pyridine was removed at reduced pressure, water (200 mL) was added and the unreacted triphenylphosphine and triphenylphosphine oxide were removed by filtration. The filtrate was extracted with toluene and the water layer was evaporated under reduced pressure to give a syrup. The syrup was purified by column chromatography (iPrOH–NH_4OH–H_2O, 77.5:15:2.5→60:30:5). The resulting white powder was further purified by HPLC (C-18, CH_3CN–MeOH–0.05% HCOOH in H_2O, 45:45:10, 3 mL/min) and the fractions containing the title compound were lyophilised to yield **4** (306 mg, 69%) as a white powder. ^{1}H NMR (300 MHz, D_2O): ***d*** 1.92 (3 H, s, 5-CH_3), 2.32–2.50 (2H, m, H-2’), 2.74–2.82 (1H, m, H-3’), 3.12–3.26 (2H, 2dd, H-6’), 4.05–4.12 (3H, m, H-4’ and H-5’), 6.17 (1H, dd, *J* = 3.7 and 7.3 Hz, H-1’), 7.78 (1H, d, *J* = 1.2 Hz, H-6); ^{13}C NMR (75 MHz, D_2O): ***d*** 11.76 (5-CH_3), 166.79 (C-2), 151.74 (C-4), 137.70 (C-5), 111.40 (C-6), 85.29 (C-1’), 82.72 (C-4’), 63.94 (C-5’), 40.80 (C-6’), 36.88 (C-3’), 35.95 (C-2’); ^{31}P NMR (500 MHz, D_2O): ***d*** 2.82; HRMS (ESI-MS) for $C_{11}H_{19}N_3O_7PNa$ [M + Na]$^+$: found, 336.0980; calcd, 336.0960.

1-[5-*O*-Benzyl-3-deoxy-3-(hydroxymethyl)-b -D-ribofuranosyl]thymine (31)

This compound was synthesised from **23** (346 mg, 0.74 mmol) using the procedure described for **28** to yield 130 mg (49%) of the title compound as a foam. ^{1}H NMR (300 MHz, DMSO-d_6): ***d*** 1.42 (3 H, s, 5-CH_3), 2.31 (1H, m, $J_{3',6'}$ = 6.6 Hz, H-3’), 3.49 and 3.68 (2H, 2m, 6’-H), 3.64 (1H, m, H-5’A), 3.98 (1H, m, $J_{5'A,5'B}$ = –11.1 Hz, H-5’B), 4.13 (1H, m, H-4’), 4.19 (1H, m, H-2’), 4.58 (3H, m, C*H*$_2$Ph and 6’-OH), 5.60 (1H, d, *J* = 5.0 Hz, 2’-OH), 5.67 (1H, d, *J* = 1.9, H-1’), 7.37 (5H, m, CH_2*Ph*), 7.70 (1H, br s, 6-H); HRMS (ESI-MS) for $C_{18}H_{22}N_2O_6Na$ [M + Na]$^+$: found, 385.1386; calcd, 385.1375.

1-[3-Azidomethyl-5-*O*-benzyl-3-deoxy-b -D-ribofuranosyl]thymine (32)

This compound was synthesised from **31** (130 mg, 0.36 mmol) using the same procedure as described for the synthesis of **30** to yield 123 mg (89%, 2 steps) of the title compound as a foam. ^{1}H NMR (300 MHz, DMSO-d_6): ***d*** 1.42 (3 H, s, 5-CH_3), 2.46 (1H, m, H-3’), 3.35–3.90 (4H, m, H-5’ and H-6’), 4.10 (1H, m, H-4’), 4.22 (1H, m, H-2’), 4.59 (2H, s, C*H*$_2$Ph), 5.67 (1H, d, *J* = 1.6 Hz, H-1’), 5.93 (1H, d, *J* = 5.1 Hz, 2’-OH), 7.37 (CH_2*Ph*), 7.67 (1H, br s, H-6); HRMS (ESI-MS) for $C_{18}H_{21}N_5O_5Na$ [M + Na]$^+$: found, 410.1504; calcd, 410.144.

1-[3-Azidomethyl-3-deoxy-b -D-ribofuranosyl]thymine (13)

Debenzylation of **32** (346 mg, 0.89 mmol) was performed as described for the synthesis of **9** to yield 210 mg (79%) of the title compound as a foam. ^{1}H NMR (300 MHz, DMSO-d_6): ***d*** 1.76 (3 H, s, 5-CH_3), 2.37 (1H, m, H-3’), 3.35–3.78 4H, m, H-5’ and H-6’), 3.91 (1H, m, H-4’), 4.20 (1H, app d, H-2’), 5.24 (1H, br s, 5’-OH), 5.66 (1H, d, $J_{1',2'}$ = 1.9 Hz, H-1’), 5.94 (1H, br s, 2’-OH), 7.95 (1H, br s, H-6). The assignment, done by a cosy-experiment, differs from that reported in ref. 8. ^{13}C NMR (75 MHz, DMSO-d_6): δ 12.95 (5-CH_3), 41.35 (C-3’), 47.90 (C-6’), 61.14 (C-5’), 75.36 (C-2’), 82.90 (C-4’), 91.26 (C-1’), 109.10 (C-5), 136.93 (C-6), 151.11 (C-2), 164.53 (C-4); HRMS (ESI-MS) for $C_{11}H_{15}N_5O_5Na$ [M + Na]$^+$: found, 320.0975; calcd, 320.0971. Anal. ($C_{11}H_{15}N_5O_5$) C, H, N.

1-[3-Aminomethyl-3-deoxy-b -D-ribofuranosyl]thymine (14)

Reduction of azide **13** (173 mg, 0.58 mmol) was accomplished using the procedure described for the synthesis of **11** to yield 123 mg (73%) of amine **14** as a foam. ^{1}H NMR (300 MHz, DMSO-d_6): δ 1.76 (3 H, d, 5-CH_3), 2.16 (1H, m, H-3’), 2.63–2.89 (2H, 2dd, H-6’), 3.59 (1H, dd, H-5’A), 3.76 (1H, dd, , $J_{5'A,5'B}$ = –12.3 Hz, H-5’B), 3.92 (1H, m, H-4’), 4.21 (1H, app d, H-2’), 5.63 (1H, d, *J* = 1.4 Hz, H-1’), 7.94 (1H, d, *J* = 1.1 Hz, H-6); HRMS (ESI-MS) for $C_{11}H_{18}N_3O_5$ [M + H]$^+$: found, 272.1245; calcd, 272.1246. Anal. ($C_{11}H_{17}N_3O_5$) C, H, N.

1-[3-Azidomethyl-3-deoxy-5-*O*-phosphoryl-b -D-ribofuranosyl]thymine (7)

13 was phosphorylated as described in the general procedure to yield 51% of nucleotide **7**. ^{1}H NMR (300 MHz, D_2O): ***d*** 1.92 (3 H, d, 5-CH_3), 2.59 (1H, m, H-3’), 3.56 and 3.66 (2H, 2dd, $J_{6',3'}$ = 5.8 and 8.1 Hz, H-6’), 4.04 (1H, m, H-5’A), 4.26 (1H, m, H-5’B), 4.32 (1H, app d, H-4’), 4.52 (1H, dd, H-2’), 5.86 (1H, d, *J* = 2.0 Hz, H-1’), 7.89 (1H, d, *J* = 1.0 Hz, H-6);

^{13}C NMR (125 MHz, D_2O): ***d*** 14.28 (5-CH_3), 43.40 (C-3’), 49.71 (C-6’), 66.68 (C-5’, $^{2}J_{C,\ P}$ = 36.0 Hz), 77.95 (C-2’), 84.52 (C-4’, $^{3}J_{C,\ P}$ = 8.9 Hz), 93.83 (C-1’), 113.62 (C-5), 139.84 (C-6), 154.25 (C-2), 169.33 (C-4); ^{31}P NMR (500 MHz, D_2O): ***d*** 1.27; HRMS (ESI-MS) for $C_{11}H_{17}N_5O_8P$ [M + H]$^+$: found, 378.0813; calcd, 378.0814.

1-[3-Aminomethyl-3-deoxy-5-*O*-phosphoryl-b -D-ribofuranosyl]thymine (8)

Azide **7** (346 mg, 0.74 mmol) was reduced to the corresponding amine following the procedure described for the preparation of **4** to yield 110 mg (65%) of the amino-nucleotide **8** as a foam. ^{1}H NMR (300 MHz, D_2O): ***d*** 1.92 (3 H, s, 5-CH_3), 2.69 (1H, m, H-3’), 3.17 and 3.38 (2H, 2dd, *J* = 5.2 and 10.2 Hz, H-6’), 4.07 and 4.17 (2H, 2m, H-5’), 4.30 (1H, app d, H-4’), 4.56 (1H, dd, H-2’), 5.84 (1H, d, *J* = 1.8 Hz, H-1’), 7.86 (1H, d, *J* = 1.1 Hz, H-6); ^{13}C NMR (125 MHz, D_2O): ***d*** 14.30 (5-CH_3), 38.26 (C-6’), 42.22 (C-3’), 65.74 (C-5’, $^{2}J_{C,\ P}$ = 4.9 Hz), 77.88 (C-2’), 84.43 (C-4’, $^{3}J_{C,P}$ = 7.8 Hz), 94.17 (C-1’), 113.72 (C-5), 139.95 (C-6), 155.51 (C-2), 169.32 (C-4); ^{31}P NMR (500 MHz, D_2O): ***d*** 3.45; HRMS (ESI-MS) for $C_{11}H_{19}N_3O_8P$ [M + H]$^+$: found, 352.0902; calcd, 352.0909.

3'-Deoxy-3'-*C*-(2-hydroxyethyl)thymine (15)

To a mixture of 5'-*O*-*tert*-butyldiphenylsilyl-3'-C-allyl-2',3'-dideoxy-thymidine (**33**)^{14} (0.80 g, 1.58 mmol) and 4-methylmorpholine *N*-oxide (0,26 g, 1.91 mmol) in dioxane (10 mL) was added an aqueous solution of OsO_4 (0.09 mmol, 1% in water). After stirring 3 h at room temperature under light protection, the reaction mixture was complete (TLC), then sodium periodate (0.53 g, 2.49 mmol) was added in small portions. After completion of the reaction (2 h), the mixture was diluted with ethyl acetate, filtered through celite and solids washed with ethyl acetate. The combined filtrates were washed with saturated aqueous NaCl, dried and evaporated under vacuum. To the crude aldehyde **34** in ethanol/water (6/2 mL) was added dropwise $NaBH_4$ (0.18 g, 4.90 mmol) in ethanol (30 mL). After 2 h at room temperature, the reaction was complete. The mixture was diluted in ethyl acetate and washed with water, the organic layer was dried and concentrated to dryness. After purification by column chromatography (CH_2Cl_2/MeOH), compound **35** (0.24 g, 0.48 mmol) was isolated in 30% yield from **33** as a white foam. Compound **35** (50 mg, 0.098 mmol) was treated with a 1M solution of TBAF in THF (0.5 mL). After stirring 1 h at room temperature, solvent was evaporated and the residue was purified by HPLC on a C18 reverse phase column (5-25 % linear gradient of acetonitrile in 10 mM TEAA) to give compound **15** (22 mg, 81%). Rt = 8.98 min. ^{1}H NMR (400 MHz, D_2O): ***d*** 1.50 (1H, m, H-6'A), 1.75 (1H, m, H-6'B), 1.81 (3 H, d, $J_{6,\ 5\text{-}CH3}$ = 1.1 Hz, 5-CH_3), 2.15 (1H, m, H-2'A), 2.25 (2H, m, H-2B and H-3’), 3.58 (2H, m, H-7'A and H-7'B), 3.70 (1H, dd, *J* = 8.6 and 4.4, H-5’A), 3.79 (1H, m, H-4’), 3.86 (1H, dd, *J* = -12.7 Hz, *J* = 2.5 Hz, H-5’B), 6.06 (1H, dd, *J* = 7.2 and 2.1 Hz, H-1’), 7.71 (1H, d, $J_{6,\ 5\text{-}CH3}$ = 1.1 Hz, H-6). ^{13}C NMR (100 MHz, D_2O) δ: 11.92 (CH_3), 33.83 (C6’), 34.46 (C3’), 37.90 (C2’), 60.51 (C7’), 61.34 (C5’), 86.96 (C1’), 85.61 (C4’), 111.19 (C5), 138.17 (C6), 152.09 (C2), 167.00 (C4); HRMS (ESI-MS) for $C_{12}H_{19}N_2O_5$ [M + H]$^+$: found, 271.1288; calcd, 271.1283.

Supporting Information Available

HPLC retention times of all target compounds. This material is available free of charge via the Internet at http://pubs.acs.org.

References

---

[1] Duncan, K. Towards the Next Generation of Drugs and Vaccines for Tuberculosis. *Chem. Ind.* **1997**, 861–865

[2] Web site://www.who.org.

[3] (a) Nelson, D. J.; Carter, C. E. Purification and characterisation of thymidine 5'-monophosphate kinase from *E. coli* B. *J. Biol. Chem.* **1969**, *244*, 5254–5262. (b) Jong, A. Y. S.; Campbell, J. L. Characterisation of *Saccharomyces cerevisiae* thymidylate kinase, the CDC8 gene product. General properties, kinetic analysis, and subcellular localisation. *J. Biol. Chem.* **1984**, *259*, 14394–14398. (c) Lee, L.-S.; Cheng, Y.-C. Human thymidylate kinase. Purification, characterisation, and kinetic behavior of the thymidylate kinase derived from chronic myelocytic leukemia. *J. Biol. Chem.* **1977**, *252*, 5686–5691.

[4] (a) Lavie, A.; Vetter, I. R.; Konrad, M.; Goody, R. S.; Reinstein, J.; Schlichting, I. Structure of thymidylate kinase reveals the cause behind the limiting step in AZT activation. *Nature Struct. Biol.* **1997**, *4*, 601–604. (b) Lavie, A.; Ostermann, N.; Brundiers, R.; Goody, R. S.; Reinstein, J.; Konrad, M.; Schlichting, I. Structural basis for efficient phosphorylation of 3'-azidothymidine monophosphate by Escherichia coli thymidylate kinase. *Proc. Natl. Acad. Sci. U.S.A.* **1998**, *95*, 14045–14050. (c) Lavie, A.; Konrad, M.; Brundiers, R.; Goody, R. S.; Schlichting, I.; Reinstein, J. Crystal structure of yeast thymidylate kinase complexed with the bisubstrate inhibitor P1-(5'-adenosyl) P5-(5'-thymidyl) pentaphosphate (TP5A) at 2.0 Å resolution: implications for catalysis and AZT activation. *Biochemistry* **1998**, *37*, 3677–3686. (d) Ostermann, N.; Schlichting, I.; Brundiers, R.; Konrad, M.; Reinstein, J.; Veit, T.; Goody, R. S.; Lavie, A. Insights into the phosphoryltransfer mechanism of human thymidylate kinase gained from crystal structures of enzyme complexes along the reaction coordinate. *Structure* **2000**, *8*, 629–642.

[5] Li de la Sierra, I.; Munier-Lehmann, H.; Gilles, A. M.; Bârzu, O.; Delarue, M. X-ray structure of TMP kinase from *Mycobacterium tuberculosis* complexed with TMP at 1.95 Å resolution. *J. Mol. Biol.* **2001**, *311*, 87–100.

[6] Vanheusden, V.; Munier-Lehmann, H.; Pochet, S.; Herdewijn, P.; Van Calenbergh, S. Synthesis and evaluation of thymidine-5’-O-monophosphate analogues as inhibitors of *Mycobacterium tuberculosis* thymidylate kinase. *Bioorg. Med. Chem. Lett.* **2002**, *12*, 2695–2698.

[7] An, H.; Wang, T.; Maier, M. A.; Manoharan, M.; Ross, B. S.; Cook, P. D. Synthesis of novel 3'-*C*-methylene thymidine and 5-methyluridine/cytidine H-phosphonates and phosphonamidites for new backbone modification of oligonucleotides. *J. Med. Chem.* **2001**, *66*, 2789–2801.

[8] Lin, T. S.; Zhu, J.-L.; Dutschman, G. E.; Cheng, Y.-C.; Prusoff , W. H. Synthesis and biological evaluations of 3’-deoxy-3’-*C*-branched-chain-substituted nucleosides. *J. Med. Chem.* **1993**, *36*, 353–362.

[9] Acton, E. M.; Goerner, R. N.; Uh, H. S.; Ryan, K. J.; Henry, D. W. Improved anti-tumor effects in 3’-branched homologues of 2’-deoxythioguanosine. Synthesis and evaluation of thioguanine nucleosides of 2,3-dideoxy-3-(hydroxymethyl)-D-*erythro*-pentofuranose. *J. Med. Chem.* **1979,** *22*, 518–525.

[10] Doboszewski, B; Herdewijn, P. Branched-chain Nucleosides: Synthesis of 3’-deoxy-3’-*C*-hydroxymethyl-α-L-Lyxopyranosyl thymine and 3’-deoxy-3’-*C*-hydroxymethyl-α-L-threofuranosyl thymine. *Tetrahedron* **1996**, *52*, 1651–1668.

[11] Fukuyama, T.; Laird, A. A.; Hotchkiss, L. M. *p*-Anisyl group: a versatile protecting group for primary alcohols. *Tetrahedron Lett.* **1985**, *26*, 6291–6292.

[12] Tino, J. A.; Clark, J. M.; Field, A. K.; Jacobs, G. A.; Lis, K. A.; Michalik, T. L.; McGeever-Rubin, B.; Slusarchyk, W. A.; Spergel, S. H.; Sundeen, J. E.; Tuomari, A. V.; Weaver, E. R.; Young, M. G.; Zahler, R. Synthesis and antiviral activity of novel isonucleoside analogues. *J. Med. Chem.* **1993**, *36*, 1221–1229.

[13] Vorbrüggen, H.; Krolikiewicz, K.; Bennua, B. Nucleoside Synthesis with trimethylsilyl triflate and perchlorate as catalysts. *Chem. Ber.* **1981**, *114*, 1234–1255.

[14] Chu, C. K.; Doboszewski, B.; Schmidt, W.; Ullas, G. V.; Van Roey, P. Synthesis of pyrimidine 3'-allyl-2',3'-dideoxyribonucleosides by free-radical coupling. *J. Org. Chem.* **1989**, *54*, 2767–2769.

[15] Fiandor, J.; Tam, S. Y. Synthesis of 3'-deoxy-3'-(2-propynyl)thymidine and 3'-cyanomethyl-3'-deoxythymidine, analogues of AZT. *Tetrahedron Lett.* **1990**, *31*, 597–600.

[16] Butterfield, K.; Thomas, E. J. Synthesis of analogues of nucleotides with all-carbon backbones: synthesis of *N*-protected *C*-linked dinucleotides. *J. Chem. Soc., Perkin Trans. 1* **1998**, 737–745.

---

[17] Blondin, C.; Serina, L.; Wiesmüller, L.; Gilles, A. M.; Bârzu, O. Improved spectrophotometric assay of nucleoside monophosphate kinase activity using the pyruvate kinase/lactate dehydrogenase coupling system. *Anal. Biochem.* **1994**, *220*, 219–222.

[18] Word, M.; Lovell, S.C.; Richardson, J.S.; Richardson, D.C. Asparagine and glutamine: using hydrogen atom contacts in the choice of sidechain amide orientation. *J. Mol. Biol.* **1999**, *285*, 1733–1745.

[19] Shah, A.; Walters, P.; Stahl, M. Babel: chemical format conversion program., W. P. Walters, M. T. Stahl, A. V. Shah and D. P. Dolata, *Abs. Papers Am. Chem. Soc.* **1994**, *207*, 36-Cinf, 37-Cinf, http://www.eyesopen.com/babel/.

[20] Jones, G.; Willett, P.; Glen, R.C. Molecular recognition of receptor sites using a genetic algorithm with a description of desolvation. *J. Mol. Biol.* **1995**, *245*, 43–53.

[21] Jones, G.; Willett, P.; Glen, R.C.; Leach, A.R.L., Taylor, R. Development and validation of a genetic algorithm for flexible docking. *J. Mol. Biol.* **1997**, *267*, 727–748.

[22] Kraulis, P.J. MOLSCRIPT: a program to produce both detailed and schematic plots of protein structures. *J. Appl. Crystallogr.* **1991**, *24*, 946–950.

Chapter 5

THYMIDINE AND THYMIDINE-5'-*O*-MONOPHOSPHATE ANALOGUES AS INHIBITORS OF *MYCOBACTERIUM TUBERCULOSIS* THYMIDYLATE KINASE

Veerle Vanheusden, Philippe Van Rompaey, Hélène Munier-Lehmann, Sylvie Pochet, Piet Herdewijn, Serge Van Calenbergh

Bioorg. Med. Chem. Lett. **2003**, *13*, 3045-3048.

THYMIDINE AND THYMIDINE-5'-*O*-MONOPHOSPHATE ANALOGUES AS INHIBITORS OF *MYCOBACTERIUM TUBERCULOSIS* THYMIDYLATE KINASE

Veerle Vanheusden, Philippe Van Rompaey, Hélène Munier-Lehmann, Sylvie Pochet, Piet Herdewijn, Serge Van Calenbergh

Bioorg. Med. Chem. Lett. **2003**, *13*, 3045-3048.

Abstract

The affinity of a series of 2', 3'-and 5-modified thymidine analogues for Mycobacterium tuberculosis *thymidine monophosphate kinase (TMPKmt) was evaluated. The affinities of several non-phosphorylated analogues are in the same order of magnitude as those of their phosphorylated congeners. In view of drug delivery problems associated with phosphorylated compounds, these "free" nucleosides seem more promising leads in the search of TMPKmt inhibitors as novel anti-tuberculosis agents.*

Recently, *Mycobacterium tuberculosis* thymidine monophosphate kinase (TMPKmt) was put forward as an attractive target for the design of a novel class of anti-tuberculosis agents.[1,2,3]

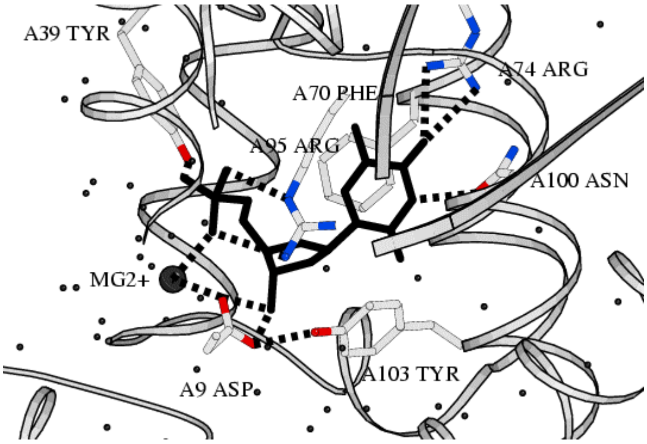

Figure 1: Schematic representation of the most important amino acid residues of TMPKmt interacting with TMP (in black).

TMPK accounts for the phosphorylation of thymidine monophosphate (dTMP) to thymidine diphosphate (dTDP), using ATP as a preferred phosphoryl donor.[4] Because TMPK lies at the junction of the *de novo* and salvage pathways of thymidine triphosphate (dTTP) synthesis and in view of its low (22%) sequence identity with the human isozyme,[5] it represents an attractive target for selectively blocking mycobacterial DNA synthesis. Recently, the X-ray structure of TMPKmt was solved at 1.95 Å as a complex with dTMP,[6] allowing structure-based design of TMPKmt ligands (Figure 1).

In order to establish initial structure-activity relationships, a series of sugar- and base-modified nucleoside-5'-*O*-monophosphates were examined for TMPKmt affinity. The aim of conserving the 5'-*O*-monophosphate moiety was to preserve its hydrogen bonding and ionic interactions with Tyr39, Arg95 and Mg^{2+}. These bindings, together with the stacking interaction between the pyrimidine ring and Phe70 should account for a dTMP-like orientation of the substrate analogues under investigation, thereby rendering prediction and modeling of the interactions of the various dTMP substituents with the enzyme more straightforward. Next, alternative substitution patterns at the 5'-position would be explored and combined with optimal sugar and base modifications. These sugar- and base-modified nucleotides were examined on their affinity for the enzyme using a reported spectrophotometric assay,[7] unless mentioned otherwise.

First, systematic substitution of the 5-methyl group for various halogen atoms was explored. 5F-dUMP, 5Br-dUMP and 5I-dUMP turned out to be substrates for TMPKmt.[5] 5Br-dUMP (K_m = 33 μM) showed the highest affinity, probably because a bromine occupies about the same steric space as a methyl group. The presence of the guanidinium group of Arg74 in the otherwise hydrophobic pocket around the 5-position could explain the measured affinity of the halogenated substrates. It is believed that the difference in the kinetic parameters of these compounds essentially reflects a size effect, with the halogen atoms serving as cavity filling atoms.[5] A co-crystal of 5I-dUMP with TMPKmt[6] showed that it, indeed, binds the phosphate acceptor binding site in a very similar fashion to dTMP.[2]

Since these findings confirmed the assumption that TMPKmt can accommodate sterically larger substituents at the 5-position, **1** was synthesised to accomplish a favourable interaction with a water molecule (W12), detected in the crystal structure. In contrast to the 5-halogeno-substituted substrates, this compound behaves as a (relatively weak) inhibitor of TMPKmt. Co-crystallisation with TMPKmt proved the predicted interaction with W12.[2] Other dTMP analogues with sterically more demanding substituents that maintain one polar atom (**2** and **3**) were found less active inhibitors than **1**, indicating that the volume of the cavity cannot be stretched too much. It is inferred that these three compounds are inhibitors because any modification, significantly perturbing the volume at the 5-position, changes the orientation of the sugar moiety as well as that of the α-phosphate.[2] Surprisingly, removal of the 5-methyl-group of dTMP (dUMP) caused a drastic decrease in affinity (K_m = 2100 μM compared to 4.5 μM for dTMP) (Table 1).[5]

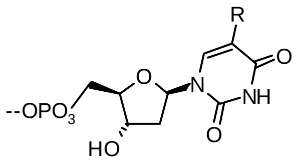

Compounds	**R**	**K_m (μM)**	**V_m[a]**	**K_i (μM)**
dTMP[5]	CH_3	4.5	10.6	
dUMP[5]	H	2100	3.5	
5F-dUMP[6]	F	420	4.7	
5Br-dUMP[6]	Br	33	9.8	
5I-dUMP[6]	I	140	7.5	
1[2]	CH_2OH			110[b]
2[2]	furan-2-yl			140[b]
3[2]	thien-2-yl			270[b]
4[2]	benzyl			28

Table 1: Kinetic parameters of TMPKmt with base-modified nucleoside monophosphates.

[a] *V_m in mmole/min.mg of protein*

[b] *The TMP kinase activity of these compounds was not determined using the spectrometric test described by Blondin et al.[7] but using HPLC chromatography. The K_m for dTMP obtained with this test is 40 mM.[2]*

The observation that TMPKmt, as opposed to all TMPKs of other species examined so far,[5] is strongly inhibited by AZTMP ($K_i = 10\ \mu M$) offered good prospects for finding selective inhibitors of TMPKmt through altering the sugar part of the dTMP scaffold. At the 3'-position, the crystal structure reveals a hydrogen bonding network (denoted by the dotted lines, Figure 1): the 3'-OH of dTMP interacts with the terminal carboxyl of Asp9, which, in its turn, is linked to the Mg^{2+}-ion that is responsible for positioning a phosphate oxygen of TMP. Through its interaction with Asp9, the 3'-azido function of AZTMP is believed to perturb the aforementioned hydrogen bonding interplay that is essential for catalysis, hence completely impeding the phosphoryl transfer.[6] Although an analogous interaction was expected upon reduction of the 3'-azido group of AZTMP to a 3'-amine (**5**), this drastically increased the K_i-value to 235 μM. Replacing the 3'-OH of dTMP by a 3'-F (**8**), on the other hand, afforded an analogue that behaves as a substrate with a K_m of 30 μM.

The presence of Tyr103 close to the 2'-position is believed to render the enzyme catalytically selective for 2'-deoxynucleotides versus ribonucleotides. The ribo analogue (**6**) of **5**, however, unexpectedly showed a much higher affinity for the enzyme (45 μM versus 235 μM), this compound being the first example of a ribonucleotide with good affinity for TMPKmt. Modeling indicates that, in this case, Tyr103 stays somewhat further away from the 2'-position and is, therefore, unable to clash with the 2'-hydroxyl.[1] Introduction of halogens at the 2'-position (**9** and **10**) is better tolerated than a hydroxyl group at that position. Modeling showed that the halogen affects the relative position of the sugar ring. As a result, the 2'-chlorine occupies the pocket, in which the 3'-hydroxyl usually resides. As previously demonstrated with AZTMP, this particular domain can, indeed, accommodate more voluminous substituents.[1]

Replacing the 5-membered sugar ring of dTMP by a 1,5-anhydrohexitol yielded a moderately active inhibitor. This effect is probably due to the inability of **11** to position both the phosphate and the 3'-hydroxyl groups in a favourable arrangement for catalysis.[2] With a K_i of 30 μM, the bisubstrate analogue Ap_5T, emerged as a good inhibitor of TMPKmt. The crystal structure of the complex of TMPKmt with Ap_5T, which has been established at 2.45 Å resolution,[2] revealed an unexpected binding mode for the adenine moiety of this compound. While the thymidine residue of this bisubstrate analogue occupies the binding pocket of dTMP, its ADP unit, surprisingly, fits a cavity on the surface of TMPKmt. This finding opens avenues to the design of branched molecules at the α-phosphate of Ap_5T, with an additional group reaching out to this cavity present only in TMPKmt (Table 2).[2]

Obviously, monophosphate derivatives are unable to enter cells and, as a consequence, can not be delivered in such a way. Generally, nucleosides cross the cell membrane barrier in a non-phosphorylated form and are then converted by intracellular kinases to the corresponding nucleotides. In this particular case where TMPK is the drug target, a thymidine analogue could be activated by thymidine kinase (TK), which converts the analogue into the corresponding monophosphorylated compound. However, a search of the *M. tuberculosis* genome[8] did not identify any gene coding for a TK. This result aligns with other biochemical studies indicating a lack of TK activity in mycobacteria.[9] At first sight, the absence of TK seems to be a severe limitation on the use of thymidine analogues or related compounds as anti-tuberculosis drugs. However, the finding that dT behaves as a competitive inhibitor of TMPKmt (with K_i in the same order of magnitude as K_m of dTMP[3]), raises the possibility of discovering non-phosphorylated nucleosidic inhibitors of TMPKmt. Enhancing the specific delivery of such inhibitors to bacteria within macrophages by modifying the 5'-position of dTMP is another option. Such modifications may also decrease toxicity by reducing interaction with the host cellular TK. Replacement of the 5'-hydroxyl by an azido or amino an group (**13** and **14**) yielded two high-affinity inhibitors of TMPKmt (K_i values of 7 and 12 µM, respectively).[3]

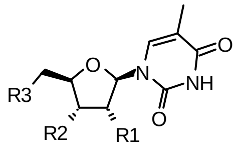

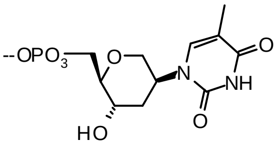

15

Compounds	R1	R2	R3	K_i (µM)
dTMP	H	H	OPO_3^{2-}	4.5[a]
AZTMP[5]	H	N_3	OPO_3^{2-}	10
D4T-MP[5]	dehydro	dehydro	OPO_3^{2-}	140[a]
5[1]	H	NH_2	OPO_3^{2-}	235
6[1]	OH	NH_2	OPO_3^{2-}	45
7[1]	NH_2	OH	OPO_3^{2-}	120
8[1]	H	F	OPO_3^{2-}	30[a]
9[1]	Cl	OH	OPO_3^{2-}	19
10[1]	F	OH	OPO_3^{2-}	43
11[2]				150[b]
Ap$_5$T[2]				30[b]

Table 2: Kinetic parameters of TMPKmt with sugar-modified nucleoside monophosphates.
[a] *K_m-value*
[b] *The TMP kinase activity of these compounds was not determined using the spectrophotometric assay by Blondin et al.*[7]*, but using HPLC chromatography. K_m for dTMP is 40 mM.*[2]

We investigated whether the negligible effect on TMPKmt affinity, observed upon deletion of the phosphate moiety of dTMP, is parallelled in other series. AZT, 5-BrdU and **22**[1] exhibited similar affinities as their nucleotide congeners. In the case of **23**,[1] the affinity decreased only 2.8 times upon removal of the 5'-*O*-phosphoryl. With regard to these observed similar affinities of nucleosides and nucleotides and in view of the drug delivery problems of phosphorylated compounds, nucleosides seem more useful leads for further drug design.

To further explore other substitution patterns at the 5'-position, the 5'-hydroxymethyl was substituted for a 5'-methyl. In **25**,[10] this caused a 42-fold decrease in affinity compared to **6**. The affinities of **20**[11] and **19**[11], on the contrary, were similar, making assumptions about the removal of the 5'-hydroxyl group unreliable. Compound **24**,[10] with a 5'-iodo group, showed a low affinity (K_i = 490 µM), but it's not clear if the 5'-iodo group or the 2'-hydroxyl function accounts for this effect.

Because **6** conveyed the impression that ribo analogues are well tolerated by TMPKmt, two other ribonucleosides (**15**[12] and **19**) were examined. The affinity of **15** was 26 times lower than the affinity of dT and **19** showed to be a poor inhibitor as well. These results indicate that the affinity improvement resulting from the introduction of a 2'-hydroxyl function in **5** (**6**) is exceptional. **16**[13] even indicates that a 2'-β-OH is better tolerated.

Because AZTMP is one of the best known inhibitors, another nitrogen-containing substituent, a guanidine group (**26**),[10] was introduced at the 3'-position. Although one would expect the delocalised positive charge of the guanidine moiety to strengthen the interaction with Asp9, the K_i value of 140 µM was not affirmative.

Since the efficient affinity of **1** proved that the 5-position can accommodate intermediately sized substituents, **17**[11] (which has a 5-CF_3 mimicking the size of the 5-methyl) and **18**[11] were investigated as well. However, with K_i-values of 97 and 1140 μM, they proved to be poor inhibitors of TMPKmt (Table 3).

In our search for high-affinity TMPKmt ligands as anti-tuberculosis agents, most of the base- and sugar-modified dTMP-analogues (with the 5-halogeno dUMP derivatives, dUMP, 3'-F-dTMP and D4T-MP as exceptions) proved to be inhibitors of the enzyme. However, conversion to prodrugs is the only way to deliver phosphorylated compounds into cells. Since this recent work indicates that in many cases (AZT, 5-BrdU, **22** and **23**) nucleoside analogues show affinities that approach those of their phosphorylated counterparts, this problem could be easily circumvented by focusing on nucleosides instead of nucleotides. Concerning the 5'-modifications we can conclude that a 5'-amino and a 5'-azidofunction are a good alternative for a 5'-hydroxyl and that further study is required to probe the effect of the deletion of the 5'-hydroxyl. At the 2'-position, a 2'-hydroxyl has proven to reduce the affinity for TMPKmt, with compounds **5** and **6** as the only exception known so far.

Future research will be directed towards finding other high-affinity 5'-substituents that are unable to be phosphorylated by cellular kinases, thereby diminishing the risk for toxicity and further exploration of the 3'-position to improve the current inhibitors. Also, analogues exhibiting interesting inhibitory activity towards TMPKmt will be examined for selectivity vis-à-vis the human enzyme.

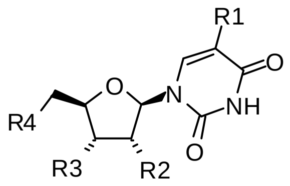

Compounds	**R1**	**R2**	**R3**	**R4**	**K_i (μM)**
dTMP	CH_3	H	OH	OPO_3^{--}	4.5[a]
dT	CH_3	H	OH	OH	27
AZT	CH_3	H	N_3	OH	28
5Br-dU[3]	Br	H	H	H	5
12[3]	CH_3	H	OH	$NHCOCH_3$	90
13[3]	CH_3	H	OH	N_3	7
14[3]	CH_3	H	OH	NH_2	12
15	CH_3	OH	OH	OH	715
16	CH_3	OH[b]	OH	OH	238
17	CF_3	H	OH	OH	97
18	CH_2CH_3	H	OH	OH	1140
19	F	OH	OH	OH	521
20	F	OH	OH	H	560
21	CH_3	H	NH_2	OH	230
22	CH_3	H	F	OH	28
23	CH_3	F	OH	OH	122
24	CH_3	OH	N_3	I	490
25	CH_3	OH	NH_2	H	1900
26	CH_3	OH	$NHC(NH)NH_2$	OH	140

Table 3: Kinetic parameters of TMPKmt with sugar- and base-modified thymidine analogues.
[a] K_m-value; [b] This hydroxyl lies at the b-side of the sugar ring.

References

---

[1] Vanheusden, V.; Munier-Lehmann, H.; Pochet, S.; Herdewijn, P.; Van Calenbergh, S. Synthesis and evaluation of thymidine-5’-O-monophosphate analogues as inhibitors of *Mycobacterium tuberculosis* thymidylate kinase. *Bioorg. Med. Chem. Lett.* **2002**, *12*, 2695–2698.

[2] Haouz, A.; Vanheusden, V.; Munier-Lehmann, H.; Froeyen, M.; Herdewijn, P.; Van Calenbergh, S.; Delarue, M. Enzymatic and structural analysis of inhibitors designed against *Mycobacterium tuberculosis* thymidylate kinase. New insights into the phosphoryl transfer mechanism. *J. Biol. Chem.* **2003**, *278*, 4963–4971.

[3] Pochet, S.; Dugué, L.; Douguet, D.; Labesse, G; Munier-Lehmann, H. Nucleoside analogues as inhibitors of thymidylate kinases: possible therapeutic applications. *ChemBioChem*. **2002**, *3*, 108–110.

[4] Anderson, E. In *The Enzymes*; Boyer, P. D., Ed.; Academic Press: New York, **1973**; Vol. 8, pp. 49–96.

[5] Munier-Lehmann, H.; Chafotte, a.; Pochet, S.; Labesse, G. Thymidylate kinase of *Mycobacterium tuberculosis*: a chimera sharing properties common to eukaryotic and bacterial enzymes. *Protein Sci.* **2001**, *10*, 1195–1205.

[6] Li de la Sierra, I.; Munier-Lehmann, H.; Gilles, A. M.; Bârzu, O.; Delarue, M. X-ray structure of TMP kinase from *Mycobacterium tuberculosis* complexed with TMP at 1.95 Å resolution. *J. Mol. Biol.* **2001**, *311*, 87–100.

[7] Blondin, C.; Serina, L.; Wiesmüller, L.; Gilles, A. M.; Bârzu, O. Improved Spectrophotometric Assay of Nucleoside Monophosphate Kinase Activity Using Pyruvate Kinase/Lactate Dehydrogenase Coupling System. *Anal. Biochem.* **1994**, *220*, 219–222.

[8] Cole, S. T.; Brosch, R.; Parkhill, J.; Garnier, T.; Churcher, C.; Harris, D.; Gordon, S. V.; Eiglmeier, K.; Gas, S.; Barry III, C. E.; Tekaia, F.; Badcock, K.; Basham, D.; Brown, D.; Chillingworth, T.; Connor, R.; Davies, R.; Devlin, K.; Feltwell, T.; Gentles, S.; Namlin, N.; Holroyd, S.; Hornsby, T.; Jagels, K.; Barrel, B. G. Deciphering the biology of *Mycobacterium tuberculosis* from the complete genome sequence. *Nature* **1998**, *393*, 537.

[9] Saito, H.; Tomioka, H. *J.* Thymidine Kinase of Bacteria - Activity of the Enzyme in Actinomycetes and Related Organisms. *Gen. Microbiol*. **1984**, *130*, 1863–1870.

[10] Synthesised by Philippe Van Rompaey.

[11] Purchased from Sigma-Aldrich.

[12] Vorbrüggen H.; Krolikiewicz K.; Bennua B.; Nucleoside Synthesis with Trimethylsilyl Triflate and Perchlorate as Catalysts. *Chem. Ber.*, **1981**, *114*, 1234–1255.

[13] Schinazi, R. F.; Chen, M. S.; Prusoff, W. H. Antiviral and Antineoplastic Activities of Pyrimidine Arabinosyl Nucleosides and Their 5'-Amino Derivatives. *J. Med. Chem.* **1979**, *22*, 1273–1276.

Chapter 6

DISCOVERY OF BICYCLIC THYMIDINE ANALOGUES AS SELECTIVE AND HIGH AFFINITY INHIBITORS OF *MYCOBACTERIUM TUBERCULOSIS* THYMIDINE MONOPHOSPHATE KINASE

Veerle Vanheusden, Hélène Munier-Lehmann, Matheus Froeyen, Roger Busson, Jef Rozenski, Piet Herdewijn and Serge Van Calenbergh.

Submitted for J. Med. Chem.

DISCOVERY OF BICYCLIC THYMIDINE ANALOGUES AS SELECTIVE AND HIGH AFFINITY INHIBITORS OF *MYCOBACTERIUM TUBERCULOSIS* THYMIDINE MONOPHOSPHATE KINASE

Veerle Vanheusden, Hélène Munier-Lehmann, Matheus Froeyen, Roger Busson, Jef Rozenski, Piet Herdewijn, and Serge Van Calenbergh.

Submitted for J. Med. Chem.

Abstract

Thymidine monophosphate kinase of Mycobacterium tuberculosis *represents an attractive target for selectively blocking the bacterial DNA synthesis. Hereby, we report on the discovery of a novel class of bicyclic nucleosides (**10** and **11**) and one dinucleoside (**12**), belonging to the most selective inhibitors of TMPKmt discovered so far.*

Introduction

The appearance of multiple drug-resistant strains of *Mycobacterium tuberculosis* and the synergism between HIV and *M. tuberculosis* infection has caused a steeply rising incidence of tuberculosis during the last decades. This has made the development of new anti-tuberculosis agents, preferably acting on novel targets, a research priority for many health organisations.[1]

M. tuberculosis thymidine monophosphate kinase (TMPKmt) recently emerged as a potentially attractive target for the design of a novel class of anti-tuberculosis agents.[2]

TMPK catalyses the γ-phosphate transfer from ATP to thymidine monophosphate (dTMP) in the presence of Mg^{2+}, yielding thymidine diphosphate (dTDP) and ADP.[3] Because TMPK is essential for thymidine triphosphate (dTTP) synthesis and in view of its low (22%) sequence identity with the human isozyme (TMPKh),[2] it represents an attractive target for selectively inhibiting mycobacterial DNA synthesis. Recently, the X-ray structure of TMPKmt was solved at 1.95Å as a complex with dTMP,[4] allowing structure-based design of TMPKmt ligands.

A series of 2'-, 3'- and 5-modified nucleosides and nucleotides was tested for their affinities with respect to TMPKmt.[5,6,7,8] The results showed that, in general, nucleosides and their corresponding 5'-*O*-monophosphate esters were nearly equivalent inhibitors of TMPKmt. The low permeability of the cell wall for phosphorylated compounds (i.e. nucleotides) prompted us to focus on nucleosides as new drug leads. Recently, we reported a series of 3'-*C*-branched chain nucleosides and nucleotides that exhibit micromolar inhibitory activity against TMPKmt.[9] The introduction of 3'-CH_2OH, 3'-CH_2NH_2, 3'-CH_2N_3 and 3'-CH_2F substituents was aimed at occupying a cavity in the enzyme near the 3'-position. Biological results and modeling confirmed this hypothesis. Modeling also indicated that these nucleosides bind to TMPKmt in the (*N*) (northern, 2'-*exo*-3'-*endo*) conformation [dTMP, in contrast, binds to TMPKmt in the (*S*) (southern, 2'-*endo*, 3'-*exo*) conformation]. This *N*-type sugar pucker enables interactions between the 6'-substituent and Asp9.[9] From this, 1-[3-*C*-(azidomethyl)-2,3-dideoxy-β-D-*erythro*-pentofuranosyl]thymine (**1**) emerged as a promising lead for further research, since it combines a low K_i-value with a favourable selectivity profile for TMPKmt versus TMPKh (Table 1). Moreover, conformational analysis of a series of 2'- and 3'-modified nucleosides showed that the presence of a halogen at the α-face of the 2'-position, especially a 2'-fluorine, biases the sugar pucker of thymidine analogues strongly towards the (*N*) conformation.[10] Based on these results and the high affinities of 2'-halogeno substituted nucleotides for TMPKmt[5] (**3** and **4**, Table 1), it was considered interesting to combine a 2'-chlorine or a 2'-fluorine substituent with a 3'-aminomethyl or a 3'-azidomethyl group (**5-8**).[9] In an attempt to supersede the good affinities of the 3'-*C*-branched-chain nucleosides, we also further explored the enzyme cavity near the 3'-position with alternative nitrogen containing substituents.

Results and Discussion

Chemistry

The synthesis of **5**-**9** started from **14** (obtained from 1,2-*O*-isopropylidene-α-D-xylofuranose in 11 steps[11]) (Scheme 1). After protection of the 5'-hydroxyl group, **15** was converted into anhydronucleoside **16** upon treatment with trifluoromethanesulfonyl chloride and DMAP.[12] Opening of the anhydro ring with HCl in dioxane yielded **5**, the 2'-α-chloro analogue of **1**.[13] The corresponding 2'-fluoro derivative **7** was obtained via formation of *ara*-nucleoside **17** from **16** with NaOH,[14] followed by fluorination with DAST[15] and removal of the trityl protective group. Reduction of **5** and **7** with Ph_3P and NH_3 yielded the corresponding 3'-amino analogues **6** and **8**, respectively.[11] Due to unwanted intramolecular attack of the 2-carbonyl of thymine on the 5'-*O*-diethylaminosulphur difluoride intermediate, reaction of **7** with DAST afforded **9** in low yield.

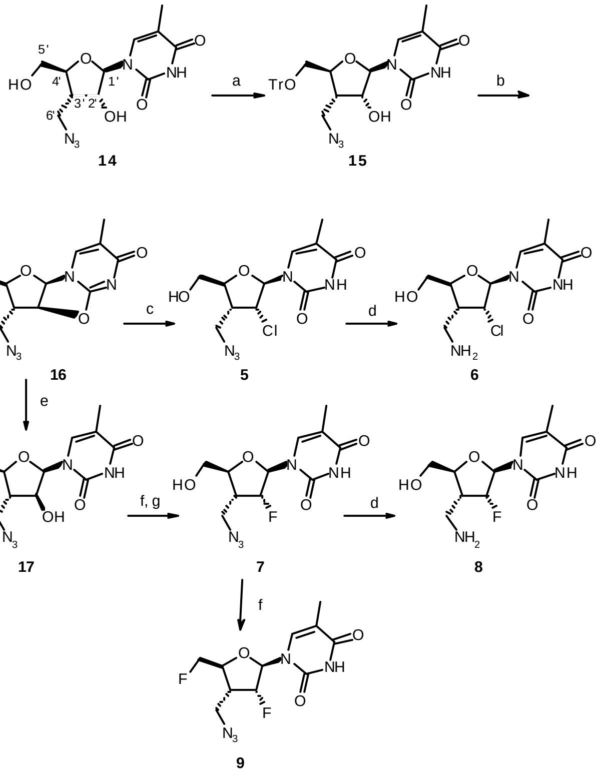

Scheme 1: Reagents: (a) trityl chloride, DMAP, pyridine; (b) trifluoromethanesulfonyl chloride, DMAP, CH_2Cl_2; (c) HCl, dioxane; (d) Ph_3P, NH_4OH, pyridine; (e) NaOH, EtOH, H_2O; (f) DAST, toluene, pyridine; (g) 80% HOAc in H_2O.

In an attempt to prepare intermediate **20** for further derivatisation, the 5'-hydroxyl group of **14** was first protected as *t*-butyldimethylsilyl ether **18** (Scheme 2). After esterification of the 2'-hydroxyl with phenylchlorothionocarbonate (→**19**),[11] however, attempted simultaneous reduction of the azido function and Barton deoxygenation at the 2'-position to give **20** failed. Instead three peculiar nucleoside analogues **21**, **22** and **23** were formed. In a similar attempt, Robins *et al.* found that, apart from a low yield of the desired aminonucleoside, Barton deoxygenation of an azide in the presence of a phenoxythiocarbonyl ester led to some uncharacterised byproducts.[16] Compounds **21** and **22** represent a novel class of bicyclic nucleoside analogues.

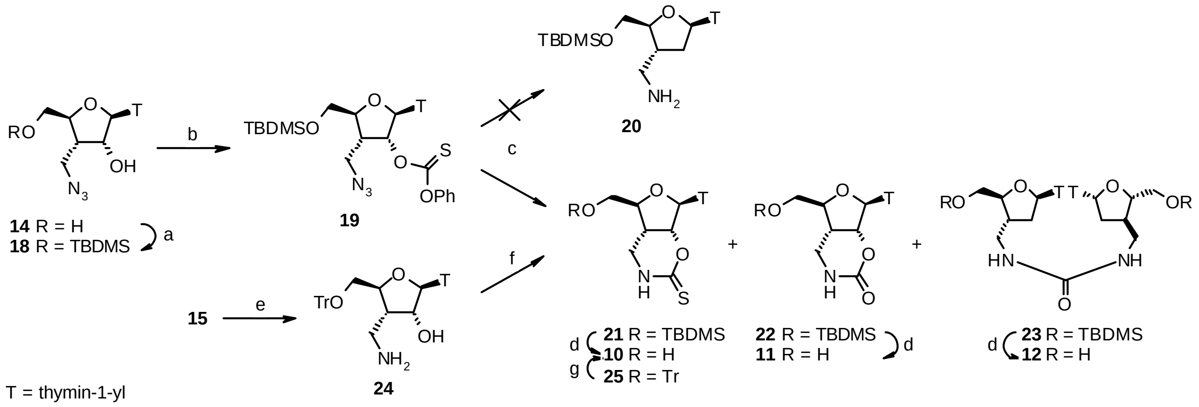

Scheme 2: Reagents: (a) t-butyldimethylsilyl chloride, imidazole, DMF; (b) phenyl chlorothionocarbonate, DMAP, CH_3CN; (c) AIBN, Bu_3SnH, toluene; (d) n-Bu_4NF, THF; (e) Ph_3P, NH_4OH, pyridine; (f) 1,1-thiocarbonyldiimidazole, DMF; (g) 80% HOAc in H_2O.

The formation of carbamates through reaction of thioacids with azides has recently been studied by Shangguan *et al.*[17] A mechanism is proposed in which the three nitrogens of the azide take part in formation of the carbamate. However, since access to the thiocarbamate cannot be explained this way, it is suggested that a radical intermediate of the reduction of the azide interacts with a radical resulting from attack of a tributyltin radical on the thioester.

Another surprising byproduct of this radical-mediated reduction is dinucleoside **23**. Most probably, the ureum moiety of this dimer is formed through attack of the 6'-amines (resulting from reduction of the 6'-azide of **19**) on the carbonoxysulfide, arising from decomposition of the 2'-phenylthionocarbonate ester.[18]

The TBDMS-protective groups of **21**, **22** and **23** were removed with TBAF in THF and the free nucleosides (**10**, **11** and **12**) were tested for their affinity for TMPKmt.

In view of the interesting biological properties of **10** (see below), a more efficient way for its synthesis was desirable. Tritylation of the 5'-hydroxyl of **14**, followed by reduction of the 6'-azido group (→**24**), treatment with thiocarbonyldiimidazole, and subsequent acidic removal of the 5'-trityl group afforded **10** in 62 % overall yield. Likewise, **11** can be obtained by using carbonyldiimidazole.

Binding Assay

All nucleosides were tested for their affinity for TMPKmt (Table 1) via a reported spectrometric assay.[19] The affinities of most 2'-halo substitued nucleosides were not as expected. In **5-8**, the introduction of the 2'-halogen led to a drastic decrease in affinity compared to the corresponding 2'-deoxynucleosides. Due to the presence of the 2'-fluorine, **8** even didn' show inhibition at 1 mM for the enzyme. Instead of enhancing the (*N*) conformation, necessary for optimal interaction between Asp9 and the 3'-substituent, the 2'-halogens probably compete with the 3'-substituents for the same binding pocket,[5] thereby abolishing the affinity for the enzyme. Remarkably, introduction of a 5'-fluorine slightly increases the affinity of **7** (K_i of **9** = 80 μM).

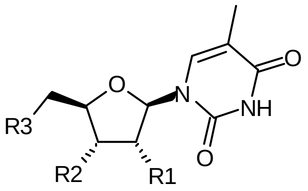

Compound	**R1**	**R2**	**R3**	**K_i (mM) TMPKmt**	**K_i (mM) TMPKh**
dTMP	H	OH	OPO_3^{2-}	4.5[a]	5.0[a]
thymidine	H	OH	OH	27[7]	180[8]
1	H	CH_2N_3	OH	40[9]	1040[9]
2	H	CH_2NH_2	OH	57[9]	220[9]
3	F	OH	OPO_3^{2-}	43[5]	n.d.[d]
4	Cl	OH	OPO_3^{2-}	19[5]	n.d.[d]
5	Cl	CH_2N_3	OH	180	n.d.[d]
6	Cl	CH_2NH_2	OH	390	n.d.[d]
7	F	CH_2N_3	OH	165	n.d.[d]
8	F	CH_2NH_2	OH	n.i.[c] at 1 mM	n.d.[d]
9	F	CH_2N_3	F	80	n.d.[d]
10	2'-OC(S)NHCH$_2$-3'		OH	3.5	700
11	2'-OC(O)NHCH$_2$-3'		OH	13.5	1100
12	Scheme 2		OH	37	n.i.[c] at 1 mM
13[b]	H	CH_2N_3	OH	29	n.i.[c] at 2 mM

Table 1:. Kinetic parameters of TMPKmt and TMPKh with compounds 1-13.

[a] *K_m-value*

[b] *Thymine is oriented at the a-side of the sugar ring.*

[c] *n.i.: no inhibition*

[d] *n.d.: not determined*

Compounds **10**, **11** and **12** were, likewise, assayed for their affinity for TMPKmt. Unexpectedly, these compounds are among the highest affinity inhibitors for TMPKmt found so far. Due to the lack of a binding site for a second nucleoside at the 3'-position, the K_i-value of **12** (37 μM) was most unexpected. A modeling experiment in GOLD showed that the sugar ring of the first monomer I binds the TMP-pocket upside down, which enables hydrogen bonding of its 5'-hydroxyl with Asp9 (Figure 1). This binding mode permits the sugar ring of the second monomer (II) to be directed towards the outside of the enzyme, where normally the phosphoryl donor binds. This orientation is the only feasible conformer to have **12** accommodated by the enzyme. The thymine base of II undergoes only few hydrophobic interactions with Phe36, Ala35 and Tyr39. Comparison with the binding positions of ATP[4] and bisubstrate inhibitor Ap5T[20] showed that nucleoside II does not bind to the pocket where adenosine normally resides. Instead, it is buried deeper in the enzyme. The fact that these two nucleosides in **12** are bound via their 3'-positions makes it a unique example of a bisubstrate inhibitor, thereby paving the way for the design of much larger molecules as inhibitors for TMPKmt than explored thus far.

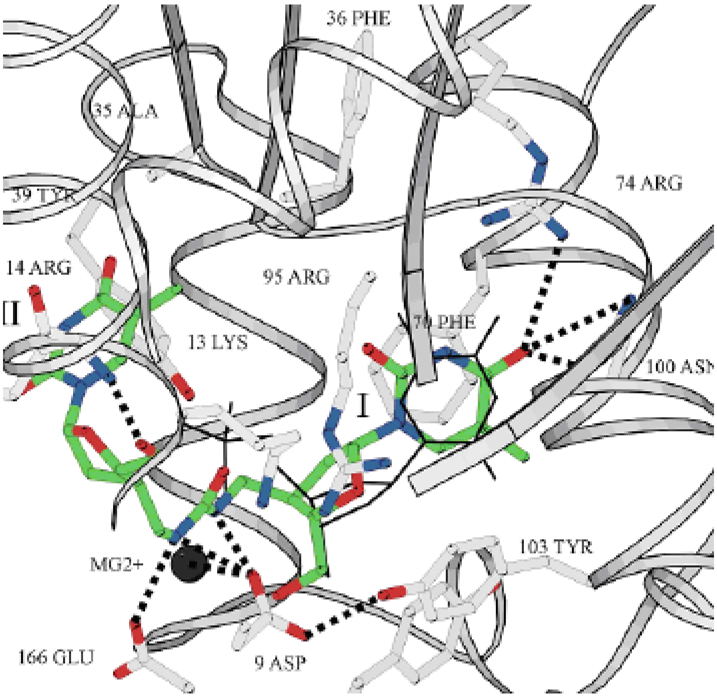
36 PHE
35 ALA
39 TYR
14 ARG
95 ARG
13 LYS
74 ARG
70 PHE
100 AS
I
MG2+
103 TYR
166 GLU
9 ASP

*Figure 1: Predicted binding mode of **12** with TMPKmt. A ribbon follows the backbone atoms of the enzyme. Hydrogen bonds are drawn as dashed lines. dTMP, as observed in the X-ray structure with TMPKmt,[4] is shown in black sticks.Residues of which atoms make contact with **12**, based on the Ligplot analysis, are Lys13, Ala35, Tyr39, Phe36, Phe70, Arg95, Asn100, Tyr103 and Tyr 165.*

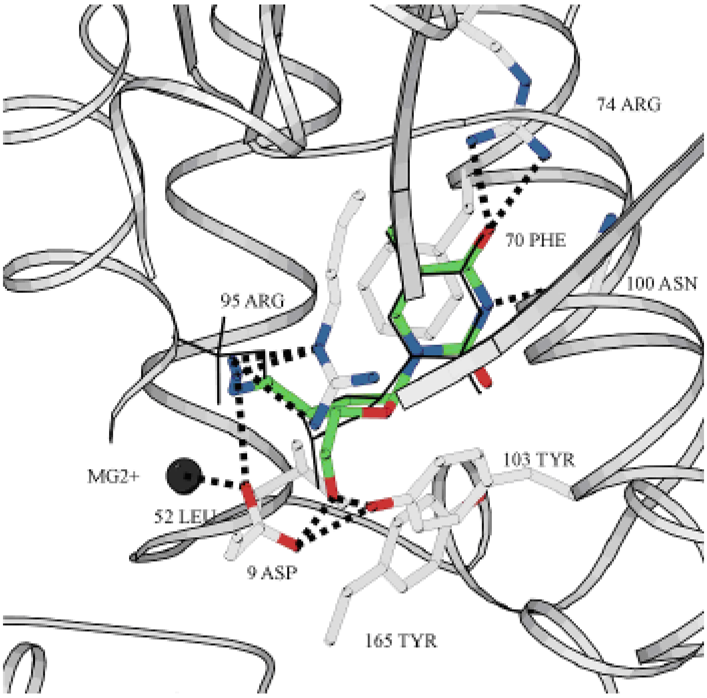
74 ARG
70 PHE
100 ASN
95 ARG
MG2+
52 LEU
103 TYR
9 ASP
165 TYR

*Figure 2: Predicted binding mode of **13** with TMPKmt. A ribbon follows the backbone atoms of the enzyme. Hydrogen bonds are drawn as dashed lines. dTMP, as observed in the X-ray structure with TMPKmt,[4] is shown in black sticks.Residues of which atoms make contact with **13**, based on a Ligplot analysis, are Asp9, Leu52, Phe70, Arg95, Tyr103 and Tyr165.*

The observed affinity of α-nucleoside **13** (an undesired anomer formed during the synthesis of 1[9]) could confirm the postulated binding mode of monomer I. A similar sugar orientation would position the thymine base ideally for stacking with Phe70. Indeed, with a K_i-value of 29 μM, this compound proves to be a good inhibitor of TMPKmt. Docking in GOLD showed a similar binding mode of the sugar ring, rendering stacking interaction with Phe70 possible (Figure 2). The 5'-hydroxyl interacts through hydrogen bonding with Asp9 and the azido group, lying in the cavity where normally the 5'-phosphoryl of dTMP resides, is engaged in a polar interaction with Arg95 and Asp9. This exceptional flexibility of TMPKmt towards the orientation of the sugar ring is of great interest for further inhibitor design.

Bicyclic nucleosides **10** and **11** showed excellent binding affinities. With a K_i-value of 3.5 μM, **10** exceeds the K_m-value of the natural substrate (4.5 μM). Compound **10** was modelled into the crystal structure of TMPKmt (Figure 3).[4] The six-membered ring, fused to the the C-2', C-3'-bond of the sugar, apparently forces the 6'-nitrogen into the most appropriate position for interaction with the Asp9 residue in the enzyme cavity. The sulphur atom, in its turn, undergoes hydrophobic interactions with Tyr103 and Tyr165 residues. When the sulphur atom in **10** is replaced by a smaller oxygen in **11**, the cavity near the 3'-position is filled less efficiently, which is reflected in the somewhat lower affinity of **11**. The functionalities of the extra ring convincingly contribute to the high affinity interactions with the biological target.

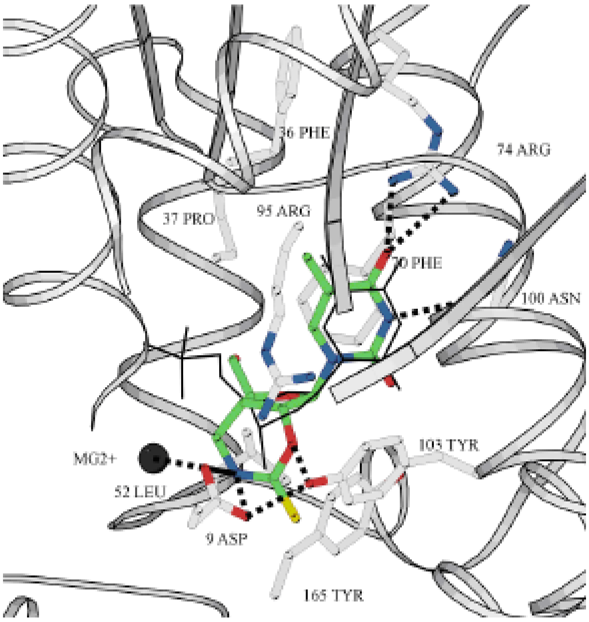

*Figure 3: Predicted binding mode of **10** with TMPKmt. A ribbon follows the backbone atoms of the enzyme. Hydrogen bonds are drawn as dashed lines. dTMP, as observed in the X-ray structure with TMPKmt,[4] is shown in black sticks. Residues of which atoms make contact with **10**, based on a Ligplot analysis, are Phe36, Pro37, Leu52, Phe70, Arg95, Tyr103 and Tyr165.*

The highest affinity inhibitors of this series were tested for their affinity for TMPKh. The low affinities of **12** and **13** for the human enzyme indicate that the flexibility towards the orientation of the sugar ring is unique for TMPKmt. Most interesting, however, is compound **10**, with a selectivity index (K_i TMPKh/ K_i TMPKmt) of 200, superseding **1** not only in affinity, but also in selectivity.

Conclusions

In inhibitor design the binding pocket of the nucleoside in nucleoside and nucleotide metabolising enzymes is generally explored by introducing small modifications to the substrate. In the present example, however, a variety of sugar modified thymidine analogues have been discovered with apparently different binding modes to TMPKmt involving Asp9, Tyr103 and Phe70 as common amino acids to anchor the inhibitors. These molecules may function as leads for further drug design, increasing considerably the variety of nucleoside analogues that may be considered for further synthesis. Of particular importance is the bicyclic nucleoside **10** with a K_i for TMPKmt of 3.5 μM and a SI of 200, which will be used as starting compound to increase further affinity forTMPKmt.

Experimental Section

Spectrophotometric binding assay

TMPKmt and TMPKh activities were determined using the coupled spectrophotometric assay described by Blondin et al.[19] at 334 nm in an Eppendorf ECOM 6122 photometer. The reaction medium (0.5 mL final volume) contained 50 mM Tris-HCl pH 7.4, 50 mM KCl, 2 mM $MgCl_2$, 0.2 mM NADH, 1 mM phosphoenol pyruvate and 2 units each of lactate dehydrogenase, pyruvate kinase and nucleoside diphosphate kinase. The concentrations of ATP and dTMP were kept constant at 0.5 mM and 0.05 mM respectively, whereas the concentrations of analogues varied between 0.1 and 2.5 mM.

Modeling: docking experiments using GOLD

The X-ray structure published by Li de la Sierra et al.[4] (pdb entry 1G3U) was used in all docking experiments. Water molecules and sulphate counter ions were removed. The Mg^{2+} was considered as being part of the enzyme. Explicit hydrogen atoms were added to the enzyme and inhibitor structures using Reduce.[21] The inhibitor structures **10**, **12** and **13** were created using Macromodel 5.0,[22] based on the dTMP substrate from pdb entry 1G3U. Their geometry was optimised in the AM1 force field using Mopac6.0.[23] PDB files were then converted to mol2 files using Babel.[24] The position of atom C1' in the dTMP ligand in the pdb file 1G3U was used as the center of a 20 Å docking sphere. Default settings were used in Gold for all dockings.[25,26] The structures in the top 50 of the docking scores were retained for visual inspection and comparison with published X-ray structures 1G3U [4] and 1MRN.[20] Criteria for selection were the same position (but not necessarily same orientation) of the base, the nonbonded interactions as calculated by Ligplot[27] and HBPLUS.[28] Figures 1-3 were generated using Molscript.[29]

Synthesis

General

NMR spectra were obtained with a Varian Mercury 300 spectrometer. Chemical shifts are given in ppm (δ) relative to residual solvent peakof DMSO-d_6 (2.5 ppm). All signals assigned to amino and hydroxyl groups were exchangeable with D_2O. Mass spectra and exact mass measurements were performed on a quadrupole/orthogonal-acceleration time-of-flight (Q/oaTOF) tandem mass spectrometer (qTof 2, Micromass, Manchester, UK) equipped with a standard electrospray ionisation (ESI) interface. Samples were infused in a 2-propanol:water (1:1) mixture at 3 μL/min. Precoated Merck silica gel F_{254} plates were used for TLC and spots were examined under UV light at 254 nm and revealed by sulfuric acid-anisaldehyde spray. Column chromatography was performed on Uetikon silica (0.2-0.06 mm).

Anhydrous solvents were obtained as follows: THF was distilled from sodium/benzophenone; pyridine was refluxed overnight over potassium hydroxide and distilled; dichloromethane, dichloroethane and toluene were stored over calcium hydride, refluxed, and distilled; DMF was stored over Linde 4 Å molecular sieves, followed by distillation under reduced pressure.

1-[3-Azidomethyl-3-deoxy-5-*O*-trityl-b-D-ribofuranosyl]thymine (15)

To a solution of **14**[11] (700 mg, 2.35 mmol) in pyridine (6 mL) containing DMAP (345 mg, 2.82 mmol) trityl chloride (786 mg, 2.82 mmol) was added in different portions. The mixture was heated to 65 °C and stirred overnight. Then it was diluted with CH_2Cl_2 (50 mL), washed with saturated aqueous $NaHCO_3$ (50 mL), and dried over anhydrous $MgSO_4$. The solvent was removed under diminished pressure and the resulting residue was purified by column chromatography (CH_2Cl_2-MeOH, 98:2) affording **15** (1.15 g, 92%) as a white foam. ^{1}H NMR (300 MHz, DMSO-d_6): *d* 1.42 (3H, d, *J* = 1.2 Hz, 5-CH_3), 2.50 (1H, m, H-3'), 3.13-3.22 (2H, m, H-5'A and H-6'A), 3.37 (1H, dd, *J* = 1.8 Hz and 10.8 Hz, H-5'B), 3.60 (1H, dd, *J* = 6.9 and 12.6 Hz, H-6'B), 4.03 (1H, ddd, *J* = 2.1, 3.9 and 9.0 Hz, H-4'), 4.32 (1H, dd, *J* = 2.1 and 6.0 Hz, H-2'), 5.68 (1H, d, *J* = 2.4 Hz, 2'-OH), 5.86 (1H, d, *J* = 5.4 Hz, H-1'), 7.35 (15H, m, arom H), 7.55 (1H, d, H-6); HRMS (ESI-MS) for $C_{30}H_{29}N_5O_5Na$ $[M + Na]^+$: found, 562.2067; calcd, 562.2066.

2,2'-Anhydro-1-(3-azidomethyl-3-deoxy-5-*O*-trityl-b-D-arabinofuranosyl)thymine (16)

A solution of **15** (940 mg, 1.74 mmol) and DMAP (854 mg, 7.00 mmol) in CH_2Cl_2 (17 mL) was stirred at room temperature. After stirring for 30 minutes trifluoromethanesulfonyl chloride (0.37 mL, 3.50 mmol) was added to the cooled (4 °C) solution. After further stirring for 3h at the same temperature, the reaction was quenched with water (20 mL) and extracted with CH_2Cl_2 (20 mL). The organic layer was successively washed with an aqueous saturated solution of Na_2CO_3 (20 mL), dried over anhydrous $MgSO_4$ and evaporated under reduced pressure. The obtained residue was purified by column chromatography (CH_2Cl_2-MeOH, 97:3) to yield **16** (743 mg, 82 %) as a white foam.^{1}H NMR (300 MHz, DMSO-d_6): *d* 1.76 (3H, d, 5-CH_3), 2.66 (1H, m, H-3'), 2.82 (1H, dd, *J* = 6.6 and 10.2 Hz, H-5'A), 3.01 (1H, dd, *J* = 3.9 and -10.5 Hz, H-5'B), 5.57 (2H, m, H-6'A and H-6'B), 5.21 (1H, m, H-4'), 5.27 (1H, dd, *J* = 2.1 and 5.4 Hz, H-2'), 6.20 (1H, d, *J* = 6.0 Hz, H-1'), 7.22 (15H, m, arom H), 7.80 (1H, d, *J* = 1.5 Hz, H-6); HRMS (ESI-MS) for $C_{30}H_{28}N_5O_4$ $[M + H]^+$: found, 522.2138; calcd, 522.2141.

1-(3-Azidomethyl-2-chloro-2,3-dideoxy-b-D-ribofuranosyl)thymine (5)

An ice-cooled suspension of **16** (220 mg, 0.42 mmol) in dry dioxane (50 mL) was saturated with anhydrous hydrogen chloride. The mixture was heated in a sealed tube at 75-80 °C for 24 h. After cooling, the solution was concentrated and the obtained residue purified by column chromatography (CH_2Cl_2-MeOH, 97:3), yielding **5** (90 mg, 71%) as a white foam. ^{1}H NMR (300 MHz, DMSO-d_6): *d* 1.74 (3H, s, 5-CH_3), 2.72 (1H, m, H-3'), 3.57 (3H, m, H-5'A and H-6'A and H-6'B), 3.84 (1H, m, H-5'B), 4.01 (1H, app d, $J_{3', 4'}$ = 9.9 Hz, H-4'), 4.81 (1H, app d, $J_{2', 3'}$ = 5.4 Hz, H-2'), 5.36 (1H, t, *J* = 4.8 Hz, 5'-OH), 5.89 (1H, d, *J* = 1.5 Hz, H-1'), 8.01 (1H, d, H-6), 11.30 (1H, s, NH); ^{13}C NMR (75 MHz, DMSO-d_6): *d* 12.96 (5-CH_3), C-3'hidden by DMSO signal, 48.73 (C-6'), 60.15 (C-5'), 65.32 (C-2'), 83.57 (C-4'), 91.36 (C-1'), 109.07 (C-5), 136.06 (C-6), 151.04 (C-2), 162.12 (C-4); HRMS (ESI-MS) for $C_{11}H_{14}ClN_5O_4Na$ $[M+Na]^+$: found, 338.0615; calcd, 338.0632. Anal. ($C_{11}H_{14}ClN_5O_4$) C,H,N.

1-[3-Aminomethyl-2-chloro-2,3-dideoxy-b-D-ribofuranosyl]thymine (6)

Compound **5** (60 mg, 0.20 mmol) and triphenylphosphine (87 mg, 0.33 mmol) were dissolved in pyridine (3 mL) and stirred at room temperature. After 1h, concentrated NH_4OH (2 mL) was added and the solution was allowed to stir for an additional 6.5 h. Pyridine was removed at reduced pressure, water (50 mL) was added and the unreacted triphenylphosphine and triphenylphosphine oxide were removed by filtration. The filtrate was extracted with toluene and the water layer was evaporated under reduced pressure to give a syrup, which was purified by column chromatography (0.175 N NH_3 in CH_2Cl_2-MeOH, 90:10) to yield **6** (42 mg, 72 %) as a white foam. ^1H NMR (300 MHz, DMSO-d_6): *d* 1.73 (3H, s, 5-CH_3), 2.52 (1H, m, H-3'), 2.77 (2H, m, H-6'A and H-6'B), 3.65 (1H, d, H-5'A), 3.87 (1H, dd, *J* = 2.7 and 12.9 Hz, H-5'B), 3.97 (1H, app d, $J_{3',4'}$ = 10.5 Hz, H-4'), 4.79 (1H, d, $J_{2',3'}$ = 4.8 Hz, H-2'), 5.85 (1H, s, H-1'), 8.04 (1H, s, H-6); ^{13}C NMR (75 MHz, DMSO-d_6): *d* 12.93 (5-CH_3), 38.06 (C-3'), 42.90 (C-6'), 60.04 (C-5'), 66.39 (C-2', 84.06 (C-4'), 91.53 (C-1'), 108.90 (C-5), 136.06 (C-6), 150.89 (C-2), 164.47 (C-4); HRMS (ESI-MS) for $C_{11}H_{17}ClN_3O_4$ $[M + H]^+$: found, 290.0911; calcd, 290.0907. Anal. ($C_{11}H_{16}ClN_3O_4$**.**$2H_2O$) C,H,N; N:calcd, 12.90; found: 11.81.

1-(3-Azidomethyl-3-deoxy-5-*O*-trityl-b-D-arabinofuranosyl)thymine (17)

A mixture of **16** (590 mg, 1.13 mmol), 1N NaOH (3.2 mL), dioxane (45 mL) and EtOH-H_2O (1:1, 45 mL) was stirred at room temperature for 2h. The solution was neutralised with HOAc/EtOH (1:1, v/v) to pH 7. The resulting mixture was extracted with CH_2Cl_2 (100 mL) and the organic layer was dried over anhydrous $MgSO_4$, evaporated under reduced pressure and purified by column chromatography (CH_2Cl_2-MeOH, 90:10), yielding **17** (530 mg, 87 %) as a white foam. ^1H NMR (300 MHz, DMSO-d_6): *d* 1.53 (3H, s, 5-CH_3), 2.32 (1H, m, H-3'), 3.21-3.43 (3H, m, H-5'A and H-5'B, H-6'A), 3.56 (1H, dd, *J* = 5.7 and -12.6 Hz, H-6'B), 3.80 (1H, m, H-4'), 4.11 (1H, t, *J* = 5.4 Hz, H-2'), 5.60 (1H, d, *J* = 5.1 Hz, 2'-OH), 5.97 (1H, d, *J* = 5.7 Hz, H-1'), 7.32 (15H, m, arom H).

1-(3-Azidomethyl-2,3-dideoxy-2-fluoro-b-D-ribofuranosyl)thymine (7)

To a solution of **17** (640 mg, 1.19 mmol) in toluene (12 mL) containing pyridine (1.2 mL), DAST (0.59 mL, 4.42 mmol) was added and the mixture was stirred for 2 h at room temperature and then for 3 h at 50 °C. The reaction was quenched with ice-water (50 mL) and extracted with CH_2Cl_2 (50 mL). The organic layer was dried over anhydrous $MgSO_4$, evaporated under reduced pressure and purified by column chromatography (CH_2Cl_2-MeOH, 97:3), yielding 1-[3-azidomethyl-2,3-dideoxy-2-fluoro-5-*O*-trityl-β-D-ribofuranosyl]thymine (460 mg, 72 %) as a white foam. ^1H NMR (300 MHz, DMSO-d_6): *d* 1.45 (3H, s, 5-CH_3), 2.85 (1H, m, $J_{3',F}$ = 33.0 Hz, H-3'), 3.20 (4H, m, H-5'A, H-5'B, H-6'A and H-6'B), 4.11 (1H, app d, $J_{4',F}$ = 9.6 Hz, H-4'), 5.40 (1H, dd, $J_{2',3'}$ = 3.9 Hz, $J_{2',F}$ = 52.2 Hz, H-2'), 5.87 (1H, d, $J_{1',F}$ = 21.6 Hz, H-1'), 7.32 (15H, m, arom H), 7.55 (1H, s, H-6); HRMS (ESI-MS) for $C_{30}H_{28}FN_5O_4Na$ $[M + Na]^+$: found, 564.2020; calcd, 564.2023.

The obtained foam was dissolved in 80% HOAc in H_2O (7 mL). The mixture was heated to 90°C during 1h. The solvent was removed under reduced pressure and the residue purified by column chromatography (CH_2Cl_2-MeOH, 90:10), yielding **10** (221 mg, 62% from **17**) as a white foam. ^1H NMR (300 MHz, DMSO-d_6): *d* 1.75 (3H, s, 5-CH_3), 2.62 (1H, m, $J_{3',F}$ = 32.7 Hz, H-3'), 3.46-3.62 (3H, m, H-5'A, H-6'A and H-6'B), 3.83 (1H, d, *J* = -12.0 Hz, H-5'B), 3.99 (1H, dt, $J_{3',4'}$ = 2.7, $J_{4',F}$ = 10.5 Hz, H-4'), 5.27 (1H, br s, 5'-OH), 5.31 (1H, dd, $J_{2',3'}$ = 4.2 Hz, $J_{2',F}$ = 52.5 Hz, H-2'), 5.87 (1H, d, $J_{1',F}$ = 19.5 Hz), 7.84 (1H, s, H-6); ^{13}C NMR (75 MHz, DMSO-d_6): *d* 12.90 (5-CH_3), C-3’ hidden by DMSO signal, 47.79 (C-6', $J_{6',F}$ = 8.6 Hz), 60.42 (C-5'), 83.44 (C-4'), 89.46 (C-1', $J_{1',F}$ = 37.0 Hz), 97.46 (C-2', $J_{2',F}$ = 180.8 Hz), 109.38 (C-5), 136.67 (C-6), 150.91 (C-2), 164.54 (C-4); ^{19}F NMR (300 MHz, D_2O): *d* -195.046; HRMS (ESI-MS) for $C_{11}H_{14}FN_5O_4Na$ $[M + Na]^+$: found, 322.0908; calcd, 322.092. Anal. ($C_{11}H_{14}FN_5O_4$) C, H, N.

1-(3-Aminomethyl-2,3-dideoxy-2-fluoro-b-D-ribofuranosyl)thymine (8)

This compound was synthesised from **7** (80 mg, 0.26 mmol) using the procedure described for the synthesis of **6**, yielding 54 mg (77 %) of amine **8** as a foam. ^{1}H NMR (300 MHz, DMSO-d_6): *d* 1.73 (3H, s, 5-CH_3), 2.30 (1H, m, $J_{3', F}$ = 34.2 Hz, H-3'), 2.57 (1H, m, H-6'A), 2.76 (1H, m, H-6'B), 3.62 (1H, d, *J* = -12.0 Hz, H-5'A), 3.79 (1H, d, H-5'B), 3.89 (1H, app d, $J_{4', F}$ = 10.2 Hz, H-4'), 5.03 (1H, br s, 5'-OH), 5.22 (1H, d, $J_{2', F}$ = 51.9 Hz, H-2'), 5.82 (1H, d, $J_{1', F}$ = 18.3 Hz, H-1'), 7.85 (1H, s, H-6); ^{13}C NMR (75 MHz, DMSO-d_6): *d* 12.95 (5-CH_3), 36.95 (*J* = 7.7 Hz) and 44.76 (*J* = 18 Hz) (C-3' and C-6'), 60.63 (C-5'), 84.41 (C-4'), 89.07 (C-1', $J_{1', F}$ = 36.3 Hz), 97.89 (C-2', $J_{2', F}$ = 179.4 Hz), 109.21 (C-5), 136.43 (C-6), 150.79 (C-2), 164.51 (C-4); ^{19}F NMR (300 MHz, D_2O): *d* –195.70; HRMS (ESI-MS) for $C_{11}H_{17}FN_3O_4$ [M + H]$^+$: found, 274.1191; calcd, 274.1202. Anal. ($C_{11}H_{16}FN_3O_4$.1/2H_2O) C, H, N; N: calcd, 14.89; found, 13.61.

1-(3-Azidomethyl-2,5-difluoro-2,3,5-trideoxy-b-D-ribofuranosyl)thymine (9)

This compound was synthesised from **7** (66 mg, 0.22 mmol) using the procedure described for the synthesis of **7**, to yield 12 mg (18 %) of **9**. ^{1}H NMR (300 MHz, DMSO-d_6): *d* 1.75 (3H, s, 5-CH_3), 2.67 (1H, m, $J_{3', F}$ = 24.0 Hz, H-3'), 3.60 (2H, m, H-6'A and H-6'B), 4.61 (1H, ddd, $J_{5', 4'}$ = 4.2 Hz, $J_{5', 5''}$ = -10.8 Hz, $J_{5', F}$ = 49.5 Hz, H-5'A), 4.80 (1H, dd, H-5'B), 5.41 (1H, dd, $J_{2', 3'}$ = 4.8 Hz, $J_{2', F}$ = 52.5 Hz, H-2'), 5.88 (1H, d, $J_{1', F}$ = 21.3 Hz, H-1'), 7.40 (1H, s, H-6); ^{13}C NMR (75 MHz, DMSO-d_6): *d* 12.87 (5-CH_3), under DMSO signal (C-3'), 46.68 (C-6'), 81.10 (C-4', $J_{4', F}$ = 18.1 Hz), 83.02 (C-5', $J_{5', F}$ = 170.0 Hz), 90.60 (C-1', $J_{1', F}$ = 38.0 Hz), 96.90 (C-2', $J_{2', F}$ = 181.2 Hz), 110.01 (C-5), 136.81 (C-6), 150.87 (C-2), 164.52 (C-4); ^{19}F NMR (300 MHz, D_2O): *d* –194.04 and –228.74; HRMS (ESI-MS) for $C_{11}H_{13}F_2N_5O_3Na$ [M + Na]$^+$: found, 324.0881; calcd, 324.0884. Anal. ($C_{11}H_{13}F_2N_5O_3$) C, H, N.

1-[3-Aminomethyl-3-deoxy-5-*O*-(*tert*-butyldimethyl)silyl-2-*O*,6-*N*-(thiocarbonyl)-b-D-ribofuranosyl]thymine (21), 1-(3-aminomethyl-2-*O*,6-*N*-carbonyl-3-deoxy-5-*O*-(*tert*-butyldimethyl)silyl-b-D-ribofuranosyl)thymine (22) and 1,3-bis[(3*R*)-(3'-deoxy-5'-*O*-(*tert*-butyldimethyl)silyl-thymidin-3'-yl)methyl]urea (23)

To a solution of **19**[11] (460 mg, 0.84 mmol) in toluene was added 2,2'-azobis(2-methylpropionitrile) (354 mg, 2.1 mmol) and tri-*n*-butyltinhydride (0.48 g, 1.65 mmol) at 50-60° C under N_2. The reaction mixture was stirred at 95-100 °C for 5h. The solvent was removed in vacuo and the residue was purified by silica gel column chromatography (CH_2Cl_2-MeOH, 99:1 $\rightarrow$ 95:5), affording produce **21** (0.16 mmol, 20 %), **22** (17 %) and **23** (19 %) as white solids. **21**: ^{1}H NMR (300 MHz, DMSO-d_6): *d* 0.00 (6H, s, $(CH_3)_2Si$), 0.80 (9H, s, $C(CH_3)_3$), 1.70 (3H, s, 5-CH_3), 2.76 (1H, m, H-3'), 3.11 (1H, d, H-6'A), 3.39 (1H, dd, *J* = 5.70 and -13.5 Hz, H-6'B), 3.86 (3H, m, H-4' and H-5'A and H-5'B), 4.95 (1H, d, $J_{2', 3'}$ = 5.1 Hz, H-2'), 5.75 (1H, s, H-1'), 7.45 (1H, s, H-6), 9.81 (1H, s, 6'-NH), 11.36 (1H, s, N(3)H); HRMS (ESI-MS) for $C_{18}H_{30}N_3O_5SSi$ [M + H$^+$]: found, 428.1675; calcd, 428.1675.

22: ^{1}H NMR (300 MHz, DMSO-d_6): *d* 0.00 (6H, s, $(CH_3)_2Si$), 0.81 (9H, s, $C(CH_3)_3$), 1.70 (3H, s, 5-CH_3), 2.61 (1H, m, H-3'), 3.07 (1H, br d, H-6'A), 3.37 (1H, dd, *J* = 5.7 Hz and -12.3 Hz, H-6'B), 3.78 (1H, dd, *J* = 3.6 and -12.0 Hz, H-5'A), 3.91 (1H, dd, H-5'B), 3.98 (1H, dt, *J* = 2.7 and 9.6 Hz, H-4'), 4.90 (1H, br d, $J_{2', 3'}$ = 5.7 Hz, H-2'), 5.70 (1H, d, *J* = 1.2 Hz, H-1'), 7.37 (1H, br s, 6'-NH), 7.44 (1H, d, = 1.2 Hz, H-6); HRMS (ESI-MS) for $C_{18}H_{30}N_3O_6Si$ [M + H]$^+$: found, 412.1897; calcd, 412.1903.

23: ^{1}H NMR (300 MHz, DMSO-d_6): *d* 0.15 (12H, s, $(CH_3)_2Si$), 0.83 (18H, s, $(CH_3)_3C$), 1.73 (6H, s, 5-CH_3), 2.03 (4H, m, H-2'), 2.30 (2H, m, H-3'), 3.05 (4H, m, H-6'A and H-6'B), 3.71

(6H, m, H-4' and H-5'A and H-5'B), 5.94 (2H, t, *J* = 5.4 Hz, H-1'), 6.01 (2H, t, 6'-NH), 7.46 (2H, d, *J* = 1.2 Hz, H-6); HRMS (ESI-MS) for $C_{35}H_{60}N_6O_9Si_2Na$ $[M + Na]^+$: found, 787.3970; calcd, 787.3858.

1-[3-Aminomethyl-3-deoxy-2-*O*,6-*N*-(thiocarbonyl)-b-D-ribofuranosyl]thymine (10), 1-(3-aminomethyl-2-*O*,6-*N*-carbonyl-3-deoxy-b-D-ribofuranosyl)thymine (11) and 1,3-bis[(3*R*)-(3'-deoxythymidin-3'-yl)methyl]urea (12)

Solutions of **21**, **22** and **23** were treated with 5 equivalents TBAF in THF. After 1 hour the mixtures were evaporated to dryness and purified by column chromatography (CH_2Cl_2-MeOH, 95:5), yielding **10**, **11** and **12** as white powders. **10**: ^{1}H NMR (300 MHz, DMSO-d_6): *d* 1.73 (3H, s, 5-CH_3), 2.80 (1H, m, H-3'), 3.45 (1H, d, H-6'A), 3.42 (1H, dd, *J* = 6.0 and -14.1 Hz, H-6'B), 3.66 (1H, br d, H-5'A), 3.85 (1H, br d, *J* = -12.6 Hz, H-5'B), 3.92 (1H, m, H-4'), 4.95 (1H, d, $J_{2',3'}$ = 5.0 Hz, H-2'), 5.34 (1H, t, 5'-OH), 5.82 (1H, s, H-1'), 7.97 (1H, s, H-6), 9.83 (1H, br s, 6'-NH), 11.35 (1H, br s, N(3)H); ^{13}C NMR (75 MHz, DMSO-d_6): *d* 12.89 (5 CH_3), 31.54 (C-3'), 37.18 (C-6'), 59.65 (C-5'), 82.57 (C-4'), 83.98 (C-2'), 89.28 (C-1'), 109.30 (C-5), 136.84 (C-6), 150.84 (C-2), 164.43 (C-4), 184.48 (C=S); HRMS (ESI-MS) for $C_{12}H_{15}N_3O_5SNa$ $[M + Na]^+$: found, 336.0636; calcd, 336.0630. Anal. ($C_{12}H_{15}N_3O_5S$) C, H, N.

11: ^{1}H NMR (300 MHz, DMSO-d_6): *d* 1.74 (3H, s, 5-CH_3), 2.66 (1H, m, H-3'), 3.13 (1H, m, H-6'), 3.42 (1H, dd, $J_{6'',3'}$ = 5.4 Hz, $J_{6'',6''}$ = -12.9 Hz, H-6''), 3.64 (1H, m, H-5'), 3.82 (1H, m, H-5''), 4.02 (1H, dt, *J* = 2.7 and 10.2 Hz, H-4'), 4.90 (1H, d, $J_{2',3'}$ = 5.4 Hz, H-2'), 5.31 (1H, t, *J* = 5.1 Hz, 5'-OH), 5.72 (1H, s, H-1'), 7.39 (1H, d, *J* = 3.0 Hz, H-6), 7.97 (1H, s, 6'-NH), 11.29 (1H, br s, N(3)H); ^{13}C NMR (75 MHz, DMSO-d_6): *d* 12.88 (5-CH_3), 32.44 (C-3'), 36.73 (C-6'), 59.94 (C-5'), 82.50 (C-4'), 83.31 (C-2'), 89.83 (C-1'), 109.28 (C-5), 136.62 (C-6), 150.86 (C=O), 151.84 (C-4), 164.44 (C-2); HRMS (ESI-MS) for $C_{12}H_{15}N_3O_6Na$ $[M + Na]^+$: found, 320.0856; calcd, 320.0858. Anal. ($C_{12}H_{15}N_3O_6$) C, H, N.

12: ^{1}H NMR (300 MHz, DMSO-d_6): *d* 1.75 (6H, s, 5-CH_3), 2.04 (4H, m, H-2'), 2.33 (2H, m, H-3'), 3.08 (4H, m, H-6'A and H-6'B), 3.52 (2H, dd, *J* = 4.5 and -12.6 Hz, H-5'A), 3.66 (4H, m, H-4' and H-5'B), 5.03 (2H, t, *J* = 5.1 Hz, 5'-OH), 5.94 (2H, t, *J* = 6.6 Hz, H-1'), 6.00 (2H, t, *J* = 6.0 Hz, 6'-NH), 7.84 (2H, s, H-6); ^{13}C NMR (75 MHz, DMSO-d_6): *d* 12.96 (5-CH_3), 36.74 (C-2'), 38.97 and hidden by DMSO-signal (C-3' and C-6'), 61.78 (C-5'), 84.58 (C-1' and C-4'), 109.30 (C-5), 137.05 (C-6), 150.97 (C-2), 158.82 (NH*CO*NH), 164.47 (C-4); HRMS (ESI-MS) for $C_{23}H_{32}N_6O_9Na$ $[M+Na]^+$: found, 559.2121; calcd, 559.2128. Anal. ($C_{23}H_{32}N_6O_9$) C, H, N.

1-(3-Aminomethyl-3-deoxy-5-*O*-trityl-b-D-ribofuranosyl)thymine (24)

Compound **15** (450 mg, 0.83 mmol) and triphenylphosphine (356 mg, 1.36 mmol) were dissolved in pyridine (10 mL) and stirred at room temperature. After 1h concentrated NH_4OH (8.5 mL) was added, and the solution was allowed to stir for an additional 2h. Pyridine was removed under reduced pressure, water (5 mL) was added, and the unreacted triphenylphosphine and triphenylphosphine oxide were removed by filtration. The filtrate was extracted with toluene, and the water layer was evaporated under reduced pressure to give a syrup. The syrup was purified by column chromatography (0.175 N NH_3 in CH_2Cl_2-MeOH, 90:10) to yield the title compound (415 mg, 97 %) as a white foam. ^{1}H NMR (300 MHz, DMSO-d_6): *d* 1.37 (3H, s, 5-CH_3), 2.25 (1H, m, H-3'), under DMSO signal (1H, H-5'A), 2.67 (1H, dd, *J* = 7.8 and -12.6 Hz, H-5'B), 3.18 (1H, dd, *J* = 4.5 and -10.5 Hz, H-6'A), under H_2O signal (1H, H-6'B), 4.04 (1H, d, *J* = 7.8 Hz, H-4'), 4.30 (1H, d, *J* = 5.4 Hz, H-2'), 5.64 (1H, s, H-1'), 7.33 (15H, m, arom H), 7.54 (1H, s, H-6); HRMS (ESI-MS) for $C_{30}H_{31}N_3O_5Na$ [M + Na]$^+$: found, 536.2162; calcd, 536.2161.

1-[3-Aminomethyl-3-deoxy-2-*O*,6-*N*-(thiocarbonyl)-5-*O*-trityl-b-D-ribofuranosyl]thymine (25)

A solution of amine **24** (200 mg, 0.39 mmol) and thiocarbonyldiimidazole (78 mg, 0.43 mg) in THF (6 mL) was stirred overnight. The solvent was removed under reduced pressure and the obtained residue was purified by column chromatography (CH_2Cl_2-MeOH, 95:5) to yield **25** as a white powder (162 mg, 75 %). ^{1}H NMR (300 MHz, DMSO-d_6): *d* 1.44 (3H, d, *J* = 1.2 Hz, 5-CH_3), 2.90 (1H, d, *J* = 13.8 Hz, H-6'A), 3.02 (1H, m, H-3'), H-5’A hidden by residual H_2O signal, 3.38 (1H, dd, *J* = 3.0 and -11.7 Hz, H-5'B), 3.46 (1H, dd, *J* = 5.4 and -13.8 Hz, H-6'B), 3.99 (1H, dt, *J* = 4.2 and 10.5 Hz, H-4'), 5.07 (1H, d, *J* = 5.7 Hz, H-2'), 5.80 (1H, d, *J* = 0.9 Hz, H-1'), 7.33 (15H, m, arom H), 7.53 (1H, s, H-6), 9.83 (1H, s, 6’-NH), 11.48 (1H, s, N(3)H); HRMS (ESI-MS) for $C_{31}H_{29}N_3O_5SNa$ [M + Na]$^+$: found, 578.1825; calcd, 578.1725.

1-[3-Aminomethyl-3-deoxy-2-*O*,*N*-(thiocarbonyl)-b-D-ribofuranosyl]thymine (10) from 25

Compound **24** (148 mg, 0.26 mmol) was dissolved in 80% HOAc in H_2O (6mL). The mixture was heated to 90 °C during 1h. The solvent was removed under reduced pressure and the residue purified by column chromatography (CH_2Cl_2-MeOH, 90:10) yielding **10** (69 mg, 85%) as a white powder. For characterisation data: see above.

1-[3-(Azidomethyl)-2,3-dideoxy-a-D-*erythro*-pentofuranosyl]thymine (13)

α-Anomer **13** was a minor unreported byproduct from the synthesis of **1**.[9] ^{1}H NMR (300 MHz, DMSO-d_6): *d* 1.76 (3H, d, 5-CH_3), 1.80 (1H, m, H-2'A), 2.25 (1H, ddd, *J* = 5.6, 7.0 and 12.3 Hz, H-2'B), 2.73 (1H, m, H-3'), 3.50-3.67 (4H, m, H-5'A and H-5'B and H-6'A and H-6'B), 4.02 (1H, dt, *J* = 3.9 and 8.1 Hz, H-4'), 5.06 (1H, t, 5'-OH), 5.99 (1H, dd, *J* = 5.7 and 8.7 Hz, H-1'), 7.83 (1H, d, H-6), ^{13}C NMR (75 MHz, DMSO-d_6): *d* 12.95 (5-CH_3), 35.46 (C-2'), 39.43 (C-3'), 51.03 (C-6'), 61.68 (C-5'), 80.00 and 84.23 (C-1' and C-4'), 109.98 (C-5), 136.77 (C-6), 151.17 (C-2), 164.39 (C-4); HRMS (ESI-MS) for $C_{11}H_{16}N_5O_4$ [M + H]$^+$: found, 282.1205; calcd, 282.1202. Anal. ($C_{11}H_{15}N_5O_4$) C, H, N.

Appendix: Elemental analysis

	C	H	N	C	H	N
5	41.85	4.47	22.18	41.78	4.81	21.74
6 + 2 H_2O	40.56	6.19	**12.90**	41.04	5.96	**11.81**
7	44.15	4.72	23.40	44.14	4.96	23.04
8 + 1/2 H_2O	46.81	6.07	**14.89**	46.58	6.00	**13.61**
9	46.00	4.83	13.41	45.67	4.84	13.21
10	43.86	4.35	23.25	43.74	4.32	23.16
11	48.49	5.09	14.14	48.61	5.31	13.92
12	51.49	6.01	15.66	51.48	5.78	15.34
13	46.97	5.38	24.90	46.95	5.24	24.63

References

---

[1] Duncan, K. Towards the Next Generation of Drugs and Vaccines for Tuberculosis. *Chem. Ind.* **1997**, 861–865.

[2] Munier-Lehmann, H.; Chafotte, a.; Pochet, S.; Labesse, G. Thymidylate kinase of *Mycobacterium tuberculosis*: a chimera sharing properties common to eukaryotic and bacterial enzymes. *Protein Sci.* **2001**, *10*, 1195–1205.

[3] Anderson, E. In *The Enzymes*; Boyer, P. D., Ed.; Academic: New York, 1973; Vol. 8, p 49.

[4] Li de la Sierra, I.; Munier-Lehmann, H.; Gilles, A. M.; Bârzu, O.; Delarue, M. X-ray structure of TMP kinase from *Mycobacterium tuberculosis* complexed with TMP at 1.95 Å resolution. *J. Mol. Biol.* **2001**, *311*, 87–100.

[5] Vanheusden, V.; Munier-Lehmann, H.; Pochet, S.; Herdewijn, P.; Van Calenbergh, S. Synthesis and evaluation of thymidine-5’-O-monophosphate analogues as inhibitors of *Mycobacterium tuberculosis* thymidylate kinase. *Bioorg. Med. Chem. Lett.* **2002**, *12*, 2695–2698.

[6] Vanheusden, V.; Van Rompaey, P.; Munier-Lehmann, H.; Pochet, S.; Herdewijn, P.; Van Calenbergh, S. Thymidine and thymidine-5'-*O*-monophosphate analogues as inhibitors of *Mycobacterium tuberculosis* thymidylate kinase. *Bioorg. Med. Chem. Lett*. **2003**, *13*, 3045–3048.

[7] Pochet, S.; Dugué, L.; Douguet, D.; Labesse, G; Munier-Lehmann, H. Nucleoside analogues as inhibitors of thymidylate kinases: possible therapeutic applications. *ChemBioChem*. **2002**, *3*, 108–110.

[8] Pochet, S.; Dugué, L.; Labesse, G.; Delepierre, M.; Munier-Lehmann, H. Comparative study of purine and pyrimidine nucleoside analogues acting on the thymidylate kinases of Mycobacterium tuberculosis and of humans. ChemBioChem. 2003, 4, 742–747.

[9] Vanheusden, V.; Munier-Lehmann, H.; Froeyen, M.; Dugué, L.; Heyerick, A.; De Keukeleire, D.; Pochet, S.; Herdewijn, P.; Van Calenbergh, S.. 3’-C-Branched-chain-substituted nucleosides and nucleotides as inhibitors of *Mycobacterium tuberculosis* thymidine monophosphate kinase. *J. Med. Chem.* **2003**, *46*, 3811–3821.

[10] Van Rompaey, P.; Nauwelaerts, K.; Vanheusden, V.; Rozenski, J.; Munier-Lehmann, H.; Herdewijn, P.; Van Calenbergh, S. *Mycobacterium tuberculosis* thymidine monophosphate kinase inhibitors: biological evaluation and conformational analysis of 2'- and 3'-modified thymidine analogues. *Eur. J. Org. Chem.* **2003**, 2911–2918.

[11] Lin, T. S.; Zhu, J.-L.; Dutschman, G. E.; Cheng, Y.-C.; Prusoff , W. H. Synthesis and biological evaluations of 3’-deoxy-3’-C-branched-chain-substituted nucleosides. *J. Med. Chem.* **1993**, *36*, 353–362.

[12] Aoyama, Y.; Sekine, T.; Iwamoto, Y.; Kawashima, E.; Ishido, Y. Efficient synthesis of 2'-bromo-2'-deoxy-3', 5'-TPDS-pyrimidine nucleosides by boron trifluoride catalyzed reaction of O^2, 2'-anhydro-(1-β-D-arabinofuranosyl)pyrimidine nucleosides with lithium bromide. *Nucleosides Nucleotides* **1996**, *15*, 733–738.

[13] Codington J. F.; Doerr I. L.; Fox J. J. Synthesis of 2’-Fluorothymidine, 2’-Fluorodeoxyuridine and Other 2’-Halogeno-2’-Deoxy Nucleosides. *J. Am. Chem. Soc.* **1964**, *29*, 558–564.

[14] Lin, T.; Yang, J. H.; Liu, M. C.; Shen, Z. Y.. Cheng, Y. C.; Prusoff, W. Birnbaum, G. I.; Giziewicz, J.; Ghazzouli, I.; Brankovan, V.; Feng, J. S.; Hsiung, G. D. Synthesis and anticancer activity of various pyrimidine nucleoside analogues and crystal structure of 1-(3-deoxy-β-D-threo-pentofuranosyl)cytosine. *J. Med. Chem.* **1991**, *34*, 693–701.

[15] Huang, J. T.; Chen, L. C.; Wang, L.; Kim, M. H.; Warshaw, J. A.; Armstronf, D.; Zhu, Q. Y.; Chou, T.C.; Watanabe, K. A.; Matulicadamic, J.; Su, T. L.; Fox, J. J.; Polsky, B.; Baron, P. A.; Gold, J. W. M.; Hardy, W. D.; Zuckerman, E. Fluorinated sugar analogues of potential anti-HIV-1 nucleosides. *J. Med. Chem.* **1991**, *34*, 1640–1646.

[16] Robins, M. J.; Wnuk, S. F.; Hernández, A. E.; Samano, M. C. Nucleic Acid Related Compounds. 91 Biomimetic Reactions Are in Harmony with Loss of 2'-Substituents as Free Radicals (Not Anions) during Mechanism-Based Inactivation of Ribonucleotide Reductases. Differential Interactions of Azide, Halogen, and Alkylthio Groups with Tributylstannane and Triphenylsilane. *J. Am. Chem. Soc.* **1996**, *118*, 11341–11348.

[17] Shangguan, N.; Katukojvala, S.; Greenberg, R.; Williams, L. J. The reaction of Thio Acids with Azides: A New Mechanism an New Synthetic Applications. *J. Am. Chem. Soc.* **2003**, *125*, 7754–7755.

---

[18] Barton, D. H.; McCombie, S. A new method for the deoxygenation of secondary alcohols. *J. Chem. Soc. Perkin I* **1975**, *16*, 1574–1585.

[19] Blondin, C.; Serina, L.; Wiesmüller, L.; Gilles, A. M.; Bârzu, O. Improved Spectrophotometric Assay of Nucleoside Monophosphate Kinase Activity Using Pyruvate Kinase/Lactate Dehydrogenase Coupling System. *Anal. Biochem.* **1994**, *220*, 219–222.

[20] Haouz, A.; Vanheusden, V.; Munier-Lehmann, H.; Froeyen, M.; Herdewijn, P.; Van Calenbergh, S.; Delarue, M. Enzymatic and structural analysis of inhibitors designed against *Mycobacterium tuberculosis* thymidylate kinase. New insights into the phosphoryl transfer mechanism. *J. Biol. Chem.* **2003**, *278*, 4963–4971.

[21] Word, M.; Lovell, S. C.; Richardson, J. S.; Richardson, D. C. Asparagine and glutamine: using hydrogen atom contacts in the choice of sidechain amide orientation. *J. Mol. Biol.* **1999**, *285*, 1733–1745.

[22] Mohamadi, F.; Richards, N. G. J.; Guida, W. C.; Liskamp, R.; Lipton, M.; Caufield, C.; Chang, G.; Hendrickson, T.; Still, W. C. MacroModel- An Integrated Software System for Modeling Organic and Bioorganic Molecules Using Molecular Mechanics. *J. Comp. Chem.* **1990**, *11*, 440–467.

[23] MOPAC6.0 QCPE #455 by JJP Stewart

[24] Shah, A.; Walters, P.; Stahl, M. Babel: chemical format conversion program. Walters, W. P.; Stahl, M. T.; Shah, A. V.; Dolata, D. P. *Abstr. Pap. –Am. Chem. Soc.* **1994**, *220*, 219–222.

[25] Jones, G.; Willett, P.; Glen, R. C. Molecular Recognition of Receptor Sites Using a Genetic Algorithm with a Description of Desolvation. *J. Mol. Biol.* **1995**, *245*, 43–53.

[26] Jones, G.; Willett, P.; Glen, R. C.; Leach, A. R. L., Taylor, R. Development and Validation of a Genetic Algorithm for Flexible Docking. *J. Mol. Biol.* **1997**, *267*, 727–748.

[27] Wallace, A. C.; Laskowski, R. A.; Thornton, J. M. LIGPLOT: A program to generate schematic diagrams of protein-ligand interactions. *Prot. Eng* **1995**, *8*, 127–134.

[28] McDonald, I. K.; Thornton, J. M. Satisfying Hydrogen Bonding Potential in Proteins. *J. Mol. Biol.* **1994**, *238*, 777–793.

[29] Kraulis, P. J. MOLSCRIPT: a program to produce both detailed and schematic plots of protein structures. *J. Appl. Crystallography* **1991**, *24*, 946–950.

Chapter 7

SYNTHESIS OF 1-[2,4-DIDEOXY-4-*C*-HYDROXYMETHYL-α-L-LYXOPYRANOSYL]THYMINE: A POTENTIAL INHIBITOR OF *MYCOBACTERIUM TUBERCULOSIS* THYMIDINE MONOPHOSPHATE KINASE

Veerle Vanheusden, Roger Busson, Piet Herdewijn and Serge Van Calenbergh

Submitted for J. Org. Chem.

SYNTHESIS OF 1-[2,4-DIDEOXY-4-*C*-HYDROXYMETHYL-α-L-LYXOPYRANOSYL]THYMINE: A POTENTIAL INHIBITOR OF *MYCOBACTERIUM TUBERCULOSIS* THYMIDINE MONOPHOSPHATE KINASE

Veerle Vanheusden, Roger Busson, Piet Herdewijn and Serge Van Calenbergh

Submitted for J. Org. Chem.

Abstract

*Due to the assumed equatorial orientation of its base moiety, 1-[2,4-dideoxy-4-*C*-hydroxymethyl-a-L-lyxopyranosyl]thymine (**2**) was put forward as an interesting thymidine mimic and inhibitor of Mycobacterium tuberculosis thymidine monophosphate kinase (TMPKmt). The key to the synthesis of **2** involves the stereoselective introduction of the hydroxymethyl group onto the C-4 carbon of the pyranose sugar. Attempts to achieve this via hydroboration/oxidation of a C-4'-exocyclic vinylic intermediate selectively yielded the undesired a-directed hydroxymethyl group. Therefore, we envisaged another approach in which the C-4 substituent was introduced upon treatment of 2,3-*O*-isopropylidene-1-*O*-methyl-4-*O*-phenoxythiocarbonyl-a-L-lyxopyranose with b-tributylstannyl styrene. This allowed stereoselective b-directed introduction of a 2-phenylethenyl group at C-4, which was converted via oxidation/reduction (OsO_4, $NaIO_4/NaBH_4$) into the desired 4-hydroxymethyl group (**17**). The resulting 1-*O*-methyl-2,3,6-tri-*O*-acetyl protected sugar was coupled with silylated thymine, using $SnCl_2$ as Lewis acid (**19**). After suitable protection, Barton deoxygenation of the 2'-hydroxyl function of the obtained ribo-nucleoside yielded the desired 2'-deoxynucleoside **2**, indeed showing the aimed equatorial orientation of the thymine ring ($^4C_1$).*

Introduction

Recently *Mycobacterium tuberculosis* thymidine monophosphate kinase (TMPKmt) emerged as an interesting target for the design of new anti-tuberculosis agents.[1,2] A series of 1,5-anhydrohexitol nucleosides was tested for its affinity for the enzyme to probe the effect of a six-membered sugar ring. 1',5'-Anhydro-2',3'-dideoxy-6'-*O*-phosphoryl-2'-(thymin-1-yl)-D-*arabino*-hexitol and its nucleoside analogue **1** proved to be inhibitors of TMPKmt (K_i-values of 30 and 103 μM), indicating that nucleosides with six-membered sugar rings can be accomodated by the target enzyme. In these two nucleoside analogues the base is preferentially in an axial ($^1C_4$) conformation,[3] in contrast to dTMP, where thymine prefers an equatorial-like position.[4]

When co-crystallised with a similar enzyme, herpes simplex virus-1 thymidine kinase, the 5-iodouracil-analogue of **1**, was forced in the $^4C_1$ (base oriented equatorially) conformation.[5] Because this conformational change upon binding of the kinase occurs at the expense of energy, a six-membered ring nucleoside analogue of **1**, in which thymine preferably adopts an equatorial position, was expected to be a better inhibitor of TMPKmt. Since modeling suggested that the thymine moiety in 1-[2,4-dideoxy-4-*C*-hydroxymethyl-α-L-lyxopyranosyl]thymine (**2**), a structural isomer of **1**, prefers an equatorial position,[5] this nucleoside seems a very promising thymidine mimic (Figure 1).

Furthermore, due to their difficult synthetic availability, pyranose nucleosides with a 1,4-substitution pattern have not been studied yet for their antiviral and antibiotic properties and as building blocks in nucleic acid synthesis. For those purposes synthesis of **2** is also considered interesting.

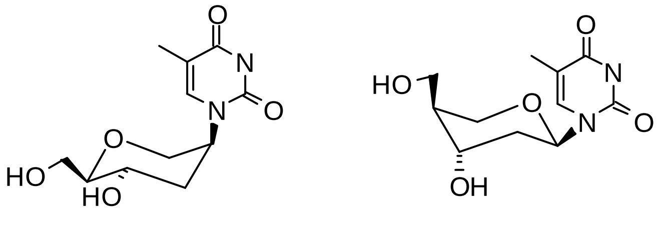

1 **2**

*Figure 1: Strucures of nucleosides **1** and **2***

Results and Discussion

Chemistry

Two strategies towards the synthesis of **20**, a precursor of the target nucleoside, were already attempted.[6] Both reaction schemes are not useful for the synthesis of significant amounts of the target molecule due low yields and separation problems at different stages. In these attempts, the key to the synthesis of **2**, i.e. the introduction of the hydroxymethyl moiety precursor onto C-4 of the pyranose sugar, was achieved by displacement of a 4-*O*-triflate group by the sodium salt of diethyl malonate or via the formation of a C-4-exocyclic vinylic intermediate by Wittig reaction at the C-4-ketone of an oxidised pentopyranose.[6] The first procedure starting from β-D-ribopyranose, required an extensive purification to isolate the desired 2,3-*O*-isopropylidene protected sugar from the unavoidably formed 3,4-*O*-isopropylidene protected isomer.[7] The hydroxyl group at carbon atom 4 (*R*-configuration) was efficiently substituted for a β-directed diethyl malonyl group.[6] However, problems of ring opening during acetolytic deprotection of the obtained 4-hydroxymethyl-1-*O*-methylglycoside, prior to sugar-base coupling, were the reason that **20** could be obtained in a low yield only. On the other hand, Doboszewski and Herdewijn[6] experienced that treatment of 4-deoxy-2,3-*O*-isopropylidene-1-*O*-methyl-4-*C*-methylene-β-D-*erythro*-pentopyranose (**3**) with borane in THF, followed by oxidation with H_2O_2 yielded mainly the undesired 4-α-hydroxymethyl sugar, probably caused by sterical hindrance of the 2,3-*O*-isopropylidene protective group during borane addition.

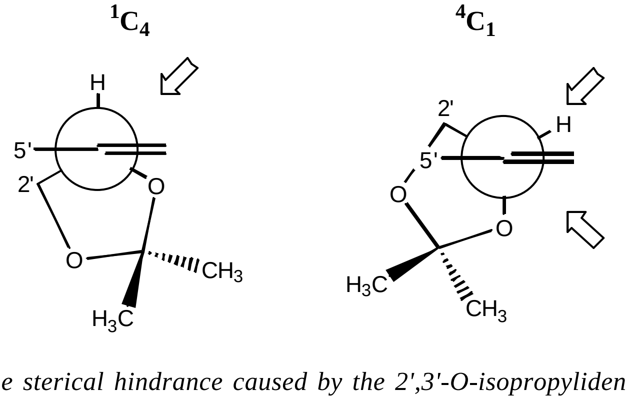

Figure 2: Image of the sterical hindrance caused by the 2',3'-O-isopropylidene in the $^1C_4$ and $^4C_1$ conformation.

In other studies, we observed that preferential attack of borane on an exo double bond is not always predictable and may be governed by complexation of the reagent and steric effects.[8] By carrying out the hydroboration/oxidation of the 4-methylene function after sugar-base coupling, we postulated that the presence of the thymine moiety would favor a $^4C_1$ conformation of the pyranose, which reduces the steric hindrance caused by the isopropylidene protective group (Figure 2). We hoped this would influence the stereochemical outcome of this reaction towards the formation of the 4-β-hydroxymethylcompound (**20**).

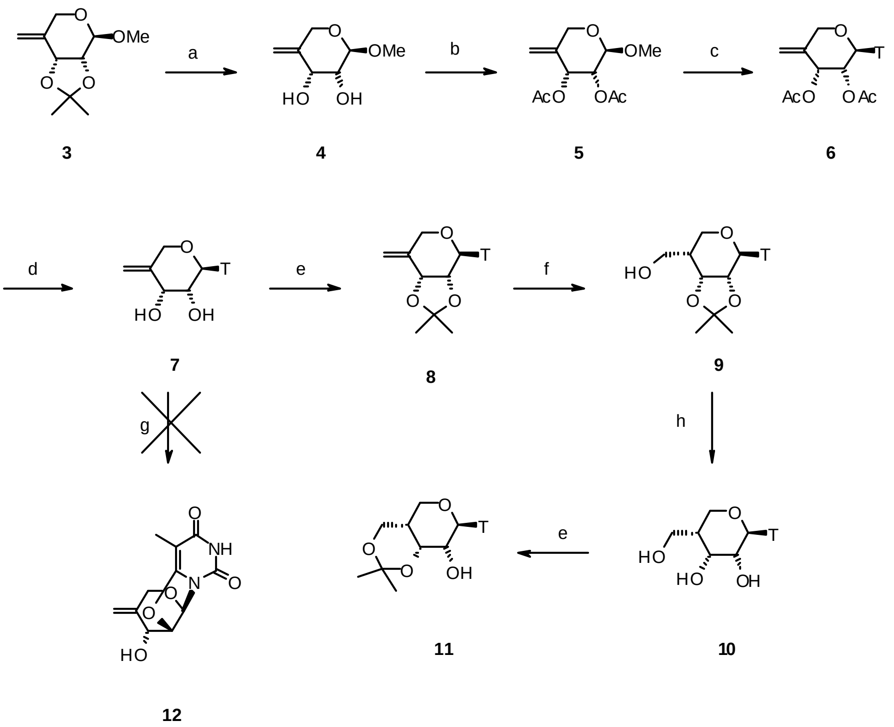

T = thymin-1-yl

Scheme 1: Reagents: (a) CF_3COOH, H_2O; (b) $(CH_3CO)_2O$, pyridine; (c) 5-methyl-2,4-bis[(trimethylsilyl)oxy]pyrimidine, CH_3CN, $SnCl_2$; (d) NH_3, MeOH; (e) 2,2-dimethoxypropane, acetone, p-toluenesulphonic acid; (f) (i) 9-BBN, THF, (ii) H_2O_2, NaOH; (g) $(PhO)_2CO$, $NaHCO_3$, DMF; (h) HOAc, H_2O.

Synthesis was started from 4-deoxy-2,3-*O*-isopropylidene-1-*O*-methyl-4-*C*-methylene-β-D-*erythro*-pentopyranose (**3**), obtained in 4 steps from L-lyxose.[6] Because acid catalysed exchange of the 1-*O*-methyl group of **3** by an 1-*O*-acetylgroup with HOAc, Ac_2O and H_2SO_4, is known to cause partial ring opening,[6] it was decided to maintain the methyl protective group at the 1-*O*-position. The 2,3-*O*-isopropylidene protective group of **3** was selectively removed upon short treatment with CF_3COOH[6] and the 2- and 3-hydroxyl groups were reprotected by acetylation. Coupling of the resulting sugar **5** with silylated thymine in the presence of trimethylsilyl triflate or $SnCl_4$ as catalysts proceeded slowly and yielded an uncharacterised side product with a similar polarity as **6**, rendering purification of the desired nucleoside difficult. This problem could be overcome by performing the coupling reaction under reflux conditions in CH_3CN using $SnCl_2$ as a Lewis acid, which selectively yielded the desired 1-β-nucleoside in 48% yield.[9] The remaining starting material **5**, could be recuperated (37 %). To avoid possible side reactions during hydroboration,[10] the 2'- and 3'-hydroxyl-groups were deprotected and reprotected with an isopropylidene protective group to yield **8**.

However, reaction of **8** with 9-BBN exclusively yielded **9**, the undesired epimer. The selectivity of the formation of **9** was most unexpected. Analysis of its ^{1}H-NMR spectrum reveals an axial-axial coupling between H-1' and H-2' and another one between H-4' and H-5'. The former is indicative for an equatorial orientation of the thymine ring, while the latter and the narrow H-3' signal (half band width of 7.8 Hz), suggest a $^{4}C_{1}$ chair conformation with an α-directed 4'-hydroxymethyl. This assumption was supported by a NOEDIF experiment, showing a weak increase (0.53 %) of the H-2' signal upon irradiation of the H-4' signal. After deprotection of **9** with acetic acid to give **10**, the α-orientation of the 4'-CH_2OH was confirmed via protection of the 6'- and 3'-hydroxyls with an isopropylidene protective group (**11**), which would be less likely for **20**. Apparently, sterical hindrance of the 2',3'-*O*-isopropylidene and formation of the thermodynamically most stable product (both the 4'-hydroxymethyl and the base are oriented equatorially) govern the stereochemical outcome of the hydroboration.[6] Attempts to increase the sterical hindrance at the β-side of the sugar ring before hydroboration, through the formation of a 2,2'-anhydronucleoside (**12**), failed. Upon treatment of **7** with diphenylcarbonate and $NaHCO_3$, elimination of the base occurred, yielding an uncharacterised highly volatile sugar analogue.

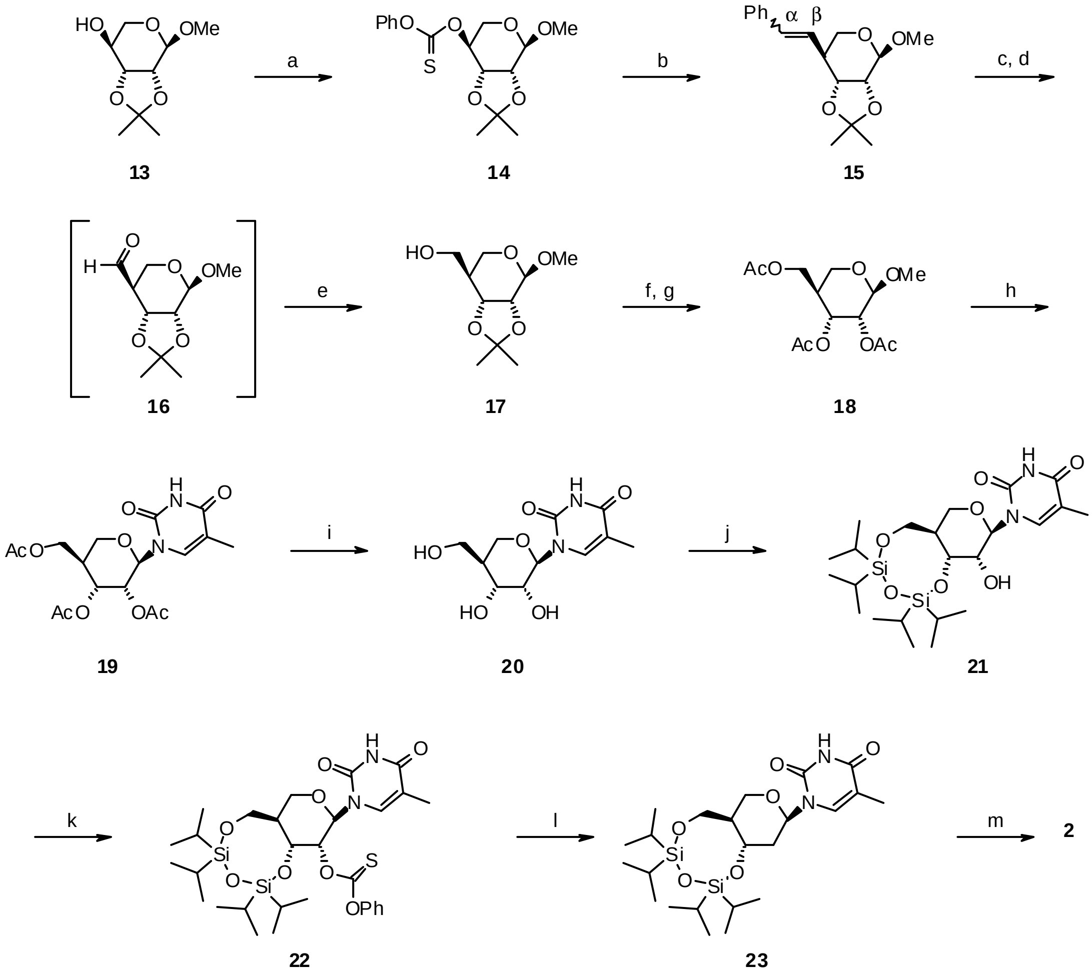

Scheme 2: Reagents: (a) PhOC(S)Cl, DMAP, CH_3CN; (b) b-tributylstannyl styrene, AIBN, benzene; (c) NMMO, OsO_4, dioxane; (d) $NaIO_4$, H_2O; (e) $NaBH_4$, EtOH, H_2O; (f) CF_3COOH, H_2O; (g) $(CH_3CO)_2O$, pyridine; (h) 5-methyl-2,4-bis[(trimethylsilyl)oxy]pyrimidine, CH_3CN, $SnCl_2$; (i) NH_3, MeOH; (j) $(iPr_2SiCl)_2O$, DMF; (k) PhOC(S)Cl, DMAP, CH_3CN; (l) Bu_3SnH, AIBN, toluene; (m) Bu_4NF, THF.

Because synthesis of **2** from **7** failed, it was decided to exploit the steric space at the β-side of the sugar ring through radical-mediated introduction of a carbon group. Thus 2,3-*O*-isopropylidene-1-*O*-methyl-4-*O*-phenoxythiocarbonyl-α-L-lyxopyranose (**14**), obtained through reaction of **13** with phenyl chlorothionocarbonate,[11] was reacted with β-tributylstannylstyrene.[12] This led to stereoselective introduction of a 2-phenylethenyl group at the β-side of the sugar ring (**15**) as indicated by its $^1C_4$ conformation and the positive NOEDIF effect between H-3' and H-β of the styrene moiety (3.9 % enhancement) (Scheme 2).[13] Via oxidative cleavage of the double bond and *in situ* reduction (OsO_4, $NaIO_4$/ $NaBH_4$) the phenylethenyl group of **15** was converted into a 4-hydroxymethyl group (**17**) in a 55% overall yield.[13] A similar reaction sequence as described for the synthesis of **7**, was employed for the conversion of **17** to ribo-analogue **20**. The yield of the sugar-base condensation reaction was only 38%. The presence of the acetoxymethyl moiety in the 4'-position (instead of the 5'-position in natural sugars) has an important effect on the reaction. The 4'-acetoxymethyl group would favor α-attack of the base moiety,[14] while the neighbouring group effect of the 2'-acetoxygroup would favor β-attack of the thymine base. To allow selective deoxygenation of the 2'-hydroxyl of **20**, we envisaged a simultaneous protection of the 3'- and 6'-hydroxyl groups as 1,1,3,3-tetraisopropyldisiloxane-1,3-diyl. At room temperature this reaction was unsuccessful due to the axial position of the 4'-hydroxylmethyl- and 3'-hydroxyl functions. Heating to 30°C allowed the sugar moiety to change its conformation from $^4C_1$ to $^1C_4$, positioning both groups equatorially what resulted in a successful protection.[15] Esterification of the 2'-hydroxyl as a phenyl thionocarbonate ester, followed by Barton deoxygenation and removal of the TIPDS group with TBAF, yielded the desired six-membered ring nucleoside **2**. Upon removal of the TIPDS-protective group, the chair conformation of the sugar ring was restored to the $^4C_1$ conformation ($J_{1',2'}$ = 11.4 Hz), indicating that the thymine ring of **2** indeed adopts an equatorial orientation.

Conformational analysis

The conformations of nucleosides **10**, **20**, **21**, **23** and **2** were studied by NMR spectroscopy. The data are given for each compound in the experimental section. A standard numbering system is used for carbon atoms as exemplified for **2** in Figure 3. All ^{13}C resonances were consistently assigned by gHMQC experiments. The ^1H-NMR results for **10**, **20**, **21**, **23** and **2** are summarised in Table 1. Due to occasional overlapping of ^1H-NMR spectra, full spectral analysis was difficult in the case of **10** and **20**. Coupling constants in the pentopyranosyl parts of **2** and **20** are essentially the same; hence the conformational analysis for compound **2** applies to compound **20** as well. This is also the case for the **21**-**23** couple.

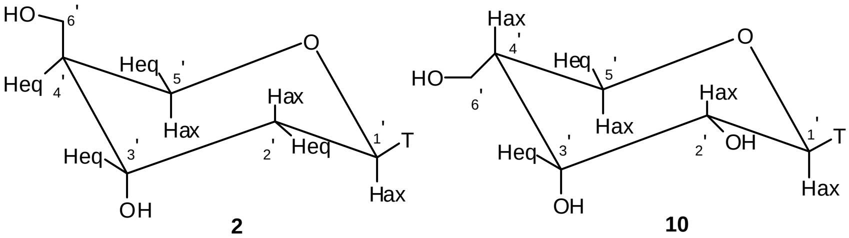

2 **10**

*Figure 3: Structure of **2** and **10**.*

According to the Karplus equation, the coupling between H-1' and H-2' ($J_{1',2'}$ = 9.6 Hz) in compound **10** indicates, that the dihedral angle between these protons is close to 180°C, consistent with an axial-axial arrangement of these bonds in a chair conformation. This points to an equatorially oriented base. The $J_{4', 5'A}$ (11.7 Hz) and the small coupling for H-3' indicate that H-4' and H-5'A are in axial and H-3' in an equatorial arrangement and thus leads to the chair conformation as shown in Figure 3. Herein the 4'-hydroxymethyl is necessarily directed equatorially.

In **2**, proton H-1' shows also a large coupling (11.4 Hz) with H-2'A, indicating an axial position of both protons. The 3' proton is in an equatorial conformation because its half band width (ν½) is about 7.2 Hz for three couplings. This cannot contain an axial-axial coupling. Also the absence of a large coupling between H-4'-H-5'A or H-4'-H-5'B points to an equatorial H-4' proton and further proves that **2** is in a chair conformation with the base in an equatorial position and the 4'-hydroxymethyl axially oriented as depicted in Figure 3.

In **21**, a $J_{1',2'}$-value of 2.7 Hz indicates an equatorial orientation of both protons and thus an axially directed thymine ring. From $J_{3',4'}$ (10.2 Hz) and $J_{4',5'A}$ (11.4 Hz) it can be concluded that H3', H4' and H5'A are all three in an axial orientation, hereby confirming the flipping of the chair conformation from $^4C_1$ to $^1C_4$ upon introduction of a TIPDS protective group on **20** (Figure 4).

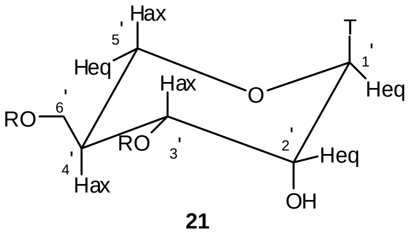

21

Figure 4: Structure of ***21****.*

Summarising, the values of the vicinal H,H-coupling constants lead to the conclusion that **10**, **20** and **2** are in chair conformations with the base in an equatorial position, contrary to **21** and **23** where the base is in an axial orientation.

The data for **20** and **2** indicate that the conformational preference of 4-deoxy-4-hydroxymethyl-α-L-lyxopyranosyl nucleosides is opposite to that of the anhydro-hexitol nucleosides.[3] When **2** is considered, an axially oriented heterocycle would lead to an unfavorable 1,3-diaxial interaction between the nucleoside base and the 3'- and 5'-positions. With an equatorially oriented heterocycle, this unfavorable interaction is present between the 4'-hydroxymethyl function and the hydrogen atom in the 2'-positon and also between the 3'-OH and the H-5' and H-1'. These latter interactions may be less unfavorable than the ones with the thymine ring. Considering the anhydro-hexitol nucleosides, on the contrary, only one sterically unfavorable 1,3-diaxial interaction is present when the nucleoside base is oriented axially. Apart from this, a hydrogen bond between the 6'-CH_2OH and the ring oxygen may also stabilise the $^4C_1$ conformation in **20** and **2**.

Binding Assay

Nucleosides **20** and **2** were tested for their affinities for TMPKmt. Unfortunately **2** showed to be a lower affinity inhibitor of TMPKmt (K_i-value of 320 μM) compared to its anhydro-hexitol congener **1**. **20** even didn't show any inhibition at a final concentration of 3 mM.

		10		**20**		**21**		**23**		**2**	
proton	coupling	δ	*J*	δ	*J*	δ	*J*	δ	*J*	δ	*J*
1'	–	5.60		5.59		5.36		5.93		5.82	
	1'–2'A		9.6		9.6		2.7		4.8		11.4
	1'–2'B		–		–		–		0		0
2'A	–	3.63		3.66		4.49		2.18		1.51	
	2'A–2'B		–		–		–		-14.7		-11.4
	2'A–3'		3.6		n.d.		2.7		10.4		n. d.
	2'A–2'OH		n.d.		n.d.		5.1		–		–
2'B	–	–		–		–		2.54		1.96	
	2'B–3'		–		–		–		3.3		<1
3'	–	3.95		3.97		3.99		4.26		4.02	
	3'–4'		n.d.		n.d.		10.2		10.4		n.d.
	3'–3'OH		n.d.		n.d.		–		–		2.7
4'	–	1.91		1.77		2.22		1.79		1.51	
	4'–5'A		11.7		0		11.4		11.7		0
	4'–5'B		4.8		2.4		5.7		4.8		2.1
	4'–6'A		n.d.		n.d.		0		0		7.2
	4'–6'B		6.3		n.d.		2.1		2.7		8.4
5'A	–	3.52		3.66		3.75		3.72		3.77	
	5'A–5'B		-11.7		-11.7		-11.4		-11.7		-11.4
5'B	–	3.68		3.83		3.87		3.86		3.92	
6'A	–	H_2O		3.50		3.55		3.57		3.50	
	6'A–6'B		-10.8		-11.7		-11.1		-11.7		-10.1
	6'A–6'OH		n.d.		n.d.		–		–		5.1
6'B	–	3.41		3.59		3.92		4.14		3.60	
	6'B–6'OH		n.d.		n.d.		–		–		5.1

*Table 1: ^{1}H NMR Chemical shifts (δ in ppm) and Coupling Constants (J in Hz) in sugar parts of **10**, **20**, **21**, **23** and **2**. Chemical shifts indicated in the first column are δ-values relative to the residual solvent peak in DMSO-d_6 (2.48 ppm) in the case of **10**, **20**, **21**, and **2** and in $CDCl_3$ (7.26 ppm) in the case of **23**. Coupling constants between the protons indicated in the second column are values in Hz. Protons are labeled by the number of the carbon atom to which they are bonded; if two protons are bonded to the same carbon atom, the one resonating at a higher field is denoted by A and the other by B. Geminal coupling constants are assumed to be negative. Abbreviation n.d.: not determined.*

Conclusions

We have successfully developed a stereoselective approach for the synthesis of 1-[2,4-dideoxy-4-*C*-hydroxymethyl-α-L-lyxopyranosyl]thymine (**2**) from 2,3-*O*-isopropylidene-1-*O*-methyl-α-L-lyxopyranose (**13**) in 13 steps. The key steps of this synthesis route involve the stereoselective introduction of the 6'-carbon on the β-side of the sugar ring, via the radical mediated substitution of the 4'-OH by a phenylethenylgroup (**14** → **15**) followed by the introduction of the base via a $SnCl_2$-mediated coupling. Conformational analysis proves that **2** indeed shows the expected $^4C_1$ conformation with an equatorially orientated thymine ring.

Experimental Section

Spectrophotometric binding assay.

TMPKmt activities were determined using the coupled spectrophotometric assay described by Blondin et al.[16] at 334 nm in an Eppendorf ECOM 6122 photometer. The reaction medium (0.5 mL final volume) contained 50 mM Tris-HCl pH 7.4, 50 mM KCl, 2 mM $MgCl_2$, 0.2 mM NADH, 1 mM phosphoenol pyruvate and 2 units each of lactate dehydrogenase, pyruvate kinase and nucleoside diphosphate kinase. The concentrations of ATP and dTMP were kept constant at 0.5 mM and 0.05 mM respectively, whereas the concentrations of the analogues varied between 0.1 and 2.5 mM.

Synthesis

General

NMR spectra were obtained with a Varian Mercury 300 spectrometer. Chemical shifts are given in ppm (δ) relative to residual solvent peak, in the case of DMSO-d_6 2.54 ppm for ^{1}H and 40.5 ppm for ^{13}C, in the case of $CDCl_3$ 7.26 ppm for ^{1}H and 77.4 ppm for ^{13}C. All signals assigned to hydroxyl groups were exchangeable with D_2O. Mass spectra and exact mass measurements were performed on a quadrupole/orthogonal-acceleration time-of-flight (Q/oaTOF) tandem mass spectrometer (qTof 2, Micromass, Manchester, UK) equipped with a standard electrospray ionisation (ESI) interface. Samples were infused in a 2-propanol:water (1:1) mixture at 3 µL/min. Precoated Merck silica gel F_{254} plates were used for TLC and spots were examined under UV light at 254 nm and revealed by sulfuric acid-anisaldehyde spray. Column chromatography was performed on Uetikon silica (0.2-0.06 mm).

Anhydrous solvents were purchased from Sigma-Aldrich.

2,3-Di-*O*-acetyl-4-deoxy-1-*O*-methyl-4-methylene-b -D-*erythro*-pentopyranose (5)

Compound **3**^{6} (1.02 g, 5.08 mmol) was treated with 90 % trifluoroacetic acid (9 mL) during 5 minutes. After evaporation, water was added, followed by Dowex 1x2 (OH^- form) to neutralise residual acid. The resin was removed by filtration and washed with water. The combined water filtrates were evaporated and the residue was thoroughly dried under high vacuum. The resulting 4-deoxy-1-*O*-methyl-4-methylene-β-D-*erythro*-pentopyranose (**4**) was dissolved in pyridine. Ac_2O was added and the mixture was stirred at room temperature for 2 h. Evaporation and coevaporation with toluene yielded crude **5** (980 mg, 79 %). ^{1}H-NMR (300 MHz, $CDCl_3$): ***d*** 2.10 (6H, s, $OCOCH_3$), 3.43 (3H, s, OCH_3), 4.09 (1H, d, *J* = -12.3 Hz, H-5A), 4.34 (1H, ddd, *J* = -12.3, 1.5 and 0.6 Hz, H-5B), 4.72 (1H, d, *J* = 2.4 Hz, H-1), 5.02 and 5.10 (2H, 2m, methylene), 5.14 (1H, m, H-2), 5.78 (1H, m, H-3); ^{13}C NMR (75 MHz, $CDCl_3$): ***d*** 20.09 ($OCOCH_3$), 21.04 ($OCOCH_3$), 55.57 (OCH_3), 64.21 (C-5), 68.77 (C-3), 70.68 (C-2), 99.53 (C-1), 110.63 (C-6), 138.19 (C-4), 169.76 (CO), 170.39 (CO); HRMS (ESI-MS) for $C_{11}H_{16}O_6$ $[M+Na]^+$: found, 267.0849; calcd, 267.0844.

1-[2,3-Di-*O*-acetyl-4-deoxy-4-methylene-b -D-*erythro*-pentopyranosyl]thymine (6)

Thymine (991 mg, 7.86 mmol) was suspended in hexamethyldisilazane (87.8 mL, 416 mmol), containing trimethylsilylchloride (0.71 mL, 5.6 mmol) and pyridine (7 mL). The mixture was heated to 125° C and stirred overnight. The reaction mixture was evaporated and co-evaporated with toluene. The resulting residue and **5** (980 mg, 4.01 mmol) were dissolved in CH_3CN (27 mL), $SnCl_4$ (anhydrous, 1.98 g, 10.5 mmol) was added and the mixture was refluxed under nitrogen during 39 h. After cooling, the mixture was poured in 10 % Na_2CO_3 (500 mL) and extracted with CH_2Cl_2 (3 times 300 mL). After drying and evaporation of the organic layer, the obtained residue was purified by column chromatography (CH_2Cl_2–MeOH, 100:0 → 98:2) yielding pure **6** (640 mg, 48%) and recuperated starting material **5** (355 mg, 37 %). ^{1}H-NMR (300 MHz, DMSO-d_6): ***d*** 1.73 (3 H, s, 5-CH_3), 1.90 (3H, s, $OCOCH_3$), 2.11 (3H, s, $OCOCH_3$), 4.28 (1H, d, *J* = -12.6 Hz, H-5'A), 4.35 (1H, d, *J* = -12.1 Hz, H-5'B), 5.16 (1H, dd, *J* = 3.3 and 9.9 Hz, H-2'), 5.34 and 5.36 (2H, 2s, methylene), 5.78 (1H, d, *J* = 3.0 Hz, H-3'), 5.93 (1H, d, *J* = 9.9 Hz, H-1'), 7.67 (1H, s, H-6); HRMS (ESI-MS) for $C_{15}H_{18}N_2O_7$ $[M+Na]^+$: found, 361.1011; calcd, 361.1011.

1-[4-Deoxy-4-methylene-b-D-*erythro*-pentopyranosyl]thymine (7)

A solution of **6** (30 mg, 0.089 mmol) in methanolic ammonia solution 7 N (5 mL) was stirred 2h at room temperature and was evaporated under reduced pressure. The resulting residue was purified by column chromatography (CH_2Cl_2–MeOH, 90:10) yielding **7** (20 mg, 89%) as a white foam. ^1H-NMR (300 MHz, DMSO-d_6): *d* 1.75 (3 H, d, *J* = 1.2 Hz, 5-CH_3), 3.68 (1H, m, H-2'), 4.02 and 4.28 (3H, d and m, H-3' and H-5'), 5.00 (1H, br s, methylene), 5.07 (1H, d, *J* = 1.8 Hz, methylene), 5.74 (1H, d, *J* = 9.3 Hz, H-1'), 7.52 (1H, q, H-6); ^{13}C NMR (75 MHz, DMSO-d_6): *d* 12.48 (5-CH_3), 67.38, 69.90 and 73.01 (C-2', C-3' and C-5'), 80.28 (C-1'), 110.27 (C-5), 114.53 (C-6'), 137.51 (C-6), 143.98 (C-4'), 151.74 (C-2), 164.55 (C-4); HRMS (ESI-MS) for $C_{11}H_{14}N_2O_5Na$ $[M+Na]^+$: found, 277.0812; calcd, 277.0800.

1-[4-Deoxy-2,3-*O*-isopropylidene-4-methylene-b-D-*erythro*-pentopyranosyl]thymine (8)

To a stirred suspension of **7** (129 mg, 0.51 mmol) in anhydrous acetone (3 mL) and 2,2-dimethoxypropane (0.31 mL, 2.52 mmol) was added *p*-toluenesulphonic acid monohydrate (97 mg, 0.51 mmol). After 4 h the resulting solution was poured slowly into stirred aqueous 0.5 M $NaHCO_3$ (2 mL). The solution was concentrated *in vacuo* to ca 1.5 mL, diluted with water (100 mL) and extracted with CH_2Cl_2 (3 times 75 mL). The combined organic layers were dried, evaporated under reduced pressure and quickly chromatographed (CH_2Cl_2–MeOH, 97:3) yielding **8** (124 mg, 83%) as a white foam. HRMS (ESI-MS) for $C_{14}H_{18}N_2O_5Na$ $[M + Na]^+$: found, 317.1109; calcd, 317.1113.

1-[4-Deoxy-4-(hydroxymethyl)-2,3-*O*-isopropylidene-b-D-ribopyranosyl]thymine (9)[17]

To an ice cooled solution of **8** (102 mg, 0.40 mmol) in anhydrous THF (1 mL), under nitrogen, was added dropwise 9-BBN (2.0 mL of a 0.5 M solution in THF, 1.0 mmol). The mixture was slowly warmed to room temperature and stirred for 24h. The reaction mixture was cooled to 0°C, treated sequentially with EtOH (1.6 mL), a 2 N solution of NaOH (0.78 mL, 1.56 mmol) and 30% aqueous H_2O_2 solution (0.78 mL, 6.8 mmol). The resulting mixture was stirred 24 h and then poured into a mixture of EtOAc (10mL) and water (10mL). The layers were separated and the aqueous layer was extracted with EtOAc (3 times). The combined organic layers were dried over $MgSO_4$ and evaporated under reduced pressure. The obtained residue was purified by column chromatography (CH_2Cl_2–MeOH, 95:5→98:2) yielding pure **9** (77 mg, 62%). ^1H-NMR (300 MHz, DMSO-d_6): *d* 1.09 (3 H, s, $C(CH_3)_2$), 1.26 (3H, s, $C(CH_3)_2$), 1.76 (3H, s, 5-CH_3), 2.23 (1H, m, H-4'), 3.20 (1H, dd, *J* = -11.2 and 5.4 Hz, H-6'A), 3.37 (1H, dd, *J* = 8.31 and -10.8 Hz, H-5'A), 3.43 (1H, t, *J* = -11.72, H-6'B), 3.53 (1H, dd, *J* = -10.8 and 6.35 Hz, H-5'B), 4.33 (1H, m, H-2'), 4.42 (1H, m, H-3'), 4.71 (1H, t, 6'-OH), 5.41 (1H, d, *J* = 9.0 Hz, H-1'), 7.63 (1H, q, *J* = 0.9 Hz, 6-H); ^{13}C NMR (75 MHz, DMSO-d_6): *d* 12.53 (5-CH_3), 28.38 and 26.95 ($C(CH_3)_2$), under DMSO signal (C-4'), 59.52 (C-6'), 66.55 (C-5'), 72.70 and 74.06 (C-2' and C-3'), 82.02 (C-1'), 110.05 (C-5), 110.77 ($\mathit{C}(CH_3)_2$), 137.27 (C-6), 151.38 (C-2), 164.18 (C-4); HRMS (ESI-MS) for $C_{14}H_{20}N_2O_6Na$ $[M+H]^+$: found, 335.1232; calcd, 335.1219.

1-[4-Deoxy-4-(hydroxymethyl)-b-D-ribopyranosyl]thymine (10)

Compound **9** (70 mg, 0.21 mmol) was refluxed for 3 hours in a 1:1 mixture of HOAc–H_2O (5 mL). The mixture was evaporated under reduced pressure, co-evaporated with EtOH and the resulting residue was purified by column chromatography (CH_2Cl_2–MeOH, 95:5), yielding **10** (51 mg, 98%) as a white foam. ^1H-NMR (300 MHz, DMSO-d_6): *d* 1.76 (1H, d, *J* = 0.9 Hz, 5-CH_3), 1.91 (1H, m, H-4'), under H_2O-signal (1H, H-6'A), 3.41 (1H, dd, *J* = 6.3 and -10.8 Hz, H-6'B), 3.52 (1H, t, *J* = -11.7 Hz, H-5'A), 3.63 (1H, dd, *J* = 3.6 and 9.3 Hz, H-2'), 3.68 (1H, dd, *J* = 4.8 and -10.8 Hz, H-5'B), 3.95 (1H, br s, H-3'), 4.49 (1H, br s, 6'-OH), 4.92 (1H, br s, 3'-OH, 5.11 (1H, br s, 2'-OH), 5.60 (1H, d, *J* = 9.6 Hz, H-1'), 7.57 (1H, q, *J* = 1.2 Hz, 6-H); ^{13}C NMR (75 MHz, DMSO-d_6): *d* 12.66 (5-CH_3), 43.86 (C-4'), 59.83 (C-6'), 64.92 (C-5'), 68.81 and 69.40 (C-2' and C-3'), 80.74 (C-1'), 109.85 (C-5), 137.71 (C-6), 151.83 (C-2), 164.46 (C-4); HRMS (ESI-MS) for $C_{11}H_{16}N_2O_6Na$ [M + Na]$^+$: found, 295.9010; calcd, 295.0906.

1-[4-Deoxy-4-(hydroxymethyl)-3,6-*O*-isopropylidene-b-D-ribopyranosyl]thymine (11)

To a stirred suspension of **10** (13 mg, 0.048 mmol) in anhydrous acetone (0.1 mL) and 2,2-dimethoxypropane (0.03 mL, 0.24 mmol) was added *p*-toluenesulphonic acid monohydrate (0.15 mg, 0.8 µmol). After 1 h the resulting solution was poured slowly into stirred aqueous 0.5 M $NaHCO_3$ (2 mL). The solution was concentrated *in vacuo*, diluted with water (10 mL) and extracted with CH_2Cl_2 (3 times 10 mL). The combined organic layers were dried, evaporated under reduced pressure and purified by column chromatography (CH_2Cl_2–MeOH, 98:2 → 97:3) yielding pure **11**. ^{1}H-NMR (300 MHz, DMSO-d_6): *d* 1.33 (3 H, s, $C(CH_3)_2$), 1.41 (3H, s, $C(CH_3)_2$), 1.76 (4H, m, 5-CH_3 and H-4'), 3.45-4.05 (5H, m, H-5', H-6' and H-2'), 4.38 (1H, m, ν1/2 = 6.6 Hz, H-3'), 5.09 (1H, br s, 2-OH), 5.59 (1H, d, *J* = 9.9 Hz, H-1'), 7.58 (1H, s, 6-H); ^{13}C NMR (75 MHz, DMSO-d_6): *d* 12.63 (5-CH_3), 19.28 and 30.30 ($C(\mathit{C}H_3)_2$), 34.02 (C-4'), 60.07 (C-6'), 64.84, 67.44 and 69.28 (C-2', C-3' and C-5'), 80.15 (C-1'), 99.15 ($\mathit{C}(CH_3)_2$), 110.13 (C-5), 137.40 (C-6), 151.70 (C-2), 164.43 (C-4); HRMS (ESI-MS) for $C_{14}H_{20}N_2O_6$ [M+Na]$^+$: found, 335.1207; calcd, 335.1219.

2,3-*O*-Isopropylidene-1-*O*-methyl-4-*O*-phenoxythiocarbonyl-a-L-lyxopyranose (14)

To an ice-cold solution of **13** (2.50 g, 12.2 mmol) and DMAP (3.00 g, 24.5 mmol) in CH_3CN (100 mL) was gradually added phenyl chlorothionocarbonate (2.3 mL, 16.4 mmol). The mixture was stirred at 0 °C for 5 h. The solvent was removed *in vacuo*, and the residue was dissolved in CH_2Cl_2 (500 mL). The solution was washed with water (2 x 500 mL), dried over anhydrous $MgSO_4$, filtered, and evaporated *in vacuo*. The obtained residue was purified by column chromatography (CH_2Cl_2–MeOH, 95:5) to give **14** (3.6 g, 87 %) as a syrup. ^{1}H NMR (300 MHz, $CDCl_3$): *d* 1.39 (3H, s, $C(CH_3)_2$), 1.58 (3H, s, $C(CH_3)_2$), 3.46 (3H, s, OCH_3), 3.83 (1H, dd, *J* = 7.5 and -12.0 Hz, H-5A), 3.92 (1H, dd, *J* = 4.2 and -12.1 Hz, H-5B), 4.16 (1H, dd, *J* = 5.4 and 3.2 Hz, H-2), 4.45 (1H, m, H-3), 4.71 (1H, d, *J* = 3.0 Hz, H-1), 5.49 (1H, m, H-4), 7.10-7.44 (5H, m, arom H); ^{13}C NMR (75 MHz, $CDCl_3$): *d* 26.49 and 28.09 ($C(\mathit{C}H_3)_2$), 56.07 (OCH_3), 58.67 (C-5), 74.48 (C-3), 75.39 (C-2), 78.89 (C-4), 100.31 (C-1), 110.21 ($\mathit{C}(CH_3)_2$), 122.07 (arom C^o), 126.89 (arom C^p), 129.78 (arom C^m), 153.63 (arom C^i), 194.73 (O(CS)O); HRMS (ESI-MS) for $C_{16}H_{20}O_6SNa$ [M + Na]$^+$: found, 363.0865; calcd, 363.0878.

2,3-*O*-Isopropylidene-1-*O*-methyl-4-*C*-(2-phenylethenyl)-a-L-lyxopyranose (*E*-isomer) (15)

To a solution of **14** (1.47 g, 4.3 mmol) in benzene (34 mL) was added β-tributylstannylstyrene (4.02 g, 10.22 mmol). The resulted solution was degassed three times with nitrogen at room temperature and 45°C. After 2,2'-azobisisobutyronitrile (AIBN) (230 mg, 1.4 mmol) was added, the solution was refluxed for 2h. Another part of AIBN (230 mg, 1.4 mmol) was added after cooling the reaction mixture to 40° C. The reaction mixture was then refluxed again for 2h. This procedure was repeated until the starting material disappeared (6 times). The solvent was evaporated, and the residue was purified by column chromatography (CH_2Cl_2–MeOH, 98:2) to give **15** (773 mg, 62 %) as an oil. ^{1}H NMR (300 MHz, $CDCl_3$): *d* 1.26 (3H, s, CCH_3), 1.44 (3H, s, CCH_3), 2.55 (1H, m, H-4), 3.46 (3H, s, OCH_3), 3.50 (2H, app d, H-5), 3.92 (1H, dd, *J* = 2.1 and 5.1 Hz, H-2), 4.11 (1H, dd, *J* = 5.1 and 7.2 Hz, H-3), 4.78 (1H, d, *J* = 2.1 Hz, H-1), 6.15 (1H, dd, *J* = 16.2 and 7.8 Hz, H-β styrene), 6.52 (1H, d, *J* = 16.1 Hz, H-α styrene), 7.11-7.40 (5H, m, arom H); ^{13}C NMR (75 MHz, $CDCl_3$): *d* 26.58 (C*C*H_3), 28.53 (C*C*H_3), 42.83 (C-4), 55.72 (OCH_3), 61.31 (C-5), 73.90 (C-3), 76.05 (C-2), 99.94 (C-1), 109.29 (*C*CH_3), 126.47 (arom C^o), 127.20 and 127.74 (arom C^p and Cα styryl), 128.72 (arom C^m), 132.78 (Cβ styryl), 137.10 (arom C^i); HRMS (ESI-MS) for $C_{17}H_{22}O_4Na$ [M + Na]$^+$: found, 313.1412; calcd, 313.1415.

4-Deoxy-4-*C*-hydroxymethyl-2,3-*O*-isopropylidene-1-*O*-methyl-a -L-lyxopyranose (17)

To a solution of styrene **15** (330 mg, 1.1 mmol) and *N*-methylmorpholine-*N*-oxide (NMMO) (200 mg, 1.7 mmol) in dioxane (20 mL), was added a catalytic amount of osmium tetraoxide 4% in H_2O (0.3 mL, 0.04 mmol). The flask was covered by aluminium foil, and the reaction mixture was stirred at room temperature overnight. A solution of $NaIO_4$ (731 mg, 3.4 mmol) in water (1 mL) was added to the stirred reaction mixture. It was stirred for 1 h at 0° C and 2h at room temperature, followed by addition of EtOAc (20 mL). The mixture was filtered through a celite pad and washed with EtOAc. The filtrate was washed three times with 10 % aqueous $Na_2S_2O_3$ solution until the color of the aqueous phase disappeared. The organic phase was further washed with water, dried ($MgSO_4$) and concentrated. The obtained aldehyde was dissolved in EtOH–H_2O (4:1 v/v, 16 mL). $NaBH_4$ (190 mg, 5.0 mmol) was added in portions at 0° C. The resulting reaction mixture was stirred at room temperature for 2 h and then treated with ice water. The mixture was extracted with EtOAc. The organic phase was washed with water and brine, dried ($MgSO_4$) and concentrated. The obtained residue was purified by column chromatography (CH_2Cl_2–MeOH, 9:1) to give **17** (127 mg, 53 % over three steps). ^{1}H NMR (300 MHz, DMSO-d_6): *d* 1.24 (3H, s, C*C*H_3), 1.38 (3H, s, C*C*H_3), 1.78 (1H, m, H-4), 3.28 (3H, s, OCH_3), 3.30-3.55 (4H, m, H-5 and H-6), 3.79 (1H, dd, *J* = 3.0 and 5.4 Hz, H-2), 4.03 (1H, dd, *J* = 5.1 and 6.6 Hz, H-3), 4.60 (1H, d, *J* = 3.0 Hz, H-1), 4.66 (1H, t, *J* = 5.7 Hz, 6-OH); ^{13}C NMR (75 MHz, DMSO-d_6): *d* 26.93 (C*C*H_3), 22.77 (C*C*H_3), under DMSO signal (C-4), 55.51 (OCH_3), 59.94 and 60.10 (C-5 and C-6), 72.49 (C-3), 73.81 (C-2), 100.50 (C-1), 108.57 (*C*CH_3); HRMS (ESI-MS) for $C_{10}H_{18}O_5Na$ [M + Na]$^+$: found, 241.1050; calcd, 241.1052.

2,3,6-Tri-*O*-acetyl-4-deoxy-4-*C*-hydroxymethyl-1-*O*-methyl-a -L-lyxopyranose (18)

A solution of **17** (72 mg, 0.3 mmol) in trifluoroacetic acid–H_2O (9:1 v/v, 1 mL) was stirred for 5 minutes. The solution was neutralised with Dowex 1x2 (OH^-). The resin was removed by filtration and washed with MeOH–H_2O (3:1). The filtrate was evaporated under diminished pressure and purified by column chromatography (CH_2Cl_2–MeOH, 90:10), yielding 4-deoxy-4-*C*-hydroxymethyl-1-*O*-methyl-α-L-lyxopyranose[6] (45 mg, 77 %) as a glassy solid. ^{1}H NMR (300 MHz, DMSO-d_6): *d* 1.91 (1H, m, H-4), 3.20 (3H, s, OCH_3), 3.30-3.61 (6H, m, H-6, H-2, H-3 and H-5), 4.35 (2H, t, 6- and 3-OH), 4.45 (1H, d, *J* = 4.5 Hz, H-1), 4.47 (1H, app d, *J* = 2.1 Hz, 2-OH); ^{13}C NMR (75 MHz, DMSO-d_6): *d* under DMSO signal (C-4), 54.90 (OCH_3), 60.06, 61.78, 66.65 and 69.35 (C-6, C-2, C-3 and C-5), 102.54 (C-1); HRMS (ESI-MS) for $C_7H_{14}O_5Na$ [M + Na]$^+$: found, 201.0750; calcd, 201.0739. The above mentionned glassy solid (40 mg, 0.2 mmol) was dissolved in pyridine (2.5 mL) and acetic anhydride (2.5 mL) was added. The solution was stirred at room temperature for 3 h. The solvent was removed under vacuum and the resulting residue was purified by column chromatography (CH_2Cl_2–MeOH, 99:1) to yield **18** (60 mg, 89 %) as a foam. ^{1}H NMR (300 MHz, CD_3OD): *d* 1.97, 2.02 and 2.10 (OCO*C*H_3), 2.47 (1H, m, H-4), 3.38 (3H, s, OMe), 3.70 (1H, t, *J* = -11.4 Hz, H-5A), 3.77 (1H, dd, *J* = -11.4 and 5.4 Hz, H-5B), 4.01 (1H, dd, *J* = -11.4 and 2.7 Hz, H-6A), 4.11 (1H, dd, *J* = 6.0 and -11.7 Hz, H-6B), 4.65 (1H, d, *J* = 5.1 Hz, H-1), 5.09 (1H, dd, *J* = 5.1 and 3.0 Hz, H-2), 5.13 (1H, dd, *J* = 3.0 and 11.0 Hz, H-3); ^{13}C NMR (75 MHz, CD_3OD): *d* 19.29, 19.40 and 19.51 (OCO*C*H_3), 35.70 (C-4), 54.028 (OCH_3), 60.34 (C-5), 61.04 (C-6), 67.31 (C-3), 68.10 (C-2), 99.32 (C-1), 170.58, 170.88 and 170.25 (O*C*OCH$_3$); HRMS (ESI-MS) for $C_{13}H_{20}O_8Na$ $[M + Na]^+$: found, 327.1058; calcd, 327.1056.

1-[2,3,6-Tri-*O*-acetyl-4-deoxy-4-*C*-hydroxymethyl-a -L-lyxopyranosyl]thymine (19)^6

Thymine (615 mg, 4.9 mmol) was suspended in hexamethyldisilazane (55 mL, 260 mmol), containing trimethylsilylchloride (0.48 mL, 3.8 mmol) and pyridine (4 mL). The mixture was heated to 125° C and stirred overnight. The reaction mixture was evaporated and co-evaporated with toluene. The resulting residue and **18** (744 mg, 2.44 mmol) were dissolved in CH_3CN (17 mL), $SnCl_2$ (anhydrous, 1.23 g, 6.5 mmol) was added and the mixture was refluxed under nitrogen during 39 h. After cooling it was poured in 10 % Na_2CO_3 (500 mL) and extracted with CH_2Cl_2 (3 times 300 mL). After drying and evaporation of the organic layer, the obtained residue was purified by column chromatography (CH_2Cl_2–MeOH 99:1 → 97:3) yielding pure **19** (367 mg, 38%) as a white foam and residual starting product **18** (315 mg, 42 %). ^{1}H NMR (300 MHz, DMSO-d$_6$): *d* 1.75 (3H, s, 5-CH$_3$), 1.88, 2.04 and 2.11 (OCOCH$_3$), 2.18 (1H, m, H-4'), 3.86 (1H, d, *J* = -12.3 Hz, H-5'A), 3.97 (1H, d, *J* = -12.3 Hz, H-5'B), 4.36 (2H, m, H-6'A and H6'B), 5.30 (1H, dd, *J* = 2.7 Hz and 9.9 Hz, H-2'), 5.45 (1H, br s, H-3'), 5.80 (1H, d, *J* = 9.9 Hz, H-1'), 7.82 (1H, s, 6-H), 11.40 (1H, s, NH); ^{13}C NMR (75 MHz, DMSO-d$_6$): *d* 12.50 (5-CH$_3$), 21.02, 21.34 and 21.45 (OCO*C*H$_3$), 55.60 (C-4'), 62.47 and 64.86 (C-5' and C-6'), 66.23 and 68.40 (C-2' and C-3'), 79.22 (C-1'), 110.70 (C-5), 137.05 (C-6), 151.36 (C-2), 164.19 (C-4), 169.80, 170.27 and 170.91 (O*C*OCH$_3$); HRMS (ESI-MS) for $C_{17}H_{22}N_2O_9Na$ $[M + Na]^+$: found, 421.1253; calcd, 421.1223.

1-[4-Deoxy-4-*C*-hydroxymethyl-a -L-lyxopyranosyl]thymine (20)^6

Compund **19** (410 mg, 1.03 mmol) was treated with a 7N methanolic ammonia solution (30 mL) at room temperature for 7 h. Evaporation yielded a residue which was purified by column chromatography (CH_2Cl_2–MeOH, 90:10) to afford **20** (218 mg, 78%) as a white foam. ^{1}H NMR (300 MHz, DMSO-d$_6$): *d* 1.77 (4H, br s, 5-CH$_3$ and H-4'), 3.50 (1H, m, H-6'A), 3.59 (1H, m, H-6'B), 3.66 (2H, m, H-5'A and H-2'), 3.83 (1H, dd, *J* = 2.4 and -11.1 Hz, H-5'B), 3.97 (1H, br s, H-3'), 4.65 (1H, t, *J* = 5.1 Hz, 6'-OH), 4.97 (2H, br s, 2'-OH and 3'-OH), 5.59 (1H, d, *J* = 9.6 Hz, H-1'), 7.56 (1H, s, 6-H), 11.25 (1H, s, NH); ^{13}C NMR (75 MHz, DMSO-d$_6$): *d* 12.56 (5-CH$_3$), 45.95 (C-4'), 60.00 (C-6'), 63.92 (C-2') and 66.17 (C-5'), 68.83 (C-3'), 81.18 (C-1'), 109.93 (C-5), 137.74 (C-6), 151.71 (C-2), 164.40 (C-4); HRMS (ESI-MS) for $C_{11}H_{16}N_2O_6Na$ $[M + Na]^+$: found, 295.0902; calcd, 295.0906; Anal. ($C_{11}H_{16}N_2O_6$) C, H, N.

1-[4-Deoxy-4-*C*-hydroxymethyl-3,6-*O*-(1,1,3,3,-tetraisopropyldisiloxan-1,3-diyl)-a -L-lyxopyranosyl]thymine (21)

Compound **20** (46 mg, 0.17 mmol) and imidazole (60 mg, 0.88 mmol) were dissolved in DMF (1 mL) at 0°C. 1,3-Dichloro-1,1,3,3-tetraisopropyldisiloxane (58 µL, 0.19 mmol) was added dropwise. The mixture was stirred 3h at room temperature and overnight at 30°C. Water (10 ml) was added and the mixture was extracted with CH_2Cl_2 (10 mL). The organic layer was dried over $MgSO_4$ and evaporated under reduced pressure. The obtained residue was purified by column chromatography (CH_2Cl_2–MeOH, 99:1) to afford **21** (78 mg, 89%) as a white foam. ^{1}H NMR (300 MHz, DMSO-d$_6$): *d* 0.95 (28H, m, *C*H(C*H*$_3$)$_2$), 1.75 (3H, s, 5-CH$_3$), 2.22 (1H, m, H-4'), 3.55 (1H, d, *J* = -11.1 Hz, H-6'A), 3.75 (1H, t, *J* = -11.4 Hz, H-5'A), 3.87 (1H, dd, *J* = 5.7 and -11.4 Hz, H-5'B), 3.92 (1H, dd, *J* = 2.1 and -11.1 Hz, H-6'B), 3.99 (1H, dd, *J* = 2.7 and 10.2 Hz, H-3'), 4.49 (1H, br, H-2'), 5.30 (1H, d, *J* = 5.1 Hz, 2'-OH), 5.36 (1H, d, *J* = 2.7 Hz, H-1'), 7.41 (1H, s, 6-H), 11.31 (1H, s, NH); ^{13}C NMR (75

MHz, DMSO-d_6): *d* 12.63, 12.66, 12.77, 13.44, 13.47 (*C*H(CH_3)$_2$ and 5-CH_3), 17.12, 17.79, 17.84, 17.87, 17.90 (CH(*C*H_3)$_2$), 38.83 (C-4'), 59.41 (C-6'), 65.23(C-5'), 66.48 (C-3'), 68.21 (C-2'), 88.47 (C-1'), 109.83 (C-5), 137.59 (C-6), 151.33 (C-2), 164.40 (C-4); HRMS (ESI-MS) for $C_{23}H_{43}N_2O_7Si_2$ $[M + H]^+$: found, 515.2619; calcd, 515.2608.

1-[4-Deoxy-4-*C*-hydroxymethyl-3,6-*O*-(1,1,3,3,-tetraisopropyldisiloxan-1,3-diyl)-2-*O*-phenoxythiocarbonyl-a -L-lyxopyranosyl]thymine (22)

Compound **21** (126 mg, 0.24 mmol) was dissolved in anhydrous CH_3CN (4 mL). DMAP (58 mg, 0.48 mmol) was added at 0°C. The mixture was stirred 15 min at 0°C, then phenylchlorothionocarbonate (46 µL, 0.33 mmol) was added dropwise and the resulting solution was stirred overnight at room temperature. After adding 7% $NaHCO_3$ solution (7mL), the mixture was evaporated to dryness, the obtained residue was dissolved in EtOAc, washed with water, dried over $MgSO_4$, evaporated under reduced pressure and purified by column chromatography (CH_2Cl_2–MeOH, 99.5:0.5) to afford **22** (140 mg, 89%) as a white foam. ^{1}H NMR (300 MHz, $CDCl_3$): *d* 1.03 (28H, m, C*H*(C*H*$_3$)$_2$), 1.94 (3H, s, 5-CH_3), 2.25 (1H, m, H-4'), 3.60 (1H, d, *J* = -11.7 Hz, H-6'A), 3.82-3.99 (2H, m, H-5'A and H-5'B), 4.10 (1H, dd, *J* = -11.7 and 2.4 Hz, H-6'B), 4.52 (1H, dd, *J* = 2.8 and 11.1 Hz, H-3'), 5.61 (1H, d, *J* = 2.6 Hz, H-1'), 6.58 (1H, t, *J* = 2.7 Hz, H-2'), 7.09-7.44 (5H, m, arom H), 8.06 (1H, s, 6-H); ^{13}C NMR (75 MHz, $CDCl_3$): *d* 12.61 (5-CH_3), 12.82, 13.04, 13.45, 13.73 (*C*H(CH_3)$_2$), 17.43, 17.51, 17.55, 17.66, 17.74 (CH(*C*H_3)$_2$), 39.73 (C-4'), 58.68 (C-6'), 64.97 and 65.02 (C-3' and C-5'), 80.78 (C-2'), 85.84 (C-1'), 112.03 (C-5), 122.00 (arom C^o), 126.88 (arom C^p), 129.77 (arom C^m), 136.71 (C-6), 150.03 (arom C^i), 153.58 (C-2), 163.35 (C-4), 194.84 (O*C*(S)O); HRMS (ESI-MS) for $C_{30}H_{46}N_2O_8SSi_2Na$ $[M + Na]^+$: found, 673.2409; calcd, 673.2411.

1-[2,4-Dideoxy-4-*C*-hydroxymethyl-3,6-*O*-(1,1,3,3,-tetraisopropyldisiloxan-1,3-diyl)-a -L-lyxopyranosyl]thymine (23)

Compound **22** (134 mg, 0.20 mmol) was co-evaporated three times with anhydrous toluene, dissolved in toluene (32 mL) and degassed with nitrogen for 30 minutes. In a second flask, AIBN (17 mg, 0.10 mmol) and Bu_3SnH (166 µL, 0.62 mmol) in toluene (2 mL) were degassed with nitrogen for 30 minutes. The first flask was heated to 80°C, the second solution was added dropwise via a syringe. The mixture was heated to 90°C for 2h. After cooling to room temperature, the mixture was evaporated, and the residue was purified by column chromatography (CH_2Cl_2–MeOH, 99.5:0.5) to afford **23** (81 mg, 79%) as a white foam. ^{1}H NMR (300 MHz, $CDCl_3$): *d* 1.05 (28H, m, C*H*(C*H*$_3$)$_2$), 1.79 (1H, m, H-4'), 1.90 (3H, s, 5-CH_3), 2.18 (1H, m, H-2'A), 2.54 (1H, dd, *J* = 3.3 and -14.1 Hz, H-2'B), 3.57 (1H, d, *J* = -11.7 Hz, H-6'A), 3.72 (1H, t, *J* = -11.7 Hz, H-5'A), 3.86 (1H, dd, *J* = 4.8 and -11.7 Hz, H-5'B), 4.14 (1H, dd, *J* = 2.7 and -12.0 Hz, H-6'B), 4.26 (1H, m, H-3'), 5.93 (1H, d, *J* = 4.8 Hz, H-1'), 8.04 (1H, s, 6-H); ^{13}C NMR (75 MHz, $CDCl_3$): *d* 12.71 (5-CH_3), 12.78, 13.46, 13.77 (*C*H(CH_3)$_2$), 17.37, 17.40, 17.50, 17.53, 17.57, 17.63 (CH(*C*H_3)$_2$, 36.36 (C-2'), 45.69 (C-4'), 58.94 (C-6'), 64.77 and 63.29 (C-3' and C-5'), 82.31 (C-1'), 110.51 (C-5), 136.64 (C-6), 150.52 (C-2), 163.47 (C-4); HRMS (ESI-MS) for $C_{23}H_{43}N_2O_6Si_2$ $[M + H]^+$: found, 499.2571; calcd, 499.2659.

1-[2,4-Dideoxy-4-C-hydroxymethyl-a -L-lyxopyranosyl]thymine (2)

Compound **23** (76 mg, 0.15 mmol) was dissolved in THF (8 mL) and Bu_4NF (1M in THF, 0.76 mL, 0.76 mmol) was added. The mixture was stirred for 1h at room temperature, evaporated to dryness and purified by column chromatography (CH_2Cl_2–MeOH, 93:7) to afford **2** (38 mg, 97%) as a white foam. ^{1}H NMR (300 MHz, DMSO-d_6): *d* 1.51 (2H, m, H-2'A and H-4'), 1.76 (3H, s, 5-CH_3), 1.96 (1H, app t, *J* = -11.4 Hz, H-2'B), 3.50 (1H, m, *J* = 8.4 and -10.2 Hz, H-6'A), 3.60 (1H, m, *J* = 7.2 and -10.2 Hz, H-6'B), 3.77 (1H, d, *J* = -11.4 Hz, H-5'A), 3.92 (1H, dd, *J* = 2.1 and -11.4 Hz, H-5'B), 4.02 (1H, m, H-3'), 4.58 (1H, t, *J* = 5.1 Hz, 6'-OH), 4.98 (1H, d, *J* = 2.7 Hz, 3'-OH), 5.82 (1H, d, *J* = 11.4 Hz, H-1'), 7.57 (1H, s, 6-H), 11.25 (1H, s, NH); ^{13}C NMR (75 MHz, DMSO-d_6): ***d*** 12.57 (5-CH_3), 33.79 (C-2'), 43.43 (C-4'), 60.53 (C-6'), 64.66 (C-5'), 64.75 (C-3'), 78.07 (C-1'), 110.08 (C-5), 137.27 (C-6), 150.91 (C-2), 164.36 (C-4); HRMS (ESI-MS) for $C_{11}H_{16}N_2O_5Na$ $[M + Na]^+$: found, 279.0952; calcd, 279.0957; Anal. ($C_{11}H_{16}N_2O_5$) C, H, N.

References

---

[1] Munier-Lehmann, H.; Chafotte, A.; Pochet, S.; Labesse, G. Thymidylate kinase of *Mycobacterium tuberculosis*: a chimera sharing properties common to eukaryotic and bacterial enzymes. *Protein Sci.* **2001**, *10*, 1195–1205.

[2] Vanheusden, V.; Munier-Lehmann, H.; Pochet, S.; Herdewijn, P.; Van Calenbergh, S. Synthesis and evaluation of thymidine-5’-*O*-monophosphate analogues as inhibitors of *Mycobacterium tuberculosis* thymidylate kinase. *Bioorg. Med. Chem. Lett.* **2002**, *12*, 2695–2698.

[3] Verheggen, I.; Van Aerschot, A.; Toppet, S.; Snoeck, R.; Janssen, R.; Balzarini, J.; De Clercq, E.; Herdewijn, P. Synthesis and Antiherpes Virus Activity of 1,5-Anhydrohexitol Nucleosides. *J. Med. Chem.* **1993**, *36*, 2033–2040.

[4] Wang, J.; Herdewijn, P. Enantioselective Synthesis and Conformational Study of Cyclohexene Carbocyclic Nucleosides. *J. Org. Chem.* **1999**, *64*, 7820–7827.

[5] Ostrowski, T.; Wroblowski, B.; Busson, R.; Rozenski, J.; De Clercq, E.; Bennet, M. S.; Champness, J. N.; Summers, W. C.; Sanderson, M. R.; Herdewijn, P. 5-Substituted pyrimidines with a 1,5-anhydro-2,3-dideoxy-D-arabino-hexitol moiety at N-1: Synthesis, antiviral activity, conformational analysis, and interaction with viral thymidine kinase. *J. Med. Chem.* **1998**, *41*, 4343–4353.

[6] Doboszewski, B.; Herdewijn, P. A. M. Synthesis of 4-deoxy-4-*C*-hydroxymethyl-α-L-lyxopyranosyl thymine. *Nucleosides Nucleotides* **1996**, *15*, 1495-1518.

[7] Hughes, N. A.; Maycock, C. The reaction of methyl β-D-ribopyranoside with acetone. *Carbohydrate Research.* **1974**, *35*, 247–250.

[8] Wang, J.; Busson, R.; Blaton, N.; Rozenski, J.; Herdewijn, P. Enantioselective Approach to the Synthesis of Cyclohexane Carbocyclic Nucleosides. *J. Org. Chem.* **1998**, *63*, 3051–3058.

[9] Martin, P. Stereoselective synthese von 2'-*O*-(2-Methoxyethyl)ribonucleosiden: nachbargruppenbeteiligung der methoxyethoxy-gruppe bei der ribosylierung von heterocyclen. *Helv. Chim. Acta*, **1996**, *79*, 1930–1938.

[10] Koga, M.; Schneller, S. Synthesis of (+)-5'-nor-2'-deoxyaristeromycin and (-)-5'-nor-3'-deoxyaristeromycin. *J. Org. Chem.* **1993**, *58*, 6471–6473.

[11] Lin, T. S.; Zhu, J.-L.; Dutschman, G. E.; Cheng, Y.-C.; Prusoff , W. H. Synthesis and biological evaluations of 3’-deoxy-3’-*C*-branched-chain-substituted nucleosides. *J. Med. Chem.* **1993**, *36*, 353–362.

[12] Saihi, M. L.; Pereyre, M. Réactivité des organostanniques viniliques vis-à-vis de chlorures et anhydrides d'acide et d'α-halogénoesters. B*ull. Soc. Chim. Fr.* **1977**, 1251–1255.

[13] An, H.; Wang, T.; Maier, M. A.; Manoharan, M. M.; Ross, B. S.; Cook, P. D. Synthesis of novel 3'-*C*-methylene thymidine and 5-methyluridine/cytidine H-phosphonates and phosphonamidites for new backbone modification of oligonucleotides. *J. Org. Chem.* **2001**, *66*, 2789–2801.

[14] Augustyns, K.; Rozenski, J.; Van Aerschot, A.; Busson, R.; Claes, P.; Herdewijn, P. Synthesis of a New Branched Chain Hexopyranosyl Nucleoside: 1-[2',3'-Dideoxy-3'-C-(hydroxymethyl)-α-D-erythro-pentopyranosyl]thymine. *Tetrahedron* **1994**, *50*, 1189–1198.

[15] Mouroud, E.; Biala, E.; Strazewski, P. Synthesis and Enzymatic digestion of an RNA Nonamer in Both Enantiomeric Forms. *Tetrahedron* **2000**, *56*, 1475–1484.

[16] Blondin, C.; Serina, L.; Wiesmüller, L.; Gilles, A. M.; Bârzu, O. Improved Spectrophotometric Assay of Nucleoside Monophosphate Kinase Activity Using Pyruvate Kinase/Lactate Dehydrogenase Coupling System. *Anal. Biochem.* **1994**, *220*, 219–222.

[17] The nomenclature derived from β-D-ribopyranose is maintained in analogy with Bogdan and Herdewijn. The unambigous name for this compound would be 1-[4(S)-deoxy-4-hydroxymethyl-2,3-*O*-isopropylidene-β-D-*erythro*-pentopyranosyl]thymine

Chapter 8

GENERAL DISCUSSION, CONCLUSIONS AND PERSPECTIVES

GENERAL DISCUSSION, CONCLUSIONS AND PERSPECTIVES

The incidence of tuberculosis has drastically increased during the last 20 years. Especially the appearance of multi-drug resistant strains of *Mycobacterium tuberculosis* is a major concern. Therefore, more potent anti-tuberculosis drugs, preferably acting on novel targets, are eagerly awaited.[1] Thymidine monophosphate kinase (TMPK) catalyses the conversion of dTMP to dTDP. Because *M. tuberculosis* thymidine monophosphate kinase (TMPKmt) plays a crucial role in the thymidine triphosphate synthesis and in view of its low (22%) sequence identity with the human isozyme, it emerged as an attractive target for new drug design.[2] Recently the structure of TMPKmt was elucidated,[3] enabling the structure based design of TMPKmt inhibitors.

Chapters 2, 3 and 5

In order to establish a first structure-activity relationship, modifications were carried out at the 2'-, 3'- and 5-positions of the dTMP scaffold. From these results, the following general tendencies could be observed:

- At the 2'-position the only well-tolerated modifications are a 2'-chlorine and a 2'-fluorine substituent (**2.12** and **2.13**). Modeling suggested that the introduction of the chlorine affects the position of the sugar ring in the active pocket. As a result the 2'-chlorine occupies the pocket where normally the 3'-hydroxyl group resides. Apparently Tyr103, believed to be responsible for the discrimination between ribo- and deoxy-nucleotides, hampered the introduction of other substituents like a 2'-amine or a 2'-hydroxyl group (**2.9**, **5.15**, **5.16**, **5.22**).

- Introduction of a fluorine at the 3'-position of the dTMP scaffold yielded a substrate with a K_m-value of 30 μM (**2.20**). Introduction of a 3'-amine (**2.1**), on the other hand yielded a weak inhibitor, not able to establish a similar interaction with Asp9 as the one observed for AZTMP. However, when a 2'-hydroxyl was combined with a 3'-amine (**2.8**), the affinity increased (K_i = 45 μM). Modeling showed an interaction between the amine and Asp9 and a larger distance between Tyr103 and the 2'-position than the one present in the crystal structure. So far, this compound remains the only example of a ribo-nucleotide showing higher affinity than its corresponding 2'-deoxy-analogue.

- At the 5-position, introduction of a CH_2OH (**3.1**) yielded a moderately active inhibitor as compared to AZTMP. This nucleotide was co-crystallised with TMPKmt, showing hydrogen bonding interactions between the 5-CH_2OH, Ser99 and a water molecule, which is held in place by Asp73 and Arg74. Compounds bearing larger substituents at the 5-position (a furanyl-, a benzyloxymethyl- or a thienyl group) were less active, indicating that the cavity near the 5-position cannot be stretched too much. However, introduction of smaller 5-substituents (a 5-ethyl, 5-fluorine and 5-trifluoromethyl) also proved unsuccessful.

- The affinities of a series of nucleosides and their corresponding nucleotides were compared. The deletion of the phosphate moiety typically resulted in a modest, in many cases negligible affinity loss. In view of the drug delivery problems of phosphorylated compounds, nucleosides seem more useful leads for further drug design. Exploration of other substitution patterns at the 5'-position (e. g. a 5'-H and a 5'-iodine) only yielded poor affinity inhibitors.

Chapter 4

Because TMPKmt represents the first TMPK that does not phosphorylate AZTMP (K_i = 10 µM), modifications of the 3'-position were considered attractive to find good and selective inhibitors. Most probably, an interaction between the 3'-azido group and Asp9 abolishes the catalysis. Since the X-ray structure[3] showed a cavity near the 3'-position, a series 3'-*C*-substituted branched-chain nucleosides and nucleotides was synthesised. Although an efficient synthetic route for the synthesis of 3'-*C*-branched-chain substituted nucleosides **4.9-4.14** has been reported,[4] we developed a route that gives access to both 2'-deoxy- and ribo-analogues and allows easier conversion to the corresponding monophosphates. In the procedure of Lin et al.,[5] all 3'-*C*-modifications are introduced on the sugar moiety before coupling with thymine. In our approach, the 3'-*C*-modifications are effected after sugar-base coupling, which allows synthesising all derivatives from a single key intermediate. A judicious choice of 5'- and 6'-*O*-protective groups permitted conversion of the key compound to the phosphorylated 3'-hydroxymethylanalogues, on one hand and to the 3'-azidomethyl-, 3'-aminomethyl- and 3'-fluoromethyl-derivatives, on the other hand.

The 3'-aminomethyl, 3'-azidomethyl- and 3'-fluoromethyl dTMP analogues **4.3**, **4.4** and **4.5** indeed showed to be potent inhibitors of TMPKmt with K_i-values in the 10-15 µM respectively. Modeling indicated that **4.4** adopts a 2'-*exo*-3'-*endo* conformation (dTMP, in contrast, is in the 2'-*endo*-3'-*exo* conformation). Consequently, the amino group occupies the same space as the 3'-hydroxyl group of dTMP; hence, it is in an appropriate position to interact with Asp9. However, the 3'-fluoromethylnucleotide indicated that an ionic interaction with Asp9 is not a prerequisite for good affinity. Interestingly, deletion of the phosphate moiety typically resulted in a modest (at most 6-fold) affinity loss. The affinities of the ribo-analogues of these compounds were disappointing, indicating that **2.8** was an exceptional example of a ribonucleotide exhibiting better affinity than its 2'-deoxy-analogue. The modest affinity of **4.15** indicated that the ideal length of the spacer between the 3'-position and the introduced functionality is one carbon atom. The selectivity of all target compounds for TMPKmt versus TMPKh was evaluated. All, except **4.6**, are inhibitors of TMPKh. Most nucleotides (**4.3**-**4.8**) showed affinities for the human enzyme in the same order of magnitude as for the *M. tuberculosis* enzyme. The corresponding nucleosides (**4.9**, **4.11** and **4.12**), however, exhibit very low affinities for the human enzyme, resulting in selectivity indices between 10 and 26. Therefore, these nucleosides, combining a low K_i-value with a favorable selectivity index are put forward as the most promising leads for further research.

Chapter 6

Encouraged by the promising affinities of the 3'-*C*-branched-chain nucleosides, attempts were made to combine these favourable 3'-substitution patterns with 2'-halogen substituents (**6.5-6.9**). However, introduction of the 2'-halogen led to a drastic decrease in affinity compared to the corresponding 2'-deoxy-nucleosides. Probably, the 2'-halogens compete with the 3'-substituents for the same binding pocket.

In an attempt to supersede the good affinities of the 3'-*C*-branched-chain nucleosides, we wanted to further explore the enzyme cavity near the 3'-position with alternative nitrogen containing substituents. However, attempted simultaneous reduction of the 6'-azido function and the 2'-hydroxyl of compound **19** (chapter 6) failed, yielding three peculiar nucleoside analogues (**6.10**, **6.11** and **6.12**).

Bicyclic nucleosides **6.10** and **6.11** showed excellent binding affinities. With a K_i-value of 3.5 μM, **6.10** exceeds the K_m-value of the natural substrate (4.5 μM), making it the best TMPKmt inhibitor found so far. Compound **6.10** was modelled into the crystal structure of TMPKmt. The six-membered ring, fused to the C-2', C-3'-bond of the sugar, apparently forces the 6'-nitrogen into the most appropriate position for interaction with the Asp9 residue in the enzyme cavity. The sulphur atom undergoes hydrophobic interactions with the Tyr103 and Tyr165 residues. When the sulphur atom in **6.10** is replaced by a smaller oxygen in **6.11**, the cavity near the 3'-position is filled less efficiently, which is reflected in the somewhat lower affinity of **6.11** (K_i = 13.5 μM).

Due to the lack of a binding site for a second nucleoside at the 3'-position, the K_i-value of **6.12** (37 μM) was most unexpected. A modeling experiment in GOLD showed that the sugar ring of the first monomer **I** binds the dTMP-pocket upside down, which enables hydrogen bonding of its 5'-hydroxyl with Asp9. This binding mode permits the sugar ring of the second monomer (**II**) to be directed towards the outside of the enzyme, where normally the phosphoryl donor binds. With α-nucleoside **6.13** the postulated binding mode of monomer **I** was confirmed. The observed exceptional flexibility of TMPKmt towards the orientation of the sugar ring is of great interest for further inhibitor design.

The low affinities of **6.12** and **6.13** for the human enzyme indicate that the flexibility towards the orientation of the sugar ring is unique for TMPKmt. Most interesting, however, is compound **6.10**, with a selectivity index (K_i TMPKh/ K_i TMPKmt) of 200, superseding **4.9** not only in affinity, but also in selectivity.

These three inhibitors are very interesting leads for further drug design, considerably increasing the variety of nucleoside analogues that may be considered for future synthesis. Especially **6.12** forms an interesting challenge for finding other bisubstrate inhibitors with an improved fit in the enzyme cavity.

Chapter 7

1',5'-Anhydro-2',3'-dideoxy-5'-*O*-phosphoryl-2'-(thymin-1-yl)-D-*arabino*-hexitol (**7.1**) proved to be a good inhibitor of TMPKmt (K_i-value of 30 μM), indicating that six-membered sugar rings can be accomodated by the target enzyme. In **7.1**, the base is preferentially in an axial ($^1C_4$) conformation, in contrast to dTMP, were thymine prefers an equatorial-like position. Because modeling showed that the thymine moiety in 1-[2,4-dideoxy-4-*C*-hydroxymethyl-α-L-lyxopyranosyl]thymine (**7.2**) would prefer an equatorial position,[6] this nucleoside was considered a promising inhibitor of TMPKmt.

The key to the synthesis of **7.2**, involves the introduction of the hydroxymethyl moiety onto the 4'-carbon of the pyranose sugar. This was first attempted through hydroboration/oxidation of an exocyclic 4'-methylene bond. Preferential attack of the hydroboration reagent at the β-side of the sugar ring due to steric hindrance caused by the 2'-3'-*O*-isopropylidene protective group, however, led to the undesired α-directed 4'-hydroxymethyl nucleoside. The preferential attack at the β-side of the sugar ring was then exploited through radical mediated introduction of a carbon nucleophile. Treatment 2,3-*O*-isopropylidene-1-*O*-methyl-4-*O*-phenoxythiocarbonyl-α-L-lyxopyranoside with β-tributylstannylstyrene allowed stereoselective introduction of a 2-phenylethenyl group at C-4, that via oxidation/reduction (OsO_4, $NaIO_4$/$NaBH_4$) was converted to the desired 4-hydroxymethyl group. In conclusion, a high yield method was developed for the synthesis of **7.2** in 13 steps from 2,3-*O*-isopropylidene-1-

O-methyl-α-L-lyxopyranose**.** NMR analysis showed that the obtained nucleoside is indeed characterised by the intended equatorial orientation of the thymine ring ($^4C_1$). However, affinity results of this nucleoside for TMPKmt were disappointing.

In conclusion, this work yielded some high affinity and selective inhibitors for TMPKmt that open interesting perspectives in the search for new anti-tuberculosis agents. Based on their high selectivity indices, especially dinucleoside **6.12** and bicyclic nucleosides **6.10** and **6.11** will be used as the starting point for the search of inhibitors with an even better fitting in the active pocket of TMPKmt.

REFERENCES

---

[1] Web site://www.who.org.

[2] Munier-Lehmann, H.; Chaffotte, A.; Pochet, S.; Labesse, G. Thymidylate kinase of *Mycobacterium tuberculosis*: A chimera sharing properties common to eukaryotic and bacterial enzymes. *Protein Sci.* **2001**, *10*, 1195–1205.

[3] Li de la Sierra, I.; Munier-Lehmann, H.; Gilles, A. M.; Bârzu, O.; Delarue, M. X-ray Structure of TMP Kinase from *Mycobacterium tuberculosis* Complexed with TMP at 1.95 Å Resolution. *J. Mol. Biol.* **2001**, *311*, 87–100.

[4] An, H.; Wang, T.; Maier, M. A.; Manoharan, M.; Ross, B. S.; Cook, P. D. Synthesis of novel 3'-*C*-methylene thymidine and 5-methyluridine/cytidine H-phosphonates and phosphonamidites for new backbone modification of oligonucleotides. *J. Med. Chem.* **2001**, *66*, 2789–2801.

[5] Lin, T. S.; Zhu, J.-L.; Dutschman, G. E.; Cheng, Y.-C.; Prusoff , W. H. Synthesis and biological evaluations of 3’-deoxy-3’-*C*-branched-chain-substituted nucleosides. *J. Med. Chem.* **1993**, *36*, 353–362.

[6] Ostrowski, T.; Wroblowski, B.; Busson, R.; Rozenski, J.; De Clercq, E.; Bennet, M. S.; Champness, J. N.; Summers, W. C.; Sanderson, M. R.; Herdewijn, P. 5-Substitted pyrimidines with a 1,5-anhydro-2,3-dideoxy-D-arabino-hexitol moiety at N-1: Synthesis, antiviral activity, conformational analysis, and interaction with viral thymidine kinase. *J. Med. Chem.* **1998**, *41*, 4343–4353.

OVERVIEW OF THE EVALUATED COMPOUNDS

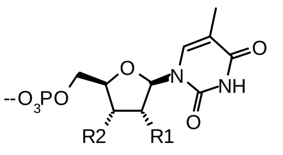

2.1 R1= H, R2= NH_2
2.8 R1= OH, R2= NH_2
2.9 R1= NH_2, R2= OH
2.12 R1= Cl, R2= OH
2.13 R1= F, R2= OH
2.20 R1= H, R2= F

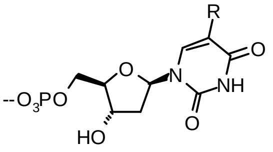

3.1 R= CH_2OH
3.2 R= CH_2OBn
3.3[a] R= CH_2OH
3.4 R= furan-2-yl
3.5 R= thien-2-yl

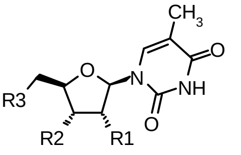

5.15 R1= OH, R2= OH, R3=OH
5.16 R1= OH[b] , R2= OH, R3=OH
5.21 R1= H, R2= NH_2, R3= OH
5.22 R1= OH, R2= F, R3=OH
5.23 R1= F, R2= OH, R3=OH
5.24 R1= OH, R2= N_3, R3=I
5.25 R1= OH, R2= NH_2, R3= H
5.26 R1= OH, R2= $NHC(NH)NH_2$, R3= OH

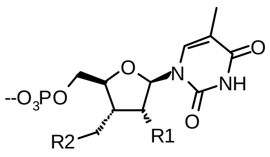

4.3 R1= H, R2= N_3
4.4 R1= H, R2= NH_2
4.5 R1= H, R2= F
4.6 R1= H, R2= OH
4.7 R1= OH, R2= N_3
4.8 R1= OH, R2= NH_2

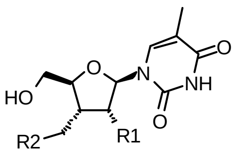

4.9 R1= H, R2= N_3
4.10 R1= H, R2= NH_2
4.11 R1= H, R2= F
4.12 R1= H, R2= OH
4.13 R1= OH, R2= N_3
4.14 R1= OH, R2= NH_2
4.15 R1= H, R2= CH_2OH

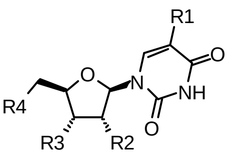

5.17 R1= CF_3, R2= H, R3=OH, R4= OH
5.18 R1= CH_2CH_3, R2= H, R3= OH, R4= OH
5.19 R1= F, R2= OH, R3= OH, R4= OH
5.20 R1= F, R2= OH, R3= OH, R4= H

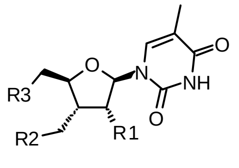

6.5 R1= Cl, R2= N_3, R3= OH
6.6 R1= Cl, R2= NH_2, R3= OH
6.7 R1= F, R2= N_3, R3= OH
6.8 R1= F, R2= NH_2, R3= OH
6.9 R1= F, R2= N_3, R3= F
6.13[a] R1= OH, R2= N_3, R3= OH

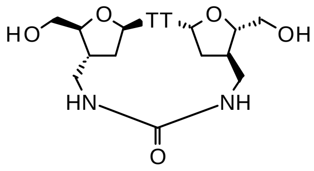

6.12
T= thymin-1-yl

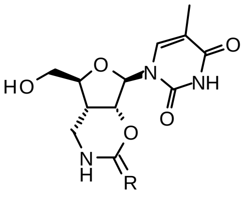

6.10 R= S
6.11 R= O

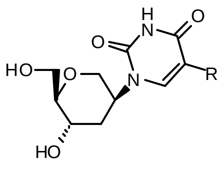

7.1

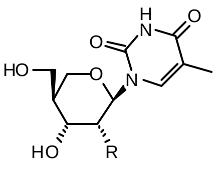

7.20 R= OH
7.2 R= H

[a] the thymine ring lies at the α side of the sugar ring
[b] the 2'-OH lies at the β side of the sugarring

LIST OF PUBLICATIONS

- Van Calenbergh, Serge; Link, Andreas; Fujikawa, Shelly; de Ligt, Rianne A. F.; Vanheusden, Veerle; Golisade, Abolfasl; Blaton, Norbert M.; Rozenski, Jef; IJzerman Adriaan P.; Herdewijn, Piet. 5'-Deoxy congeners of 9-(3-amido-3-deoxy-beta-D-*xylo*furanosyl)-*N*(6)-cyclopentyladenine: new adenosine A(1) receptor antagonists and inverse agonists. *Journal of Medicinal Chemistry* (2002), 45(9), 1845-1852.

- Vanheusden, Veerle; Munier-Lehmann, Hélène; Pochet, Sylvie; Herdewijn, Piet; Van Calenbergh, Serge. Synthesis and evaluation of thymidine-5'-*O*-monophosphate analogues as inhibitors of *Mycobacterium tuberculosis* thymidylate kinase. *Bioorganic & Medicinal Chemistry Letters* (2002), 12(19), 2695-2698.

- Haouz, Ahmed; Vanheusden, Veerle; Munier-Lehmann, Hélène; Froeyen, Mattheus; Herdewijn, Piet; Van Calenbergh, Serge; Delarue, Marc. Enzymatic and structural analysis of inhibitors designed against *Mycobacterium tuberculosis* thymidylate kinase. New insights into the phosphoryl transfer mechanism. *Journal of Biological Chemistry* (2003), 278(7), 4963-71.

- Vanheusden, Veerle; Munier-Lehmann, Hélène; Froeyen, Matheus; Dugué, Laurence; Heyerick, Arne; De Keukeleire, Denis; Pochet, Sylie; Herdewijn, Piet; Van Calenbergh, Serge. 3’-*C*-Branched-chain-substituted nucleosides and nucleotides as inhibitors of *Mycobacterium tuberculosis* thymidine monophosphate kinase. *Journal of Medicinal Chemistry* (2003), 46(18), 3811-3821.

- Vanheusden, Veerle; Van Rompaey, Philippe; Munier-Lehmann, Hélène; Pochet, Sylvie; Herdewijn, Piet; Van Calenbergh, Serge. Thymidine and thymidine-5'-*O*-monophosphate analogues as inhibitors of *Mycobacterium tuberculosis* thymidylate kinase. *Bioorganic and Medicinal Chemistry Letters* (2003), 13(18), 3045-3048.

- Van Rompaey, Philippe; Nauwlaerts, Koen; Vanheusden, Veerle; Rozenski, Jef; Munier-Lehmann, Hélène; Herdewijn, Piet; Van Calenbergh, Serge. *Mycobacterium tuberculosis* thymidine monophosphate kinase inhibitors: biological evaluation and conformational analysis of 2'- and 3'-modified thymidine analogues. *European Journal of Organic Chemistry* (2003), (15), 2911-2918.

- Vanheusden, Veerle; Munier-Lehmann, Hélène; Froeyen, Matheus; Busson, Roger; Rozenski, Jef; Herdewijn, Piet; Van Calenbergh, Serge. Discovery of bicyclic thymidine analogues as selective and high affinity inhibitors of *Mycobacterium tuberculosis* thymidine monophsophate kinase. *Submitted for J. Med. Chem.*

- Vanheusden, Veerle; Busson, Roger; Herdewijn, Piet; Van Calenbergh, Serge. Synthesis of 1-[2,4-dideoxy-4-*C*-hydroxymethyl-α-L-lyxopyranosyl]thymine: a potential inhibitor of *Mycobacterium tuberculosis* thymidine monophsophate kinase. *Submitted for J. Org. Chem.*